ABCA Transporters and Associated Genes in Lipid Metabolism

Dissertation zur Erlangung des Doktorgrades der Naturwissenschaften (Dr. rer. nat.) der Naturwissenschaftlichen Fakultät III – Biologie und Vorklinische Medizin der Universität Regensburg

vorgelegt von
Alexander Sigrüner
aus Altötting
Februar 2007

Die vorliegende Arbeit entstand in der Zeit von April 2002 bis Februar 2007 am Institut für Klinische Chemie und Laboratoriumsmedizin des Klinikums der Universität Regensburg unter der Anleitung von Prof. Dr. Gerd Schmitz.

Promotionsgesuch eingereicht am: 07.02.2007

Prüfungsausschuss: Vorsitzender: Prof. Dr. Reinhard Wirth
1. Gutachter: Prof. Dr. Stephan Schneuwly
2. Gutachter: Prof. Dr. Gerd Schmitz
3. Prüfer: Prof. Dr. Will Minuth

Danksagung

Besonders bedanken möchte ich mich bei Herrn Prof. Dr. Gerd Schmitz, der mir die Durchführung dieser Doktorarbeit an seinem Institut ermöglicht hat, für seine umfassende wissenschaftliche Unterstützung, und die vielen informativen Diskussionen und Anregungen.

Bei Herrn Prof. Dr. Stephan Schneuwly möchte ich mich für die Bereitschaft bedanken die fakultätsinterne Betreuung der Arbeit zu übernehmen.

Besonderer Dank gilt auch Frau PD Dr. Christa Büchler, die mich bei der Planung und Auswertung von Versuchen unterstützt hat, und die durch zahlreiche wissenschaftliche Diskussionen und Anregungen wesentlich zum Gelingen der Arbeit beigetragen hat.

Bei Prof. Dr. Charalampos Aslanidis, Dr. Guido Maa Bared, Dr. Alfred Böttcher, Dr. Margot Grandl und Dr. Christian Rudolph bedanke ich mich für viele interessante und hilfreiche Diskussionen.

Bedanken möchte ich mich auch bei Louay Jouma für seine Hilfe bei den ABCA7 Promoter- und Expressions-Analysen und bei Tamas Köbling für seine Unterstützung bei der Identifizierung TAX1BP3 und Syntaxin 13 interaktiver Proteine.

Vielen Dank an Rudolph Jung für die Durchführung und an Prof. Dr. Arndt Hartmann für die Auswertung der Immunhistochemie, und an Dr. Peter J. Wild für die statistische Auswertung dieser Daten und seine Hilfe bei der Formulierung der entsprechenden Abschnitte.

Außerdem danke ich noch meinen Laborkolleginnen Conny und Sylvia und allen anderen Mitarbeiterinnen und Mitarbeitern des Instituts für die angenehme Zusammenarbeit.

Last, but not least, möchte ich mich noch bei meinen Eltern und meinen Freunden für Ihre Unterstützung bedanken.

Abbreviations

ABC	ATP-binding cassette
ABCA1	ABC transporter A1
ABCA7	ABC transporter A7
ABCG1	ABC transporter G1
ACTH	adrenocorticotropic hormone
AHR	aryl hydrocarbon receptor
AMH	anti-Müllerian hormone
AOX1	Aldehyde oxidase 1
AP-3	Adapter Protein-3
apoA-I	apolipoprotein A-I
apoE	apolipoprotein E
ARL7	ADP-ribosylation factor-like protein 7
ARNT	AHR nuclear translocator
Arx	Aristaless-related homeobox
ATP	adenosintriphosphate
ATRA	all-trans retinoic acid
BCA	bicinchonic acid
bHLH-Zip	basic helix-loop-helix leucine zipper
BLOC	Biogenesis of Lysosome- related Organelles Complexe
BSA	bovine serum albumin
CC	cholesterol crystal
cDNA	copy desoxyribonucleic acid
CE	cholesterol ester
CYP	Cytochrome P450
DAB	3,3‘-diaminobenzidine
Dax1	DSS-AHC-critical region on the X chromosome gene 1
DHEA	dehydroepiandrosteron
Dhh	Desert hedgehog
DMSO	dimethylsulfoxide
dpc	days post coitum
dsRNA	double stranded RNA
E. coli	Escherichia coli
EC	enzyme cocktail
E-LDL	enzymatically modified LDL
ELISA	enzyme-linked immunosorbent assay
ER	endoplasmatic reticulum
FACS	Fluorescence Activated Cell Sorter
FADD	Fas-associated via death domain
Fig.	Figure
$FLIP_L$	FLICE-like inhibitory protein long form
GIPC1	GAIP C-terminus-interacting protein1
GST	gluthation S-transferase
HCC	hepatocellular carcinoma
HDL	high-density lipoprotein
HMGCR	3-hydroxy-3-methylglutaryl coenzyme A-reductase
HPS	Hermansky-Pudlak Syndrome
HSD3B2	3β-hydroxysteroid dehydrogenase
kb	kilo base pairs
kDa	kilodalton
LB	Luria Broth
LCT	Leydig cell tumor
LDL	low-density lipoprotein
LDLR	LDL receptor

LRO	lysosome-related organelle
LXR	liver X receptor
MAGI3	Membrane associated guanylate kinase, WW and PDZ domain containing 3
M-CSF	Macrophage-Colony Stimulating Factor
MFE	molybdo-flavoenzyme
MLN64	metastatic lymph node 64
mRNA	messenger RNA
mTOR	mammalian target of Rapamycin
NBD	nucleotide binding domain
NPC	Niemann-Pick type C disease
Ox-LDL	oxidized LDL
PAGE	polyacrylamide gel electrophoresis
PBS	Phosphate buffered saline
PDGF	platelet-derived growth factor
PDGFRα	PDGF receptor α
PDZ	PSD-95/Dlg/ZO-1
PI3K	phosphoinositide 3-kinase
PPAR	peroxisome proliferator activated receptor
Ptc	Patched
PUFA	polyunsaturated fatty acids
RA	retinoic acid
RAR	RA receptor
RCC	renal cell carcinoma
RNA	ribonucleic acid
ROS	reactive oxygen species
RT	reverse transcription
RXR	retinoid X receptor
S. cerevisiae	Saccharomyces cerevisiae
SAP	shrimp alcaline phosphatase
SCAP	SREBP-cleavage-activating protein
SDCBP	Syndecan-binding protein
SDS	sodium dodecyl sulfate
Sf1	steroidogenic factor 1
SFM	serum free medium
siRNA	small interfering RNA
SNARE	soluble N-ethylmaleimide-sensitive factor attachment protein receptor
SNP	single-nucleotide polymorphism
SNTA1	α1- syntrophin
SNTB1	β1-syntrophin
SNTB2	β2-syntrophin
SREBP	SRE-binding protein
StAR	steroidogenic acute regulatory protein
START	StAR-related lipid transfer
TAX1BP3	Tax1 (human T-cell leukemia virus type I) binding protein 3
TCDD	2,3,7,8-Tetrachlorodibenzo-p-dioxin
TD	Tangier disease
TG	triglyceride
TMA	tissue microarray
TMD	transmembrane domain
VSMC	vascular smooth muscle cell
Wnt4	wingless-type MMTV integration site family, member 4
Wt1	Wilms tumor 1 gene
XOR	xanthine oxidoreductase

Table of Contents

I. INTRODUCTION

1. The ATP-Binding Cassette Transporter Family

ATP-binding cassette (ABC) transporters are archaic proteins found in the three kingdoms of life, namely the prokaryotic archaea and bacteria as well as eukaryotes. Among human transporters they are the largest subgroup consisting now of 48 functional diverse members [1]. Functional ABC transporters normally contain two transmembrane domains (TMD) and two nucleotide binding domains (NBD) or ABCs. The ABC domain is determined by two short, conserved peptides, called Walker A and Walker B motifs [2]. These motifs are common in ATP-binding proteins. According to a signature motif, located between the two Walker motifs, ABC-transporters are divided in seven subfamilies (A-G) [3]. Proteins from the ABCE and ABCF family, in contrast to all other ABC-transporters, lack the TMD. The TMD and ABC domains can be coded on a single polypeptide, like the full-size transporter ABCA1, or two polypeptides that need to form homo- or heterodimers, like half-size proteins from the ABCG family (Fig. 1 and Table 1).

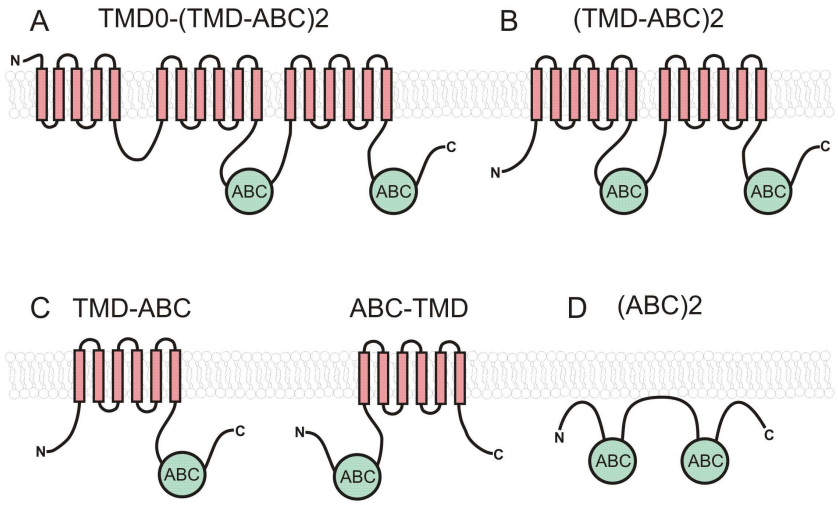

Figure 1. Diagram depicting domain arrangements of human ABC transporters. The ABC is shown as green circle, and the membrane spanning domains are depicted as barrels. **(A)** The TMD0-(TMD-ABC)2 structure. In addition to the regular full-size type, containing the (TMD-ABC)2 domain arrangement, this type displays additional five TMDs termed TMD0. **(B)** Prototype ABC transporter with the (TMD-ABC)2 structure. **(C)** Two alternative types of half size molecules, TMD-ABC and ABC-TMD. Only corresponding half-molecule organizations are able to form heterodimers. **(D)** The (ABC)2 type of molecules lacking TMDs is unlikely to function as transporter [*].

Table 1. Overview of human ABC transporters [*].

Gene	Alternative name	Location	Domain structure	Lipid regulation	Known/putative transported molecule
ABCA1	ABC1	9q31.1	(TMD-ABC)2	+	Choline-phospholipids and cholesterol
ABCA2	ABC2	9q34	(TMD-ABC)2	+	Estramustine, steroids
ABCA3	ABC3	16p13.3	(TMD-ABC)2	+	Surfactant phospholipids
ABCA4	ABCR	1p22.1-p21	(TMD-ABC)2	-	N-retinylidene-PE
ABCA5		17q24	(TMD-ABC)2	+	
ABCA6		17q24	(TMD-ABC)2	+	Phospholipids
ABCA7		19p13.3	(TMD-ABC)2	+	Sphingolipids and serine-phospholipids
ABCA8		17q24	(TMD-ABC)2	-	
ABCA9		17q24	(TMD-ABC)2	+	
ABCA10		17q24	(TMD-ABC)2	-	
ABCA12		2q34	(TMD-ABC)2	-	
ABCA13		7p11-q11	(TMD-ABC)2	-	
ABCB1	MDR1, PGY1	7p21	(TMD-ABC)2	+	Phospholipids, PAF, aldosterone, cholesterol, amphiphiles, β-amyloid peptide
ABCB2	TAP1	6p21	TMD-ABC	-	Peptides
ABCB3	TAP2	6p21	TMD-ABC	-	Peptides
ABCB4	MDR3	7q21.1	(TMD-ABC)2	+	Phosphatidylcholine
ABCB5		7p14	(TMD-ABC)2	-	
ABCB6	MTABC3	2q36	TMD-ABC	+	Fe/S clusters
ABCB7	ABC7	Xq12-q13	TMD-ABC	-	Fe/S clusters
ABCB8	MABC1	7q36	TMD-ABC	-	Fe/S clusters
ABCB9		12q24	TMD-ABC	+	
ABCB10	MTABC3	1q42	TMD-ABC	-	Fe/S clusters
ABCB11	BSEP, SPGP	2q24	(TMD-ABC)2	+	Monovalent bile salts
ABCC1	MRP1	16p13.1	TMD0-(TMD-ABC)2	+	GSH-, glucuronate-, sulfate-conjugates, GSSG, sphingolipids, LTC_4, PGA_1, PGA_2, 17β-glucuronosyl estradiol
ABCC2	MRP2	10q24	TMD0-(TMD-ABC)2	+	GSH-, glucuronate-, sulfate-conjugates, bilirubin glucuronide, LTC_4, 17β-glucuronosyl estradiol, taurolithocholate 3-sulfate, anionic drugs
ABCC3	MRP3	17q21.3	TMD0-(TMD-ABC)2	-	glucuronate-, sulfate-conjugates, 17β-glucuronosyl estradiol, taurolithocholate 3-sulfate
ABCC4	MRP4	13q32	(TMD-ABC)2	+	Xenobiotics, nucleosides
ABCC5	MRP5	3q27	(TMD-ABC)2	+	Xenobiotics, nucleosides
ABCC6	MRP6	16p13.1	TMD0-(TMD-ABC)2	-	Anionic cyclopentapeptides
ABCC7	CFTR	7q31.2	(TMD-ABC)2	-	Chloride ions, ATP
ABCC8	SUR1	11p15.1	TMD0-(TMD-ABC)2	-	Sulfonylureas
ABCC9	SUR2	12p12.1	TMD0-(TMD-ABC)2	-	Sulfonylureas
ABCC10	MRP7	6p21	TMD0-(TMD-ABC)2	-	
ABCC11	MRP8	16q11-q12	(TMD-ABC)2	-	
ABCC12	MRP9	16q11-q12	(TMD-ABC)2	-	
ABCD1	ALD	Xq28	TMD-ABC	+	Very-long-chain fatty acids
ABCD2	ALDR	12q11-q12	TMD-ABC	+	Very-long-chain fatty acids
ABCD3	PMP70, PXMP1	1p22-p21	TMD-ABC	-	Very-long-chain fatty acids
ABCD4	PMP69	14q24.3	TMD-ABC	+	Very-long-chain fatty acids
ABCE1	OABP	4q31	(ABC)2	-	Oligoadenylate
ABCF1		6p21.33	(ABC)2	-	translation elongation initiation factor 2
ABCF2		7q36	(ABC)2	-	
ABCF3		3q25	(ABC)2	-	
ABCG1	White	21q22.3	ABC-TMD	+	Phospholipids, cholesterol
ABCG2	MXR, BCRP	4q22	ABC-TMD	-	Drugs
ABCG4	White2	11q23	ABC-TMD	+	
ABCG5	White3	2p21	ABC-TMD	+	Plant- and shellfish sterols
ABCG8	White4	2p21	ABC-TMD	+	Plant- and shellfish sterols

ABC-transporters operate in two ways: as active pumps hydrolyzing ATP, like members of the ABCB family (MDR/TAP), or as transport-facilitators, like ABCC7 (CFTR) and ABCA1 that bind ATP, which induces a conformational change, but with a slowly hydrolysis of the ATP (Fig. 2).

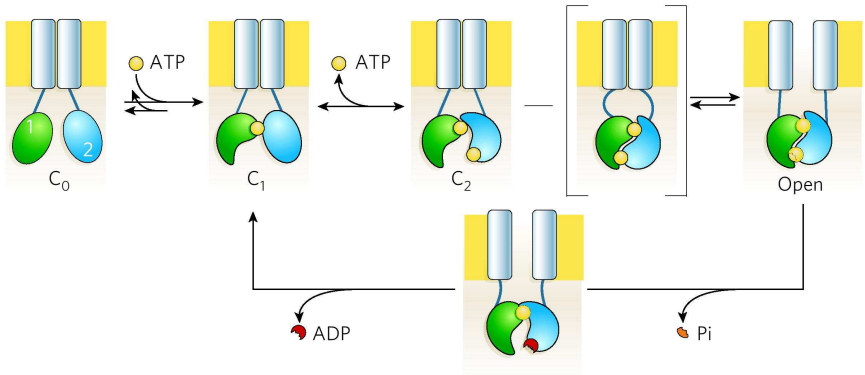

Figure 2. Structural interpretation of ATP-dependent gating cycle of CFTR. ATP remains tightly bound to NBD1 (green) for minutes, during which time many gating cycles occur. Following ATP binding to NBD2 (blue) a slow opening step (C_2-to-Open) proceeding through a transition state (square brackets) in which the intramolecular NBD1–NBD2 heterodimer is formed but the transmembrane pore (grey rectangles) has not yet opened. Hydrolysis of ATP bound at the NBD2 catalytic site and loss of inorganic phosphate (Pi) leads to channel closure (from [4]).

While the majority of full-size transporters act at the plasma membrane, most half-size transporters are found in intracellular membrane systems such as mitochondria, peroxisomes, the endoplasmatic reticulum (ER) and the Golgi. On the other hand, full-size transporters are also located intracellularly as result of vesicular trafficking events, or determined by alternative splicing.

One of the best-characterized ABC-transporters is the gene responsible for cystic fibrosis, a lethal inherited disorder that is caused by mutations in ABCC7 (CFTR) [5]. Nowadays various ABC-transporters are described in inherited monogenetic diseases (Table 2).

Table 2. Human ABC transporter genes and associated monogenetic disorders (from [6])**.**

Gene	Monogenetic disorder	OMIM no.
ABCA1	Tangier disease Familial hypoapolipoproteinemia	205400 604091
ABCA3	Respiratory distress syndrome (Neonatal surfactant deficiency)	267450
ABCA4	Stargardt disease Retinitis pigmentosa 19 Cone rod dystrophy 3 Age-related macular degeneration	248200 601718 604116 153800
ABCA12	Lamellar ichthyosis type 2 (Ichthyosis congenital IIB) Harlequin ichthyosis (Ichthyosis congenita, Harlequin fetus type)	601277 242500
ABCB4	Progressive familial intrahepatic cholestasis type 3	602347
ABCB7	X-linked sideroblastosis and anemia	301310
ABCB11	Progressive familial intrahepatic cholestasis type 2	601847
ABCC2	Dubin–Johnson Syndrome	237500
ABCC6	Pseudoxanthoma elasticum (PXE)	264800
ABCC7	Cystic fibrosis (Mucoviscidosis) Congenital bilateral absence of the vas deferens	219700 277180
ABCC8	Familial persistent hyperinsulinemic hypoglycemia of infancy	601820
ABCD1	Adrenoleukodystrophy	300100
ABCG5	β-sitosterolemia	210250
ABCG8	β-sitosterolemia	210250

1.1. The ABCA-Subfamily is Involved in Phospholipid- and Cholesterol-Trafficking

All members of the ABCA-subfamily are full-size transporters, most of which show a ubiquitous expression. Interestingly the ABCA-subgroup is the only one with no homologues in yeast, appearing in Caenorhabditis elegans for the first time [7].

In humans, the 12 ABCAs can be divided in two groups: five genes (ABCA5, ABCA6, ABCA8, ABCA9, and ABCA10) are clustered on chromosome 17q24, the remaining seven genes are distributed over six chromosomes (Fig. 3).

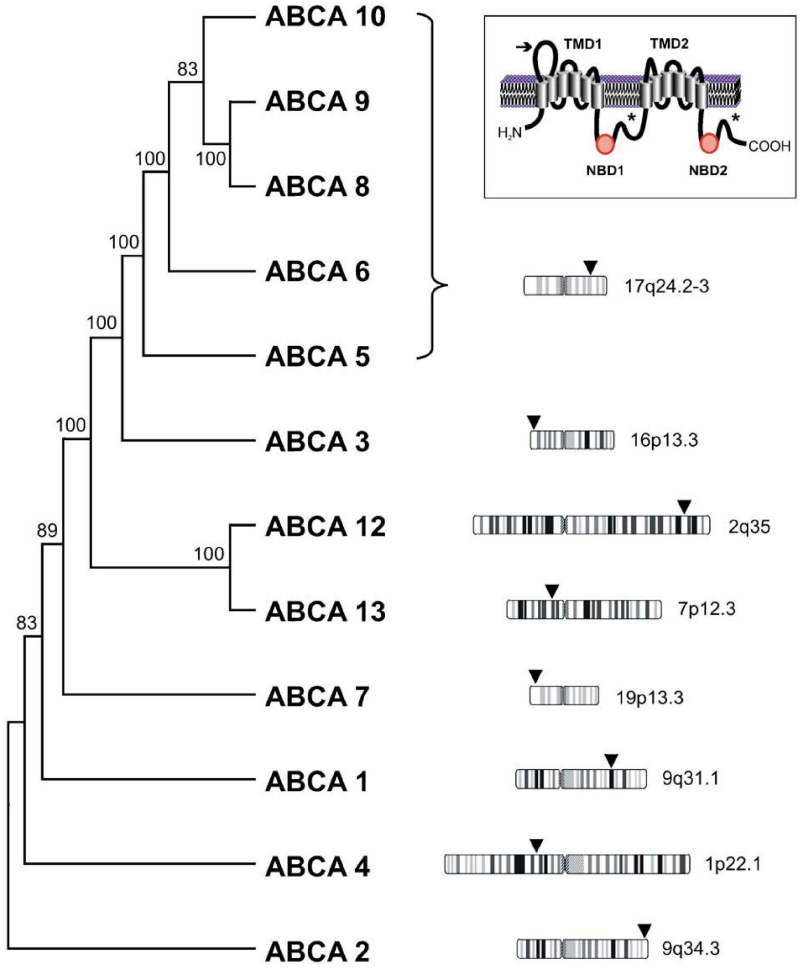

Figure 3. Phylogenetic consensus tree and chromosomal dispersion of human ABCA-subfamily transporter genes. Bootstrap values (%) out of 100 iterations are indicated at each branch point. The chromosomal loci are schematically shown for each ABC A-subfamily transporter gene (arrowheads). Inset: Schematic representation of the structural organization of ABCA transporters (from [6]).

An important role for the ABCA subfamily in lipid metabolism is indicated by the finding that the transcription of at least six members is regulated by lipids [8-11] (Table 1). The tissue distribution of the ABCA transporters is shown in Table 3.

Table 3. mRNA Expression of ABCA-class transporters in different human tissues (from [12])**.**

Tissue	ABCA1	ABCA2	ABCA3	ABCA4	ABCA5	ABCA6	ABCA7	ABCA8	ABCA9	ABCA10	ABCA12
Brain, whole	•	•••••	•	•	•	•	•	•	•	•	•
Brain, cerebellum	•	•••	•	•	•	•	•	•	•	•	•
Heart	•	•	•	•	•	•	•	•	•	•	•
Skeletal muscle	•	•	•	•	•	•	•	•	•	•	•
Trachaea	•••	•••	•	•••	•••••	•••••	•••••	••••	•••••	•••••	••••
Lung	•••	••	•••••	•	•	••	•	•	•	•	•
Kidney	•	•	•	•••	•	•	•	•	•	•	•
Liver	••	•	•	•	•	•	•	•	•	•	•
Small intestine	•	•	•	•••	•	•	•	•	•	•	•
Colon	•	•	•	•	•	•	•	•	•	•	•
Salivary gland	•	•	•	•	•	•	••	•	•	•	•
Thyroid	•	•••	•	•	•	•	••	•	•	•	•
Adrenal gland	•••••	••	•	•	•	•	•	•	•	•	•
Testis	••	•	•	•••••	•••	••	•	•••••	••••	••••	•••••
Prostate	••	••	•	••	••••	•	•••	••	••	••	••
Uterus	•••••	••	•	•	••	••	•	••	••••	••••	•
Placenta	••	•	•	•	•	•	••	•	•	•	•
Thymus	••	•	•	•	•	•	••••	•	•	•	•
Spleen	•••	••	•	•	•	•	•••	•	•	•	•
Bone marrow	•	•	•	•	•	•	••	•	•	•	•

Expression was measured by TaqMan real-time reverse transcription (RT)-PCR. Results were converted to a linear scale. Tissues with the highest expression are highlighted (yellow).

1.1.1. ABCA1

The human ABCA1 cDNA codes for a 2261 amino acid protein (220 kDa) [13] and is widely expressed in tissues with highest expression levels in placenta, liver, lung, adrenal glands and fetal tissues [11]. In macrophages, ABCA1 is upregulated by cholesterol loading and downregulated by high-density lipoprotein $(HDL)_3$-mediated cholesterol deloading [11]. The finding that mutations in ABCA1 cause familial HDL-deficiency syndromes (Tangier disease, TD) highlight ABCA1 as a major regulator of HDL metabolism [14-16]. Upregulation of ABCA1 expression is associated with increased cholesterol and phospholipid efflux and reduced efflux was found in ABCA1 deficient cells [17]. ABCA1 was expected to translocate lipids between the inner and outer plasma membrane [18]. In addition, results from overexpression of ABCA1 indicated a role in intracellular cholesterol transport [19]. Experiments performed in insect Sf9 cells imply that nucleotide binding leads to conformational changes of ABCA1 and ATP hydrolysis only takes place at very low rates [20]. ATP hydrolysis was also detected in mammalian HEK293 cells [21]. Due to the low ATP turnover, ABCA1 is probably a transport-facilitator, not an active transporter.

Macrophages have an important role in the development and progression of atherosclerotic lesions [22]. Upon continuous loading with cholesterol in lesions, they change into foam cells. In this process ABCA1 expression is enhanced [11; 17] and ABCA1 is recruited to the plasma membrane [17], where it is found in Lubrol-detergent resistant membrane domains

[23]. Besides in the plasma membrane, ABCA1 is also found in the Golgi compartment and in lysosomes [21; 24], indicating shuttling of ABCA1 between these sites. These data point to a function of ABCA1 in foam cell and atherosclerotic lesion development, which is supported by findings from chimeric low-density lipoprotein (LDL) receptor $(LDLR)^{-/-}$ mice and apolipoprotein E (apoE) null mutant mice [25; 26]. It is of note that the absence of ABCA1 in leukocytes had no influence on plasma HDL levels but alters recruitment of inflammatory cells [25]. In line with this, overexpression of human ABCA1 in transgenic apoE null mice reduced lesion size [27]. These data from in vitro and in vivo experiments emphasize the importance of ABCA1 in macrophage lipid homeostasis and its anti-atherogenic potential. These features make ABCA1 an interesting target for therapeutic approaches that modulate ABCA1 activity. Transcription of ABCA1 is among other factors regulated by zinc finger proteins 202 [28], oncostatin M [29], and geranylgeranyl pyrophosphate, which influences the nuclear hormone receptor liver X receptor (LXR) [30] (Fig. 4).

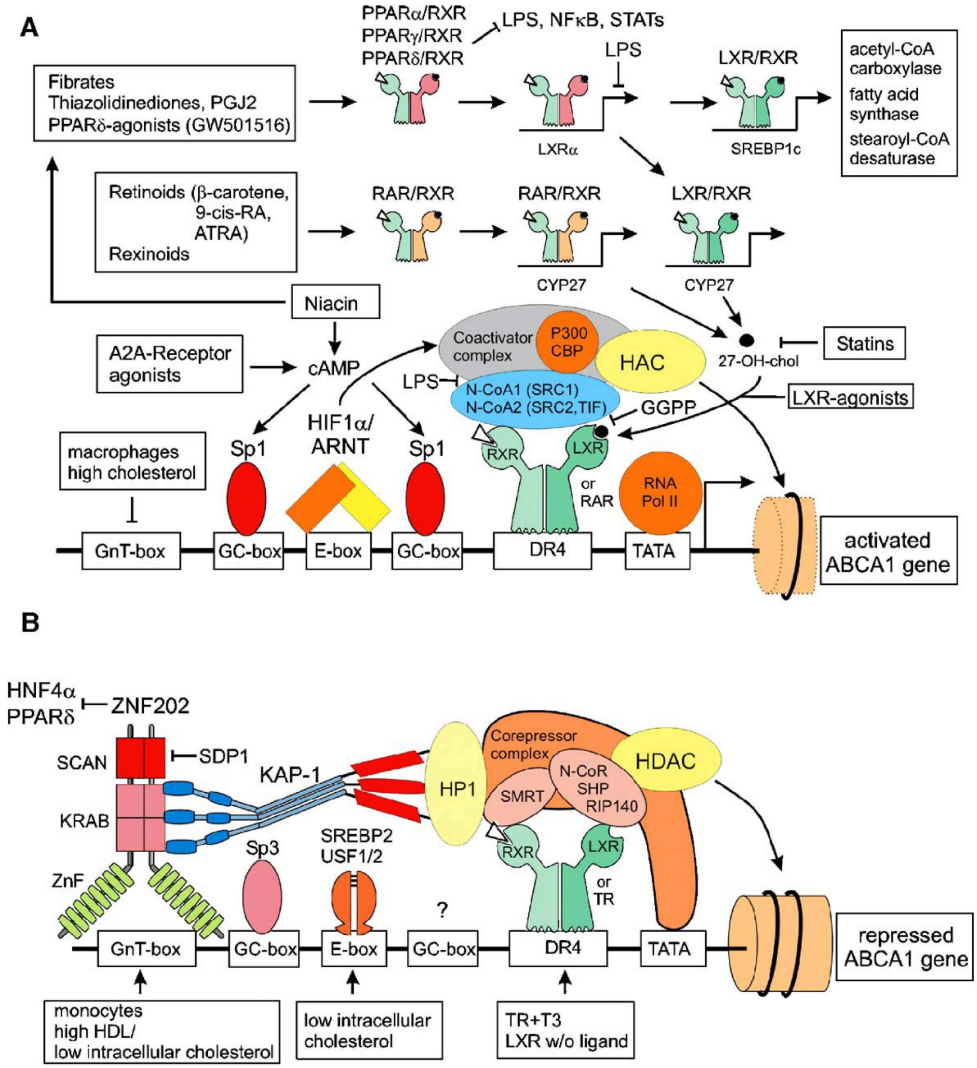

Figure 4. Transcriptional regulatory network controlling ABCA1 expression. (A) Mechanisms activating the ABCA1 promoter. **(B)** Repressing factors at the ABCA1 regulatory region (from [31]).

LXRα was already shown to be involved in sterol-dependent transactivation of ABCA1 transcription [32; 33]. In macrophages, ABCA1 expression is induced by the peroxisome proliferator activated receptors PPARα and PPARγ agonists [34; 35], supporting the influence of nuclear receptors on ABCA1 activity. Further promotion comes from chimeric $LDLR^{-/-}$ mice missing PPARγ in their bone marrow-derived cells. This leads to a higher prevalence of atherosclerosis in these animals implying that PPARγ-mediated ABCA1 upregulation in macrophages is atheroprotective in vivo [35]. Noteworthy, the protective effect of PPARγ can as well happen without reference to ABCA1, implying possible involvement in other antiatherosclerotic pathways [36].

Another interesting finding is that unsaturated fatty acids seem to regulate ABCA1 activity. They reduce ABCA1 dependent cholesterol/phospholipid efflux from macrophages [37] probably due to enhanced degradation of ABCA1 mediated by a phospholipase D2 signaling pathway [38]. In addition, polyunsaturated fatty acids (PUFA) likely inhibit ABCA1 expression [39]. Furthermore, stearoyl-CoA desaturases decrease ABCA1-mediated cholesterol efflux [40]. As systemic fatty acids are increased in type 2 diabetes mellitus, these results may link cholesterol metabolism and diabetes. Furthermore, ABCA1 is involved in phosphoinositide 3-kinase (PI3K)/Akt signaling. Akt is a kinase downstream from PI3K, and PI3K/Akt pathways are involved in insulin signaling [41] and the platelet-derived growth factor (PDGF)-dependent suppression of ABCA1 expression in vascular smooth muscle cells (VSMC) [42]. Akt activity is reduced by ABCA1 [43] and HDL-mediated activation of the PI3K/Akt pathways results in endothelial nitric oxide synthase (eNOS)-mediated nitric oxide production [44]. The PI3K/Akt signaling pathways are moreover involved in apoptosis [45; 46] and autophagy [47]. ABCA1 is also expressed in steroidogenic tissues. In mice, mRNA and protein are highly expressed in testis and adrenal gland [48], and ABCA1 mRNA was also found in rat ovarian theca-interstitial cells albeit with no effect on HDL-supported androgen production [49].

1.1.1.1. HDL Deficiency Syndromes

Loss of functional ABCA1 results in HDL deficiency syndromes [14]. Patients with genetic HDL-deficiency suffer from massive accumulation of cholesteryl esters in many tissues and a variety of clinical phenotypes like hepatosplenomegaly, atherosclerosis, and peripheral neuropathy [50] that are mainly determined by ABCA1, as data from TD patients and ABCA1 knockout-mice show. TD is a rare autosomal recessive disorder of lipid metabolism marked by almost complete absence of plasma HDL and the accumulation of cholesteryl esters in the cells of the reticulo-endothelial system leading to splenomegaly and enlargement of tonsils and lymph nodes [51]. Coherent with the finding that mutations in ABCA1 cause a HDL deficiency phenotype in humans, data from our laboratory show that mice missing functional ABCA1 manifest plasma lipid alterations that are consistent with those observed in

TD [17]. Female ABCA1$^{-/-}$ mice also suffer from placenta malformation, leading to embryo growth retardation, fetal loss, and neonatal death [52]. In male ABCA1$^{-/-}$ mice lipids accumulate in Sertoli cells, and Leydig cells reveal a decrease of lipid droplets. In addition, those animals have lower intratesticular testosterone levels and sperm count and are less fertile compared to wild type animals [53].

Up to now, various single-nucleotide polymorphisms (SNPs) have been identified in the human ABCA1 gene. Interestingly they appear in clusters located in the C-terminal half of the first extracellular domain, the N-terminal ABC and the C-terminus (Fig. 5). The type of clinical presentation seems to associate with the localization of the mutation; mutations in the first extracellular domain and the C-terminus are frequently associated with a cardiovascular phenotype while exchanges in or in the proximity of the N-terminal ABC appear to coincide with splenomegaly [6].

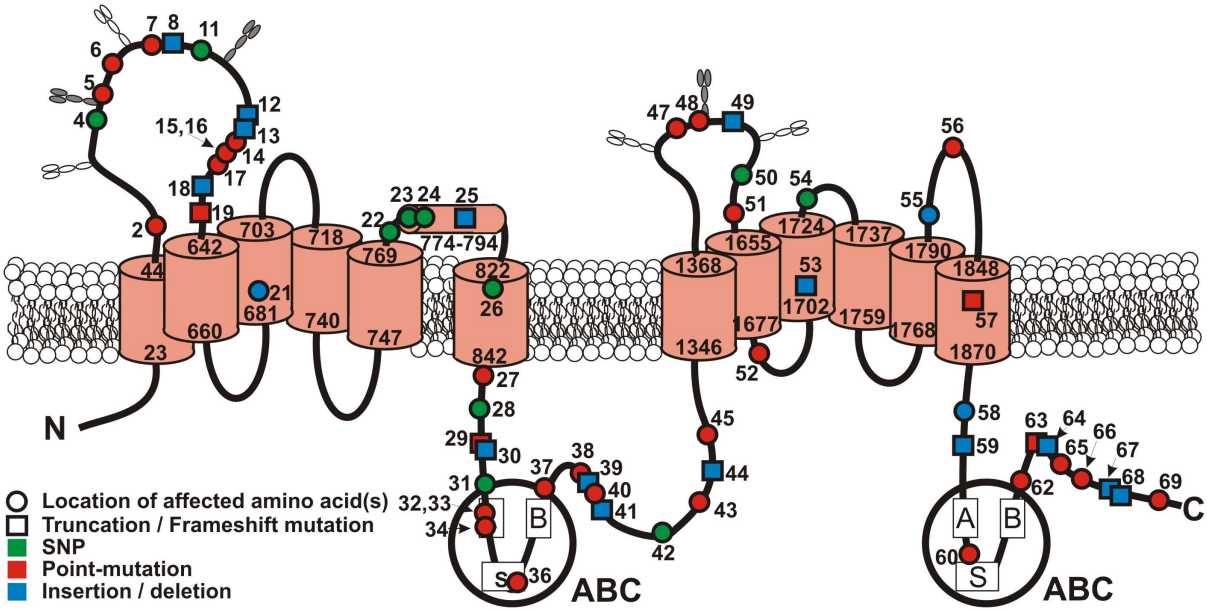

Figure 5. Overview of the published mutations in ABCA1.
(from http://www.uni-regensburg.de/Fakultaeten/Medizin/Klinische_Chemie/abca1.htm).

1.1.1.2. ABCA1 Interacting Proteins

Several ABCA1 interactive proteins have been described to modulate ABCA1 dependent lipid efflux (Fig. 6).

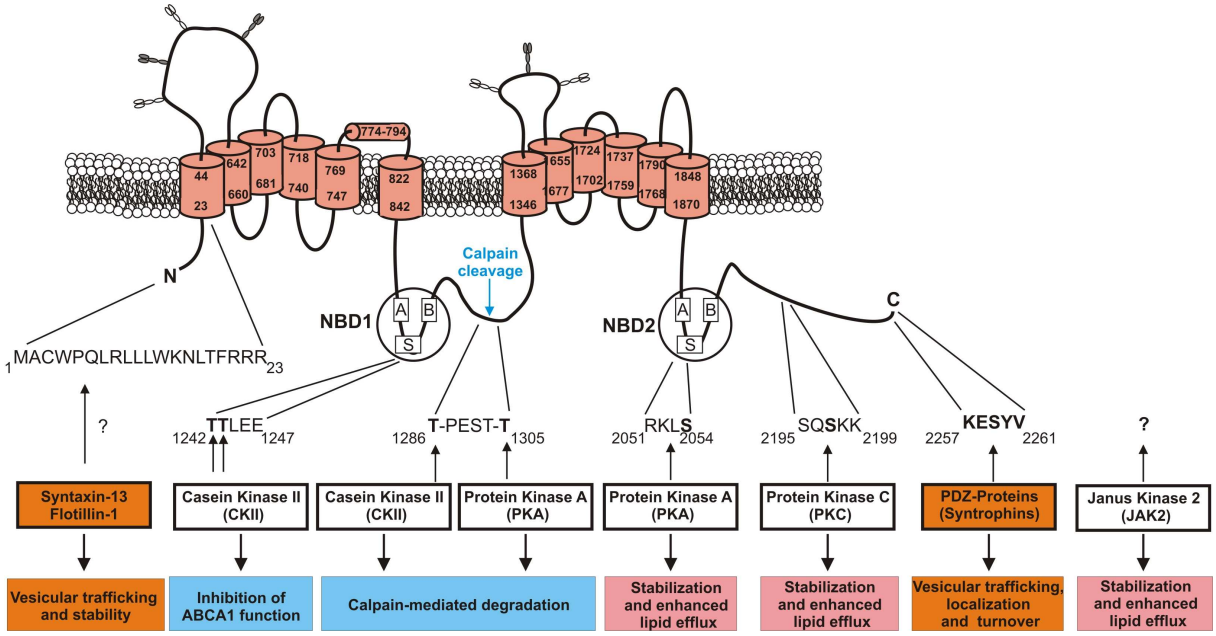

Figure 6. Overview of ABCA1 interaction sites. Sequences represent sites of interaction [*].

The PSD-95/Dlg/ZO-1 (PDZ) domain proteins α1-syntrophin (SNTA1) and β1-syntrophin (SNTB1) enhance lipid efflux by stabilizing ABCA1 [54; 55] and ABCA1 was also reported to interact with a β2-syntrophin(SNTB2)/utrophin complex, putatively linking it to the actin cytoskeleton [56]. On the other hand, lipid efflux is decreased by the expression of a dominant negative form of Fas-associated via death domain (FADD) which also interacts with the ABCA1 C-terminus [57]. This might link ABCA1 to apoptosis and host defense, in both of which FADD is implied [58; 59]. The small GTPase cdc42 was also shown to interact with ABCA1 [60], and overexpression of cdc42 leads to increased lipid efflux [61] while a dominant negative mutant substantially reduced apolipoprotein A-I (apoA-I)-induced cholesterol efflux [62]. ADP-ribosylation factor-like protein 7 (ARL7), probably in concert with ABCA1, may be involved in vesicular transport between a perinuclear compartment and an ABCA1-accessible cholesterol pool at the plasma membrane and has also been demonstrated to influence lipid efflux [63]. Recently, syntaxin 13 was identified to bind to ABCA1, and knock-down of syntaxin 13 reduced ABCA1 protein abundance and lipid efflux. Besides disturbed lipid efflux, ABCA1 deficiency is associated with enhanced phagocytic uptake. Transfection of functional ABCA1 in Tangier fibroblasts normalized enhanced uptake of lipoproteins and phagobeads. These findings suggest involvement of ABCA1 in the modulation of phagocytic uptake in type I- and type II phagocytosis [64].

1.1.2. ABCA7

ABCA7 is localized on chromosome 19 in close proximity to HA-1 [65] (Fig. 7), and, with its high homology to ABCA1 (54%), was initially described as a sterol-regulated gene similar to ABCA1 [8]. Therefore, it was assumed that ABCA7 might also be involved in lipid metabolism.

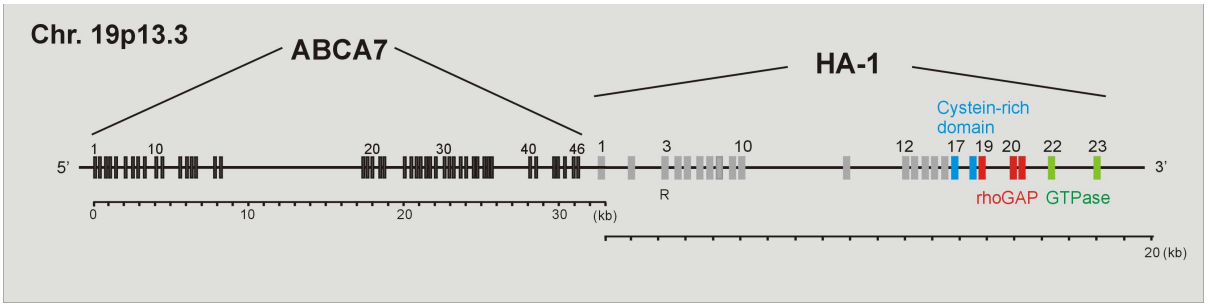

Figure 7. Structural organization of the ABCA7/HA-1 gene locus. Exons are numbered in 5´ to 3´ order and shown as black (ABCA7) or gray boxes (HA-1), respectively. Domains found in HA-1 are highlighted (adapted from [65]).

In transfection experiments it was shown that ABCA7 releases phospholipids via an apolipoprotein-mediated mechanism [66-71] and that ABCA7 may be a regulator of serine phospholipid species transport, including phosphatidylserine and ceramide [72]. Whether ABCA7 is involved in the release of cholesterol is unclear [66-68; 70; 71]. Recently two isoforms of ABCA7 have been identified, a full-length cDNA named type I and a shorter splice variant named type II [68]. Overexpression of ABCA7 type I in HEK293 cells localizes ABCA7 to the plasma membrane and mediates apoA-I-dependent release of cholesterol and phospholipids. In contrast ABCA7 type II was mainly found in the ER and did not influence apoA-I-mediated lipid efflux [68]. In spite these in vitro findings, ABCA7-mediated lipid efflux may not significantly influence plasma HDL-levels as data from macrophages and fibroblasts treated with ABCA7 small interfering (si)RNA [70; 73], from ABCA7 knockout mice [69], and ABCA7 heterozygous mice [70] indicate. More recent data show that ABCA7 is regulated inversely to ABCA1 by cholesterol loading through a sterol regulatory element/sterol regulatory element-binding protein 2 (SREBP2) dependent mechanism and suggests that this regulation of ABCA7 is involved in phagocytosis [73]. The involvement of ABCA7 in phagocytosis is supported by the finding that it has an important role in the removal of apoptotic cells and therefore ABCA7, not ABCA1 [74], might be the ortholog of Caenorhabditis elegans CED-7 [75].

The mRNA tissue distribution of ABCA7 differs from ABCA1, while ABCA1 is ubiquitously expressed with a high expression in placenta, liver, lung, adrenal glands and fetal tissues [11], ABCA7 is predominantly expressed in lymphohematopoetic tissues [8].

1.2. ABCG1

ABCG1 is a homodimer forming half-size transporter highly expressed in macrophages. Silencing of ABCG1 by siRNA reduced cholesterol and phospholipid efflux to HDL while its overexpression enhanced HDL-mediated cholesterol efflux, thereby lowering cellular cholesterol mass [76-78]. In contrast to ABCA1, that only poorly interacts with the major HDL fractions HDL_2 and HDL_3 [79; 80] and mediates efflux to lipid-poor apolipoproteins (e.g. apoA-I, apoE) [79; 81], ABCG1 uses HDL_2 and HDL_3 but not lipid-free apoA-I as acceptor [77; 78]. It was also reported that ABCG1 transfers cholesterol to LDL particles [78]. ABCG1 mRNA, similar to ABCA1, is upregulated by LXR agonists and cholesterol loading [77]. Interestingly different transcripts of ABCG1 are produced because of alternative promoters and alternative splicing [82; 83] (Fig. 8).

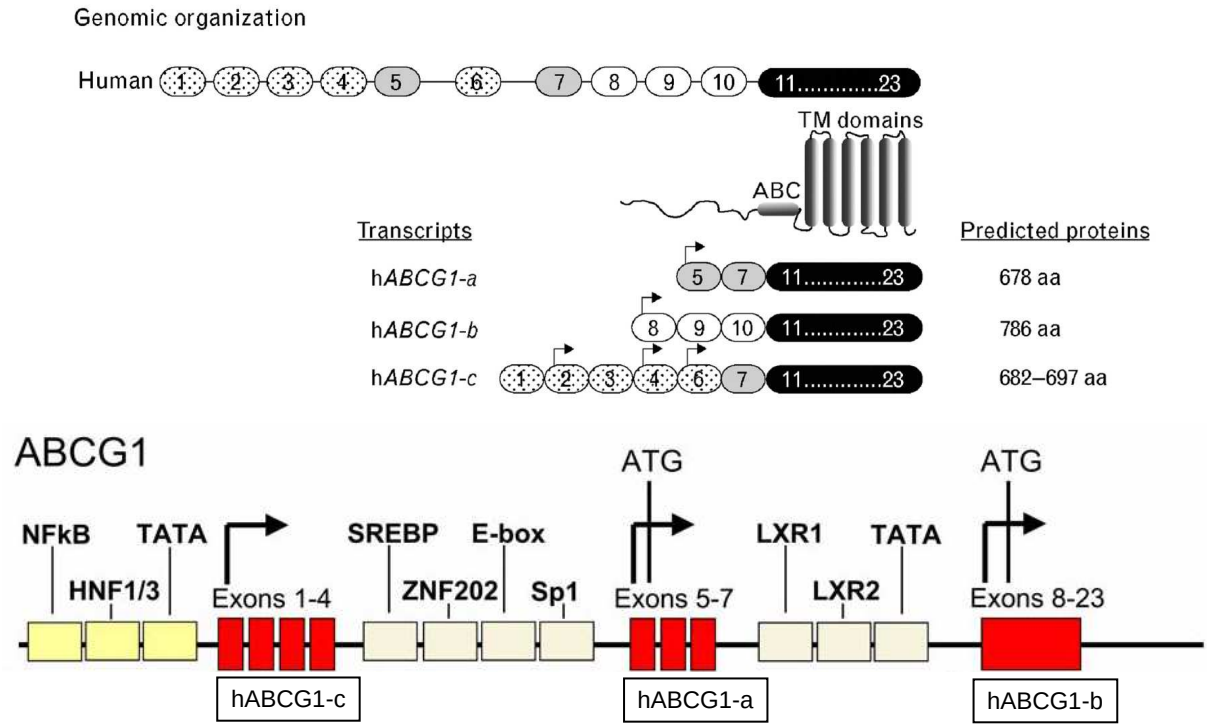

Figure 8. Genomic organization of the human ABCG1 together with the three putative promoters and resulting isoforms. Upper part: Alternative promoters and alternative splicing lead to multiple mRNA transcripts. The predicted proteins have the ABC and TM domains in common, but differ at the N-terminus. Due to alternative splicing of the exons 1-4 and 6 the N-terminus of hABCG1-c is even more variable [82]. Arrows indicate translation start (from [84]). Lower part: Putative promoters of ABCG1 with transcription factor binding sites [*].

While ABCA1 is well known to transport phospholipids (reviewed in [85]) ABCG1 appears to be less efficient [78]. On the other hand, controversial data on the ability of ABCA1 to transport cholesterol directly exist (reviewed in [85]). Recent findings suggest a two-step model, in which ABCA1 transfers phospholipids to lipid-poor apoA-I, thereby generating acceptor particles for ABCG1-mediated cholesterol efflux [86].

ABCG1$^{-/-}$ mice have defects previously linked to respiratory syndromes [87] (Fig. 9). Under normal conditions, phospholipid and cholesterol rich surfactant from the alveolar hypophase is cleared by type 2 cells (recycling and degradation) and by macrophages (degradation). In ABCG1$^{-/-}$ mice type 2 cells are transformed to hypertrophied pneumocytes, accumulating cholesterol crystals (CC) and excess lamellar bodies. In macrophages, a constant supply of cholesterol and fatty acids is generated by degrading surfactant. In ABCG1$^{-/-}$ compared to wild type macrophages lipid homeostasis is disturbed as upregulation of ABCA1 and downregulation of lipid/sterol biosynthesis are not sufficient to balance loss of ABCG1. Therefore, enhanced intracellular unesterified cholesterol content is detectable in these cells, leading to CC formation or esterification and formation or cholesterol ester (CE)-rich lipid droplets. The increased recovery of lipids in bronchioalveolar lavages from ABCG1$^{-/-}$ mice might be due to the combined hypertrophy of type 2 cells and a partial defect of both pneumocytes and macrophages in surfactant clearance [87].

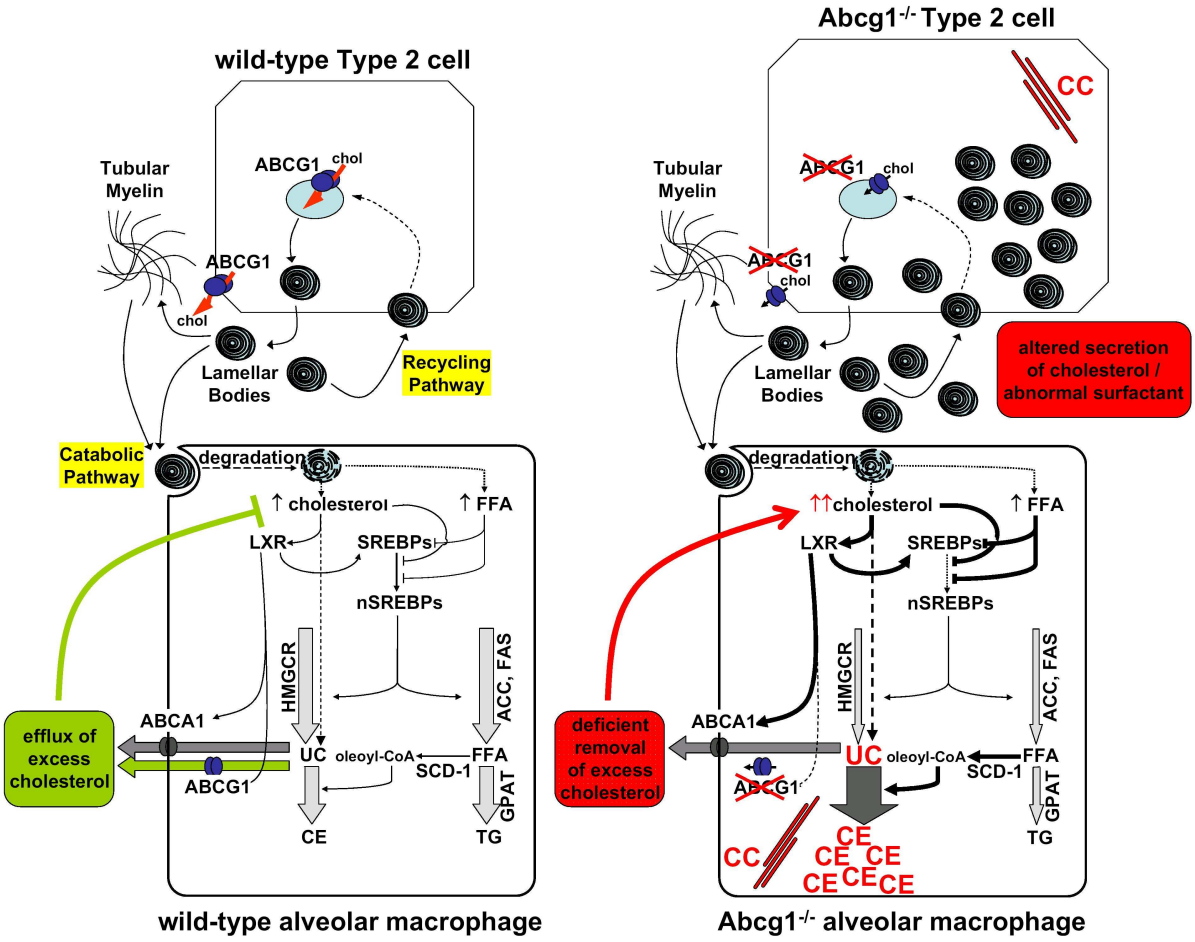

Figure 9. ABCG1 controls sterol/lipid homeostasis in type 2 cells and alveolar macrophages. For details see text. (from [87]).

2. Genes Involved in Lysosome-Related Organelle Synthesis and/or Trafficking

Trafficking of lysosome-related organelles (LROs), like melanosomes, platelet dense granules, and lamellar bodies, is accomplished through the endocytic pathway and they are characterized by subsets of shared membrane proteins, acidic pH and relatively high calcium content [88-90]. Mutations leading to Hermansky-Pudlak Syndrome (HPS) [91-93], Chediak-Higashi Syndrome [94; 95], and Griscelli Syndrome [96] exposed genes with important functions in LRO synthesis and/or trafficking (Table 4).

Table 4. Genes involved in LRO synthesis and/or trafficking.

Defective gene	Defective cells	Affected complex	Mouse mutant
Hermansky-Pudlak-Syndromes			
HPS1	Melanocytes and platelets	BLOC-4	"Pale ear"
AP3B1 (HPS2)	Immunocytes, melanocytes & platelets	AP-3	"Pearl"
HPS3	Melanocytes and platelets	BLOC-2	"Cocoa"
HPS4	Melanocytes and platelets	BLOC-3	"Light ear"
HPS5	Melanocytes and platelets	BLOC-2	"Ruby-Eye2"
HPS6	Melanocytes and platelets	BLOC-2	"Ruby-Eye"
DTNBP1 (HPS7)	Melanocytes and platelets	BLOC-1	"Sandy"
AP3D1	Melanocytes and platelets	AP-3	"Mocha"
RABGGTA	Immunocytes, melanocytes & platelets	Transient with Rabs	"Gunmetal"
PLDN	Melanocytes and platelets	BLOC-1	"Pallid"
MU	Melanocytes and platelets	BLOC-1	"Muted"
CNO	Melanocytes and platelets	BLOC-1	"Cappuccino"
VPS33A	Melanocytes and platelets	Unknown	"Buff"
Chediak-Higashi-Syndrome			
LYST	Immunocytes and melanocytes	Unknown	"Beige"
Griscelli-Syndromes			
MYO V	Melanocytes and neurons	Rab27a/MyoV/Melanophilin	"Dilute"
RAB27A	Immunocytes and melanocytes	Rab27a/MyoV/Melanophilin	"Ashen"
MLPH	Melanocytes	Rab27a/MyoV/Melanophilin	"Leaden"

The defective genes in human diseases impairing secretory lysosomes are shown together with the affected cell types, involved complex and their mouse models (from [97]).

For the genetically heterogeneous HPS, 8 and at least 15 responsible genes were identified in humans [92; 98] and mice [90], respectively, causing among others hypopigmentation, prolonged bleeding, and lung disease. Most murine HPS proteins belong to the three Biogenesis of Lysosome- related Organelles Complexes (BLOCs) [90; 99]. Mutations in HPS2 (AP3B1, pearl) and AP3D1 (mocha) affect subunits of the Adapter Protein-3 (AP-3) complex [100]. A recent study using mutant mice doubly or triply deficient in protein subunits of various BLOC complexes and/or AP-3 complex demonstrated extensive, tissue and cell type specific interactions among BLOC and AP-3 complexes in LRO synthesis [101].

At least part of cholesterol transport is mediated by vesicular transport, which requires fusion of membranes mediated by soluble N-ethylmaleimide-sensitive factor attachment protein receptors (SNAREs) [102]. The SNARE protein Syntaxin 13, besides ABCA1 [64], also binds to syntaxin 13 binding protein (pallidin) [103], which is a component of BLOC-1 [101], thereby linking ABCA1 to LRO and the AP-3 pathway. Furthermore, the Ras-related small regulatory GTPases ADP-ribosylation factors control vesicle budding in vesicular transport processes in the secretory and endosomal pathway [104] and it is assumed that ADP-ribosylation factor-like proteins undertake similar functions [105]. Together with the finding that ARL7 influences lipid efflux, this suggests ARL7 as part of the AP-3 pathway [63]. Figure 10 presents an overview of ABCA1-related AP-3 constituents.

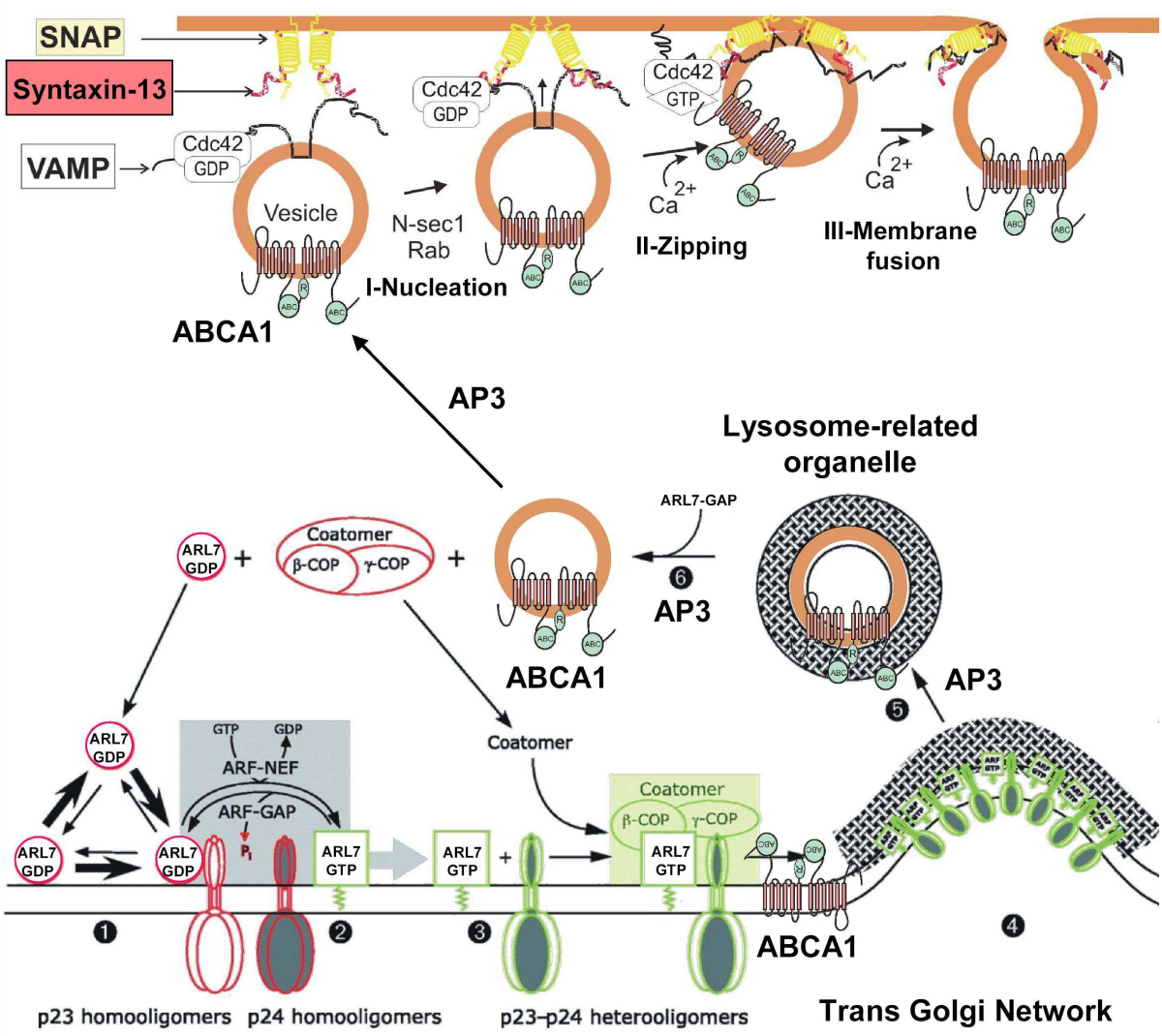

Figure 10. Overview of ABCA1-related AP-3 constituents. For details see text [*].

Interestingly, data from drosophila also link ABCG1, the human homolog of the drosophila white gene product, to the AP-3 pathway, as the garnet (homolog of AP3D1/mocha)/AP-3 transport system seems to be necessary for correct intracellular localization of the white gene product [106].

3. Cholesterol Uptake, Biosynthesis and Transport to Cellular Sites of Steroidogenesis

Cholesterol is vital as it serves as essential component of cell membranes and as precursor of steroid hormones and vitamin D that is either derived from nutrition or synthesized in the body. The liver removes excess cholesterol, either by conversion to bile acids, or secretion together with bile acids into the small intestine. Essential quantities of cholesterol are reabsorbed in the small intestine, leading to enterohepatic cholesterol cycling.

3.1. Uptake and Cellular Processing of Cholesterol

Cholesterol is found in the intestinal lumen in its free, unesterified form. After absorption, it is incorporated together with triglycerides (TG), phospholipids, and apolipoproteins into large TG-rich lipoprotein particles called chylomicrons, which are transported from the intestine to the liver. There, cholesterol is esterified with CoA-activated fatty acids (mainly oleoyl-CoA) by the enzyme Acyl coenzymeA:cholesterol acyltransferase; the same reaction is catalyzed by lecithin-cholesterol acyltransferase in the plasma with phosphatidylcholine as fatty acid donor. Accordingly, cholesterol is either transported for storage to peripheral tissues or transferred via reverse cholesterol transport to the liver for biliary excretion. Albeit most tissues are able to synthesize cholesterol the main sites of synthesis include the liver, the gut, steroidogenic tissues and the central nervous system.

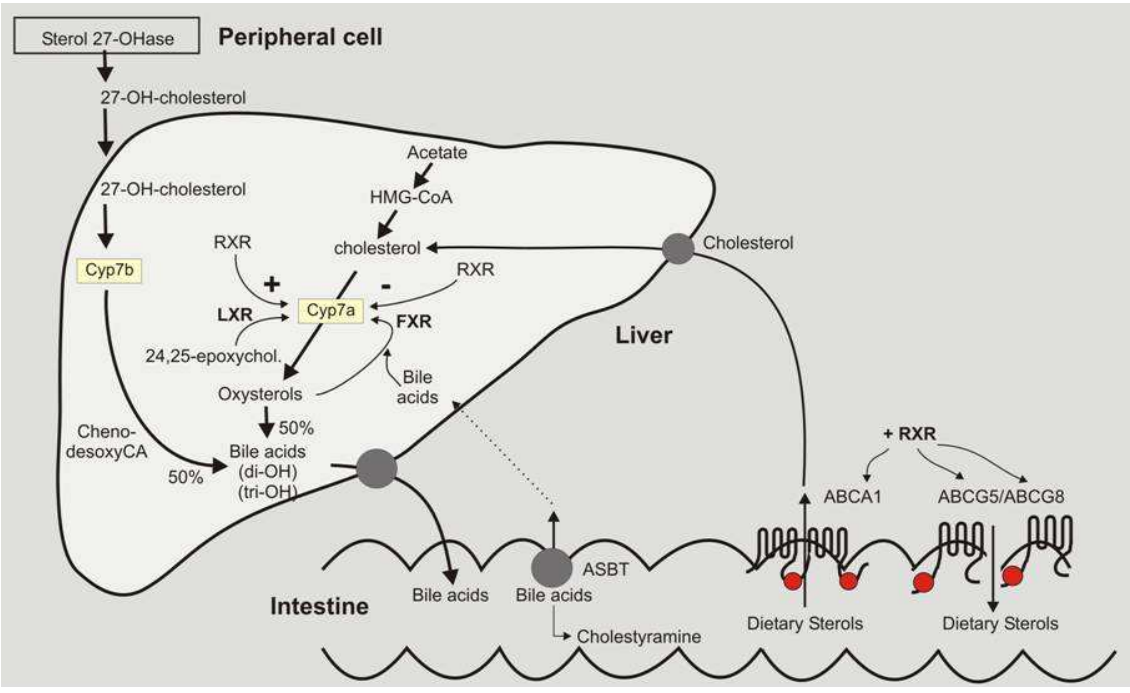

Figure 11. ABC transporters and dietary cholesterol metabolism. For details see text [*].

A key step in this process is catalyzed by 3-hydroxy-3-methylglutaryl coenzyme A-reductase (HMGCR), which can be inhibited by various substances, e.g. statins, which are of pharmacological interest in lowering cholesterol levels in the blood. ABC transporters are key molecules in these processes. ABCG5/ABCG8 are crucial for hepatobiliary and intestinal cholesterol excretion, while ABCA1 is essential for HDL formation and, hence, for inter-organ trafficking of the highly water-insoluble cholesterol molecules [107] (Fig. 11).

3.2. The NPC/Late Endosome Pathway

After delivery to its destination, cholesterol is taken up by different receptor-mediated pathways and processed along the phagosomal/endosomal route (Fig. 12).

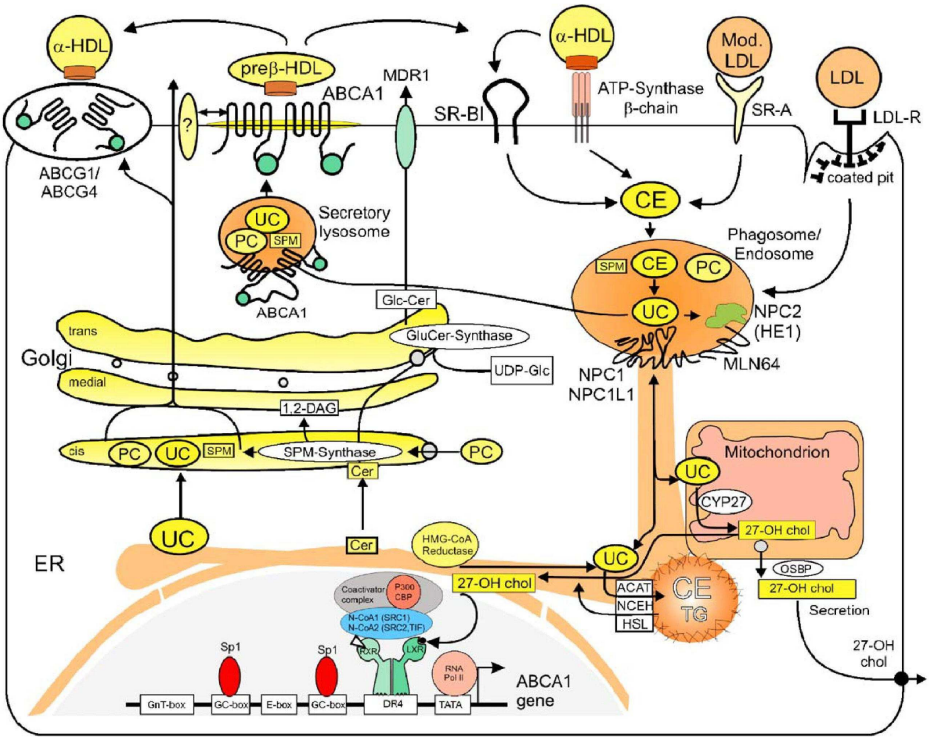

Figure 12. Rheostat model for lipid influx, synthesis, storage and efflux. Cholesterol derived from phagosomal/endosomal uptake can traffic and regulate several mechanisms in the cell: (a) mitochondrial conversion to 27-hydroxycholesterol (27-OH-chol) via CYP27 and direct secretion, (b) action as nuclear receptor ligand, (c) storage as CE in lipid droplets, and (d) export via apoA-I dependent and independent routes, involving ABC transporters (from [31]).

NPC1 and NPC2 are critically involved in post-endosomal cholesterol traffic. Mutations in these genes result in Niemann-Pick type C disease (NPC), an autosomal recessive neurovascular lipid storage disorder [108; 109]. On the cellular level this leads to accumulation of LDL-derived free cholesterol in late endosomes, lysosomes and the Golgi [110; 111]. The intact feedback regulation of cholesterol homeostasis observed by oxysterols and de novo synthesized cholesterol in NPC-deficient cells indicates that the transport of LDL-cholesterol to regulatory sites is impaired [112].

3.3. SREBP and Sterol Sensing at the ER Level

Cholesterol also modulates cell-signaling protein complexes and influences development. Seven subgroups of proteins, namely HMGCR, SREBP-cleavage-activating protein (SCAP), 7-dehydrocholesterol reductase, Dispatched/CHE-14, Patched (Ptc), NPC1 and Ptc-related, exert important functions in cholesterol homeostasis or cholesterol-mediated signaling and are evolutionary conserved (Fig. 13 A). All of them have the phylogenetically conserved sterol-sensing domain consisting of approximately 180 amino acids that are organized into five consecutive membrane-spanning domains (Fig. 13 B) in common [113]. Originally, this domain was identified in HMGCR and SCAP. Both play key roles in cholesterol homeostasis [114; 115], measuring cellular cholesterol content. Under low sterol conditions, SCAP translocates SREBP from the ER to the Golgi, where it is processed by Site-1 protease (S1P) and Site-2 protease (S2P) (Fig. 13 C). This releases the N-terminal basic helix-loop-helix leucine zipper (bHLH-Zip) domain, which enters the nucleus and activates transcription of target genes regulating lipid synthesis and uptake. Under higher sterol conditions, the SCAP/SREBP complex is retained in the ER and Golgi-mediated liberation of the bHLH-Zip domain is prevented [116].

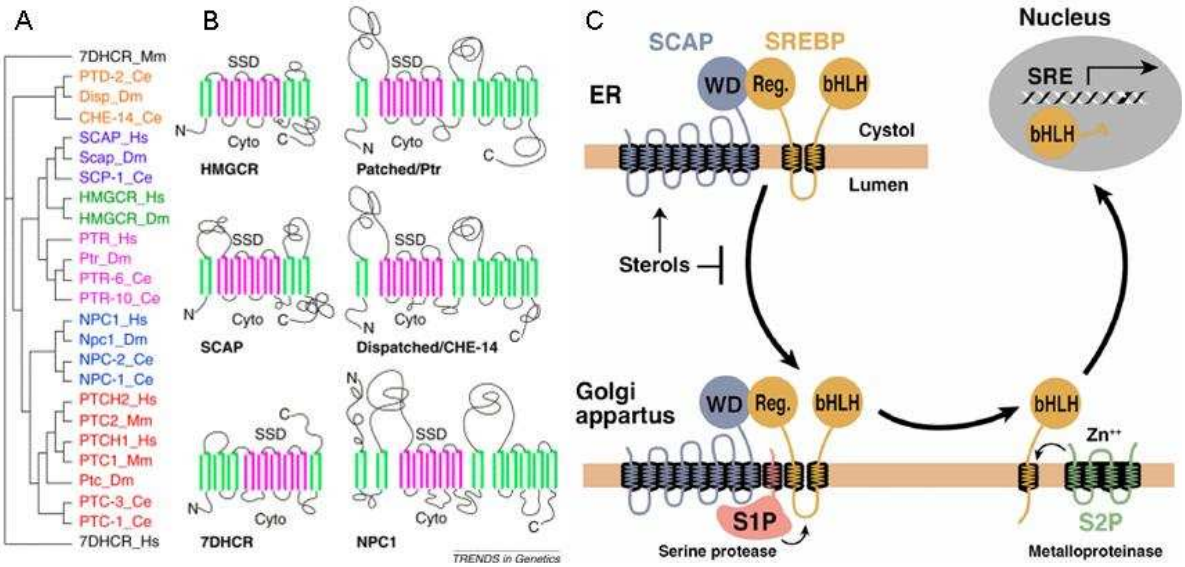

Figure 13. Sterol-sensing domain (SSD)-containing proteins and model for the sterol-mediated cleavage of membrane-bound SREBP. (A) Evolutional conservation of SSD. **(B)** Predicted topology of all known protein classes carrying SSDs. **(C)** Model of the sterol-mediated cleavage of membrane-bound SREBP. Details are found in the text. PTD, Ptc-related Disp-like; Ce, Caenorhabditis elegans; Hs, Homo sapiens; Dm, Drosophila melanogaster; Mm, Mus musculus; 7DHCR, 7-dehydrocholesterol reductase; Disp, Dispatched; PTR, Ptc-related (from [113] and [116]).

3.4. Cholesterol Biosynthesis and Relation to Uptake and ER Cholesterol Content

As mentioned above, under conditions of low cellular cholesterol levels the N-terminal bHLH-Zip domain of SREBP is released and, after entering the nucleus, activates transcription of various target genes. Figure 14 presents a schematic overview of SREBP target genes and the main metabolic intermediates in the pathways for synthesis of cholesterol, fatty acids, and TG. SREBP-2 mainly enhances transcription of genes influencing cholesterol metabolism, among others the LDLR, while SREBP-1c predominantly upregulates genes for fatty acid and TG metabolism [117].

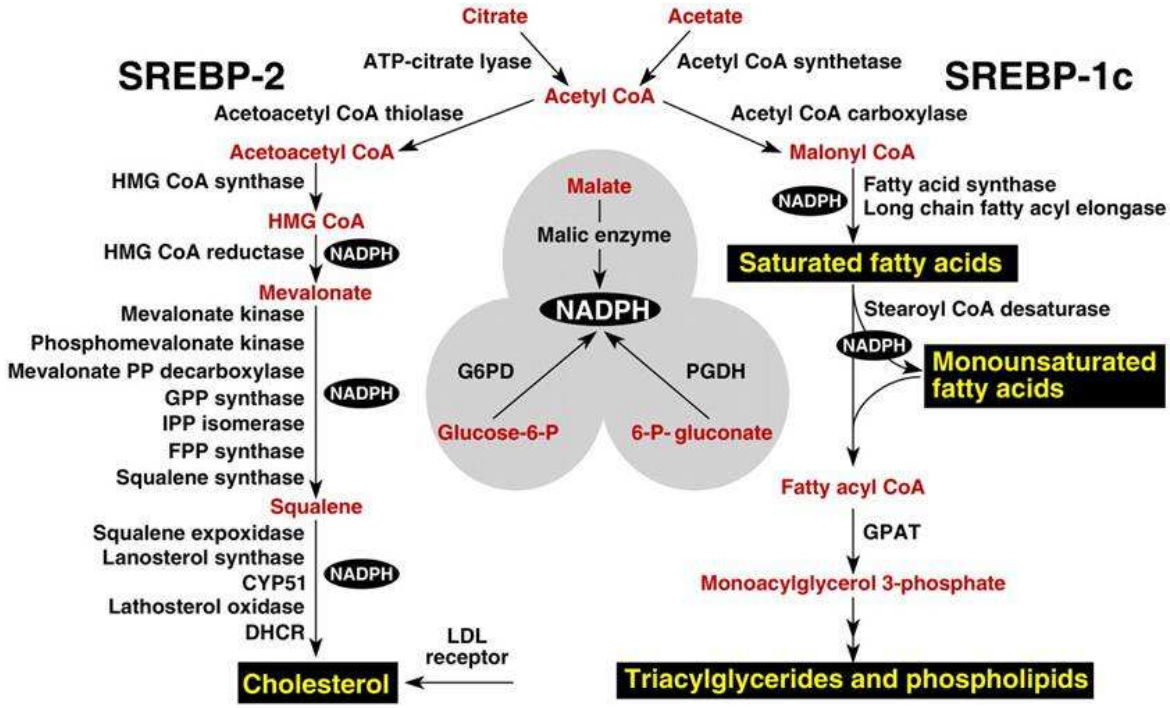

Figure 14. Overview of SREBP target genes and their metabolic function. DHCR, 7-dehydrocholesterol reductase; FPP, farnesyl diphosphate; GPP, geranylgeranyl pyrophosphate synthase; CYP51, lanosterol 14α-demethylase; G6PD, glucose-6-phosphate dehydrogenase; PGDH, 6-phosphogluconate dehydrogenase; GPAT, glycerol-3-phosphate acyltransferase (from [117]).

Interestingly SREBP-2 is reported to regulate transcription of ABCA1 and ABCA7 in opposite directions. While ABCA1 is downregulated, expression of ABCA7 in enhanced [73]. In conclusion, SREBP increases cholesterol-uptake and -synthesis, while reducing efflux under conditions when cellular cholesterol levels are low.

3.5. StAR Function and the START Family

The steroidogenic acute regulatory protein (StAR)-related lipid transfer (START) domain is evolutionary conserved in plants and animals. Fifteen human proteins comprise the START domain alone or together with other protein domains (Fig. 15) [118]. Proteins containing this domain are involved in lipid trafficking, lipid metabolism and cell signaling. By multiple sequence alignment, the 15 human members were divided in 6 subgroups (Fig. 15) [119]. StAR, playing a key role in steroidogenesis by transferring cholesterol into mitochondria, and metastatic lymph node (MLN)64, related to the NPC-proteins, belong to the STARD1/StAR group and their START domains were shown to bind cholesterol (Fig. 15) [120].

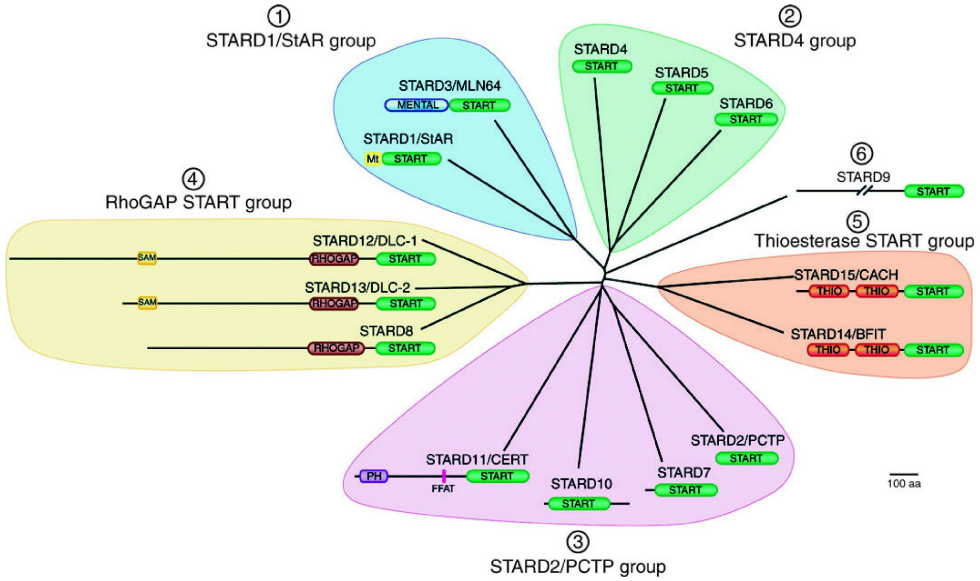

Name	Other names[a]	Lipid specificity[b]	Subcellular localization[c]	Expression pattern[d]	Mainly expressed[e]	Implicated in[f]	Gene chromosomal localization[g]
STARD1	StAR	Cholesterol[1]	Mitochondria[1]	Specific	Adrenal, Gonads, Brain[1]	Genetic disorder[1]	8p11.2
STARD2	PCTP	Phosphatidylcholine[2]	Cytosol[2]	Wide			17q21-q24
STARD3	MLN64, CAB1	Cholesterol[1]	Late-endosomes[3]	Wide		↑ Cancer[2]	17q11-q12
STARD4	None		Cytosol and Nucleus[4]	Wide			5q22.1
STARD5	None	Cholesterol, 25-hydroxycholesterol[3]	Cytosol and Nucleus[5]	Wide		↑ Cancer[3]*	15q26
STARD6	None		Nucleus?[6]	Specific	Testis[2]		18q21.2
STARD7	GTT1		?	Wide		↑ Cancer[4]	2q11.2
STARD8	RhoGAP		?	Wide	Placenta, PNS	↓ Cancer[5]*	Xq13.1
STARD9	None		?	Wide		↓ Cancer[6]*	15q15.1-q15.2
STARD10	PTCP-like, SDCCAG28, CGI-52	Phosphatidylcholine/ethanolamine[4]	Cytosol and Nucleus[7]	Wide		↑ Cancer[7]	11q13
STARD11	CERT, GPBP, COL4A3BP	Ceramides[5]	Cytosol and Golgi[8]	Wide		Autoimmune disease[8]	5q13.3
STARD12	DLC-1,Arhgap7, p122-RhoGAP		Plasma membrane[9]	Wide		↓ Cancer[9]	8p22
STARD13	DLC-2, SDCCAG13		Cytosol?[10]	Wide		↓ Cancer[10]	13q12-q13
STARD14	BFIT, THEA		?	Wide		Obesity[11]	1p32.3
STARD15	CACH		Cytosol[11]	Specific	Liver, Lung	↓ Cancer[12]*	5q14.1

Figure 15. Human START-domain proteins. Upper part: Phylogenetic tree and domain organizations of the 15 START-domain proteins. Lower part: Characteristics of the START-domain proteins. BFIT, brown fat-inducible thioesterase; CAB1, coamplified with erbB2 1; CACH, cytoplasmic acetyl-CoA hydrolase; COL4A3BP, collagen type IV alpha 3 binding protein; DLC-1, deleted in liver cancer 1; FFAT, two phenylalanines in an acidic tract motif responsible for ER targeting; GPBP, Goodpasture-antigen-binding protein; GTT1, gestational trophoblastic tumor 1; MENTAL, MLN64 N-terminal domain; MLN64, metastatic lymph node 64; Mt, mitochondrial targeting motif; PCTP, phosphatidylcholine transfer protein; PH, pleckstrin homology domain; RHOGAP, Rho-GTPase-activating-protein domain; SAM, sterile alpha motif; SDCCAG, serologically defined colon cancer antigen; StAR, steroidogenic acute regulatory protein; THEA, thioesterase-adipose-associated protein; THIO, acyl-CoA thioesterase domain (adapted from [119]).

While the START domain in some proteins eventually just works as a lipid sensor, a common function seems to be the transfer of lipids between membranes. Although the mechanism of lipid transport is not completely clear, data indicate that StAR acts at the surface of the outer mitochondrial membrane [119]. The proposed model for START-mediated translocation of lipids is shown in Figure 16. When interacting with the membrane the α4 helix makes the lipid-binding pocket accessible. After loading, the pocket closes and the lipid can be transferred to its destination membrane. The mechanism underlying targeting to membranes are not clear, but in case of StAR and MLN64, both containing membrane-targeting motifs, it is speculated that they are directed to specific contact sites by other motifs and/or binding to membrane-resident proteins [119].

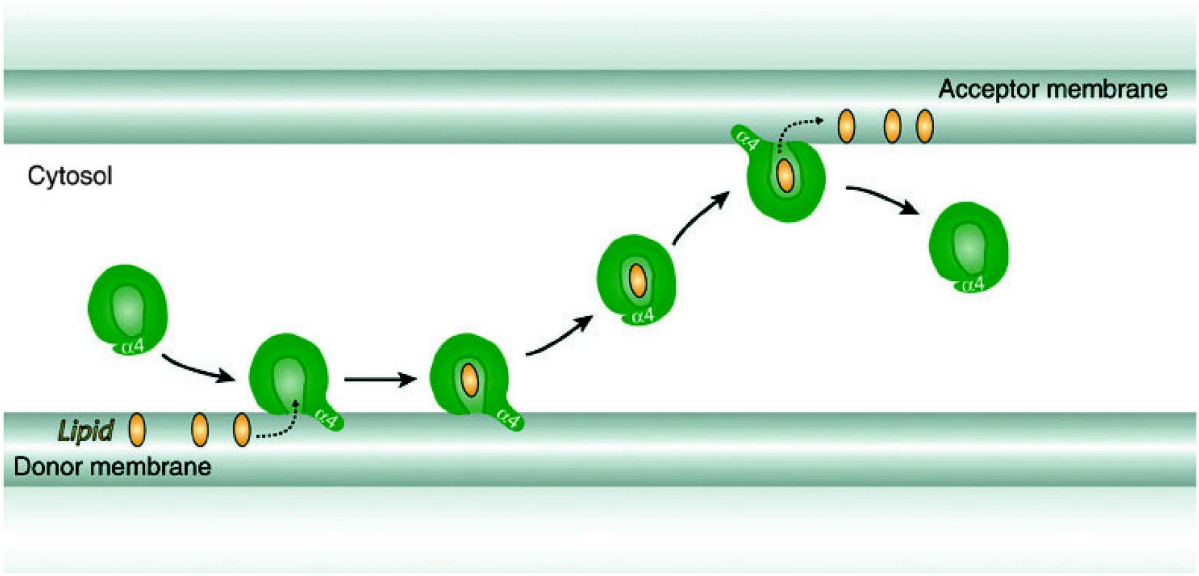

Figure 16. Model of the START-mechanism for lipid promotion. In its free form, the START domain binds to the membrane by its C-terminal α4 helix, leading to a conformational change making the lipid-binding pocket accessible. Loading with the lipid (yellow) closes the lid. Targeting of the loaded START protein to an acceptor membrane is necessary for delivery of bound lipids (from [119]).

3.6. The Adrenal Gland as Steroid Hormone Producing Organ

The adrenal gland plays a major role in the regulation of stress response by the synthesis of corticosteroids and catecholamines, including cortisol and adrenaline.

An adrenogonadal precursor lineage in the intermediate mesoderm is the common origin of the adrenal cortex and steroid-secreting cells of the gonads [121]. The adrenal gland is divided into two functional regions, the outer cortex, derived from mesoderm, and the inner medulla, derived from the neural crest. While synthesis of steroid hormones occurs in the cortex, the catecholamine hormones norepinephrine and epinephrine are produced in the medulla.

The adrenal cortex consists of three zones, namely zona glomerulosa, zona fasciculata, and zona reticularis, all of which are involved in steroidogenesis (Fig. 17).

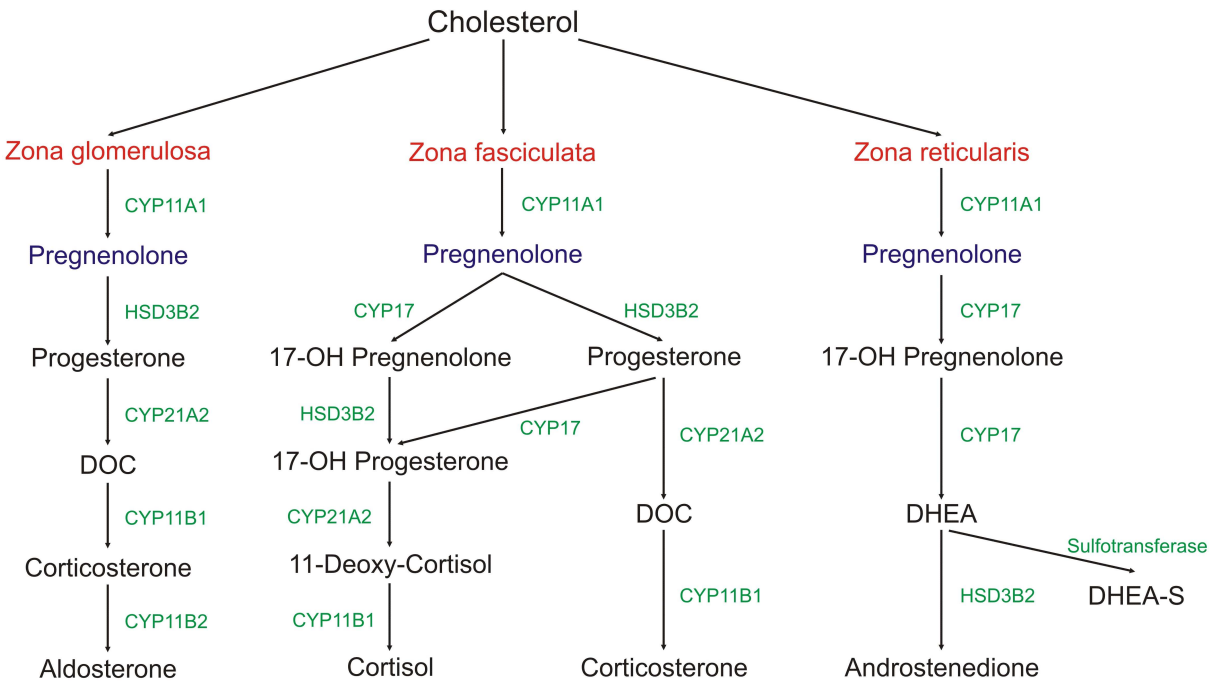

Figure 17. Steroid hormone synthesis in the cortex of the adrenal gland. Mitochondria include the enzymatic activities of CYP11A1, CYP11B1, and CYP11B2. The ER includes the rest of the enzymatic activities. The major inducers of mineralcorticoid secretion are angiotensin II and the serum concentration of potassium. Adrenocorticotropic hormone (ACTH) mainly increases the production of cortisol and corticosterone; transiently it also increases aldosterone secretion. For details see text. DOC = deoxycorticosterone; DHEA = dehydroepiandrosterone.

The synthesis of all steroid hormones starts with the conversion of cholesterol to pregnenolone, the rate-limiting and hormonally regulated step in this process carried out by the StAR/CYP11A1 system.

In the conversion process of cholesterol to pregnenolone the cholesterol side chain is cleaved by mitochondrial CYP11A1, encoded by a single gene [122; 123] on chromosome 15q23-q24 [124], mediating three distinct sequential reactions: cholesterol sequentially undergoes 20-hydroxylation, 22-hydroxylation, and scission of the 20,22 C-C bond to yield prenenolone and isocaproaldehyde (for review see [125]). As CYP11A1 only works in mitochondria [126] the transport of cholesterol to the inner mitochondrial membrane by StAR is a crucial and quantity regulating step in steroidogenesis.

Different groups demonstrated that ACTH rapidly enhances adrenal steroidogenesis and that this process is hampered by inhibitors of protein synthesis [127-130], suggesting involvement of a short-lived protein. Further experiments led to the identification of StAR. Overexpression in MA-10 and in COS-1 cotransfected with CYP11A1 increased steroidogenesis [131-133] and mutations in StAR were found in congenital lipoid adrenal hyperplasia [132].

The pathways in the adrenal cortex have many components in common, like the StAR, cholesterol side-chain cleavage enzyme CYP11A1, the type 2 isozyme of 3β-hydroxysteroid dehydrogenase (HSD3B2), and CYP21A2, but differ in certain key enzymes catalyzing terminal reactions in the steroid biosynthesis (Fig. 17).

CYP11B2 is restricted to outer zona glomerulosa, converting corticosterone to aldosterone. In the inner zones, CYP17 and the closely related isozyme CYP11B1 are expressed. Both participate in the production of cortisol, the predominant glucocorticoid in humans. When besides the 17α-hydroxylase activity of CYP17, necessary for the production of C-21 17-hydroxysteroids such as cortisol, also the 17,20 lyase activities is present, C-19 precursors of sex steroids are produced. Therefore, the activities of CYP17 direct pregnenolone towards its final metabolic pathway.

3.6.1. Adrenal Development

Two discrete proliferative/migratory events are necessary to give rise to the adrenocortical cells in human embryos (Fig. 18; reviewed in [134]).

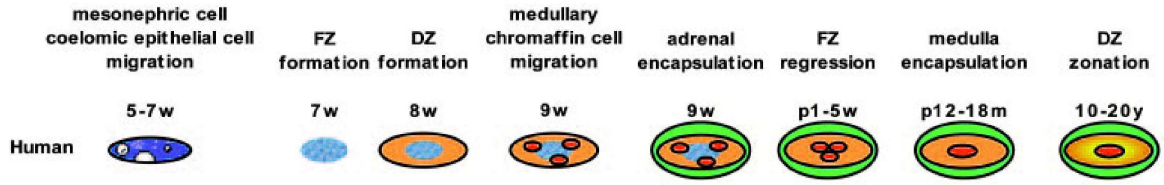

Figure 18. Time line of adrenal development in humans. The major events in adrenal development in humans are shown. w, week; p, postnatal; FZ, fetal zone; DZ, definitive zone (from [135]).

Because of the low HSD3B2 activity, the fetal adrenal produces large amounts of pregnenolone-, 17-hydroxy-pregnenolone-, and DHEA-sulfates, which cross into the placenta. The placenta is rich in sulfatases and HSD3B2 and converts the products to progesterone and 17α-hydroxyprogesterone, which are returned to the fetus, enabling the formation of aldosterone and cortisol. DHEA is metabolized to 16α-hydroxy-DHEA, the substrate for biosynthesis of estriol [136] (Fig. 19).

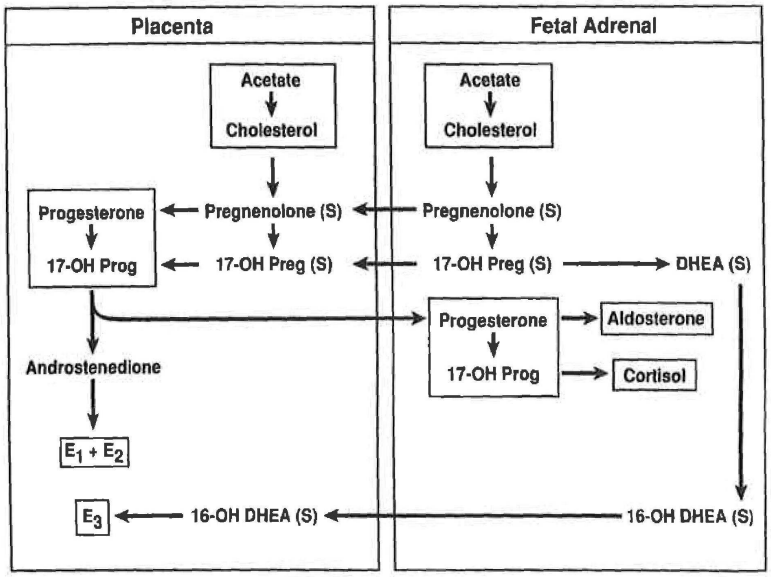

Figure 19. Steroid biosynthesis in the placental-fetal unit (from [136]). For details see text.

Postnatal notable transformation of the adrenal gland takes place: a rudimentary medulla is formed, the fetal zone forms back by the third month and the definitive zone of the human adrenal cortex forms discrete functional compartments (zona glomerulosa, zona fasciculata, zona reticularis) [134]. In the third trimester the zona glomerulosa gains steroidogenic capacity and synthesizes aldosterone under control of the renin- angiotensin system. Under the regulation of ACTH by 15 weeks of gestation, the zona fasciculata secretes glucocorticoids, whereas the zona reticularis in humans secretes dehydroepiandrosterone and its sulfates [135]. Along with regression of the fetal zone, levels of these adrenal androgens decrease, and increase again during childhood, along with adrenarche.
Several findings indicate interactions between different transcription factors in adrenal development, namely the nuclear receptors steroidogenic factor 1 (Sf1) and DSS-AHC-critical region on the X chromosome gene 1 (Dax1), and wingless-type MMTV integration site family, member 4 (Wnt4) and Dax1. Sf1 was shown to activate the expression of Dax1 [137-139], in contrast Dax1 inhibits Sf1 [140-142], suggesting a feedback loop maintaining expression level of target genes in the adrenal cortex. Impaired Dax1 expression in the absence of Wnt4 may contribute to the abnormal sexual differentiation observed [143; 144]. Wilms tumor 1 gene (Wt1) is only present in earliest adrenogonadal precursors [145]. Data from cell culture models imply that Sf1 and Wt1 directly interact to activate the expression of anti-Müllerian hormone [146]. It was suggested that Wt1, like Sf1, activates Dax1 expression [147]. Taken together these findings suggest that Sf1 and Wt1 interact at earliest stages of adrenogonadal development to permit the survival of cells that ultimately form the adrenal cortex.

3.7. The Gonads as Steroid Hormone Producing Organs

Besides the adrenal gland, the gonads play an important role in steroid hormone synthesis. The adrenal cortex and steroid-secreting cells of the gonads arise from a common adrenogonadal precursor lineage in the intermediate mesoderm [121].

3.7.1. Gonadal Development

Testis and ovary arise from the undifferentiated embryonic gonad. Both testis and ovary comprise three main cell types, Sertoli cells, Leydig cells, and germ cells in testis, and granulosa cells, theca cells, and oocytes in ovary. An overview of genetic pathways implied in gonadal development is shown in Figure 20.

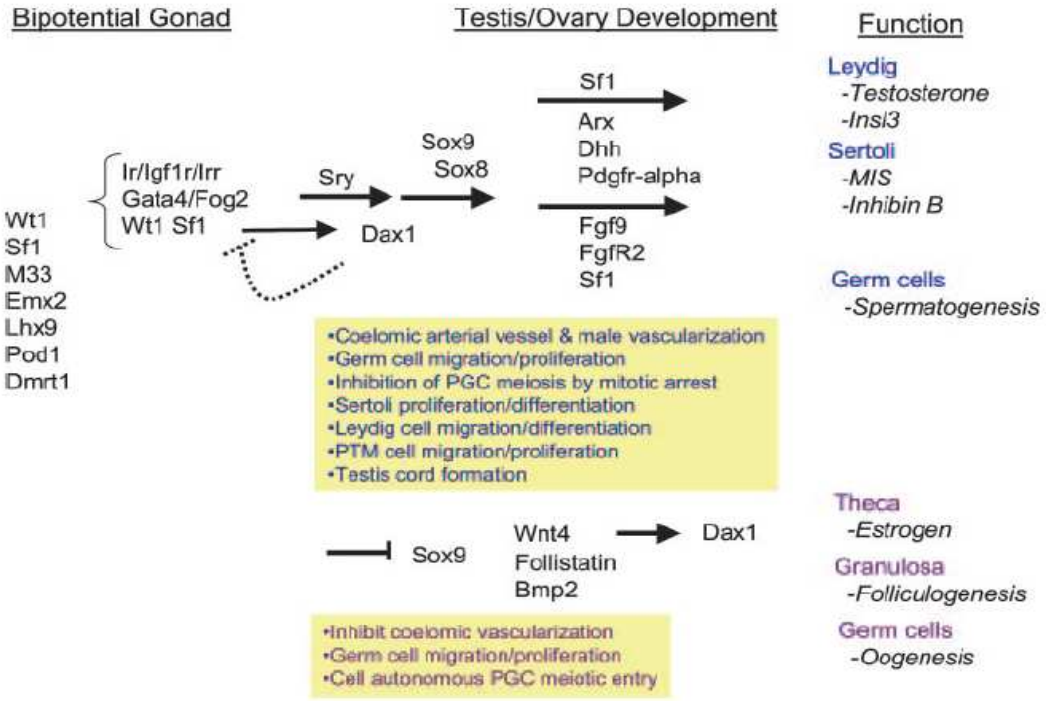

Figure 20. Genetic pathways involved in gonadal development. The bipotential gonad expresses genes such as Wt1, Sf1, Emx2, M33, Lhx9, Pod1, and Dmrt1. Subsequently, expression of the insulin receptor family Ir, Irr, and Igf1r; GATA4/Fog2; Wt1; and Sf1 are thought to promote the expression of Sry in the male. Sox9 and Sox8 are downstream of Sry. Sf1 regulates AMH activation in Sertoli cells and steroidogenesis in Leydig cells. In the male, Dax1 may repress Sf1 in a dose-dependent manner, modulating the transactivation of AMH and genes necessary for steroid hormone biosynthesis. Dax1 also supports the normal formation of testis cords. Additional factors such as Arx, Dhh, Pdgfr, Fgf9, and FgfR2 are involved in Leydig and Sertoli cell differentiation. A description of the cellular events downstream of Sry and thus specific to male development is outlined in the center box. PGC, Primordial germ cell; PTM, peritubular myoid cell. Female differentiation requires the activity of Wnt4a and repression of Sox9. Other key factors include Fst, Bmp2, and Dax1 (from [148]).

In males and females, the adrenal gland and kidney ascend toward the abdominal region. The final position of the gonad depends on its differentiation into either an ovary or testis, and on the gestation of the sex-specific Müllerian or Wolffian ducts. Due to testosterone in males, the proximal Wolffian duct is virilized to form the epididymis, vas deferens, and seminal vesicle. Anti-Müllerian hormone (AMH) imparts back formation of the distal Müllerian duct [149]. Insulin-like 3 (Insl-3) finally is responsible for testicular descent [149; 150]. In the absence of testosterone and AMH in females the Wolffian duct regresses and the Müllerian duct develops into oviduct, uterus, and upper vagina. After sex determination, steroid hormones are crucial for the succeeding phenotypic differentiation.

Little is known about the function and target genes of the testis-determining gene Sry. On the other hand, various cellular and morphological events downstream of Sry are well-characterized (Fig. 20 and Fig. 21). Following Sry expression proliferation of coelomic epithelial cells in XY gonads is notably elevated [151]. Between 11.2 and 12.5 days post coitum (dpc) the testis cord is formed by differentiating Sertoli cells that surround germ cells.

In parallel, vascular endothelial cells migrate from the mesonephros into the XY gonad giving rise to a testis-specific vasculature [152]. The steroidogenic Leydig cells differentiate between 12.5 and 13.5 dpc in the interstitial space between cords.

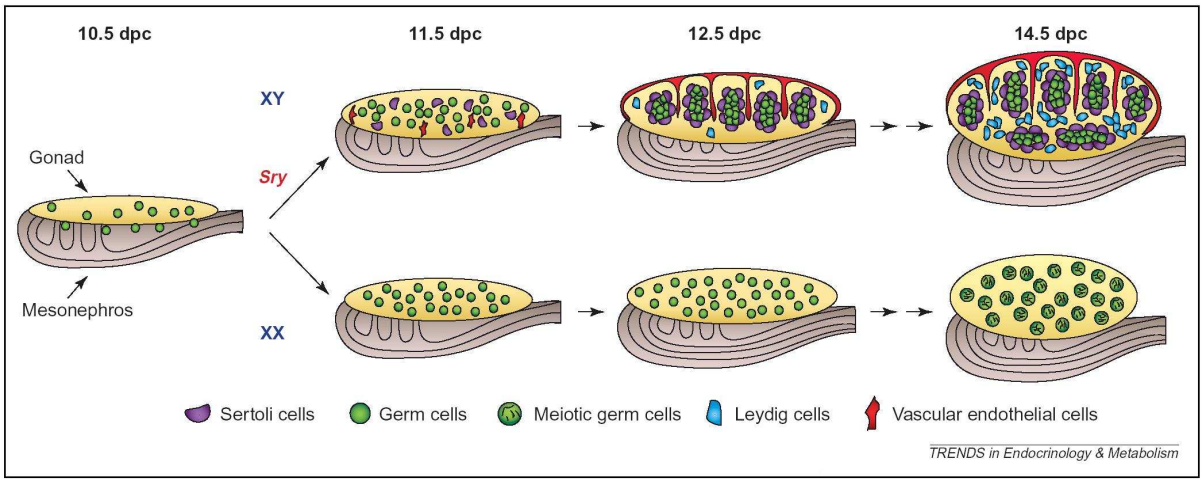

Figure 21. Early murine gonad differentiation. A thickening of the coelomic epithelium of the mesonephros (gray) gives raise to the bipotential gonad (yellow). Between 9.5 and 11.5 dpc, primordial germ cells (green) migrating from the hindgut into the urogenital ridges populate the gonads. Between 10.5 and 12.0 dpc, testis differentiation is triggered by specific expression of the Y-linked gene Sry in the XY gonads. Development starts with the differentiation of Sertoli cells (purple) and the formation of a male-specific vasculature (red). At about 12.5 dpc the differentiation of steroidogenic Leydig cells (blue) in the testis interstitium starts. In the XX gonads no marked morphological changes are observed until 13.5 to 14.5 dpc, when germ cells enter the prophase of meiosis (from [153]).

In contrast, less visible morphological changes take place in XX gonads in this time (Fig. 21). Evident aspects of ovarian development start with the entry of the germ cells into the prophase of meiosis happening in anterior-to posterior wave between 13.5 and 14.5 dpc [154]. The differentiation of granulosa cells and the formation of primordial follicles take place close to birth.

By 13.5 dpc, germ cells in male and female gonads have taken different developmental paths. In males, germ cells halt in mitosis as prospermatogonia, in contrast to females where they enter prophase of the first meiotic division (Fig. 21). The somatic environment is vital for germ cell fate, not their chromosomal sex [155]. Therefore, until now unidentified signals of somatic cells seem crucial for differentiation of embryonic germ cells.

On the other hand, signals from germ cells influence somatic cells in their environment. Germ cells in XY but not XX gonads express Prostaglandin D synthase between 11.5 and 12.5 dpc and prostaglandin D2 leads to partial masculinization of XX gonads. This indicates that signals from germ cells might be involved in testis differentiation [155]. Recent data demonstrate that meiotic germ cells can block testis cord formation when aggregated with XY somatic cells, indicating that XX germ cells determinate to the ovarian pathway countering male development [156].

3.7.2. The Role of Leydig Cells in Steroidogenesis

Sertoli cells and germ cells are found in the seminiferous tubules where spermatogenesis occurs. The interstitial compartment is populated by Leydig cells producing testosterone.
Migration of mesonephric cells into the XY gonad is an early and well-characterized step in testis differentiation [157-159]. This step is induced by XY but not XX gonads, and necessary for normal testis development as prevention of migration inhibits testis cord formation [157; 160]. The majority of migrating mesonephric cells are vascular endothelial cells decisive for building testis-specific vasculature (Fig. 21) [152; 159].
In testicular development, Sf1 is restricted to Leydig cells after 13.5 dpc. Sf1 target genes include enzymes necessary for testosterone biosynthesis including StAR, Cyp11A1, Cyp17, and HSD3B2. Factor implied in Leydig cell determination and lineage development are not well-characterized. In addition, their origin remains ambiguous. Paracrine signal seem to be essential for Leydig cell fate. The Sertoli-secreted factor Desert hedgehog (Dhh), which is supposed to have an important role in Leydig cell differentiation, binds to the receptor Ptc1 expressed on Leydig cells and induces CYP11A1 expression [161]. Other factors influencing Leydig cell development are PDGF receptor α (PDGFRA) and Aristaless-related homeobox (Arx). Genetic analysis placed PDGFRA, inducing mesonephric migration and required for full CYP11A1 expression in gonads, upstream of Dhh [162]. Arx on the other hand is predominantly expressed in peritubular myoid cells, endothelial cells, and in the epithelium of the tunica albuginea [163].
In embryonic and adult testis, Leydig cells localize to the interstitial compartment and are responsible for the production of androgen (testosterone), which is crucial for the development of the male phenotype and spermatogenesis. Anyway, embryonic and adult Leydig cells are separate populations. Embryonic Leydig cells appear between 12.5 and 13.5 dpc and produce testosterone needed to masculinize the internal and external genitalia. After birth, they are lost step-by-step. Adult Leydig cells develop during puberty and are held through adult life [164; 165].
Some data are available on molecular signals that regulate the proliferation, differentiation and function of adult Leydig cells [166], but data on origin and differentiation of embryonic Leydig population are scarce besides their vital role in male reproductive development. Dhh has been shown to be necessary for the differentiation and expansion of fetal Leydig cells. Depending on the genetically background different defects in mice deficient for Dhh are visible: on a 129/Sv background they have disturbed spermatogenesis [161], on a mixed genetic background (129/Sv, C57BL/6 and Swiss Webster) they have defects in development of peritubular myoid cells and Leydig cells in the adult testis [167; 168]. Analysis of Dhh mutants on mixed background reveal involvement of Dhh in development of

fetal Leydig cells. Sertoli cells start secreting Dhh at 11.5 dpc and its receptor Ptc1 follows at 12 dpc in the interstitial space between testis cords [161]. Gonads mutated in Dhh contain no Leydig cells at 13.5 dpc. Later some Leydig cells appear, but their number is eminently decreased compared to controls [161]. This finding explains why mutants on this background have feminized external genitalia. Data from humans with mutations in Dhh in 46,XY individuals leading to partial or complete pure gonadal dysgenesis further support the essential role of Dhh in testis development [169; 170].

Furthermore, PDGF signaling plays a key role in fetal Leydig cell differentiation. Vascular development, testis cord formation, and early Leydig cell differentiation are disturbed in XY embryos with mutations in the PDGFRA [162]. CYP11A1 is not detectable in these embryos at 12.5 dpc, proofing an impact on Leydig cell differentiation. This might just be a downstream effect but the role of PGDFα is stressed by the finding that mutants also have defects in the development of adult Leydig cells [171]. Even though effects of PGDFα mutations on embryonic Leydig cells have not been analyzed, no abnormalities in development of the external genitalia were observed, indicating that embryonic Leydig cells are not influenced. This effect might be due to redundancy among different PDGF ligands.

The very low turnover of Leydig cells in adult testis [172] is maintained by mitosis of the persistent small population of progenitor/immature cells. This is supported by experimental work that showed development of a new Leydig cell population within months [173; 174] and spontaneous recovery of steroidogenesis after elimination of mature adult Leydig cells using ethylene dimethanesulfonate [175]. In addition long-term administration of human chorionic gonadotropin/ luteinizing hormone leads to elevation in Leydig cell numbers [176-179]. The progenitors may be mesenchymal cells whose consecutive differentiation along with proliferation finally results in mature Leydig cells [180] or genuine stem cells, which like hemopoietic stem cells have side population characteristics [181].

In testis the final step in testosterone synthesis, converting androstenedione to testosterone, is mediated by 17β-hydroxysteroid dehydrogenase III [182]. In adults, the conversion takes place in Leydig cells while in fetal mouse this enzyme localizes to the tubules rather than Leydig cells. Hence androstenedione secreted by fetal Leydig cells is modified to testosterone in the tubules [183].

3.8. Genetic Defects Related to Steroid Hormone Metabolism

Cholesterol is the obligate precursor for the biosynthesis of steroid hormones, and many genes involved in disorders of steroidogenesis are known (Table 5).

Table 5. Mutations affecting the hypothalamic-pituitary-adrenal axis in humans (from [184])**.**

Protein	Gene	Locus	OMIM	Protein family	Inheri-tance	Associations
Adrenal hypoplasia						
HESX1	*HESX1*	3p21	601802	Homeodomain TF	AR AR AD	Septo-optic dysplasia, CPHD CPHD Isolated GH insufficiency
LHX3	*LHX3*	9q34	600577	Homeodomain TF	AR	CPHD (ACTH sometimes spared), spinal rigidity
LHX4	*LHX4*	1q25	602146	Homeodomain TF	AD	CPHD (gonadotrophs spared), cerebellar tonsil ectopia
PROP-1	*PROP1*	5q35	601538	Homeodomain TF	AR	CPHD (ACTH usually spared)
POMC	*POMC*	2p23.3	176830	Pro-hormone	AR	Obesity, red hair
T-PIT	*TBX19*	1q23–24	604614	T-box TF	AR	
PC-1	*PCSK1*	5q15–21	162150	Endopeptidase	AR	Obesity, hypogonadotropic hypogonadism, diarrhoea
ACTHR	*MC2R*	18p11	607397	G protein receptor	AR	Tall stature
ALADIN	*AAAS*	12q13	605378	WD-repeat motif	AR	Achalasia, alacrima, neurological abnormalities
DAX-1	*NR0B1 (ACH)*	Xp21	300200	Orphan nuclear receptor	X-linked	[a]Abnormal puberty, impaired spermatogenesis
SF-1	*NR5A1 (FTZF1)*	9p33	184757	Orphan nuclear receptor	AD/AR AD	Undervirilization, uterus (46,XY) ?Pubertal failure (46,XX)
Adrenal destruction						
ALDP	*ABCD1*	Xq28	300100	ATPase binding cassette protein	X-linked	Spastic paraparesis
mtDNA	*mtDNA*	mtDNA	530000	mtDNA	Mito	Lactic acidosis, cataracts, short stature, myopathy, hearing loss
AIRE	*AIRE*	21q22	240300	Zinc finger transcription factor	AR	Hypoparathyroidism, mucocutaneous candidiasis, alopecia, pernicious anaemia, hepatitis (APS1)
CTLA-4	*CTLA4*	2q33	123890	T-lymphocyte immuno-modulator	Polygenic	Graves disease, autoimmune hypothyroidism, type 1 diabetes mellitus (APS2)
Disorders of steroidogenesis						
Sterol Δ-7-reductase	*DHCR7*	11q12–13	270400	Reductase enzyme	AR	Undervirilization, developmental delay, micro-cephaly, short thumbs, syndactyly, cardiac defects, photosensitivity (SLO)
STAR	*STAR*	8p11	201710	Mitochondrial membrane protein	AR	Undervirilization (46,XY), arrested puberty (46,XX), hypotension/salt loss
P450 side-chain cleavage	*CYP11A1*	15q23–24	118485	Cytochrome P450 enzyme	AR	Undervirilization (46,XY), (presumed) impaired puberty (46,XX), hypotension/salt loss
3β-hydroxysteroid dehydrogenase	*HSD3B2*	1p13	201810	Dehydrogenase enzyme	AR	Undervirilization (46,XY), partial virilization (46,XX), hypotension/salt loss
17α-hydroxylase	*CYP17*	10q24–25	202110	Cytochrome P450 enzyme	AR	Undervirilization (46,XY), impaired puberty (46,XX), hypertension
21-hydroxylase	*CYP21A2*	6p21	201910	Cytochrome P450 enzyme	AR	Virilization (46,XX), hypotension/salt loss
P450 oxidoreductase	*POR*	7q11.2	124015	Cytochrome P450 reductase	AR	Antley-Bixler syndrome, disturbed CYP21, CYP17 and CYP19 activity
11β-hydroxylase	*CYP11B1*	8q24	202010	Cytochrome P450 enzyme	AR	Virilization (46,XX), hypertension
18α-hydroxylase	*CYP11B2*	8q21	124080	Cytochrome P450 enzyme	AR	Hypotension/salt loss
Steroid resistance						
Glucocorticoid receptor	*NR3C1*	5q31	138040	Nuclear receptor	AR/AD	Hypertension, hirsutism, baldness, oligomenorrhoea
Mineralocorticoid receptor	*NR3C2*	4q31	177735	Nuclear receptor	AD	Hypotension/salt loss

OMIM = Online mendelian inheritance in man; AR = autosomal recessive; AD = autosomal dominant; CPHD = combined pituitary hormone deficiency; GH = growth hormone; ACTH = adrenocorticotropic hormone; MC2R/ACTHR = melanocortin-2 receptor/adrenocorticotropin receptor; Sf1 = steroidogenic factor-1; ALDP = adrenoleukodystrophy protein; mt = mitochondrial; CTLA-4 = cytotoxic T-lymphocyte-associated 4; AIRE = autoimmune regulator; APS = autoimmune polyendocrinopathy syndrome; SLO = Smith-Lemli-Opitz; StAR = steroidogenic acute regulatory protein.

Mutations affecting synthesis, mitochondrial transport and cleavage of cholesterol interfere with both adrenal and gonadal steroid synthesis. This results in adrenal insufficiency and undervirilization and lack of pubertal development, respectively, in karyotypic (46,XY) males and (46,XX) females [185-191].

3.8.1. Adrenal Disorders

3.8.1.1. Adrenocortical Dysplasia

Adrenocortical dysplasia (acd) is an autosomal recessive disorder caused by mutations in the acd gene localized on chromosome 8 [192]. Its phenotypes are small size, hyperpigmentation, and premature death. In agreement with the assumption that they died from adrenocortical insufficiency, in mice that were assumedly homozygous for the acd mutation, low levels of corticosterone and high ACTH levels were detected. This indicates that acd mutations disturb cellular proliferation in the adrenal cortex along with secondary hypertrophy of cortical cells eventually caused by elevated ACTH levels.

3.8.1.2. Adrenal Steroid Resistance

Familial glucocorticoid resistance, caused by mutations in the glucocorticoid receptor, is accomplished by symptoms of mineralocorticoid and androgen excess (hypertension, hypokalaemia, hirsutism, baldness, oligomenorrhoea) and elevated cortisol and ACTH concentrations [193]. The molecular reasons for this are abnormalities in ligand binding, co-factor interaction, nuclear localization and DNA binding, resulting in changes of the target gene transcription [194]. Mutations in the mineralocorticoid receptor lead to aldosterone resistance in pseudohypoaldosteronism type I [195], characterized by neonatal salt wasting, hyperkalemia and hypotension, with elevated aldosterone and renin activity. In contrast to pseudohypoaldosteronism type II, which is caused by mutations in the epithelial sodium channel, these symptoms tend to remit with age.

3.8.1.3. Adrenal Hypoplasia

Adrenal hypoplasia is characterized by underdevelopment or atrophy of the adrenal glands. Reasons are intrinsic defects in adrenal development and function (primary) or disturbed ACTH secretion and action (secondary) (Fig. 22) [196].

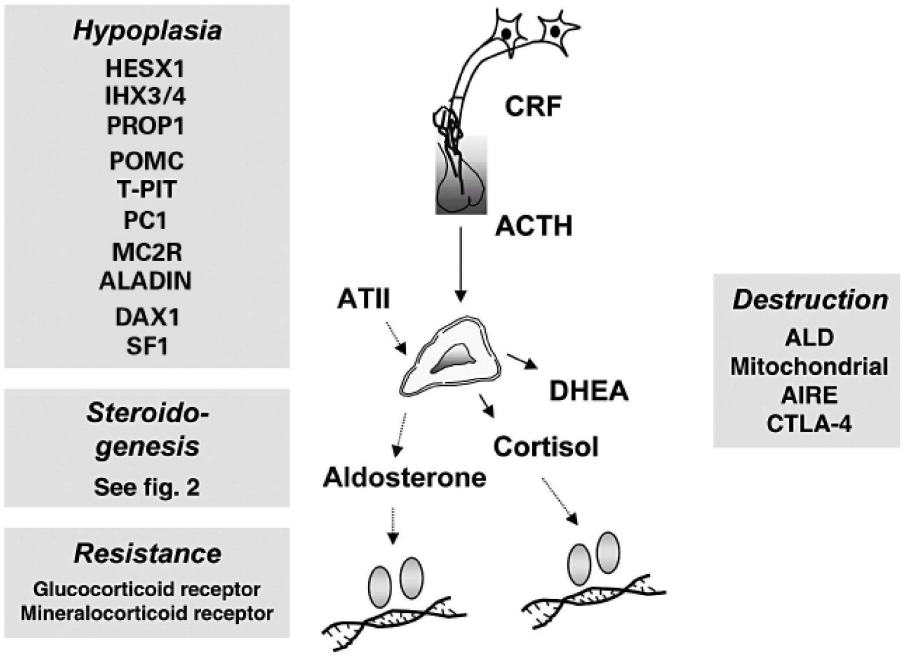

Figure 22. Overview of the hypothalamic-pituitary (corticotroph)-adrenal axis. Loss-of function mutations in the genes listed have been shown to cause single gene disorders in humans. CRF = corticotrophin-releasing factor; ACTH = adrenocorticotropic hormone; ATII = angiotensin II; DHEA = dehydroepiandrosterone; ALD = adrenoleukodystophy; AIRE = autoimmune regulator; CTLA-4 = cytotoxic T-lymphocyte-associated 4 (from [184]).

4. Physiology and Pathophysiology of Aldehyde Oxidase 1

Aldehyde oxidase 1 (AOX1) catalyses the oxidation of aldehydes and nitrogen-containing heterocyclic compounds, as well as the reduction of nitro-aromatic compounds, isoxazole, and isothiazole ring systems [197]. The physiological function of AOX1 remains largely unknown. However data from Tomita *et al*. indicate that AOX1 (EC 1.2.3.1) is identical to retinal oxidase [198], suggesting retinal as physiological substrate of AOX1. AOX1 and retinaldehyde dehydrogenase (EC 1.2.1.36) are capable of catalyzing the oxidation of retinal to retinoic acid (RA), but require different co-factors [199]. AOX1 has been suggested to be involved in ethanol-induced liver injury [200] and the generation of reactive oxygen species (ROS) during ethanol metabolism [201; 202]. A comparable two-step process is involved in the metabolism of both ethanol and retinol (Fig. 23).

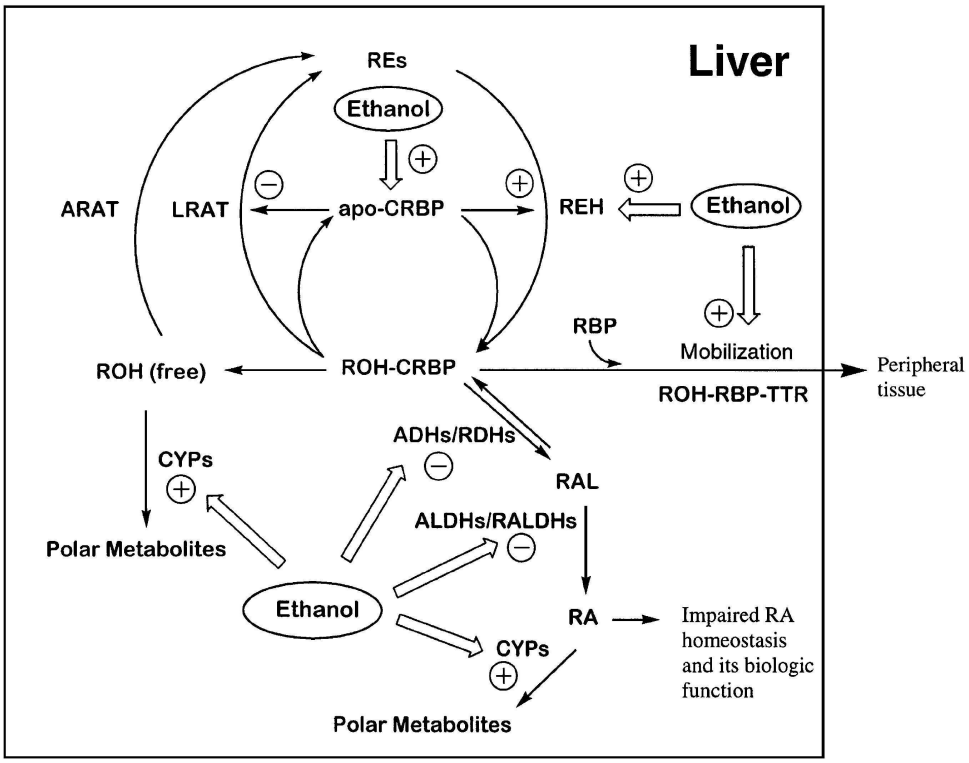

Figure 23. Schematic drawing of possible mechanisms of excessive ethanol effects on retinoid metabolism. ADHs, Alcohol dehydrogenases; ALDHs, aldehyde dehydrogenases; ARAT, acyl-coenzyme A–retinol acyltransferase; CRBP, cellular retinolbindingprotein; CYPs, cytochrome P450 enzymes; LRAT, lecithin:retinol acyltransferase; RA, retinoic acid; RAL, retinal; RALDHs, retinaldehyde dehydrogenases; RBP, plasma retinol-binding protein; RDHs, retinol dehydrogenases; REH, retinyl ester hydrolases; REs, retinyl esters;ROH, retinol; and TTR, transthyretin (from [203]).

Both are first oxidized to the aldehyde form, and the aldehyde is subsequently oxidized to the acid form [203]. Products of the retinal dehydrogenase and AOX1 metabolic pathway, 9-cis RA and all-trans RA (ATRA), modulate retinoic acid receptors (RAR) / retinoid X receptors (RXR) target genes and thereby influence ABCA1-mediated HDL maturation [204].

Data from Yang *et al*. demonstrate that 2,3,7,8-Tetrachlorodibenzo-p-dioxin (TCDD) significantly reduced hepatic all-trans-retinol level and enhanced hepatic ATRA content, and upregulated AOX1 mRNA and enzymatic activities in mice [205]. The transcriptional effect was attenuated by supplementation with vitamin A. The observed induction of AOX1 may be responsible for the changed all-trans-retinol/ATRA levels due to TCDD and addition of vitamin A may weaken the effect of TCDD on AOX1 mRNA [205].

4.1. Structure of Aldehyde Oxidase 1 Protein

The cryptozoic proteins of the mammalian molybdo-flavoenzyme (MFE) group are marked by a similar general structure. They are homodimers composed of approx. 150 kDa subunits [206-209] with a typical and easily recognized tripartite structure: the N-terminal domain of approx. 20 kDa comprising two 2Fe/2S redox centers, a 40 kDa flavin-containing region, and a 85 kDa C-terminal domain insisting the MoCo and the substrate-binding sites (Fig. 24). The final electron acceptor for xanthine oxidase (XO), AOX1, aldehyde oxidase homolog 1 (AOH1), and possibly AOH2 and AOH3 is oxygen, producing superoxide oxygen radicals or hydrogen peroxide, whereas xanthine dehydrogenase (XD) uses NAD+.

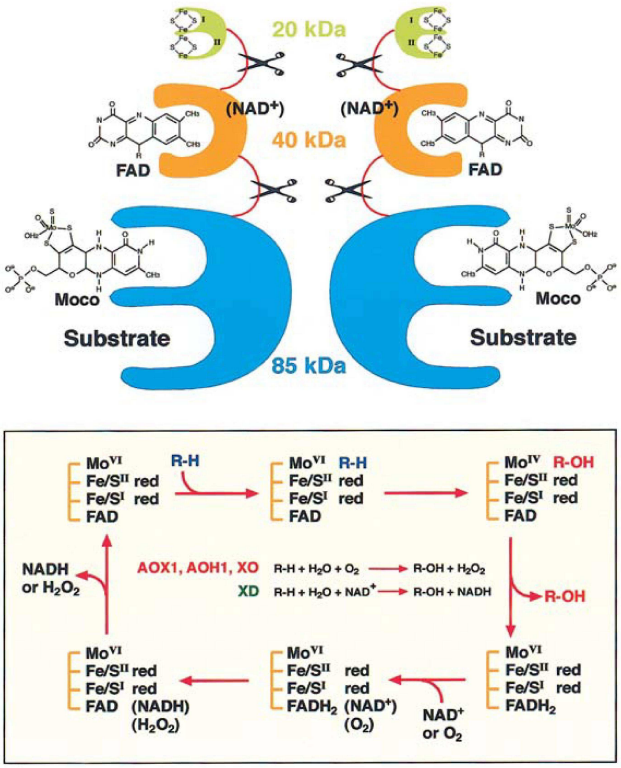

Figure 24 Structure and reaction scheme of MFEs. Upper part: MFEs consist of three domains joined by poorly conserved and unstructured hinge regions: a 20 kDa N-terminal domain (light green), the 40 kDa FAD-binding domain (orange) and a 85 kDa domains (blue). In the XD form of XOR, the FAD-containing domain binds NAD (NAD+). Lower part: The different redox centers of MFEs are displayed from top to bottom according to their implication in charge transfer. Oxidation of the substrate (R-H) takes place at the molybdenum centre. The products is shown as R-OH. Reducing equivalents are passed over flavin, to molecular oxygen (NAD+ in the case of the XD form of XOR). The Fe/S centers [always shown in their reduced ('red') state] are thought to mediate the transfer of electrons between MoCo and the flavin cofactor and to serve as electron sinks, storing reducing equivalents during catalysis (from [210]).

In humans this family consists of xanthine oxidoreductase (XOR) and AOX1 while in mouse three homologous of AOX1, named AOH1, AOH2, and AOH3, are present. Sequence

homologous of mouse AOH1, AOH2, and AOH3 are also present in humans, but do not seem to code for functional MFEs [210].
In mice and humans 34 out of 36 junctions are conserved in XOR relative to AOX1, AOH1 or AOH2. Protein alignment and gene structure data clearly indicate that all known mammalian MFEs have a common origin and have evolved from an ancestral precursor [210]. Human AOX1 maps to chromosome 2q32.3-2q33.1 [211].

4.1.1 Regulation of AOX1 Expression

The promoter of AOX1 contains no TATA sequence [212; 213] and the transcription of AOX1 in human liver starts from a consensus transcriptional initiator for mammalian RNA polymerase II [214], common to other TATA less genes [215], 298 bp upstream of the translation start site [214]. In HepG2 transcription initiation seems to arise from several sites that are located closer to the ATG [212]. Additional analysis revealed a structurally complex region upstream of AOX1, containing sequences for a proximal promoter, enhancer sites, and a silencer element, indicating the potential for complex regulation of AOX1 expression and pointing out the essential role for the transcription factors Sp1 and Sp3 in epithelial cells [216]. Up to now very little is known about expression and regulation of AOX1 and its homologs, AOX1 is regulated in a tissue type specific manner in humans [214], cattle [206], rabbits [217], and rats [218], with liver and lung showing highest expression. Besides the tissue specific regulation, AOX1 is also regulated in a gender specific way, which was shown for murine liver AOX1 and AOH1. Hepatocytes of male animals synthesize by far larger amounts than females [208]. This is in good agreement with the finding that chronic administration of testosterone to female mice induces both AOX1 and AOH1 [208; 219]. This effect is due to elevated mRNA levels, suggesting an influence of testosterone on the transcription of both genes [208]. Probably the modulation is indirect, mediated by growth hormone and/or somatomedins [220; 221]. No sex-related differences in the expression of AOX1 and AOH1 have been found in lung indicating that the effects of testosterone are tissue-specific [209]. Interestingly AOX1 is observed in target organs of testosterone, namely testis, epididymus, and prostate [222].
“Dioxin like” compounds found ubiquitous in the environment are also reported to influence AOX1 expression. In the mouse hepatoma cell line Hepa-1, AOX1 mRNA is upregulated by dioxin. Data from mutants defective in the key enzymes of the aryl hydrocarbon receptor (AHR) pathway, namely AHR and AHR nuclear translocator (ARNT), show that AOX1 mRNA expression is only enhanced if both proteins are present [223]. Upon ligand binding the cytosolic AHR migrates to the nucleus and forms heterodimers with the nuclear localized ARNT [224]. These dimers specifically recognize DNA sequences in the 5´ regulatory region

of responsive genes, known as xenobiotic response elements [225], leading to enhanced transcription [226]. Furthermore, dioxin increased AOX1 mRNA, protein, and enzymatic activity in the liver of C57BL/6 mice. An upregulation of AOX1 mRNA was detectable at 4 h after dioxin treatment, peaking at 24 h. Elevated protein levels of AOX1 and AOH1 were observed following 3 days of treatment and remained elevated at least to 6 days. Tungstate inhibiting AOX1 and eventually AOH1 activity by replacing molybdenum lowered both basal and dioxin induced aldehyde oxidase activity [223]. These data show a co-regulation of AOX1 and AOH1 in mice. The delay of time between mRNA and protein increase of AOX1 indicates that dioxin in vivo does not only enhance transcription but also affects other factors regulating AOX1 [223]. Taking into account the complex synthesis of catalytically active holoenzyme forms of the molybdo-flavoenzymes which is controlled by many genes this finding is not surprising [210]. For XOR it was demonstrated that its increase by interferons and interferon inducers in vivo is partly regulated at the translational level [227].

Recent data report downregulation of AOX1 on mRNA and protein level by the PPARα activators adiponectin and fenofibric acid and the PPARα antagonist RU486 blocks this effect, thus identifying AOX1 as PPARα target gene [228].

4.1.2. Tissue Distribution of AOX1

AOX1 expression is most prominent in the liver, as was shown for humans [229], rats [218] and cattle [206]. Significant but low levels of both mRNA and protein are also present in lung and testis [208; 209]. By northern blot analysis of tissues from unstimulated CD1 mice, the AOX1 transcript was detected in hepatocytes, cardiocytes, lung, and esophageal epithelial cells, with trace amounts in brain, spinal cord, spleen and eye. Nevertheless enzymatic activity was only detected in liver, lung and spinal cord [219]. Low expression of AOX1 mRNA and protein in mouse brain and spinal cord was also described by Bendotti *et al*. [230]. AOX1 is only active in epithelial cells of the choroid plexus, which is involved in the secretion and reabsorption of the cephalo-rachidian fluid, as well as in the motor neurons of the brain and spinal cord. In mice, AOX1 and AOH1 reveal entirely overlapping tissue distribution. In situ hybridization studies suggest that different, although partially superimposable, subpopulations of hepatocytes are the sites of AOX1 and AOH1 expression [209]. While AOH1 is present in hepatocytes in the final phase of fetal development AOX1 is only found in adult animals, implying a role of AOH1 in liver development [209].

Immunohistochemical studies demonstrated a common allocation of AOX1 in respiratory (epithelial cells from trachea and bronchium, alveolar cells), digestive (surface epithelia of small and large intestine, hepatic cells), urogenital (proximal, distal and collecting tubules of

the kidney), and endocrine tissues (ductuli epididymidis and glandular epithelia, cortex of adrenal gland) [222].

The expression of AOH2 is distinct from AOX1 and AOH1, with mRNA and protein being only detectable in keratinized epithelia, such as the epidermis and the mucosa of the oral cavity, the oesophagus and the first part of the stomach [209].

5. Apoptosis/Autophagy

It is well known that ABCA1 is upregulated in macrophage foam cells [11; 231]. Based on own unpublished observations demonstrating inverse regulation of ABCA1 and ABCA7 under this conditions and the finding that ABCA1 and ABCA7 are inversely regulated by SREBP-2 in a sterol-dependent manner [73] the current working hypothesis is that ABCA1 and ABCA7 fulfill different functions in the same pathway (Fig. 25).

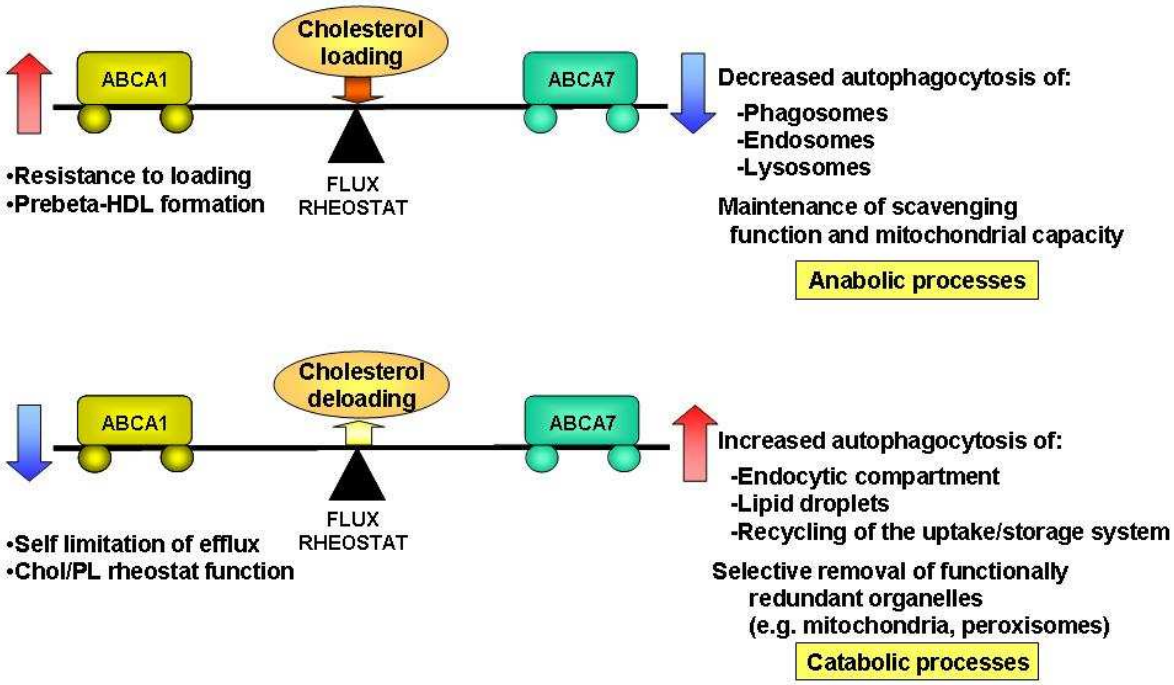

Figure 25. Model of the postulated functional relation of ABCA1 and ABCA7 [*].

When cells are loaded with cholesterol, ABCA1 is upregulated to generate acceptor-molecules for cholesterol efflux, providing the cell with the possibility to get rid of the excess cholesterol. ABCA7, on the other hand, is downregulated, and the same is expected for autophagy under this conditions. When cells are deloaded ABCA1 is downregulated, to prevent excess efflux of cholesterol, ABCA7 and autophagy on the other hand are increased to breakdown and recycle components that were needed under excessive cholesterol loading, like lipid droplets or mitochondria. The involvement of ABCA7 in phagocytic/autophagic processes is further supported by experiments demonstrating that knock-down of ABCA7 impairs engulfment of apoptotic cells by macrophages due to disturbed ERK signaling [75].

Autophagy is an evolutionary conserved mechanism in eukaryotic cells and can be divided in several subgroups, like microautophagy, macroautophagy and chaperone-mediated autophagy. The vacuolar, self-digesting process mediating removal of long-lived proteins and damaged organelles by the lysosome is termed macroautophagy [232]. Key players in

autophagy are the Atg genes primary described in yeast [233]. Macroautophagy shows basal activity in most cells, presumably liable for its anti-aging role [234; 235]. It enables the cell to get rid of damaged mitochondria [236] or functional redundant organelles [237]. Under starving conditions, macroautophagy is induced in order to provide the necessary components for survival. For example in the liver amino acids are generated and transformed into glucose to provide energy for the brain and erythrocytes [232]. Newer findings indicate that muscles also contribute amino acids under these conditions [238; 239]. Of note is that in cases of prolonged nutrient depletion macroautophagy is downregulated, eventually by ketone bodies [232]. Another important function of macroautophagy when nutrients are scarce is the generation of oxidizable substrates in neonates, indicated by transient upregulation in different tissues of the early neonate [238]. Autophagy is moreover involved in different diseases [237] resembling its dual role as cell-protective and –destructive [232]. In advanced stages of cancer, macroautophagy may be necessary to supply cells without connection to the blood stream in the inner part of solid tumors [240]. In apoptosis, again macroautophagy could play a dual role. It is able to protect cells from apoptosis by providing sufficient substrates under nutrient depletion [241] or reduced uptake of nutrients in case of a miss of growth factor [242]. Autophagy can also cause an apoptosis (Type I programmed cell death) independent cell death named autophagic cell death or Type II programmed cell death [243].

Amino acids processed by autophagic break down constitute a potent feedback inhibition of autophagic sequestration and moreover the process is inhibited by insulin (in the liver) and enhanced by glucagon (reviewed in [244]). Both hormones exert their influence on autophagy in the liver at intermediate amino acid concentrations by altering the phosphorylation state of ribosomal protein S6 (S6); insulin, like high amino acid concentrations alone, increases and glucagon reduces phosphorylation [232]. Rapamycin entirely blocks amino acid-mediated S6 phosphorylation, implying mammalian target of Rapamycin (mTOR) and p70S6 kinase as members of this pathway and partly reduced inhibition of autophagy by amino acids. Furthermore, rapamycin partly reduced protein synthesis, suggesting a common regulation of both pathways [245]. Besides activating mTOR amino acids seem capable to inhibit autophagy independent of mTOR [246; 247].

In addition to rapamycin the PI3K inhibitors wortmannin and LY294002 reduced amino acid stimulated S6 phosphorylation. In contrast to rapamycin autophagy was decreased in the absence of amino acids [248]. These results were clarified by the finding that the product of class-III PI3K is necessary for autophagy and that the products of class-I PI3K display inhibitory potentials [47]. As both classes are affected by those PI3K inhibitors, autophagy is abolished. The specific autophagy inhibitor 3-methyladenine was identified as PI3K inhibitor,

accounting for its effect on autophagy and S6 phosphorylation [47; 248]. A schematic drawing of the complex regulation of autophagy is shown in Figure 26.

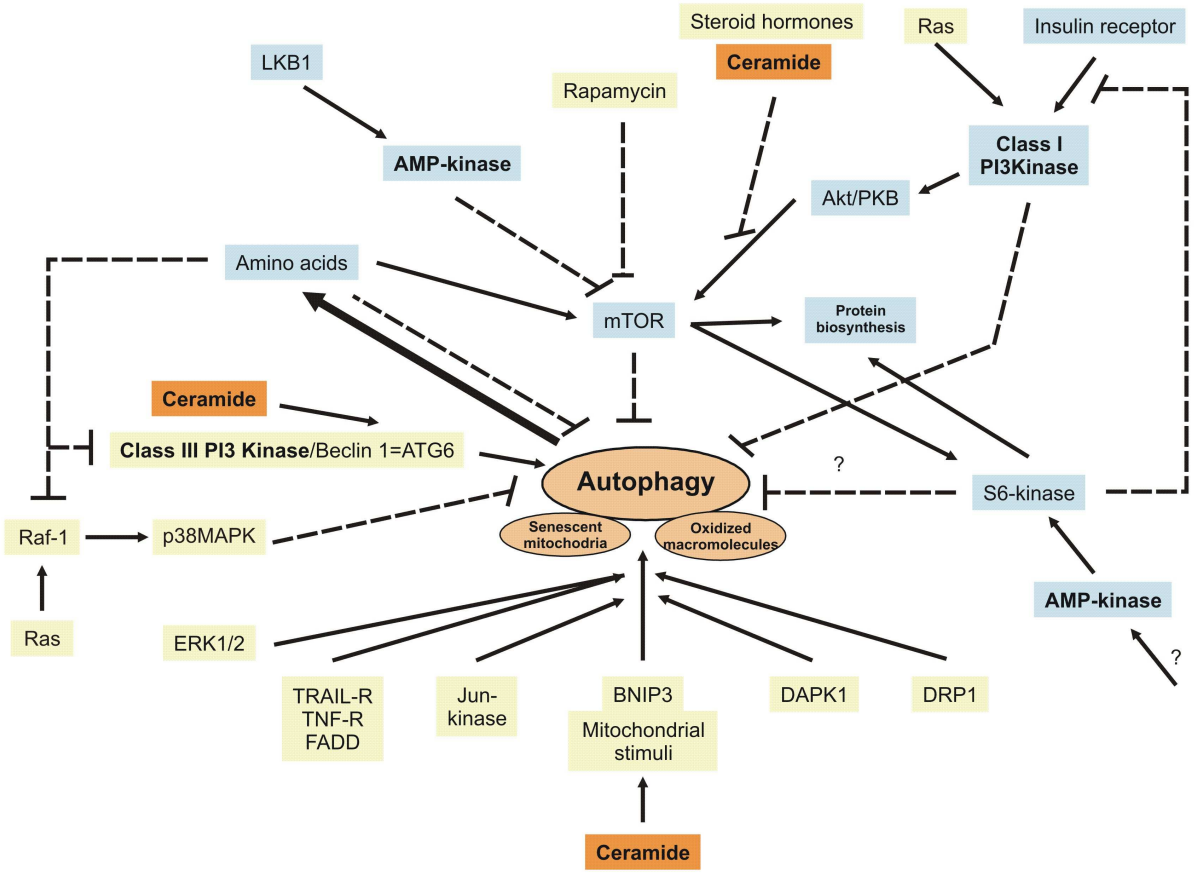

Figure 26. Diagram of autophagy signaling. Detail are found in the text (adapted from [232])**.**

5.1. Effects of Atherogenic Lipoproteins on Macrophages

The recruitment of monocytes to the arterial wall and the enhanced entrapment of LDL in the intima are the earliest events in atherogenesis [22]. LDL in the subendothelium is modified to an atherogenic particle that is taken up by lesional macrophages and leads to foam cell formation [249]. Foam cells have been detected in early and advanced lesions and influence plaque rupture eventually leading to myocardial infarction and stroke. The enhanced survival and proliferation as well as apoptotic and necrotic cell death of lesional foam cells has been reported and contributes to the development of atherosclerotic lesion and the final rupture of the plaque [250].

The oxidative modification of LDL (Ox-LDL) in the intima is catalyzed by vascular cells and generates an atherosclerotic particle. Numerous studies investigated foam cell formation in-vitro using copper oxidized LDL. Ox-LDL was demonstrated to be cytotoxic and to induce apoptotic cell death in macrophages [251]. Apoptosis was shown to depend on p53 and superoxide dismutase (MnSOD) in-vitro and in atherosclerotic lesions where MnSOD

immunoreactivity correlates to plaque advancement [252]. The expression of the proapoptotic Bcl-2 family protein BAX was found induced in lesional macrophages [253]. In addition Ox-LDL activates sphingomyelinase and the subsequent rise of intracellular ceramide leads to apoptotic cell death [254]. In contrast, lightly oxidized LDL or low amounts of Ox-LDL enhance macrophages survival and promote proliferation [255]. The mitogenic effect was attributed to lysophospholipids in Ox-LDL and was enhanced by aggregation [256]. Current research indicates that besides oxidation partial degradation of LDL by enzymes secreted from vascular cells takes place in the subendothelium [257]. Treatment of LDL with trypsin and cholesterylesterase generates an atherogenic lipoprotein called enzymatically modified LDL (E-LDL), with a similar size as lipoproteins isolated from atherosclerotic lesions [257]. Furthermore E-LDL binds C reactive protein and activates complement [258]. E-LDL induces foam cell formation more rapidly than Ox-LDL [259] and this might explain that E-LDL is a more potent inducer of gene expression as was demonstrated for monocyte chemotactic protein 1 [260], early growth response gene-1 [261] or adipophilin [262]. These studies indicate that E-LDL and Ox-LDL influence identical target genes but with different kinetics. E-LDL was also demonstrated to exert effects not identified or opposite of Ox-LDL treated cells. The expression of cathepsin H was induced by E-LDL but not Ox-LDL in macrophages and cathepsin H may also contribute to the transformation of LDL to an atherogenic moiety [263]. In contrast to Ox-LDL, E-LDL induces foam cell formation also in freshly isolated peripheral blood monocytes and cytotoxicity of E-LDL is only observed using very high amounts of this modified lipoprotein [259; 260].

II. AIMS OF THE THESIS

The goals of this thesis were to identify and functionally characterize new and previously identified ABCA1 or ABCA7 interacting proteins and genes in the ABCA1-pathway in more detail.

Firstly, yeast two-hybrid screens were performed to identify new putative ABCA1 associated proteins and these results were confirmed by independent methods.

Secondly, the interaction of AOX1 with ABCA1 was verified and the functional relevance of this interaction was analyzed, which was the major topic of my thesis.

Thirdly, syntaxin 13 and Tax1 binding protein 3 (TAX1BP3) associated proteins were identified by yeast two-hybrid screens.

Fourthly, yeast two-hybrid screens were performed to identify putative ABCA7 interacting proteins and the regulation of the promoter(s) of ABCA7 was analyzed.

Fifthly, genes were identified that are regulated by atherogenic lipoproteins in a similar manner as ABCA1.

III. MATERIAL

1. Chemicals, Enzymes, Markers, Media and Buffers

-Leu Dropout (DO) Supplement	Clontech, Palo Alto, CA, USA
-Leu/-Trp DO Supplement	Clontech, Palo Alto, CA, USA
-Leu/-Trp/-His DO Supplement	Clontech, Palo Alto, CA, USA
-Trp DO Supplement	Clontech, Palo Alto, CA, USA
1 kb plus Ladder, DNA	Gibco BRL, Berlin, Germany
Agarose	Biozym, Hameln, Germany
Alkaline Phosphatase, Shrimp	Roche, Mannheim, Germany
Ampicillin	Roche, Mannheim, Germany
Apolipoprotein A-I (apoA-I)	Calbiochem, Bad Soden, Germany
Bovine serum albumin (BSA, Lipid-free)	Sigma, Deisenhofen, Germany
DMEM with L-Glutamin	Bio WHITTAKER, Walkersville, MD, USA
EDTA (Di-sodium)	Pharmacia Biotech, Freiburg, Germany
Eicosapentaenoic acid (EPA)	Calbiochem, Bad Soden, Germany
Fetal Calf Serum (FCS)	Gibco BRL, Berlin, Germany
Fluoresbrite microparticles	Polysciences, Eppelheim, Germany
FuGene 6	Roche, Mannheim, Germany
Full-Range Rainbow Molecular Weight Markers	Amersham Pharmacia Biotech, Freiburg, Germany
H_2O Nuclease-free	Promega, Madison, AL, USA
Human recombinant M-CSF	R&D Systems, Wiesbaden-Nordenstadt, Germany
γ-linolenic acid	Biotrend, Köln, Germany
Luria Broth Agar Base	Gibco BRL, Berlin, Germany
Luria Broth Base	Gibco BRL, Berlin, Germany
Macrophage serum free medium (SFM)	Gibco BRL, Berlin, Germany
MEM (Non-essential Amino acid)	Gibco BRL, Berlin, Germany
Minimal SD Agar Base	Clontech, Palo Alto, CA, USA
Minimal SD Base	Clontech, Palo Alto, CA, USA
Complete Mini Protease inhibitor Cocktail	Roche, Mannheim, Germany
Phosphate Buffered Saline (PBS) w/o Ca+2/Mg+2	Gibco BRL, Berlin, Germany
Protein A-Dynabeads	Dynal, Hamburg, Germany
Pwo-DNA-Polymerase	Roche, Mannheim, Germany
Ready Gels, 4-20%	BioRad, Hercules, CA, USA
Restrictionendonucleases	Roche, Mannheim, Germany
RNAiFect	Qiagen, Hilden, Germany
Taq-DNA-Polymerase	Roche, Mannheim, Germany
TaqMan PCR Mastermix	Applied Biosystems, Darmstadt, Germany
T4-DNA-Ligase	Gibco BRL, Berlin, Germany
Triton X-100	Boehringer, Mannheim, Germany
Trypsin / EDTA	Sigma, Deisenhofen, Germany
YEASTMAKER Carrier DNA	Clontech, Palo Alto, CA, USA
YPD Agar Base	Clontech, Palo Alto, CA, USA
YPD Base	Clontech, Palo Alto, CA, USA
All other chemicals and solvents	Sigma, Deisenhofen, Germany

2. Kit Systems

BCA Protein Assay Kit	Pierce, Rockford, IL, USA
BigDye Terminator Cycle Sequencing Kit v.1.1	Applied Biosystems, Darmstadt, Germany
Cell Death Detection ELISA^{PLUS}	Roche, Penzberg, Germany
Centrisep spin columns	Princeton Separations, Adelphia, NJ, USA
ECL+ Western Blotting Analysis System	Amersham Pharmacia Biotech, Freiburg, Germany
Galactosidase enzyme assay	Promega, Madison, AL, USA
MATCHMAKER Two-Hybrid System II and III	Clontech, Palo Alto, CA, USA
MicroSpin GST Purification Module	Amersham Pharmacia Biotech, Freiburg, Germany
Ni-NTA Spin Kit	Qiagen, Hilden, Germany
Protein Assay	BioRad, Hercules, CA, USA
QIAprep Spin Miniprep Kit	Qiagen, Hilden, Germany
QIAquick Gel Extraction Kit	Qiagen, Hilden, Germany

QIAquick PCR Purification Kit	Qiagen, Hilden, Germany
Reverse Transcription System	Promega, Madison, AL, USA
RNeasy Mini Kit	Qiagen, Hilden, Germany
Soluble Fas ELISA	R&D Systems, Wiesbaden-Nordenstadt, Germany
TNT Quick Coupled Transcription/Translation System	Promega, Madison, AL, USA
YEASTMAKER™ Yeast Plasmid Isolation Kit	Clontech, Palo Alto, CA, USA

3. Oligonucleotides, AODs, and siRNA

All sequences are denoted from 5´ to 3´.

3.1. Oligonucleotides

Oligonucleotides were ordered from Qiagen/Operon.

3.1.1. For Cloning

3.1.1.1. Constructs Related to ABCA7

Bait-constructs for the yeast two-hybrid screen:

YTHA7Crev	GGA TCC GTC GAC TTA GAG CAC AGT CTC GGC AGT GC
ABCA7Ctermuni	GGG GAA TTC CGC TGC CTG GGC AGC CCG CAA
ABCA7Ntermrev	CCC GGA TCC CCC TAG GCC AGC CAG CGT CCT GTG
ABCA7Ntermuni	GGG GAA TTC GCC TTC TGG ACA CAG CTG ATG CTG

Constructs for the verification of the interaction in yeast:

CAP37 Fwd_Eco:	GGG GAA TTC ATG ACC CGG CTG ACA GTC CTG
CAP37 Rev_Bam:	GGG GGA TCC CTA GGC TGG CCC CGG TCC CGG
FB5_uni_Eco	GGG GAA TTC ATG CCA GGA ATA AAA AGG ATA
FB5_rev_Xho	GGG CTC GAG TCA GAA TGG GTA CTG CGA CAC
GIP2_uni_Bam_ACT2	GGG GGA TCC AA ATG CCC CTG AAG CTG CGG GGG
GIP2_rev_Xho_ACT2	GGG CTC GAG TCA TAA TCC TCT TCG TTT GGC
VC_uni_Eco	GAG GAA TTC GAG CAT CGC AAG GCG GTG CCA
VC_rev_Bgl	GGG AGA TCT TCA CTC CGG GCA CTG AGT GGT
MT2_uni_Eco	GGG GAA TTC ATG GAT CCC AAC TGC TCC TGC
MT2_rev_Bgl	GGG AGA TCT TCA GGC GCA GCA GCT GCA CTT
JAM_uni_Mun	GGG CAA TTG ATG GGG ACA AAG GCG CAA GTC
JAM_rev_Bam	GGG GGA TCC TCA CAC CAG GAA TGA CGA GGT
JAB_uni_Eco	GGG GAA TTC ATG GCG GCG TCC GGG AGC GGT
JAB_rev_Bam	GGG GGA TCC TTA AGA GAT GTT AAT TTG ATT
C1Q_uni_Eco	GGG GAA TTC ATG GAG GGT CCC CGG GGA TGG
C1Q_rev_Bam	GGG GGA TCC TCA GGC AGA TGG GAA GAT GAG

Constructs for pull-down assays and coimmunoprecipitation:

capTOPODIRuni	CAC CAT GAC CCG GCT GAC AGT CCT G
capTOPODIRrev	CGG TCC CGG GTT GTT GAG AAC
capTOPODIRreifuni	CAC CAT GAT CGT TGG CGG CCG GAA GGC G

JAM_TD_uni	CACC ATG GGG ACA AAG GCG CAA GTC
JAM_TD_rev	CAC CAG GAA TGA CGA GGT CTG
JAB_TD_uni	CACC ATG GCG GCG TCC GGG AGC GGT
JAB_TD_rev	AGA GAT GTT AAT TTG ATT AAA CAG
GIP2_TD_uni	CACC ATG CCC CTG AAG CTG CGG GGG
GIP2_TD_rev	TAA TCC TCT TCG TTT GGC ATC ACC
VC_TD_uni	CACC ATG GCG GCG GTG GCT GGA TC
VC_TD_rev	CTC CGG GCA CTG AGT GGT CGG
VC3uniTD	CACC GGA TCC CGT GCC CCT GGC C
VC3revTD	GAA CTC CAC CTT GCA GGC CGG G
FB_TD_uni	CACC ATG CCA GGA ATA AAA AGG ATA C
FB_TD_rev	GAA TGG GTA CTG CGA CAC ATA TAT C
C1Q_TD_uni	CACC ATG GAG GGT CCC CGG GGA TGG
C1Q_TD_rev	GGC AGA TGG GAA GAT GAG GAA GCC

Constructs for promoter-assay:

(+) 65	CCC AAG CTT GGC TGT CTC CGG CGA TAC ATG
-1170	CCC AAG CTT CCG AGT CCT TCT CAC CTT CC
H1	CTC GAG AAT GCG GGG TTG GGG CCG GGA GGG
B8	CCC ACG CGT ATA GCA GCG TGC AGA GGC AG
A	CCC ACG CGT GGA GCA GGC CAG TGA GTG ACG
B7	CCC ACG CGT TGA TCC CGT CTC CTC CCT T
B6	CCC ACG CGT AAG AAA CCC GGC TAG GCG A
B5	CCC ACG CGT CTA CGG TGA TGC AGC AAG AG
B4	CCC ACG CGT AAG ACA GCG CAG CCT CGT T
B3	CCC ACG CGT GTT ATA CAA CGT GGG GAG
B2	CCC ACG CGT GAA CTC CTG CAA TTC GGA G
B1	CCC ACG CGT GAG TCT GGA CTA AAC TAG AG
B	CCC ACG CGT GAA CGA ATG ATC TAG TGG AAC CC
H	CCC ACG CGT AGG AGG AGC AAA AGC TGA AGC

3.1.1.2. Constructs Related to ABCA1

Bait-constructs for the yeast two-hybrid screen:

YTHA1Cuni	GAA TTC GTC AAT GGA AGG TTC AGG TGC
YTHA1Crev	GGA TCC GTC GAC TCA TAC ATA GCT TTC TTT CAC

Constructs for the verification of the interaction in yeast:

A1CT2rev	GGA TCC TAC ATA GCT TTC TTT CAC TTT C
A1CTrev3del	GGA TCC TCA TTT CAC TTT CTC ATC CTG
A1CTrev4mut	GGA TCC TCA TCC ATA TCT TTC TTT CAC TTT C
GIPC1 Fwd_Eco:	GGG GAA TTC ATG TTT TGC ACC CTG AAC AC
GIPC1 Rev_Bam:	GGG GGA TCC CTA GTA GCG GCC GAC CTT GGC
TIP1 Fwd_Eco:	GGG GAA TTC ATG TCC TAC ATC CCG GGC CAG
TIP1 Rev_Bam:	GGG GGA TCC CTA GGA CAG CAT GGA CTG CTG
SDCBP Fwd_Mun:	GGG CAA TTG ATG TCT CTC TAT CCA TCT CTC
SDCBP Rev_Bam:	GGG GGA TCC TTA AAC CTC AGG AAT GGT GTG
b2_YTH_ECO	GAA TTC CCC GCG GGT GAG GCG GGC

b2_YTH_BAM	GGA TCC GCG TAG GAT CAA CGT GTT CCT G

Constructs for pull-down assays and coimmunoprecipitation:

MAGITDuni	CAC CAT GTC GAA GAC GCT GAA GAA GAA GAA GCA C
MAGITDrev	ATG TTG CTC GGG TTT CAC GTA GGA G
GIPC1 Fwd:	CAC CAT GCC GCT GGG ACT GGG GCG
GIPC1 Rev:	GTA GCG GCC GAC CTT GGC GTC
TIP1 Fwd:	CAC CAT GTC CTA CAT CCC GGG CCA G
TIP1 Rev:	GGA CAG CAT GGA CTG CTG CAC
SDCBP Fwd:	CAC CAT GTC TCT CTA TCC ATC TCT C
SDCBP Rev:	AAC CTC AGG AAT GGT GTG GTC

Construct for PDZ-Array:

QE_A1_uni	GGA TCC GTC AAT GGA AGG TTC AGG TG
QE_A1_rev	AAG CTT TCA TAC ATA GCT TTC TTT CAC TTT C

3.1.1.3. Constructs Related to TOSO

For cloning in the pcDNA3.1D/V5-His-TOPO TOSO was amplified using the primers

FWD: CAC CAT GGA CCT CTG GCT TTG GCC ACT TTA

REV: GGC AGG AAC ATT GAT GTA GTC ATC TGA ATC AC

The TOSO probe for northern blots was generated using the primers

FWD: TGA GGA TCC TCC CAG AAG TA

REV: CCT CCC AGA CTG TGA GCC AT

3.1.2. For Sequencing

capTDsequni	CCC CGG GGT TAG CAC CGT GG
capTDseqrev	GCC ACT CGG GTG AAG AAG TC
FBTDuni	CTC CAG GCC TCT TAT ATG CC
FBTDrev	GAT AAG GCT CCT CAC AGC GG
JABTDseq	GCA TAT GAA TAC ATG GCT GC
pACT2Seqrev	GCA CGA TGC ACA GTT GAA GTG
SeqFBuni	GTG CAA CAG ATT CCC ACC AG
SeqFBrev	AGA TAA GGC TCC TCA CAG CG
SeqJAMuni	ACC ATT GGG AAC CGG GCA GTG
SeqGIP2uni	AAA GAT GGT GGT GTT ATT GAC
YTH_VER_UNI	GAG CGC CGC CAT GGA GTA C
YTH_VER_REV	CAG TTG AAG TGA ACT TGC GG
TD_UNI	CTC ACT ATA GGG AGA CCC AAG
TD_REV	CCT CTA GAC TCG AGC GGC C
A1_CT_sequin	TGC TAC AAT ACC AGC TTC
A1_CT-seqrev	TGT CTG AGA AAC AGA GTA G
pAS2-1rev	CGT TTT AAA ACC TAA GAG TCA C
PAS2-1uni	TCA TCG GAA GAG AGT AG
GADT7uni	CTA TTC GAT GAT GAA GAT ACC CCA CCA AAC CC
GADT7rev	GCG GGG TTT TTC AGT ATC TAC GAT TCA TCT GC

INSERTuni	CAG TGA ATT CCA CCC AAG C
INSERTrev	CCC GTA TCG ATG CCC ACC C
pACT2_Seq_uni	GCT TAC CCA TAC GAT GTT CCA G
pUCuni	GTA AAA CGA CGG CCA GT
pUCrev	CAG GAA ACA GCT ATG AC
MAG340	CGG CAT TAC CTA AGT CTT CAG
MAG640	CAA GTC CTC TTT GAT AAT GAG
MAG940	CAC TGA CAC AGG GAT GAT C
MAG1240	GGT GTC CTT GTT CGA GCA TC
MAG1540	CAG TGA AGA TCC TGT TGT GG
MAG1840	GTG TCA AGG CCT TCA GAA AGG
MAG2140	GGA TCC CCA AAA TTG GAT CC
MAG2440	ACG GAA GAT CTT CTA TGG AG
MAG2740	CAT TGT TGA ACT GTC TCA TG
MAG3040	CCA GTA GAG CTG GAG AGA GG
MAG3220	GAA CCT ACA CAA GGA ATC AC
GIP360	CAC TTG GTC TCA CCA TTA CAG
VC325	CCT GCC TCT CAC AAG CTA CTG
VC640	GGA GTA CGT GGC TGA GTC TC
VC940	GCG CTC CGA GGT GGC TGC TG
VC1240	CTC TGT GTG CGC CCT GCT GG
VC1540	CAC GCA AGA CTG AGA AAG AAG
VC1840	CCT GGA GCT GGG GCC GAT C
VC2140	CAC CAG TGA GGC TGG GCT GAG
QE uni	CGG ATA ACA ATT TCA CAC AG
QE rev	GTT CTG AGG TCA TTA CTG G
QE prom	CCC GAA AAG TGC CAC CTG

3.2. TaqMan-Assays

3.2.1. Gene Expression Assays

Assays on Demand (AOD) were purchased from Applied Biosystems.

Gene	Assay ID
ABCA1	Hs00194045_m1
SNTA1	Hs00162045_m1
SNTB1	Hs00221412_m1
SNTB2	Hs00198844_m1
GIPC1	Hs00194807_m1
TIP1	Hs00205924_m1
Scribble	Hs00363005_m1
MAGI3	Hs00326365_m1
GIPC2	Hs00214273_m1
AOX1	Hs01565229_m1

Primers and Probes.

The mRNA sequences for ABCA7 type I and type II, TOSO and SDCBP were derived from GenBank and primers and TaqMan probes were designed using the PrimerExpressSoftware v2.0 (Applied Biosystems). Primers for ABCA7 and SDCBP and 6-carboxyfluoresceine (FAM)-labeled probes, quenched by a non-fluorescent quencher (TAMRA) at its 3´ end, were obtained from Applied Biosystems. Primers for TOSO were obtained from MWG-Biotech (Ebersberg, Germany).

ABCA7 type I:

FWD	TCT TCA TCC TGG TGG CTG TTC
Probe	CCA CTC CCA CCC GCC CCT G
REV	ACC ATG AAT GCC ACT TCC CA

ABCA7 type II:

FWD	GGA CCC CTA GTG AGT GTT CAA AA
Probe	CAT TGT CCC CCT TGT GGT CTT TCT CCC
REV	AGG AAT CCC TGG GGT TGG

TOSO:

FWD	TGG TGC CAA GGA GTC TCA TCT
Probe	TCT GCT GAT GTC CAA TAC CTG CTT CAT GTG
REV	GGG AAT GAT GAG GGC TCT GA

SDCBP:

FWD	GCT CAA ACT GCT TTT TCT GCA A
Probe	CCC TGC CAA TCC AGC AAT TTT GTC A
REV	TGA GGG ATA GGA GCA GAA GCT T

3.2.2. SNP Genotyping Assay

SNP Genotyping assays located in or near AOX1 (Assay IDs: C____144529_1_, C____144530_10, C___8130525_10, C__25473600_20, C__27967310_10, C__29454081_20, C__30787305_10) were purchased from Applied Biosystems.

3.3. siRNA

siRNAs were supplied by Ambion, Austin, TX, USA.

Aldehyde Oxidase 1 (AOX1, NM_001159):

Sense:	GCC AAU GCC UGU CUG AUU Ctt
Antisense:	GAA UCA GAC AGG CAU UGG Ctg

Silencer Negative Control #1 siRNA

4. Antibodies

Antigen	Host	Clonality	Provider
ABCA1 (AB.H10)	mouse	monoclonal	Abcam, Cambridge, UK
AOX1	mouse	monoclonal	BD Biosciences, Erembodegem, Belgium
β-Actin	mouse	monoclonal	Sigma, Deisenhofen, Germany
Caspase-8	mouse	monoclonal	BD Biosciences, Erembodegem, Belgium
CD95 (DX2)	mouse	monoclonal	Calbiochem, Bad Soden, Germany
CD95L	mouse	monoclonal	Santa Cruz, Heidelberg, Germany
FADD	mouse	monoclonal	BD Biosciences, Erembodegem, Belgium
$FLIP_L$	rabbit	polyclonal	Chemicon, Hampshire, UK
GST	goat	polyclonal	Abcam, Cambridge, UK
HA	mouse	monoclonal	Clontech, Palo Alto, CA, USA
Mouse	goat	polyclonal	Jackson ImmunoResearch, Suffolk, UK
Rabbit	goat	polyclonal	BD Biosciences, Erembodegem, Belgium
V5	mouse	monoclonal	Invitrogen, Carlsbad, CA, USA

5. Radioactive Materials

[3H]Choline phospholipid	Amersham Pharmacia Biotech, Freiburg, Germany
[14C]Cholesterol	Amersham Pharmacia Biotech, Freiburg, Germany
[α^{32}P]dCTP	Amersham Pharmacia Biotech, Freiburg, Germany

6. Films and Membranes

ECL Hyperfilm	Amersham Pharmacia Biotech, Freiburg, Germany
Fluorotrans Membrane (PVDF)	Pall Filtron GmbH, Dreieich, Germany
Genescreen membrane	NEN Life Science, Boston, MA, USA)
Instant Picture Film Typ 667	Polaroid, Offenbach, Germany
X-Ray Films Biomax	Kodak, Rochester, NY, USA

7. Organisms and Plasmids

Organisms	Characteristics	Reference
Monocytes	Primary human-derived monocytes	this work
COS-7	African green monkey kidney fibroblast-like cells	[264]
HepG2	Human hepatoblastoma cells	[265]
HL-60	Human acute myeloid leukemia	[266]
Jurkat	Human T cell leukemia	[267]
S. cerevisiae Y187	*MATα, ura3-52, his3-200, ade2-101, trp1-901, leu2-3, 112, gal4Δ, met⁻, gal80Δ, URA3::GAL1*$_{UAS}$*-GAL1*$_{TATA}$*-lacZ*	Clontech, Palo Alto, CA, USA
S. cerevisiae PJ69-2A **AH109**	*MATa, trp1-901, leu2-3, 112, ura3-52, his3-200, gal4Δ, gal80Δ, LYS2::GAL1*$_{UAS}$*-GAL1*$_{TATA}$*-HIS3, GAL2*$_{UAS}$*-GAL2*$_{TATA}$*-ADE2,* ***ura3::MEL1***$_{UAS}$***-MEL1***$_{TATA}$***-lacZ***	Clontech, Palo Alto, CA, USA
E. coli BL21-Gold	F⁻, *omp*T, *hsd*S (r_B^-, m_B^-), dcm^+, Tet^r, *gal*, *end*A, Hte	Stratagene, La Jolla, CA, USA
E. coli TOP10 GC10	F⁻, *mcr*A, Δ(*mrr-hsd*RMS-*mcr*BC), Φ80*lac*ZΔM15, Δ*lac*X74, *deo*R, *rec*A1, *ara*D139, Δ(*ara-leu*)7697, *gal*U, *gal*K, *rpsL*(Str^R), *end*A1, *nup*G	Invitrogen, Carlsbad, CA, USA Biomol, Hamburg, Germany
E. coli TOP10F´	F´{*lac*I^q, Tn10(Tet^R)}, *mcr*A, Δ(*mrr-hsd*RMS-*mcr*BC), Φ80*lac*ZΔM15, Δ*lac*X74, *deo*R, *rec*A1, *ara*D139, Δ(*ara-leu*)7697, *gal*U, *gal*K, *rpsL*(Str^R), *end*A1, *nup*G	Invitrogen, Carlsbad, CA, USA

Plasmid	Marker	Reference
pGEX-5X-1	Amp^r	Amersham Pharmacia Biotech
constructs based on pGEX-5X-1	Amp^r	this work
pQE30	Amp^r	Qiagen, Hilden, Germany
pQE30-ABCA1-CT	Amp^r	this work
pAS2-1	Amp^r, *TRP*1	Clontech, Palo Alto, CA, USA
constructs based on pAS2-1	Amp^r, *TRP*1	this work
pACT2	Amp^r, *LEU*2	Clontech, Palo Alto, CA, USA
constructs based on pACT2	Amp^r, *LEU*2	this work
pGADT7	Amp^r, *LEU*2	Clontech, Palo Alto, CA, USA
constructs based on pGADT7	Amp^r, *LEU*2	this work
Human Matchmaker cDNA-Libraries	Amp^r, *LEU*2	Clontech, Palo Alto, CA, USA
pCR2.1-TOPO	Amp^r, Kan^r, *lac*Z	Invitrogen, Carlsbad, CA, USA
pCRII-TOPO	Amp^r, Kan^r, *lac*Z	Invitrogen, Carlsbad, CA, USA
pcDNA3.1D/V5-His-TOPO	Amp^r, Neo^r	Invitrogen, Carlsbad, CA, USA
constructs based on pcDNA3.1D/V5-His-TOPO	Amp^r, Neo^r	this work
pcDNA3.1D/V5-His-*lac*Z	Amp^r, Neo^r	Invitrogen, Carlsbad, CA, USA
pGL3-Basic	Amp^r	Promega, Madison, AL, USA
constructs based on pGL3-Basic	Amp^r	this work
pSV-β-Galactosidase Control Vector	Amp^r	Promega, Madison, AL, USA

8. Technical Equipment

2100 Bioanalyzer, Caliper	Agilent, Palo Alto, CA, USA
Autoclave Steam Sterilizer Type 24	Melag, Berlin, Germany
Automatic Gamma Counter 1470 WIZARD	Berthold, München, Germany
Biofuge 15R	Heraeus, Hanau, Germany
Cell culture Incubator 6000	Heraeus, Hanau, Germany
ELISA-reader	Tecan, Stuttgart, Germany
FACScan	BD, Heidelberg, Germany
GeneQuant pro RNA/DNA Calculator	Amersham Pharmacia Biotech, Freiburg, Germany
GeneChip Fluidics Station 450	Affymetrix, Santa Clara, CA, USA
GeneChip Scanner 3000	Affymetrix, Santa Clara, CA, USA
Horizontal Shaker GFL-3016	GFL, Großburgwedel, Germany
Hybridization Oven 640	Affymetrix, Santa Clara, CA, USA
Incubator B 6120	Heraeus, Hanau, Germany
Instant Camera MP4	Polaroid, Offenbach, Germany
Kodak X-Omat 2000 processor	Kodak, Rochester, NY, USA
LaminAir Hood	Heraeus, Hanau, Germany
Liquid Scintillation Counter Wallac 1410	Berthold, München, Germany
Lumi Imager F1	Boehringer, Mannheim, Germany
LUMAT LB9501	Berthold, München, Germany
Megafuge 1.0 R	Heraeus, Hanau, Germany
Microscope (Visible) Leitz Laborlux S	Leitz GmbH, Wetzlar, Germany
Milli-Q UF Plus System	Millipore, Bradford, VT, USA
MiniSpin Plus Centrifuge	Eppendorf, Hamburg, Germany
Mini Transblot Cell	BioRad, München, Germany
Mini Protean-3 Electrophoresis Cell	BioRad, München, Germany
Mini-Sub Cell GT Electrophoresis	BioRad, München, Germany
pH-Meter pH537	WTW, Weilheim, Germany
Precision Balance Sartorius MD BA 200	Sartorius, Göttingen, Germany
Power Supply PAC 300	BioRad, München, Germany
Princeton MicroMax CCD-1317-K/1	Roper Scientific, Trenton, NJ, USA
Shaking Incubator GFL-3032	GFL, Großburgwedel, Germany
Shaking Water Bath Julabo SW-20C	Julabo, Seelbach, Germany
Spectrophotometer UV/VIS Lambda 2	Perkin Elmer, Überlingen, Germany
Stirrer with Heating Surface IKAMAG	Labor Center, Nürnberg, Germany
SpeedVaq Alpha RVC	Christ, Osterode, Germany
Sysmex Micro-Cell Counter F-300	Digitana AG, Hamburg, Germany
Thermocycler Gene Amp PCR System 9600	Perkin Elmer, Uberlingen, Germany
Thermomixer Comfort	Eppendorf, Hamburg, Germany
Ultrasonic Disintegrator Soniprep 150	MSE, Watford Herts, United Kingdom
Ultracentrifuge (fixed angle) J2-21 M/E	Beckman, München, Germany
Ultracentrifuge L-70	Beckman, München, Germany
Ultracentrifuge Optima TLX	Beckman, München, Germany
Vortex-Mixer REAX 2000	Heidolph, Kelheim, Germany
Zeiss Axiovert S-100 Spectral Microscope	Carl Zeiss, Goettingen, Germany

9. Preparation of Solutions

PBS-Tween

10 l PBS

100 ml 10% Tween

Transfer-buffer (western blot)

1 l Methanol

30.3 g TRIS

144 g Glycine

Ad 10 l H_2O

5x SDS-Gel running buffer (western blot)

75 g TRIS

360 g Glycine

250 ml 10% SDS

Ad 5 l H_2O

5x sample loading buffer (Laemmli dye - western blot)

5 ml Glycerol

1 g SDS

2.56 ml ß-Mercapto-Ethanol

2.13 ml 0.5M TrisHCl pH 6.8+ 0.4% SDS

Bromphenolblue Traces

5x TBE-buffer (DNA)

54 g Tris

27.5 g Boric acid

20 ml 0.5 M EDTA (pH 8.0)

Ad 1 l H_2O

6x Sample buffer (DNA)

0.25 % (w/v) Bromphenolblue

0.25% (w/v) Xylencyanol

15% (w/v) Ficoll 400 in H_2O

Ethidiumbromid stock solution (DNA – RNA)

10 mg/ml ethidium bromide in H_2O

E. coli and yeast media

were prepared according to the manufacturers´ instructions**.**

IV. METHODS

1. Cell Culture Techniques

1.1. Elutriation of Human Monocytes

Suspensions enriched in human peripheral blood leukocytes were isolated by leukapheresis in a Spectra cell-separator (Gambro BCT), supplemented with the anticoagulant ADCA and diluted with an equal volume of PBS (w/o $Ca2^+$, $Mg2^+$). The diluted apheresate was subjected to counterflow centrifugation (J2-MC centrifuge with JE- 6B Rotor, Beckmann) using buffers and centrifuge adjustment as follows:

Running buffer:
PBS (w/o Ca2+, Mg2+)
1.0 % (v/v) penicillin / streptomycin-solution
0.5 % (w/v) BSA
0.1 % (w/v) Glucose

Rotation: 2040 rpm
Rotor temperature: 15℃

	Flow rate (ml/min)	Volume of fraction (ml)
Loading	7	-
Pre-run	9	150
Fractions 1 - 4	12	50
Fractions 5 - 8	15	50
Fractions 9 - 12	18	50
Fractions 13 - 16	20	50
Fractions 17 - 19	22	50
Fractions 20 - 22	24	50

The monocyte content of each fraction was determined using flow cytometry based on the different scatter properties of lymphocytes, granulocytes and monocytes. Fractions that were devoid of granulocytes with a monocyte content of at least 95% of leukocytes were pooled, washed with PBS (w/o Ca2+, Mg2+) and resuspended in culture medium. The concentration of the suspension was determined with a Sysmex micro-cell counter F-300.

1.2. Cultivation of Cells and Cell Lines

Monocytes were isolated from blood donors 25 to 45 years of age with normal lipid status by counterflow elutriation. Cells were cultivated in macrophage serum free medium (SFM) with M-CSF for 4 d on plastic dishes (10^6 cells/ml) to induce phagocytic differentiation as described [268]. Incubation with atherogenic LDL (E-LDL, Ox-LDL) for 24 h was as previously described [262]. For deloading with HDL_3 the medium was removed, cells were washed with macrophage SFM and incubated in macrophage SFM with M-CSF supplemented with 100 µg HDL_3 for 24 h.
COS-7 cells were obtained from LGC Promochem (Wesel, Germany), all other cell lines were obtained from DSMZ (Braunschweig, Germany). Cells were cultivated according to the providers' recommendations in an incubator at 37℃ (95 % humidity, 10 % CO_2).

1.3. Incubation of Monocytes with Fatty Acids

For stimulation of monocytes with long-chain, free PUFA, 4 mM PUFA were complexed to BSA by incubation with 6% lipid-free BSA in PBS for 10 min. Complexed PUFA were subsequently used for stimulation at the indicated final concentrations. Lipid-free BSA at the same concentration was used for control incubations.

1.4. Phagocytic Activity

Phagocytic capacity was determined by flow cytometry. HepG2 and COS-7 cells were incubated with fluoresbrite yellow green microspheres (0.75 µm, Polysciences Europe GmbH) for one, or two, and four h, respectively (pulse). Following two washes with PBS fresh medium was added and cells were incubated for additional two h (chase). After washing with PBS fluorescence intensity of cells was determined by a FACSCalibur flow cytometer (BD Biosciences).

1.5. Assessment of ApoA-I-mediated Radioactive Lipid Efflux

Cells were labeled with [^{3}H]choline and [^{14}C]cholesterol (Amersham Pharmacia Biotech) for 31 hrs, and subsequently incubated in the presence of BSA or BSA plus apoA-I for 17 hrs and processed as described previously [269] according to the method of Bligh and Dyer [270]. Lipid efflux was calculated by subtracting the radioactivity secreted in the supernatant from total radioactivity. Specific lipid efflux was determined as lipid efflux in the presence of apoA-I subtracted by the efflux in the presence of a nonspecific acceptor (BSA).

1.6. Transfections of Cell Lines

1.6.1. Knock-down of Expression

RNA interference is based on the observation that the presence of double stranded (ds)RNA in a cell eliminates the expression of a gene having the same sequence, whereas expressions of other genes are unaffected. dsRNA is recognized and bound within the cell by the Dicer-RDE-1 (RNAi deficient-1) protein complex. This protein complex cleaves long dsRNA into 19-22 bp siRNA oligonucleotides. The antisense strand of the siRNA is used by an RNA-induced silencing complex (RISC) to guide mRNA cleavage, thus promoting mRNA degradation.

Knock-down of Aldehyde Oxidase 1 (AOX1) expression was achieved by transfection of cells with siRNA. The siRNA was designed and supplied by Ambion. A sequence of 19 nucleotides of AOX1 (EMBL-GenBank, Accession No. NM_001159; bp 312-330; see III.3.3.) was targeted. HepG2 cells were seeded in a 12-well plate at a density of 10^6 cells/well. 24 h after seeding AOX1 or non-silencing control siRNA were added using RNAifect (Qiagen) and the method was optimized according to the manufacturer's instructions. Functional studies were started 24 h (lipid efflux studies) or 48 h (phagocytic activity) after transfection.

1.6.2. Recombinant Expression

COS-7 cells were transfected with the recombinant plasmids containing the complete cDNA of TOSO using FuGene 6 (Roche) following the manufacturers instructions and stable cells were selected by G418.

1.7. Luciferase Reporter Assays

HepG2 or Jurkat cells were transiently transfected with FuGene reagent (Roche) as described by the manufacturer. Two µg of the respective reporter gene constructs were cotransfected with 1 µg of the pSV-galactosidase vector (Promega). A promoterless pGL3-basic vector served as control. Cells were lysed in reporter lysis buffer (Promega), and after centrifugation, luciferase assay reagent with luciferyl-CoA (Promega) was added to the supernatant as recommended by the manufacturer. Luciferase activity was finally determined in a LUMAT LB9501 (Berthold). All data were normalized for protein concentrations (BioRad protein assay) and -galactosidase activity (Promega -galactosidase enzyme assay). Each experiment was repeated three times, and measurements were performed in triplicate. Results are expressed as multiples in comparison to promoterless pGL3-basic vector activity.

2. Isolation of Lipoproteins

Lipoproteins and lipoprotein-deficient serum were prepared from human plasma or serum by sequential preparative ultracentrifugation in potassium bromide gradients followed by extensive dialysis and filter sterilization. All lipoprotein concentrations mentioned are protein concentrations determined by Lowry's method [271]. Lipoprotein fractions were stored at 4℃ and used within two weeks from end of dialysis.

2.1. Enzymatic and Oxidative Modifications of LDL

Enzymatic degradation of native LDL was performed as described previously [260] with the following modifications. LDL was diluted to 2 mg/ml in 20 mM 4-(2-hydroxyethyl)-1-piperazine ethan-sulfonic acid (HEPES), 150 mM NaCl, 2 mM $CaCl_2$, pH 7.0 and treated with trypsin (6.6 mg/ml, Sigma) and cholesterol esterase (40 mg/ml, Roche) for 24 h at 37^{o}C. Subsequently, trypsin inhibitor (Sigma) was added and the pH was adjusted to 5.0 by morpholinoethane sulfonic acid buffer. Ox-LDL was prepared as recently described [272]. During LDL preparation and subsequent modification, general precautions were taken to avoid lipopolysaccharide contamination. The latter was excluded by Limulus endotoxin assay (Sigma) [273].

3. Protein Methods

3.1. Protein Isolation

Cells were harvested, washed 3 times with PBS, collected by centrifugation for 7 min. at 400 g. Afterwards, cells were resuspended in lysis buffer (normally PBS, 1% Triton X-100 with protease inhibitor (Roche)) and left on ice for 20 min. After an additional incubation for 15 min at room temperature, cell debris was separated by centrifugation at 14,000g at 4℃ for 10 min and samples were stored at -20℃ until u se.

3.2. Recombinant Expression and Purification of the ABCA1 C-terminus

ABCA1 C-terminus was cloned from bp 6,352 to 6,786 (EMBL-GenBank, Accession No. AB055982) in fusion with gluthation S-transferase (GST) in pGEX-5X-1, and expressed in E. coli BL21-Gold (Stratagene) according to the manufacturer's instructions (Amersham Pharmacia Biotech). The fusion protein was purified with glutathione sepharose 4B beads in a batch procedure following manufacturer's instructions (Amersham Pharmacia Biotech).

For expression of ABCA1 with an N-terminal His-tag ABCA1 was cloned in pQE30 (Qiagen) and expressed in E. coli as suggested by the manufacturer. The fusion protein was purified under denaturating conditions using the Ni-NTA Spin Kit (Qiagen) according to the manufacturer's instructions.

3.3. Determination of Protein Concentration

For protein quantification, the bicinchonic acid (BCA) protein assay kit (Pierce) was used. The method is based on the reduction of Cu^{2+}-ions to Cu^{+}-ions in alkaline environment (Biuret reaction). The Cu^{+}-ions form a complex with BCA, a purpled colored complex with peak absorption at 562 nm. The absorption is linear in a range of 20 – 2000 µg/ml and is proportional to the protein concentration.
BCA reagent was freshly prepared by adding 4% CuSO4 to the protein solution at a ratio of 1:50. 25 µl of the sample or the standard were added to a microtiter plate and mixed with 200 µl of the prepared BCA solution. After incubation at 37℃ for 30 min the extinction was measured in an ELISA-reader and the protein concentration was calculated.

3.4. Pull-down Assays

In-vitro translation was performed according to the manufacturer's protocol (Promega). Equal amounts of GST or GST-ABCA1 were incubated with the in-vitro translated proteins overnight at 4℃ while shaking in a total volume of 500 µl of the denoted buffer. The reactions were cleaned up with the GST Micro Spin Purification Module (Amersham Pharmacia Biotech) following the manufacturer's instructions. Washing was carried out in the same buffer as overnight incubation. Bound proteins were eluted by boiling in Laemmli buffer and analyzed by immunoblot.

3.5. Coimmunoprecipitation

HepG2 cells were lysed in PBS with protease inhibitor mixture (Roche Molecular Biochemicals), 0.5% Triton X-100 as described above (IV.3.1.). Three µg of the supernatant were incubated with magnetobeads coupled with Protein-A (Dynal) linked to monoclonal anti-AOX1 antibody overnight at 4℃ while shaking. Washing was performed in PBS with protease inhibitor mixture (Roche Molecular Biochemicals), and 0.5% Triton X-100. Bound proteins were eluted by boiling in Laemmli buffer and analyzed by immunoblot.

3.6. SDS-PAGE and Immunoblot

Proteins are separated by sodium dodecyl sulfate (SDS)-polyacrylamide gel electrophoresis (PAGE) according to their size. For gel electrophoresis, pre-cast gradient gels (BioRad) were used. Protein samples were diluted in 5x Laemmli dye and incubated at 65℃ for 5 min. The samples were loaded on the gel and separated in a BioRad apparatus (25 milliampere per gel, 90 min at room temperature).
After electrophoresis, the gel was transferred to a polyvinylidene fluoride fluotrans transfer membrane using a Mini Trans-Blot electrophoretic transfer cell (BioRad). The transfer conditions were 4℃, 350 milliampere for 1.5 h.
For the immunoblot of AOX1 in different human tissues, a commercial blot from Imgenex (San Diego, CA, USA) was used according to the manufacturer's instructions.
After blotting, the membrane was blocked using 5% nonfat dry milk in PBS-Tween 0.1% at room temperature for 30 min. Afterwards, primary antibodies were applied for 1 h at room temperature or overnight at 4℃. After washing 3 ti mes with PBS-Tween 0.1%, the secondary peroxidase-conjugated antibody was diluted 1:5000 and incubated at room temperature for 1 h. Detection of the immune complexes was carried out with the ECL Western blot detection system (Amersham Pharmacia Biotech) according to manufacturer's instruction.

4. Nucleic Acid Methods

4.1. Sequencing

Cycle sequencing was performed in a Gene Amp PCR System 9600 (Perkin Elmer) using the BigDye Terminator Cycle Sequencing Ready Reaction Kit v.1.1 (Applied Biosystems) according to the manufacturer's instructions.
After purification of the sequencing reaction using Centrisept Spin Colums (Princeton Separations) 4 µl of the sample were mixed with 21 µl HighDye Formamid (Applied Biosystems) in 96-well plates (Applied Biosystems). Signal detection was carried out on an ABI PRISM 3130xl Genetic Analyser equipped with Data Collection Software v3.0 (both Applied Biosystems).

4.2. Polymerase Chain Reaction

By polymerase chain reaction (PCR), specific nucleotide sequences can in vitro be amplified exponentially. The PCR reaction consists of the three steps denaturation (segregation of the doublestrands of the template), annealing (hybridization of the specific oligonucleotides to

the singlestranded template), and elongation (polymerization, resulting in doublestrands). According to the requirements Pwo- or Taq-DNA polymerase were used following the manufacturer's protocols. Pwo-polymerase leads to blunt-end PCR products used for CACC-cloning (IV.4.9.); Taq-polymerase due to its terminal transferase activity adds a single deoxyadenosine to the 3´end of PCR products, making it usable for TA-cloning (IV.4.8.).
Thermocycling was performed in a Gene Amp PCR System 9600 (Perkin Elmer). Initially the template was denatured for 2 min at 95℃. Following 35 cycles of:

Denaturation: 15 sec, 94 ℃
Annealing: 15-60 sec, 40-70 ℃
Elongation: 30-240 sec, 72 ℃

Elongation was completed by incubation for 7 min at 72℃ and the reaction was cooled to 4℃. Afterwards the whole sample was loaded on an agarose gel and following gel electrophoresis (IV.4.3.) the PCR product was purified (IV.4.4.2.).

4.3. DNA Gel Electrophoresis

Different length DNA-molecules can be separated in agarose gels according to their mobility and the negative total charge of the DNA-double helix.
The electrophoretic mobility of the DNA is inversely proportional to the logarithm of base pairs. Polyacrylamid gels are capable of separating DNA fragments up to 1 kb of size, whereas agarose gels separate fragments up to 20 kb. In order to achieve a maximum of separation capacity gels are cast in following concentrations:

DNA fragment size < 1 kb 1.5% - 4% gel
DNA fragment size 1 – 10 kb 0.7% - 1% gel
DNA fragment size > 10 kb 0.5% gel

The applied voltage varied between 80 – 100 volt. To visualize the DNA in the gel, ethidium bromide was incorporated in the gel, and this mutagen substance binds to the DNA double helix, staining it with an orange colored fluorescent light when observed under UV (365 nm). The gel was photographed with a MP-4 camera (Polaroid) or scanned with a Lumi-imager (Boehringer-Mannheim).

4.4. DNA-Purification

4.4.1. Plasmid Purification

For plasmid purification, the QIAprep Spin Miniprep Kit (Qiagen) was used due to the manufacturer's instructions. Shortly overnight cultures of E. coli were collected, and resuspended in resuspension buffer. After lysis and neutralization, the debris including the genomic DNA was separated and the supernatant was loaded on columns containing a silica-matrix. At high salt concentrations DNA binds to this matrix and is after washing eluted in water.

4.4.2. From Agarose Gels and Solutions

DNA-fragments were purified from agarose gels or solution using the respective Qiagen Kit (QIAquick Gel Extraction Kit or PCR Purification Kit) according to the manufacturer's instructions. In brief DNA is mixed with the respective binding buffer (Gel Extraction: QG; PCR Purification: PB), bound to a silica-matrix at a high salt concentration and after washing then eluted in water (30 – 50 µl).

4.5. Enzymatic cleavage

The restriction digest can either be performed analytically to analyze the DNA or preparative to prepare DNA for further cloning. The incubation is performed with buffers obtained from Roche (10x buffers: A, B, L, M, H) for up to 2 h at the according temperature in a thermo block.

For the analytical approach, one µg DNA was digested with 10 units of restriction enzyme in 20 µl total volume. For preparative digestions the following mixture was used:

Vector DNA	50 ng
Restriktionsendonuclease	1.0 µl (3 U)
Buffer	0.7 µl
H_2O	ad 7.0 µl

Samples were incubated for 10 min at 37°C and afterwards the reaction was stopped by incubating for 15 min at 65°C.

4.6. Dephosphorylation of Plasmid-DNA

To prevent re-ligation of cohesive ends dephosphorylation was carried out. Shrimp alcaline phosphatase (SAP) was added to remove the 5´-phosphate.
To the reaction prepared for digestion (IV.4.5.) 0.9 µl 10x dephosphorylationbuffer and 1 µl (1 U) SAP were added. The reaction was incubated for 10 min at 37°C, followed by heat–inactivation of the SAP for 15 min at 65 °C. The sa mple can directly be used for ligation.

4.7. Ligation

In the presence of ATP and Mg2+-ions T4-DNA-ligase is able to covalently join blunt- or cohesive ends by a phosphodiester bridge between a 5´phosphate and a 3´OH group. For ligation the dephosphorylation reaction (IV.4.6.) was supplemented as follows:

Insert-DNA	150 ng
T4 DNA ligase	1.0 µl
5x T4 DNA ligase-buffer	4.0 µl
H_2O	variable
total	20 µL

The mixture was incubated overnight at 14°C or 25 m in at room temperature and subsequently used for transformation of E. coli.

4.8. TA-Cloning

TA cloning is based on the terminal transferase activity of different thermophile polymerases (e.g. Taq-polymerase). Due to this activity during the PCR reaction, an additional, overhanging adenosine is added to the 3´ ends of the product. TopoTA-vectors (pCR2.1-TOPO, pCRII-TOPO) are linearized and posses a 3´overhangig thymine allowing direct ligation of the PCR product. In addition, the vector binds topoisomerase I, an enzyme keeping the vector in its relaxed state.
For the ligation 4 µl purified PCR-product (10-100 ng), 1 µl salt-solution and 1 µl TopoTA vector were mixed and incubated for 15 min at room temperature. The mixture afterwards is placed on ice and used for the transformation of E. coli.

4.9. CACC-Cloning

For the generation of expression constructs for eukaryotic cells or in vitro translation pcDNA3.1D/V5-His-Topo vector was chosen. This vector allows the direct ligation of blunt-

ended PCR-products. Oligonucleotides were designed to amplify the complete coding sequence without the stop-codon. 5´before the ATG CACC was added for directional cloning of the fragment. For the ligation 4 µl purified PCR-product (10-100 ng), 1 µl salt-solution and 1 µl TopoD vector were mixed and incubated for 15 min at room temperature. The mixture afterwards is placed on ice and used for the transformation of E. coli.

4.10. Transformation and Cultivation of E. coli Cells

50 µl of competent cells were thawed on ice, mixed by pipetting with the ligation mixture (5 – 20 µl) and placed on ice for 15 min. In case of ampicillin selection cells were than directly plated on pre-warmed LB-selection plates (37℃) and placed overnight in an incubator at 37℃.

E. coli were cultivated either on agar plates or in liquid medium over night at 37℃ in an incubator. Cultures were obtained by inoculating a single colony or suspension of bacteria from a glycerol culture into LB-medium. Liquid cultures are incubated in a shaker at 37℃ and 240 rpm over night. It is necessary to add an appropriate antibiotic (Ampicillin) to select a specific plasmid. E. coli cultures were permanently stored in glycerol, to achieve this 500 µl liquid culture was mixed with 500 µl sterile glycerol (30%) in a cryotube and were shock frozen in liquid nitrogen and stored at -80℃.

4.11. RNA-Isolation

Harvesting of cells and RNA extraction was carried out according to the manufacturer's instructions using the TRIzol reagent or the RNeasy Mini Kit (Qiagen, Hilden, Germany). For Northern blot, the RNA was isolated by the guanidine isothiocyanate-cesium chloride technique.

Purity and integrity of the RNA was assessed on the Agilent 2100 Bioanalyzer with the RNA 6000 Nano LabChip reagent set (Agilent Technologies). The RNA was quantified spectrophotometrically at 260 nm and then stored at -80℃. The concentration is calculated according to the following formula:

C µg/ml = E260 * k / d

k= 40 for RNA, k = 20 for ss DNA, k = 50 for ds DNA

d = Path length of cuvette [cm]

4.12. cDNA Synthesis

First strand cDNA synthesis was performed with the Reverse Transcription System from Promega. For 2 µg of total RNA (final RNA concentration: 50 ng/µl) the following reaction mixture was prepared:

$MgCl_2$	8 µl
RT-buffer	4 µl
dNTP mix	4 µl
RNAsin	1 µl
AMV reverse transcriptase	1.5 µl
Random Hexamers	4 µl
RNA + H_2O	17.5 µl

The mix was added and the cup was incubated at 42℃ for 60 min. After heat-inactivation at 95℃, the reaction was placed on ice and diluted 1: 5 (final concentration: 10 ng/µl). For longtime storage, samples were put to -20℃.

4.13. Northern Blot Analysis

10 µg of total RNA were separated through a 1.2% agarose gel containing 6% formaldehyde after the secondary structure of RNA has been denaturated at 56℃; the formaldehyde keeps the RNA from renaturating. Following blot onto nylon membranes and crosslinking by UV-irradiation (Stratalinker model 1800, Stratagene), the membranes were hybridized with a cDNA probe amplified with TOSO specific primers. The blots were stripped and subsequently hybridized with a human GAPDH probe (Clontech). The probes were radiolabeled with [α-^{32}P]dCTP using the Oligolabeling kit from Amersham Pharmacia. Hybridization and washing conditions were performed as recommended by the manufacturer of the membrane.

4.14. Gene Chip Expression Analysis

RNA was isolated from 5 d M-CSF cultivated macrophages and macrophages incubated for 4 d with M-CSF and subsequently with 40 µg/ml E-LDL for 24 h. The HgU133A chips from Affymetrix were hybridized starting with 10 µg of total RNA according to the instructions of the manufacturer. Data analysis was performed using the Affymetrix Microarray Suite Version 5.0.

4.15. Real-Time PCR

In conventional PCR, quantification either requires multiple samples or several aliquots must be taken from a single sample at certain intervals. The accuracy of this method is limited because the amplification product has to be detected by ethidium bromide staining, a procedure which lacks sensitivity and specificity and is time consuming. These drawbacks can be eliminated by using a novel method, which uses online-detection of fluorescence as a marker for the ongoing PCR. Two different methods are used in Real-Time-PCR, both of which can be practiced either on the LightCycler system (Roche) or on the ABI Prism 7900 HT Sequence Detection System (Perkin Elmer). One method is based on the fluorescent dye SYBR-Green I, that binds to the minor groove of the DNA double helix. In solution, the unbound dye exhibits very little fluorescence, this is greatly enhanced upon DNA-binding. The second method is based on hydrolysis (TaqMan) probes and is the method of choice at our institute.

4.15.1. Gene Expression Monitoring with Hydrolysis Probes

The hybridization probe format is used for DNA detection and quantification and provides a maximal specificity for product identification. In addition to the reaction components used for conventional PCR, a specially designed, sequence specific oligonucleotide is applied in this detection method. This oligonucleotide is called TaqMan probe, it is labeled with two fluorescent dyes: one is the emitting fluorescent dye (FAM, VIC) and the other is either a fluorescent (TAMRA) or a non-fluorescent quencher. As long as the two dyes are in close proximity, the light emitted from the first dye, is quenched by the other, but as elongation occurs, the probe is hydrolyzed and the two dyes are separated from each other allowing a fluorescence emission. The increasing amount of measured fluorescence is proportional to the increasing amount of DNA generated during the ongoing PCR process.

Per well a reaction is composed of:

Template cDNA	25 ng
TaqMan Mastermix	5 µl
Assay on Demand	0.5 µl
H_2O, nuclease-free	2.5 µl

Reaction conditions are initial denaturation for 10 min at 95℃, after that 15 sec 95℃ and 1 min 60℃ for 45 cycles.

Relative quantification was carried out as described earlier [12].

4.15.2. SNP Analyses with Hydrolysis Probes

This is a common approach to detect SNP following the principle mentioned above (IV.4.15.1.). In contrast to gene expression monitoring, for this application two differently labeled (e.g. one VIC and one FAM) TaqMan probes are used, one for each allele. Hydrolysis of the probe by the 5'-3' endonuclease reaction is greatly impaired when it mismatches its target sequence by even a single nucleotide. According to the resulting fluorescence the analyzed DNA can be discriminated in homozygous (for allele A or B) and heterozygous.

5. The Yeast Two-Hybrid System

The MATCHMAKER Two-Hybrid System is a GAL4-based system providing a transcriptional assay for the identification of protein interaction in vivo in yeast. A short overview is shown in Figure 27. In principle a bait gene is expressed in fusion with the GAL4 DNA-binding domain (BD), while the library-inserts are expressed in fusion with the GAL4 activation domain (AD) [274; 275]. In case of an interaction between bait and library fusion proteins BD and AD are brought in proximity, thereby activating transcription of the reporter genes and enabling growth on selection media.

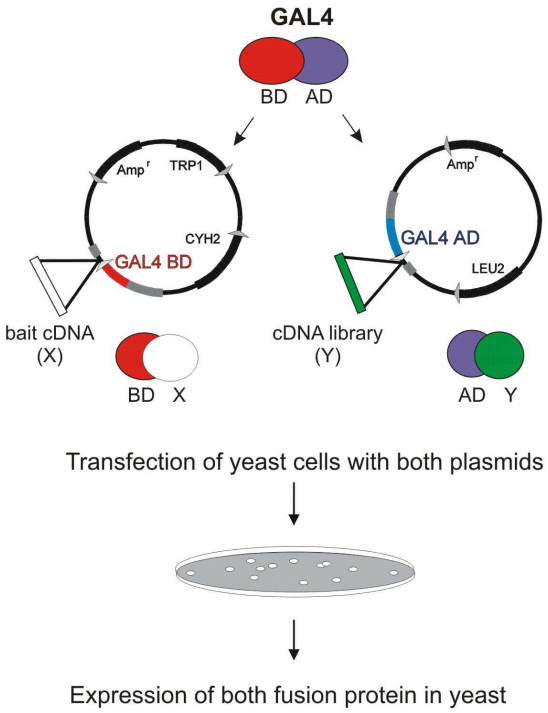

Figure 27. Principle of the yeast two-hydrid screen. Details are found in the text.

Screenings were performed according to the manufacturer's instructions and as previously described [56].

6. Flow Cytometry

The cellular light-scatter signals and three fluorescence signals of 20,000 cells per sample were analyzed in list mode at a channel resolution of 1024 with forward scatter as the trigger parameter on FACSCalibur flow cytometer (Becton Dickinson). The photomultiplier gains were calibrated with polychromatic fluorescent reference beads (Polysciences Europe GmbH). Compensation was adjusted with FITC- and R-PE–coated microbeads (Becton Dickinson). Gating of cells was based on forward- and side-scatter dot plots. Mean fluorescence values were corrected for background by subtraction of cellular autofluorescence in case of fluorochrome-conjugated primary antibodies or fluorescent beads and in case of fluorchrome-conjugated secondary antibodies by subtraction of the mean fluorescence of cells that were incubated with the secondary antibody, but without the primary antibody. For analysis of the list files the CellQuest 2.0 software (Becton Dickinson) was used on a Macintosh G3.

7. Immunohistochemistry

Rudolph Jung performed immunohistochemistry (IHC) and Prof. Dr. Arndt Hartmann evaluated the slides (both from the Institute of Pathology, University of Regensburg).
Immunohistochemical studies for the expression of ABCA1 and AOX1 utilized an avidin-biotin peroxidase method with a 3,3‘-diaminobenzidine (DAB) chromatogen. Four µm sections were cut from formalin-fixed and paraffin wax-embedded tissues. After deparaffinization for 10 min in xylol, tissue sections were rehydrated in descencing ethanol series. After antigen retrieval (microwave oven for 10 min at 250 W in citrate buffer (pH 7.1)) IHC was carried out in a NEXES immunostainer (Ventana, Tucson, AZ) following manufacturer’s instructions. The following primary antibodies were used: anti-ABCA1 (dilution 1:10), and anti-AOX1 (dilution 1:50). For target proteins the ChemMate detection kit (DAKO, Glostrup, Denmark) was used, and finally the slides were counterstained with haematoxylin for 1 min. Incubation with the primary and secondary antibody was performed according to the manufacturer’s protocol. Normal hepatocytes were chosen as internal positive control for ABCA1 and AOX1 IHC. A surgical pathologist (A.H.) performed a blinded evaluation of the slides without knowledge of clinical data. Causes of non-interpretable results included lack of tumor tissue and presence of necrosis or crush artefact. Cytoplasmic ABCA1 and AOX1 staining intensity was estimated using a semiquantitative four-step scoring system (0-3+): 0, negative; 1+, weak positive; 2+, moderate positive; 3+, strong positive.

7.1. Tissue Microarray

ABCA1 and AOX1 protein expression in hepatocellular and renal carcinomas was assessed using tissue microarrays (TMAs). Commercially available liver (LV801) and kidney (KD801) tumor TMAs were obtained from BioCat (Heidelberg, Germany). Additionally, a hepatocellular carcinoma (HCC) TMA from the Institute of Pathology, University of Basel, Switzerland and a renal tumor TMA from the Department of Urology, University of Regensburg were used. The hepatocellular TMA contained a consecutive series of 233 non-selected, formalin-fixed, paraffin-embedded primary HCC, 119 specimens with liver cirrhosis, and 18 normal liver samples. The kidney TMA contained a consecutive series of 90 non-selected, formalin-fixed, paraffin-embedded primary renal cell carcinomas (RCC) (stage I - IV) and 16 oncocytomas. Before construction of the TMAs, an experienced surgical pathologist evaluated haematoxilin-eosin-stained slides of all specimens to identify representative areas. In the process of histological review all carcinomas were graded using a three-tired nuclear grading system (G1-3) according to WHO criteria (2000).

8. Statistical Analysis

Data are given as mean value ± standard deviation. Significance was calculated using two-tailed Students t-test and $p < 0.05$ was regarded as significant.

8.1. Tissue Microarray Data

Dr. Peter J. Wild performed analyses of TMA data (from the Institute of Pathology, University Hospital Zürich, Switzerland).
Statistical analyses were performed completed using SPSS version 13.0 (SPSS, Chicago, IL, USA). Differences were considered statistically significant when P values were <0.05. Contingency table analysis and two-sided Fisher's exact tests were used to study the statistical association between clinicopathologic and immunohistochemical parameters.

V. RESULTS

The identification and characterization of proteins involved in lipid metabolism is in the main focus of the institute. Two different approaches were chosen, the first was to identify ABCA1 or ABCA7 related proteins by yeast two-hybrid screen, the other was to search for genes that reveal “ABCA1-like” regulation in response to lipid loading.

1. Constructs for the Yeast Two-Hybrid screens

For the yeast two-hybrid approaches five bait constructs were created. The denoted regions of ABCA1, ABCA7, TAX1BP3 and syntaxin 13 were cloned in pAS2-1 and the indicated Matchmaker Libraries (Clontech) were screened for putative interaction partners (Table 6).

Table 6. Bait constructs and Libraries used in this work for the yeast two-hybrid screens.

Gene	Construct	Region	Amino Acids	Accession No.[§]	Library
ABCA1	pAS-A1-CT	C-terminus (144 aa)	2118-2261	NP_005493	Placenta
ABCA7	pAS-A7-NT	N-terminus (144 aa)	1-144	NP_061985	Bone marrow
ABCA7	pAS-A7-CT	C-terminus* (144 aa)	1865-2008 2003-2146	NP_150651 NP_061985	Bone marrow Spleen
TAX1BP3	pAS-TAX1BP3	full-length (124 aa)	1-124	NP_055419	Placenta
Syntaxin 13	pAS-STX13	full-length (276 aa)	1-276	NP_803173	Placenta

[§] EMBL-GenBank
* The C-terminal 144 amino acids are identical in both isoforms.

2. ABCA1 C-terminal Interactive Proteins

In order to identify new ABCA1 C-terminus interacting proteins a yeast two-hybrid screen was performed. Furthermore the interaction of AOX1 and ABCA1 was confirmed and characterized in more detail.

2.1. ABCA1 Interacting PDZ Proteins

Screening with pAS-A1-CT (Table 6) identified 5 putative ABCA1 C-terminus interacting PDZ proteins. Those are shown together with the structure of SNTB2 in Figure 28. SNTB2 is also a PDZ protein shown to bind the ABCA1 C-terminus in our laboratory recently and therefore is also indicated here.

Short	Full name	OMIM/Accession No.[§]
GIPC1	GAIP C-terminus-interacting protein1	*605072
TAX1BP3	Tax1 (human T-cell leukemia virus type I) binding protein 3	NM_ 014604
SDCBP	Syndecan-binding protein	*602217
Scribble	Scribble, drosophila, homolog of	*607733
MAGI3	Membrane associated guanylate kinase, WW and PDZ domain containing 3	NM_020965 (variant 1) NM_152900 (variant 2)

[§] EMBL-GenBank

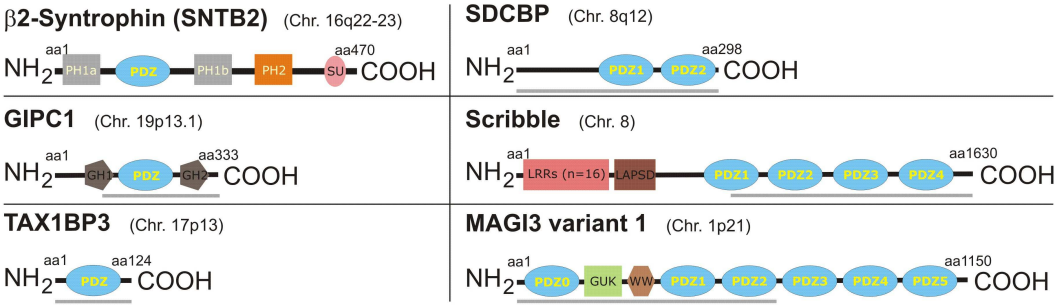

Figure 28. ABCA1 C-terminus interacting PDZ candidates. Upper panel: names and OMIM entries of the PDZ proteins found in the yeast two-hybrid screen. Lower panel: Structure of the identified PDZ proteins together with SNTB2. MAGI3 variant 1 and variant 2 differ by a region of 25 amino acids located between the WW-domain and PDZ domain 1, that is absent in variant 2. Grey bars indicate the regions found in the yeast two-hybrid screen. aa, amino acid; COOH, C-terminus; GH, GIPC1 homology domain; LAPSD, LRR and PDZ-specific domain; LRR, Leucin-rich Repeat domain; NH_2, N-terminus; PDZ, PSD95/Discs-large/ZO-1 domain; PH, pleckstrin homology domain; SU, syntrophin-unique domain.

The first aim was to confirm the interaction of ABCA1 protein with these candidates.

2.1.1. Verification of the Interaction of PDZ Proteins with ABCA1 by Co-Transformation in Yeast

To reconfirm the binding of the ABCA1 C-terminus to the putative PDZ-interaction partners in yeast a yeast cotransformation was performed. The complete coding sequence of the candidate genes was cloned in a yeast two-hybrid prey vector (GIPC1 in pAS2-1, all other in pGADT7) to get fusion proteins with the activation domain of the GAL4 transcription factor, suitable for a cotransformation according to the yeast two-hybrid principle. The PDZ protein GIPC2 initially identified as putative ABCA7 interaction partner was also included. Besides, different ABCA1-GAL4-BD constructs were created to proof the specific PDZ interaction, which is based on an intact PDZ binding sequence of ABCA1 (ESYV, class I, consensus: X-S/T-X-V/L; X: any amino acid, S: serine, T: threonine, V: valine, L: leuzine) and a free C-terminus.

1	wt	EKVKESYV Stop
2	deletion of the stop codon	EKVKESYVGSVDLQPS Stop
3	deletion of the PDZ binding sequence	EKVK Stop
4	mutation of the PDZ binding sequence	EKVKERYG Stop

GAL4-BD-construct 1 is wild type, and should enable yeast to grow on plates selecting on interaction when cotransformed with the candidate genes. In the other three constructs the PDZ binding sequence was modified by attaching additional amino acids (construct 2), deletion (construct 3) or mutation of the key amino acids (construct 4). All modifications should abolish interaction thereby preventing growth on plates selecting for interaction. Figure 29 shows that, as expected for a specific PDZ interaction, only cotransformants containing construct 1 and one of the candidate prey constructs are able to grow under conditions selecting for interaction.

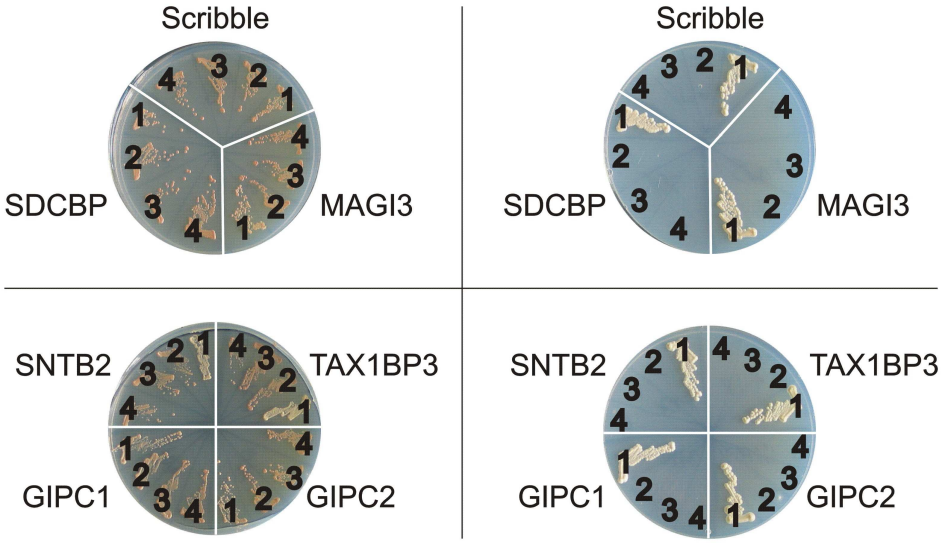

Figure 29. Verification of the specific PDZ interaction of ABCA1 C-terminus and PDZ candidates. Left: Selection medium lacking trp and leu, allowing growth of yeast containing prey and bait construct. Right: Selection medium lacking trp, leu and his, selecting for interaction of prey and bait construct.

2.1.2. Verification of the Interaction In Vitro

To validate the interaction of ABCA1 with PDZ proteins by coimmunoprecipitations expression-constructs were generated. ABCA1 C-terminus was cloned in the pGEX5X-1 vector, and expressed in E. coli as an N-terminal GST fusion protein. The N-terminal fusion was important to prevent blocking of the C-terminal PDZ binding sequence of ABCA1. The coding sequence of the candidate genes was cloned in pcDNA3.1D/V5-His-TOPO vector and used for in vitro translations, resulting in fusion proteins with C-terminal V5-tags. GST-ABCA1 and GST (control) were purified using the GST-epitope and incubated together with the products from the in vitro translation using different incubation conditions (PBS, PBS containing 0.1, 0.5, 1 % Triton X-100 or NP40). After immunoblot, detection was performed with a monoclonal anti-V5 antibody. This confirmed the specific binding of TAX1BP3 (in PBS) and GIPC1 (in PBS containing 1% Triton X-100) with the ABCA1 C-terminus (Fig. 30 A).
To proof this finding with full-length ABCA1 HepG2 lysate (PBS containing 0.5 % Triton X-100) was incubated with in vitro translated, V5-tagged TAX1BP3 and GIPC1, respectively, and precipitated with a mouse monoclonal anti-V5-antibody (control mouse monoclonal anti-MYC-antibody). Detection was done with the monoclonal anti-ABCA1 antibody. Both TAX1BP3 and GIPC1, specifically bind ABCA1 under this conditions (Fig. 30 B).

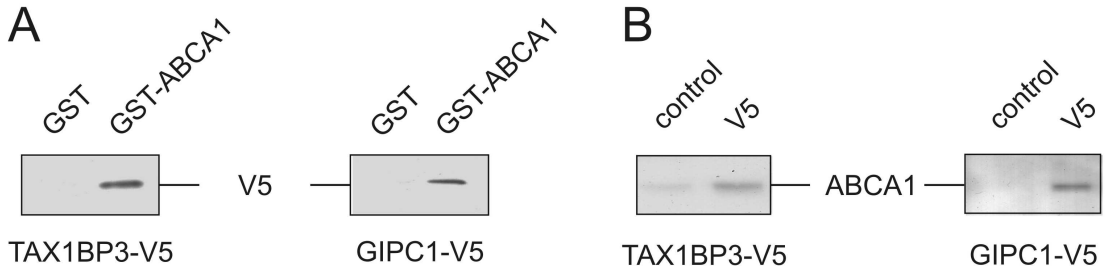

Figure 30. Specific binding of TAX1BP3 and GIPC1 to the ABCA1 C-terminus. (A) In vitro translated TAX1BP3 and GIPC1, respectively, was incubated with GST-ABCA1-C-terminus or GST alone. **(B)** HepG2 lysate was incubated with in vitro translated, V5-tagged TAX1BP3 and GIPC1, respectively, and precipitated with a mouse monoclonal anti-V5-antibody.

To further confirm the interaction of ABCA1 with MAGI3, Scribble and TAX1BP3, and to identify new ABCA1 interacting PDZ proteins a PDZ-array was screened using HIS-tagged ABCA1 C-terminus as probe. ABCA1 C-terminus was cloned in the pQE30 vector and expressed in E. coli, leading to a fusion protein with an N-terminal HIS-tag. The PDZ-array consists of single PDZ domains, enabling to specify the interaction of ABCA1 and PDZ domain proteins containing more than one PDZ domain in more detail. As shown in Figure 31 ABCA1 C-terminus strongly binds to the PDZ domain of TAX1BP3, PDZ domain 2 of MAGI3, PDZ domain 1 of Scribble and in addition to PDZ domain 3 of MAGI2. This further affirmed the direct interaction of ABCA1 with TAX1BP3, MAGI3 and Scribble and identified MAGI2 as putative new ABCA1 interaction partner.

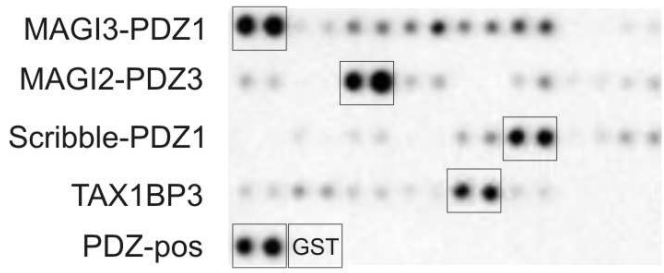

Figure 31. Screening of a PDZ-array with the His-tagged C-terminal 144 amino acids of ABCA1.

2.1.3. Co-Expression Analysis of ABCA1 and Interacting Proteins

To get more insight in the role of the PDZ-interaction with ABCA1 the co-expression of the putative ABCA1-interacting PDZ proteins with ABCA1 and the already published interaction partners SNTA1, SNTB1, and SNTB2 was analyzed in different tissues by TaqMan real-time RT-PCR. The results are presented in a linear scale, reaching from 1 (weak expression) to 5 (strong expression) dots (Table 7).

Table 7. mRNA Expression of ABCA1 and selected PDZ proteins in human tissues.

Tissue	ABCA1	SNTA1	SNTB1	SNTB2	GIPC1	GIPC2	TAX1BP3	SDCBP	MAGI3	Scribble
Brain, whole	●	●●●●●	●	●	●●	●	●●	●●●	●●●	●●
Brain, cerebellum	●	●●	●	●	●●	●	●	●●	●	●●
Spinal Cord	●●●●	●●●	●	●	●●●	●	●●●●	●●●●	●●●●	●●●
Heart	●	●●●●	●	●	●	●	●●	●	●	●
Skeletal Muscle	●	●●●●	●	●	●	●	●	●	●	●
Lung	●●●●	●	●●	●	●	●●	●●●●	●	●	●●
Kidney	●●●●	●●●●	●●	●●●●●	●●	●●●●●*	●	●●●●	●●●●●	●●
Liver	●●	●	●	●	●	●	●	●	●	●
Stomach	●●	●	●●	●	●●	●	●●●●●	●●●	●●●	●●
Small Intestine	●●	●	●	●	●●	●●●●●	●●●●	●●	●●●	●●
Colon	●●	●	●	●	●●●●●	●●	●●●●●	●	●●	●●●●●
Salivary Gland	●	●	●●	●	●	●	●	●	●	●
Thyroid	●●●	●●●	●●●●●	●●●	●●	●	●●	●●●	●●●●●	●
Adrenal Gland	●●●●●	●	●●●	●	●	●●	●●●	●	●	●
Testis	●●	●●	●	●●●●●	●	●	●	●●	●●●	●●
Prostate	●●	●	●	●●●	●	●	●	●	●	●
Uterus	●●●	●	●	●●●	●	●	●	●●●	●●	●●
Placenta	●●●●	●	●	●	●	●	●●●	●●●●●	●●	●●
Thymus	●●●	●	●	●●	●	●	●●	●	●	●
Spleen	●●●	●	●	●	●	●●●	●●	●●●	●	●
Bone Marrow	●	●	●●●	●	●	●	●	●●●●●	●	●

Experiments were performed in triplicate and results were converted to a linear scale (●●●●●: 81-100% of highest expression; ●●●●: 61-80%; ●●●: 41-60%; ●●: 21-40%; ●:>0-20%;* very high expression). Tissues with the highest expression are highlighted (yellow).

ABCA1, SNTA1, SNTB2, GIPC2, SDCBP and MAGI3 are highly expressed in kidney; ABCA1, TAX1BP3, SDCBP, and MAGI3 are highly expressed in spinal cord. In general, the proteins display a different tissue expression, though mRNA expression is not necessarily identical to protein expression.

2.2. Verification and Characterization of the Interaction of AOX1 and ABCA1

2.2.1. AOX1 is an ABCA1 Interacting Protein

In a previous yeast two-hybrid screen of a human liver library fourteen AOX1 clones (common region: amino acids 972 to 1338 (EMBL-GenBank, Accession No. NP_001150)) were found to interact with the ABCA1 C-terminus [56].

The interaction of AOX1 with ABCA1 was confirmed by a pull-down assay using a recombinant GST-fusion protein of the ABCA1-C-terminus (GST-ABCA1) and an in vitro translated human AOX1-fragment (amino acids 972 - 1338) found in the yeast two-hybrid screen. Equal amounts of purified GST-ABCA1 protein or GST alone were immobilized on glutathione sepharose beads and incubated with HA-tagged AOX1. Binding of AOX1 was investigated by immunoblot using a monoclonal anti-HA-Tag antibody. As shown in Figure 32A GST-ABCA1 binds significant amounts of AOX1, in contrast to GST alone. This indicates a direct interaction of ABCA1 and AOX1 in vitro.

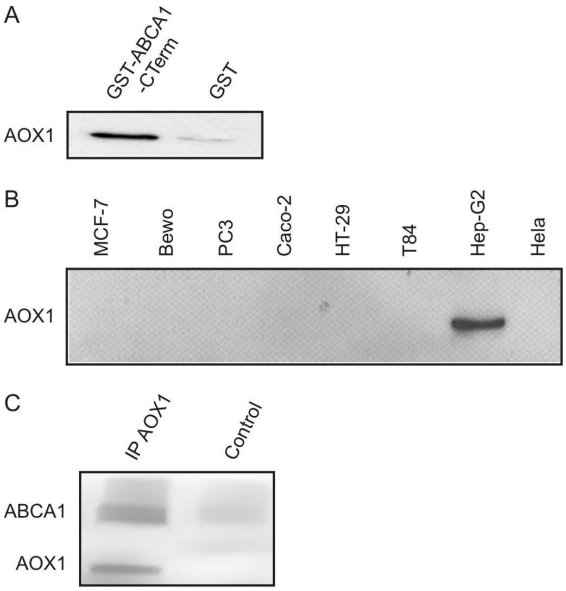

Figure 32. Confirmation of the interaction of AOX1 with ABCA1 and expression of AOX1 in human cell lines. (A) Interaction of AOX1 and ABCA1 demonstrated by pull-down assay. In vitro translated AOX1 fragment (aa 972-1338) with an N-terminal HA-Tag was precipitated by ABCA1 C-terminus with an N-terminal GST fusion or GST alone. Precipitates were analyzed on immunoblots using an anti-HA antibody. **(B)** Immunoblot showing the abundance of AOX1 in different human cell lines. **(C)** Interaction of AOX1 with ABCA1 demonstrated by coimmunoprecipitation. AOX1 antibody was linked to magnetic beads and incubated with lysate from HepG2 cells. Precipitates were analyzed on immunoblots for AOX1 and ABCA1 using the respective antibodies.

Different human adenocarcinoma cell lines (MCF-7 breast, PC3 lung, CaCo-2 colon, HT-29 colon), carcinoma cells (T84 colorectal, HepG2 hepatocellular, HeLa cervix) together with the placental choriocarcinoma BeWo cell line were analyzed by immunoblot for the expression of AOX1. Only HepG2 cells showed clearly detectable levels of AOX1 proteins (Fig. 32 B), and therefore HepG2 cells were chosen for further analysis of the AOX1/ABCA1 interaction. ABCA1 could be precipitated from HepG2 cell lysates using a monoclonal anti-AOX1-antibody, indicating that ABCA1 also interacts with AOX1 in vivo (Fig. 32 C).

2.2.2. Knock-down of AOX1 Expression by siRNA Reduces ABCA1-related Cellular Functions

The physiological role of the AOX1-ABCA1 interaction was further elucidated in HepG2 cells by an AOX1 siRNA approach. Indeed, AOX1 siRNA, but not the non-silencing RNA, significantly decreased AOX1 mRNA and protein levels at 100 nM (Fig. 33 A and B). Higher concentrations of siRNA (up to 300 nM) resulted in no further decrease of protein (data not shown). The decrease of AOX1 protein was detectable between 24 and 72 hrs after siRNA transfection by immunoblots. ABCA1 mRNA and protein levels were unaffected in response to AOX1 siRNA treatment, indicating that knock-down of AOX1 does not affect ABCA1 mRNA or protein abundance (Fig. 33 A and B).

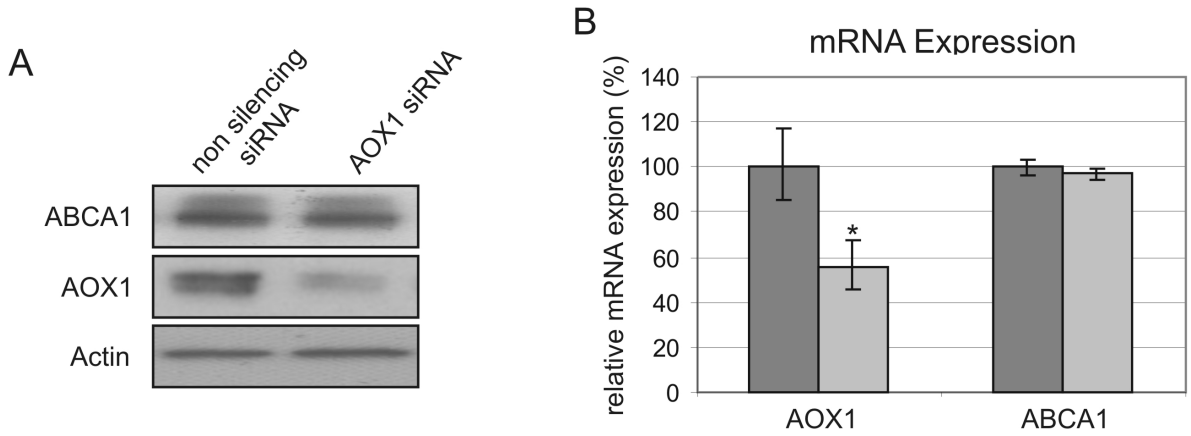

Figure 33. Effect of AOX1 siRNA on AOX1 and ABCA1 mRNA and protein level. (A) Immunoblot showing the abundance of AOX1 and ABCA1 in HepG2 cells treated with AOX1- or non silencing control-siRNA. Lysates were analyzed by immunoblot for AOX1 and ABCA1 using the respective antibodies. β-Actin is shown as loading control. **(B)** mRNA expression of AOX1 and ABCA1 in HepG2 cells treated with AOX1- or non silencing control-siRNA. Expression was analyzed using TaqMan real-time RT-PCR. Compared to control AOX1 siRNA reduced AOX1 mRNA by 50 ± 10% while ABCA1 levels were not changed.

Regarding the crucial role that ABCA1 plays in apoA-I-dependent cellular cholinephospholipid- and cholesterol-efflux, the effect of AOX1 knock-down on lipid efflux was determined. HepG2 cells treated with AOX1 siRNA showed a significantly reduced efflux for cholinephospholipids (66 ± 27 %) and cholesterol (51 ± 31 %) as compared to controls (Fig. 34 A). These results indicate that AOX1 not only interacts with ABCA1 but also enhances the functional activity of ABCA1 by a yet unknown mechanism.

Recent findings linked ABCA1 function to the phagocytic compartment [64] and hepatocytes have been described to be able to engulf apoptotic bodies [276]. Therefore, we analyzed the effect of AOX1 knock-down on phagocytic activity of HepG2 cells. Cells treated with AOX1 siRNA show enhanced uptake of fluorescence-labeled phagobeads (50 ± 6 %, Fig. 34 B), as compared to cells treated with non silencing siRNA. These data further emphasize the influence of AOX1 on ABCA1 function.

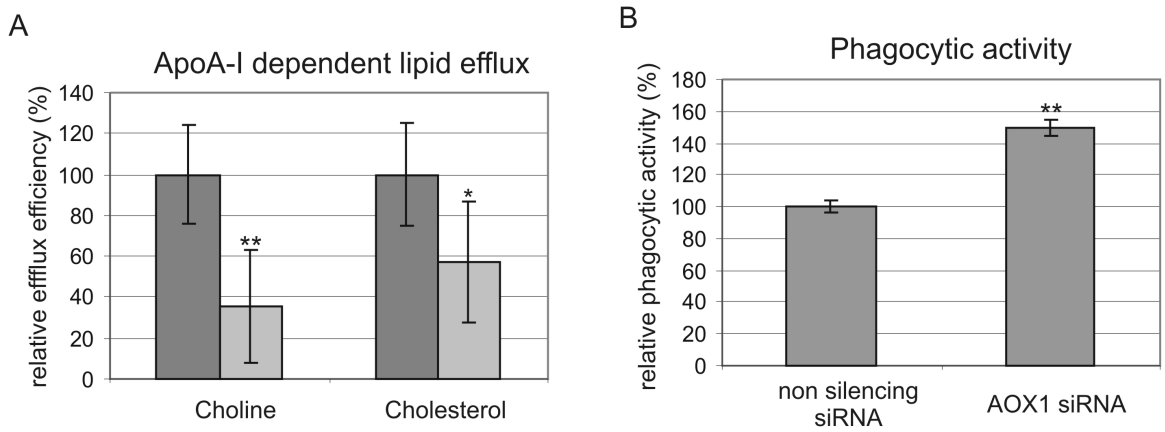

Figure 34. Analysis of lipid efflux and phagocytic activity in HepG2 cells treated with AOX1 or non-silencing control siRNA. Experiments were performed three times in triplicate and cells treated with non-silencing siRNA were set to 100%. **(A)** apoA-I-specific cholinephospholipid- and cholesterol-efflux. Bars represent non-silencing siRNA treated cells (grey) and AOX1 siRNA treated cells (light gray). **(B)** Phagocytic activity. Cells were loaded with fluoresbrite yellow green microspheres and analyzed by flow cytometry. ** $p < 0.001$; * $p < 0.01$.

2.2.3. Expression pattern of AOX1 in Human Tissues

As a next step, the mRNA expression of AOX1 in different human tissue samples was analyzed. AOX1 mRNA was significantly expressed in liver, kidney, testis, ovary, and adrenal gland. All other tissues analyzed showed relative low AOX1 mRNA levels when compared to adrenal gland (Table 8).

Table 8. Relative mRNA expression of AOX1 and ABCA1 in human tissues.

Tissue	ABCA1	AOX1
Brain, whole	●	●
Brain, cerebellum	●	●
Spinal Cord	●●●●	●
Heart	●	●
Skeletal Muscle	●	●
Lung	●●●●	●
Kidney	●●●●	●●●
Liver	●●	●●
Stomach	●●	●
Small Intestine	●●	●
Colon	●●	●
Salivary Gland	●	●
Thyroid	●●●	●
Pancreas	●	●
Adrenal Gland	●●●●●	●●●●●
Testis	●●	●●
Ovary	●●	●●
Prostate	●●	●
Mammary	●	●
Uterus	●●●	●
Placenta	●●●●	●
Thymus	●●●	●
Spleen	●●●	●
Bone marrow	●	●

Experiments were performed in triplicate and results were converted to a linear scale (●●●●●: 81-100% of highest expression; ●●●●: 61-80%; ●●●: 41-60%; ●●: 21-40%; ●:>0-20%). Tissues with the highest expression are highlighted (yellow).

AOX1 protein was also determined in different human tissues and the highest expression was found in the liver, followed by kidney, ovary and testis. Weak expression was detected in the heart, lung, brain, stomach and spleen, while no AOX1 protein could be observed in skeletal muscle and small intestine (Fig. 35).

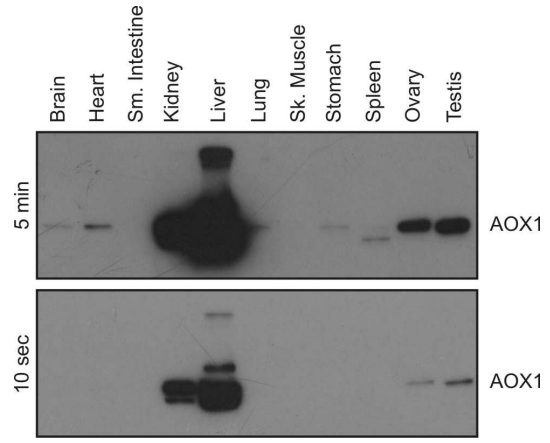

Figure 35. Immunoblot showing the abundance of AOX1 in different human tissues. Two exposure times (10 sec and 5 min) are shown because of the big difference of AOX1 expression in different tissues.

In order to assess the cellular distribution of AOX1 and ABCA1 proteins, immunohistochemistry for both proteins was performed on human tissue sections from organs with the highest AOX1 expression as detected by immunoblots. This work was performed by Rudolph Jung and evaluated by Prof. Dr. Arndt Hartmann from the Institute of Pathology, University of Regensburg. ABCA1 expression showed a broad cellular distribution in liver, kidney, adrenal, testicular and ovarian tissues. Expression of AOX1 was confined to hepatocytes, proximal tubular epithelial cells of the kidney, cortical but not medullary cells of the adrenal gland, testicular Leydig cells, and theca externa cells in ovaries (Fig. 36).

2.2.4. In Silico Promoter Analysis of AOX1

To gain more insight in the regulation of AOX1 an in silico promoter analysis was performed. The genomic regions 773 bp upstream of the translation start of human, chimpanzee, and rhesus monkey was compared using Transfac (http://www.biobase.de/cgi-bin/biobase/transfac) and Genomatix MatInspector (http://www.genomatix.de). Specific transcription factors found in all three species with both tools are shown in Figure 37.

					Genomatix			Transfac	
Factor	Strand	Start	End	Sequence	Opt. threshold	Matrix sim	Core sim	Matrix match	Core match
AREB6	-	703	715	tcccAGGTGccc	0,96	0,97	1	0,98	1
CREB	+	540	560	ccagTGACGccc	0,89	0,91	1	0,91	1
Elk-1	-	516	536	tgatTTCCGcccac	0,91	0,92	1	0,94	1
HIF-1	+	555	567	cacACGTGctgg	0,93	0,99	1	0,95	1
MAZR	-	667	679	aagCCCCGcccca	0,88	0,92	1	0,93	0,92
N-Myc	+	556	568	acacACGTGctg	0,92	0,98	1	0,99	1
Sox-5	-	285	301	tgATTGTtta	0,87	0,99	1	0,99	1
Sox-9	+	766	782	acaccACAATggac	0,9	0,92	1	0,94	1
Whn	+	465	475	acaGACGCtaa	0,95	0,97	1	0,99	1

Figure 37. Putative transcription factors influencing AOX1 transcription. TFs are shown together with their localization, sequence and similarity scores.

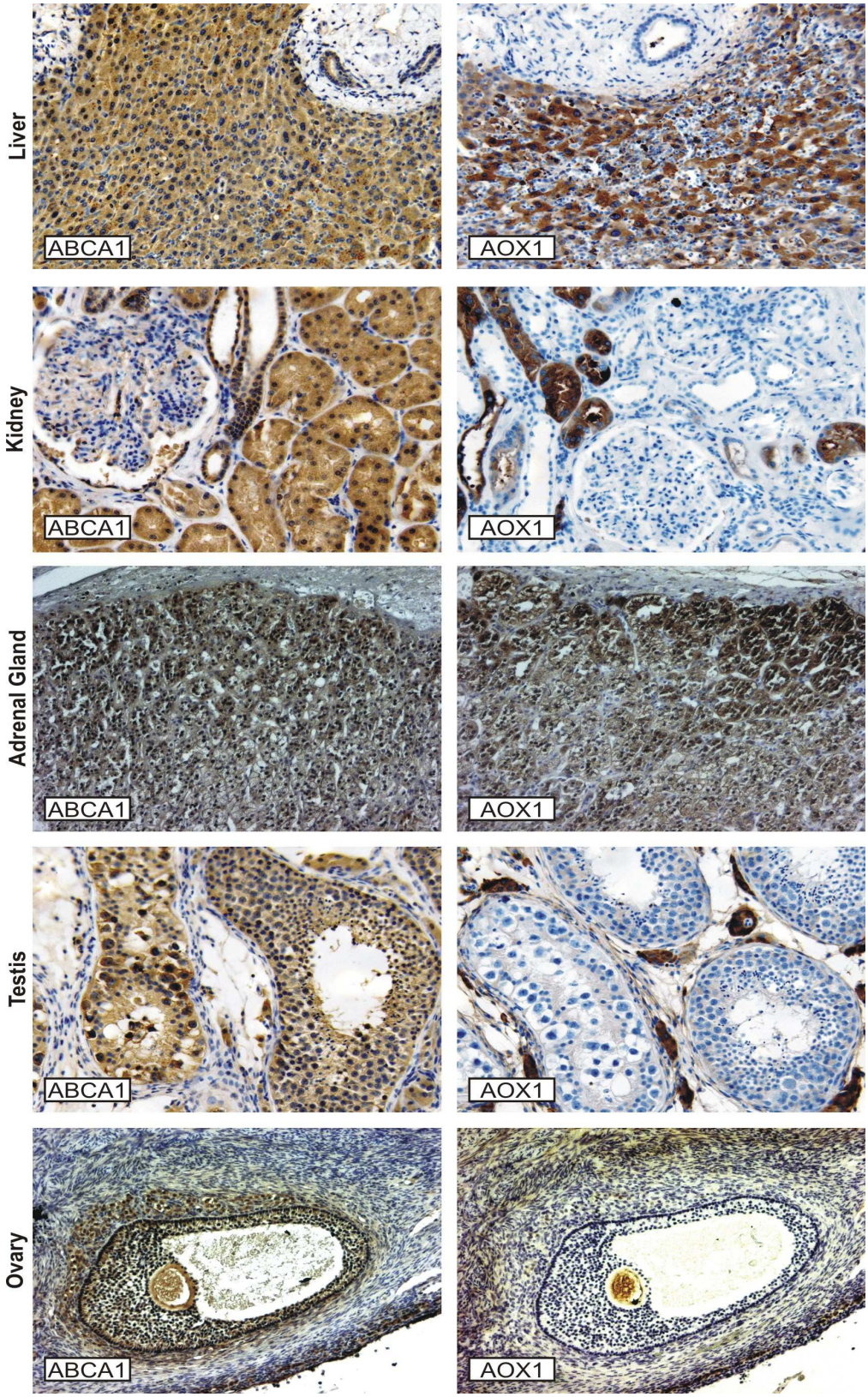

Figure 36. Immunohistochemistry of AOX1 and ABCA1 in different human tissues. Immunohistochemical analysis showed that AOX1 and ABCA1 are coexpressed in hepatocytes, kidney proximal tubules, adrenal gland cortical cells, and Leydig cells in testis. ABCA1 and AOX1 were stained utilized an avidin-biotin peroxidase method with a DAB chromatogen. Nuclei were counterstained with haematoxylin. Magnification 100 fold.

2.2.5. Analyses of ABCA1 and AOX1 in Tissue Microarrays

In order to elucidate in more detail the potential role of the AOX1/ABCA1 interaction we analyzed the protein expression of both genes by immunohistochemistry in tumors of kidney (RCC), liver (HCC), and testicular Leydig cells (Leydig cell tumor, LCT). Staining was performed by Rudolph Jung and Prof. Dr. Arndt Hartmann evaluated the results (both from the Institute of Pathology, University of Regensburg). Statistical analysis of the data was performed by Dr. Peter J. Wild (Institute of Pathology, University Hospital Zürich, Switzerland).

2.2.5.1. Expression in Normal Kidney and RCC

Expression of ABCA1 and AOX1 was investigated by immunohistochemistry using a commercial kidney TMA. In normal human kidney 100% (35/35) of controls were found positive for ABCA1 and 97% (34/35) for AOX1. In contrast, 54% (21/39) and 15% (6/39) of the samples from RCC were ABCA1 and AOX1 positive, indicating reduced AOX1 and ABCA1 expression. This finding was supported by a second independent TMA with RCC and onkozytomas (Table 9).

Table 9. ABCA1 and AOX1 protein expression in RCC and oncocytomas in relation to clinico-pathologic parameters and results of immunohistochemistry.

Variable	Categorization	AOX1 expression					p†	ABCA1 expression					p†
		n analyzable	negative	score 1+	score 2+	score 3+		n analyzable	negative	score 1+	score 2+	score 3+	
Clinico-pathologic data:													
Age at diagnosis													
	≤65 years	48	42	1	5	0	0,792	47	19	14	13	1	1,000
	>65 years	43	38	1	3	1		43	18	12	12	1	
Gender													
	female	30	27	0	2	1	0,274	30	15	12	3	0	0,212
	male	39	31	2	6	0		39	19	10	10	0	
Histologic tumor type													
	Clear cell RCC	31	28	0	3	0	0,174	31	14	9	8	0	**0,005**
	Papillary RCC	24	17	2	4	1		24	14	6	4	0	
	Chromophobe RCC	22	21	0	1	0		21	8	8	3	2	
	Oncocytoma	14	14	0	0	0		14	1	3	10	0	
Tumor stage*													
	pT1a	28	23	2	3	0	0,660	28	13	10	5	0	0,271
	pT1b	17	15	0	2	0		17	9	6	2	0	
	pT2	8	8	0	0	0		8	6	2	0	0	
	pT3a	8	6	0	1	1		8	5	2	1	0	
	pT3b	9	7	0	2	0		9	2	2	5	0	
Regional lymph node status*													
	pN0	65	58	2	5	0	**0,001**	65	35	19	11	0	**0,029**
	pN1-2	5	1	0	3	1		5	0	3	2	0	
Histologic grade*													
	G1	12	11	1	0	0	0,149	12	7	3	2	0	0,130
	G2	49	42	1	6	0		49	26	16	7	0	
	G3	10	7	0	2	1		10	2	3	5	0	
UICC stage*													
	I	38	32	2	4	0	0,158	38	18	13	7	0	0,435
	II	7	7	0	0	0		7	5	2	0	0	
	III	12	11	0	1	0		12	6	2	4	0	
	IV	8	4	0	3	1		8	2	4	2	0	
Immunohistochemistry (IHC):													
ABCA1								AOX1 IHC					
	negative	37	35	0	2	0	0,368	79	35	20	22	2	0,368
	score 1+	26	20	2	3	1		2	0	2	0	0	
	score 2+	25	22	0	3	0		8	2	3	3	0	
	score 3+	2	2	0	0	0		1	0	1	0	0	

* only RCC were included.
† Fisher's exact test (2-sided); bold face representing significant data

Investigation of immunohistochemical ABCA1 and AOX1 expression in renal tumors was informative in 84.9% (90/106) and 85.8% (91/106) of cases, respectively. Cytoplasmic ABCA1 and AOX1 protein expression of any intensity (score 1+-3+) was detected in 58.9% (53/90) and 12.1% (11/91) of informative cases. No significant association between ABCA1 and AOX1 immunoreactivity could be found (data not shown). Clinicopathologic and immunohistochemical characteristics were associated with ABCA1 and AOX1 IHC for descriptive data analysis. ABCA1 immunoreactivity was significantly lost in RCCs compared to oncocytomas (p=0.005). In the subgroup of RCCs, no significantly different ABCA1 (p=0.382) and AOX1 (p=0.160) expression between clear cell, papillary and chromophobe carcinomas was found. ABCA1 and AOX1 staining was significantly associated with positive nodal status (p=0,029 and p=0,001).

2.2.5.2. Expression in Normal Liver and HCC

Expression of ABCA1 and AOX1 was investigated by immunohistochemistry using a commercial liver TMA. In normal human liver 62% (24/39) of controls were found positive for ABCA1 and 100% (39/39) for AOX1. In contrast, 68% (28/41) and 59% (24/41) of the samples from HCC were ABCA1 and AOX1 positive, indicating reduced AOX1 and enhanced ABCA1 expression, respectively. This finding was supported by a second independent TMA with HCC, normal and cirrhotic liver specimens (Table 10). AOX1 and ABCA1 protein expression of any intensity (score 1+-3+) was detected in 77.5% (134/173) and 89.0% (146/164) of HCC, respectively. Again, AOX1 expression was significantly reduced from normal liver (100% expression) to cirrhosis (92.5%) to HCC (77.5%). Accordingly, expression of ABCA1 significantly increased from normal liver (56.3%) to cirrhosis (87.3%) to HCC (89.0%). AOX1 and ABCA1 immunoreactivity (intensity score 1+-3+) co-associated significantly in 69.5% of cases (107/154), whereas simultaneous negative AOX1 and ABCA1 expression (score 0) was found only in 6.8% (8/154) of cases (P=0.032).
For descriptive data analysis, clinico-pathologic characteristics of HCC were associated with AOX1 and ABCA1 IHC (Table 10). Loss of AOX1 staining was significantly associated with higher tumor stages (P=0.008), positive nodal status (P=0.005), and occurrence of distant metastases (P=0.037). Loss of ABCA1 expression was associated with positive nodal status (P=0.021) and occurrence of distant metastases (P=0.014). In general, loss of AOX1 and ABCA1 expression was associated with negative pathologic parameters in HCC.

Table 10. ABCA1 and AOX1 protein expression in HCC in relation to clinico-pathologic parameters and results of immunohistochemistry

Variable	Categorization	AOX1 expression						ABCA1 expression					
		n analyzable	negative	score 1+	score 2+	score 3+	p†	n analyzable	negative	score 1+	score 2+	score 3+	p†
Clinico-pathologic data:													
Histologic tumor type													
	hepatocellular carcinoma	173	39	15	36	83	**0.004‡**	164	18	45	80	21	**0.028‡**
	cirrhosis	80	6	2	17	55		71	9	23	31	8	
	normal liver	18	0	0	2	16		16	7	6	2	1	
Age at diagnosis*													
	≤70 years	94	19	11	18	46	0,576	94	8	28	44	14	0,947
	>70 years	51	12	3	13	23		45	5	12	22	6	
Gender*													
	female	24	6	2	4	12	0,694	24	3	6	12	3	0,950
	male	87	15	9	23	40		83	7	22	43	11	
Tumor stage*													
	pT1	37	3	4	7	23	**0,008**	37	3	10	22	2	0,675
	pT2	14	0	1	4	9		12	2	2	6	2	
	pT3	17	8	0	3	6		18	4	6	7	1	
	pT4	2	1	0	1	0		3	0	1	2	0	
Regional lymph node status*													
	pN0	29	3	1	6	19	**0,005**	28	1	5	20	2	**0,021**
	pN1	11	6	0	3	2		12	4	2	4	2	
Metastatic status													
	M0	22	3	1	3	15	**0,037**	20	2	2	16	0	**0,014**
	M1	17	6	0	6	5		19	2	6	7	4	
Histologic grade*													
	G1	6	0	1	1	4	0,299	5	0	2	3	0	0,056
	G2	112	24	8	23	57		100	11	22	57	10	
	G3	46	13	6	11	16		51	7	17	16	11	
Immunohistochemistry (IHC):													
ABCA1								AOX1					
	negative	18	8	3	5	2	**0.032‡**	37	8	11	14	4	**0.032‡**
	score 1+	43	11	6	4	22		14	3	6	4	1	
	score 2+	74	14	4	15	41		30	5	4	15	6	
	score 3+	19	4	1	6	8		73	2	22	41	8	

* only HCC were included
† Fisher's exact test (2-sided); bold face representing significant data
‡ Pearson Chi-Square test (2-sided); bold face representing significant data

2.2.5.3. Expression in Leydig Cell Tumors

As already shown in Figure 36 (IHC Tissues) AOX1 in the testis is restricted to Leydig cells. 24 different LCT were analyzed and AOX1 was expressed in 100% of samples. Furthermore it was found to retain its specific expression in the Leydig cell population (Fig. 38), recommending AOX1 as possible LCT marker. In contrast, ABCA1 was broadly expressed in tumor areas and adjacent tissues (Fig. 38).

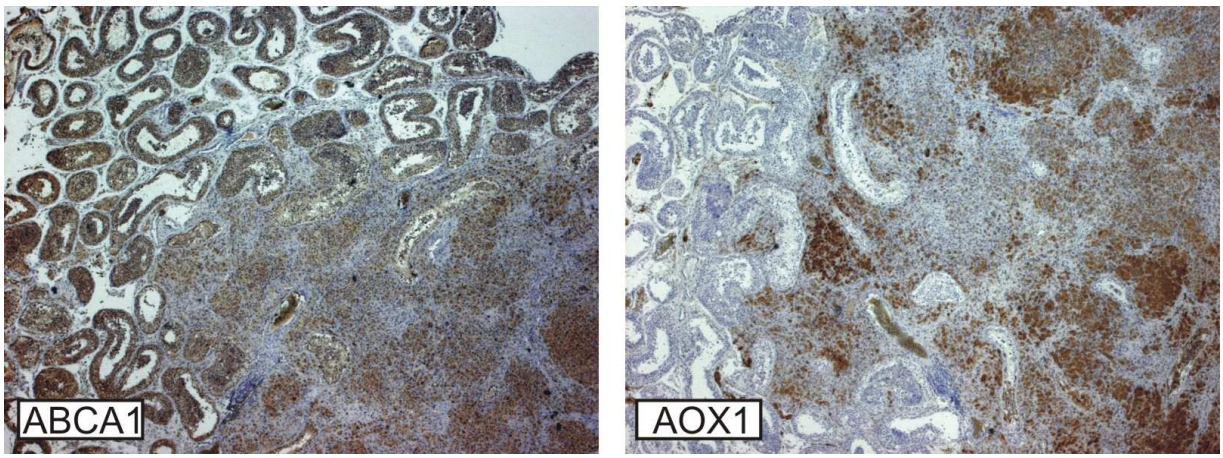

Figure 38. Immunohistochemistry of AOX1 and ABCA1 in Leydig cell tumors. For details see text. ABCA1 and AOX1 were stained utilized an avidin-biotin peroxidase method with a 3,3'-diaminobenzidine (DAB) chromatogen. Nuclei were counterstained with haematoxylin. Magnification 100 fold.

2.2.6. SNP analysis of AOX1

The role of AOX1 in acetaldehyde/acetate conversion during alcohol metabolism and ROS-dependent alcohol-mediated tissue damage is not completely solved, but AOX1 has been suggested to be involved in ethanol-induced liver injury [200] and the generation of ROS during ethanol metabolism [201; 202]. To gain further insight in this point 7 SNPs found in the database that either lead to an amino acid exchange in AOX1 or are located close to its putative promoter region were analyzed. A control collective of healthy blood donors was compared with alcoholics with or without cirrhosis.

The two assay detecting amino acid exchanges gave no evaluable results.

The other 5 assay could be evaluated and the results are shown in Table 11.

Table 11. Genotype- and allele frequencies of selected AOX1 SNPs.

		genotype N			genotypes frequency %			allele N			allele frequency %		
SNP (Assay ID)	genotype	control	cirrhosis	NO cirrhosis	control	cirrhosis	NO cirrhosis	control	cirrhosis	NO cirrhosis	control	cirrhosis	NO cirrhosis
C____144529_1_	C	60	29	65	74,1	69,0	71,4	141	70	154	87,0	83,3	84,6
	C/G	21	12	24	25,9	28,6	26,4						
	G	0	1	2	0,0	2,4	2,2	21	14	28	13,0	16,7	15,4
	total	81	42	91									
C____144530_10	C	61	32	73	74,4	72,7	72,3	143	75	169	87,2	85,2	83,7
	C/A	21	11	23	25,6	25,0	22,8						
	A	0	1	5	0,0	2,3	5,0	21	13	33	12,8	14,8	16,3
	total	82	44	101									
C___8130525_10	G	24	14	34	30,8	31,8	35,4	85	48	119	54,5	54,5	62,0
	G/A	37	20	51	47,4	45,5	53,1						
	A	17	10	11	21,8	22,7	11,5	71	40	73	45,5	45,5	38,0
	total	78	44	96									
C__27967310_10	C	5	1	4	6,1	2,3	4,1	36	16	44	22,0	18,2	22,4
	C/T	26	14	36	31,7	31,8	36,7						
	T	51	29	58	62,2	65,9	59,2	128	72	152	78,0	81,8	77,6
	total	82	44	98									
C__30787305_10	C	52	29	53	63,4	64,4	54,1	131	73	147	79,9	81,1	75,0
	C/A	27	15	41	32,9	33,3	41,8						
	A	3	1	4	3,7	2,2	4,1	33	17	49	20,1	18,9	25,0
	total	82	45	98									

The biggest differences were visible for SNP C___8130525_10. Genotype frequencies and allele frequencies in controls and cirrhosis samples are almost identical, but a shift is detectable in samples from alcoholics without cirrhosis (Table 11, p-Values: genotype frequency: control vs. NO cirrhosis p=0.18; allele frequency: control vs. NO cirrhosis p=0.19). However, more samples have to be analyzed to reveal if these changes are significant and additional experiments are necessary to proof the biological relevance.

3. TAX1BP3 or Syntaxin 13 Interacting Proteins

In cooperation with Tamas Köbling we performed yeast two-hybrid screens to identify new TAX1BP3 and STX13 interacting proteins. Screenings were performed using pAS-TAX1BP3 and pAS-STX13, respectively (Table 6). Eight putative TAX1BP3 interacting proteins and six putative STX13 interacting proteins were identified (Table 12).

Table 12. Putative TAX1BP3 interacting proteins and putative STX13 interacting proteins.

A. Candidates from the TAX1BP3 yeast two-hybrid screen.

Short	Full name	OMIM
CTNNB1	Catenin, beta 1	*116806
GAPDH	Glyceraldehyde-3-phosphate dehydrogenase	*138400
GDF15	Growth/differentiation factor-15	*605312
PFKL	Phosphofructokinase, liver type	*171860
PLOD1	Procollagen-lysine, 2-oxoglutarate 5-dioxygenase	*153454
PLXNB2	Plexin B2	*604293
PRDX5	Peroxiredoxin 5	*606583
TFAP2A	Transcrip factor AP2-alpha	*107580

B. Candidates from the STX13 yeast two-hybrid screen.

Short	Full name	OMIM
NAPA	N-ethylmaleimide-sensitive factor attachment protein alpha	*603215
SLC3A2	Solute carrier family 3, member 2	*158070
SNAP29	Synaptosomal-associated protein, 29kDa	*604202
STXBP5	Syntaxin binding protein 5	*604586
TBK1	TANK-binding kinase 1	*604834
VAT1	Vesicle amine transport protein 1	*604631

Further experiments in order to confirm these results were performed by Tamas Köbling.

4. ABCA7 Interacting Proteins and Regulation

To get more insight into ABCA7 function two different approaches were chosen. Yeast two-hybrid screens were performed to identify ABCA7 C-terminal interacting proteins and the regulation of both isoforms was analyzed.

4.1. ABCA7 Interacting Proteins

Screening with pAS-A7-CT (Table 6) identified 8 putative interacting proteins that are shown together with the corresponding OMIM entry in Table 13.

Table 13. Identified putative ABCA7 C-terminus binding candidates.

Short	Full name	OMIM/ Accession No[§]
GIPC2	GIPC1 PDZ domain containing family, member 2	NM_017655
BPY2IP1	BPY2-interacting protein 1	*607573
C1QA	Complement component 1, q subcomponent, alpha polypeptide	*120550
COPS5	Cop9, subunit 5	*604850
FBLN5	Fibulin 5	*604580
JAM1	Junction adhesion molecule 1	*605721
MT2A	Metallothionein 2A	*156360
NAZC	Neutrophil azurocidin	*162815

[§] EMBL-GenBank

In the screening with pAS-A7-NT (Table 6) no candidates have been found.
In a next step, the interaction of ABCA7 with these candidates had to be verified.

4.1.1. Verification of the Interaction by Co-Transformation in Yeast

To confirm the interaction of the candidates identified in the yeast–two-hybrid screens the complete coding sequence of the candidates was cloned in pGADT7. This resulted in AD-fusion constructs, which were cotransfected together with pAS-A7-CT or a control plasmid in yeast. In case of interaction, yeast cells should be able to grow on selection media. No growth could be detected, indicating a false positive result of the yeast two-hybrid screen or that the full length constructs fold different from the fragments found in the screen, thereby inhibiting interaction.

4.1.2. Verification of the Interaction In Vitro

As an independent second approach to confirm the interaction, recombinant ABCA7 C-terminus with an N-terminal GST fusion was used. ABCA7 C-terminus was cloned in the pGEX-5X-1 vector in fusion with an N-terminal GST-tag and expressed in E. coli. The N-terminal fusion was chosen to keep the putative C-terminal PDZ-binding-sequence (ETVL, class I, consensus X-S/T-X-V/L) free. The coding sequences of the candidate genes were cloned in pcDNA3.1D/V5-His-TOPO and used for in vitro translations, resulting in fusion proteins with C-terminal V5- and His-tags.
GST-ABCA7 and GST (control), respectively, were purified using the GST-epitope and incubated together with the products from the in vitro translation using different incubation conditions (PBS, PBS containing 0.1, 0.5, 1 % Triton X-100 or NP40). After immunoblot, detection was performed with a monoclonal anti-V5 antibody.
Under conditions tested here, no specific interaction between ABCA7 C-terminus and the candidates from the yeast two-hybrid screen could be confirmed.
In summary, the interaction of ABCA7 with the candidates could not be confirmed by two independent methods suggesting that the use of the ABCA7 C-terminus in the yeast two-hybrid led to false positive results.

4.2. Transcriptional Regulation of ABCA7

In cooperation with Louay Jouma we performed expression analyses of both isoforms in different human tissues and cell lines and analyzed the putative promoter region for transcriptional activity and possible transcription factors involved in ABCA7 regulation.

4.2.1. Expression of the two ABCA7 Isoforms

To get more insight in the function of the two published ABCA7 isoforms their mRNA expression in different human tissues was analyzed. TaqMan-Assays specifically recognizing ABCA7 Type I and Type II, respectively, were designed. The tissue distribution of both isoforms is quite similar, revealing very high expression in thymus and bone marrow and high expression in whole brain and mammary (Table 14).

Table 14. mRNA Expression of ABCA7 Type I and Type II in different human tissues.

Tissue	type I	type II
Brain, whole	●●●●●	●●●●●
Spinal Cord	●●	●●
Heart	●	●
Lung	●●	●
Kidney	●●●	●●
Liver	●	●
Stomach	●●●●	●●●
Small intestine	●●●	●●●
Colon	●●●	●●●
Salivary Gland	●●●●	●
Thyroid	●●●	●●
Pancreas	●	●
Adrenal Gland	●●	●
Ovary	●	●
Mammary	●●●●	●●●●
Uterus	●	●
Placenta	●●	●●
Thymus	●●●●●*	●●●●●*
Spleen	●●●●	●●●
Bone marrow	●●●●●*	●●●●●*

Results were converted to a linear scale (●●●●●: 81-100% of highest expression; ●●●●: 61-80%; ●●●: 41-60%; ●●: 21-40%; ●:>0-20%; * very high expression). Tissues with the highest expression are highlighted (yellow).

Furthermore, we determined the change of expression in HL-60 cells stimulated with vitamin D, ATRA or N-butyrate dissolved in ethanol to induce monocytic, granulocytic or eosinophilic differentiation. Ethanol and dimethylsulfoxide (DMSO) were included as solvent-controls. First results imply upregulation of both isoforms during eosinophlic and granulocytic differentiation and upon DMSO treatment, but to a different extent. Interestingly the ABCA7 type II isoform is strongly upregulated during monocytic differentiation (Fig. 39).

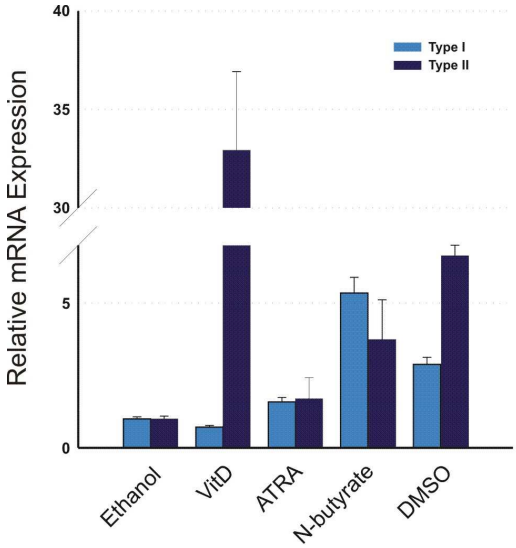

Figure 39. mRNA expression of ABCA7 type I and type II in differentiated HL-60 cells. Differentiation is induced by vitamin D (monocytic), ATRA (granulocytic) or N-butyrate (eosinophilic) dissolved in ethanol. Ethanol and DMSO were included as solvent-controls.

Therefore, we analyzed the expression of both isoforms during differentiation from monocytes to macrophages and under lipid loading (E-LDL/Ox-LDL) and deloading (HDL_3) conditions. Interestingly in this system, ABCA7 type I is significantly upregulated during differentiation from monocytes to macrophages ($p<0.05$) while type II is slightly but not significantly decreased ($p=0.08$) (Fig. 40). Upregulation of ABCA7 Type I under HDL_3-deloading is not significant because of the large inter-individual differences in the three donors.

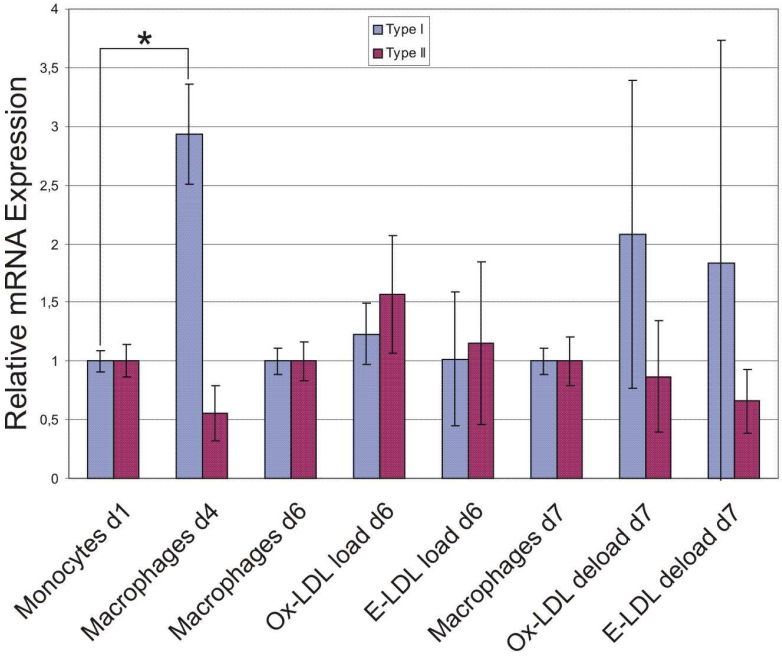

Figure 40. mRNA expression of ABCA7 type I and type II in monocytes and macrophages. Monocytes from 3 different donors were differentiated to macrophages, loaded with E-LDL or Ox-LDL and subsequently deloaded with HDL_3. Average expression levels are displayed together with their standard deviation relative to the corresponding controls (Monocytes d1 for differentiation; Macrophages d6 for loading; Macrophages d7 for deloading). * $p<0.05$.

As ABCA7 was shown to be involved in keratinocyte differentiation [72], we also analyzed the expression of both isoforms under these conditions. While ABCA7 type I was downregulated during differentiation type II mRNA was found initially reduced and increased at day 10 (Fig. 41). In summary, the two isoforms of ABCA7 were similarly expressed in human tissues but display different regulation in initial differentiation experiments of HL-60 cells, monocytes/macrophages and keratinocytes.

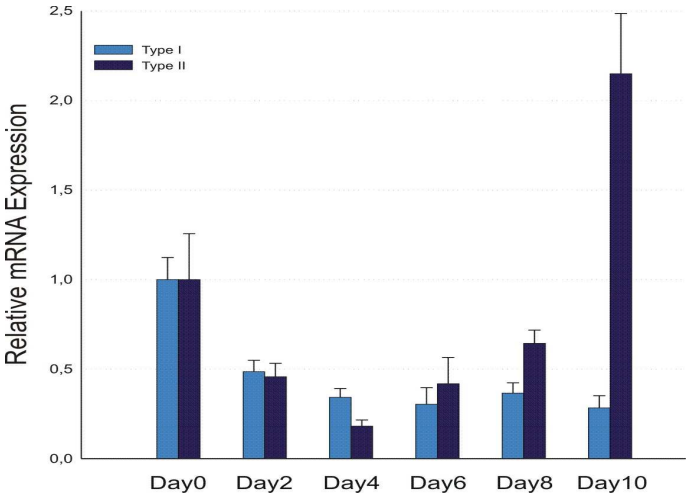

Figure 41. mRNA expression of ABCA7 type I and type II during keratinocyte differentiation.

4.2.2. Analysis of the ABCA7 Promoter(s)

To characterize the putative ABCA7 isoform1 promoter in more detail we cloned different constructs of the putative promoter area in pGL3 basic to assess their transcriptional activity in a luciferase-assay. The assay was performed in HepG2 and Jurkat cells, both expressing ABCA7. The different fragments together with their activity are shown in Figure 42. These results indicate that the ABCA7 core-promoter is localized between the base +144 and -47, the shortest fragment with significant promoter activity. Afterwards an in-silico analysis of the putative promoter was performed using Genomatix. The putative transcription factor binding sites are also displayed in Figure 42.

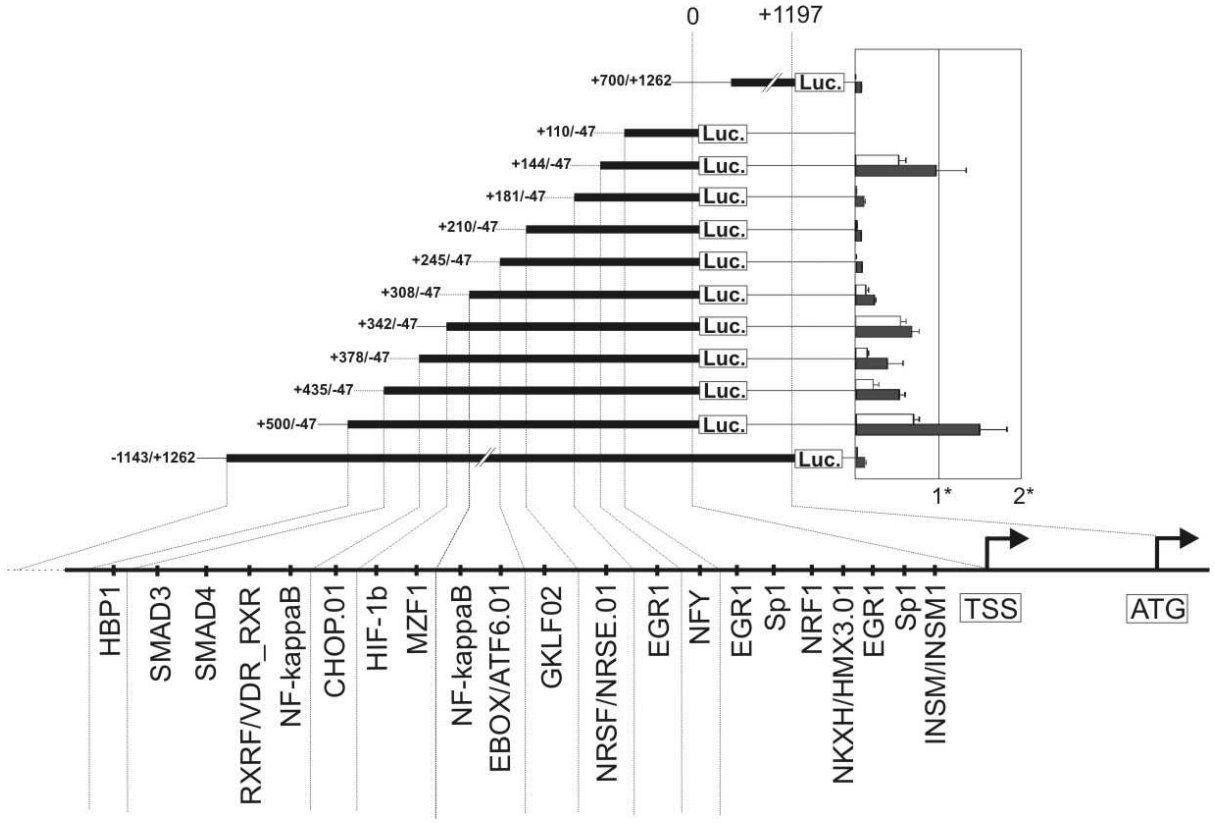

Figure 42. Promoter activity of several ABCA7 promoter fragments in HepG2 (grey bar) and Jurkat cells (white bar) with the predicted transcription factor binding sites. TSS, transcription start site; ATG, translation start; Promoter activity is calculated as luciferase activity / β galactosidase x protein concentration.

While this work was performed a competitive paper appeared, supporting our data and in addition demonstrating regulation of ABCA7 by SREBP-2 [73]. Therefore, we focused on the putative alternative promoter of ABCA7.

In silico analysis of this promoter revealed additional binding sites for transcription factors different from promoter one (Fig. 43). This supports the data indicating different regulation of both isoforms.

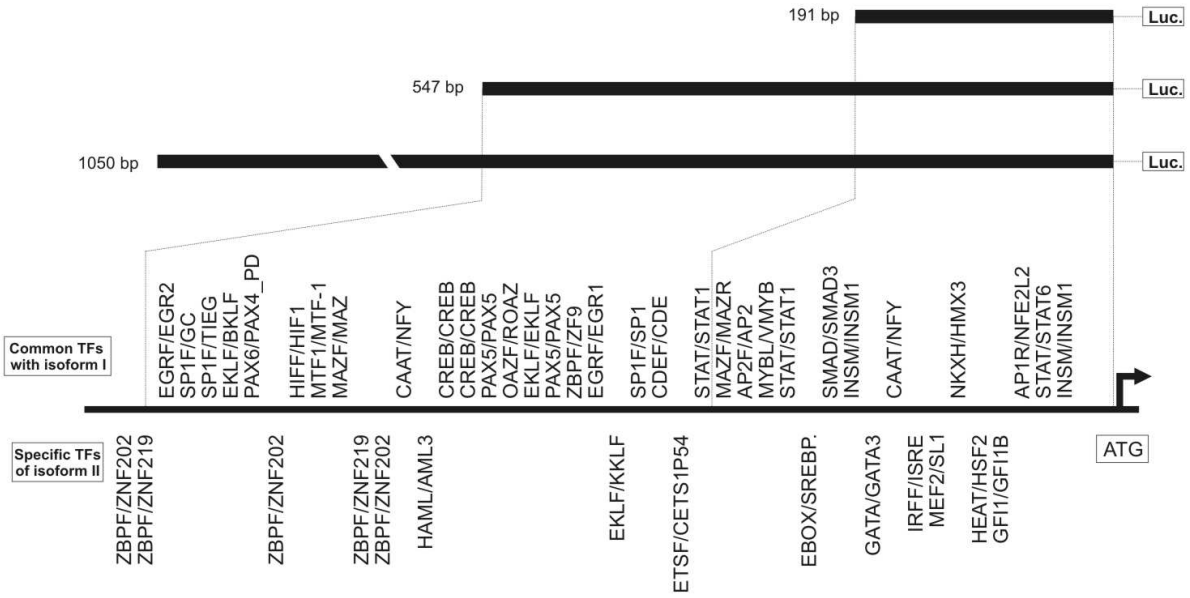

Figure 43. The putative second promoter of ABCA7. The promoter fragments for the luciferase assay and corresponding transcription factor binding sites are shown.

Detailed analysis of the second promoter is currently performed in our group.

5. Genes Regulated by Modified Lipoproteins

To study the role of cholesterol flux on ABCA1/ABCA7 and autophagy/apoptosis, loading (E-LDL, Ox-LDL) and HDL_3-deloading experiments were performed in cooperation with PD Dr. Büchler to search for apoptosis-related genes.

5.1. Identification of Apoptosis Related Genes Differentially Expressed in E-LDL Treated Macrophages

Total RNA from 5 d M-CSF differentiated macrophages and macrophages cultivated for 4 d with M-CSF and subsequently with E-LDL for 24 h was prepared and used to hybridize the HgU133A GeneChip from Affymetrix. Three independent experiments with monocytes from 3 different donors were performed and genes that were either induced or repressed in all experiments are listed in Table 15.

Table 15 Apoptosis related genes differentially regulated by E-LDL in macrophages.

A: Induced by E-LDL

Short name	Full name	Control signal	D-C	Unigene	C-C
TOSO	Regulator of Fas-induced apoptosis TOSO	170	P	Hs.58831	I
HSPA9B	Heat shock 70 kDa protein 9B	428	P	Hs.184233	I
BCL2A1	BCL2-related protein A1	488	P	Hs.227817	I
BCL2L1	BCL2-like 1	106	P	Hs.516966	I
PDCD8	Programmed cell death 8	182	P	Hs.424932	I

B: Suppressed by E-LDL

Short name	Full name	Control signal	D-C	Unigene	C-C
CARD8	Caspase recruitment domain family, member 8	163	P	Hs.446146	D
CFLAR	CASP8 and FADD-like apoptosis regulator	124	P	Hs.390736	D
Casp1	Caspase 1	142	P	Hs.2490	D
Casp6	Caspase 6	68	P	Hs.389452	D
BNIP3L	BCL2/adenovirus interacting protein 3-like	686	P	Hs.131226	D
SOD2	Superoxide dismutase 2, mitochondrial	443	P	Hs.487046	D
STK17B	serine/threonine kinase 17b	60	P	Hs.88297	D
TNFSF10	TRAIL, APO2 Ligand (APO2L)	49	P	Hs.478275	D
IER3	Immediate early response 3	613	P	Hs.591785	D

Control signal is the value for the expression of the gene in differentiated cells, D-C is the Detection Call (Present = P) and C-C the Change Call (Increase = I, Decrease = D) calculated by the software.

Several genes related to apoptosis were identified to be differentially expressed (Table 15A and B). The antiapoptotic gene BCL2A1 and BCL2L1 were found induced, like programmed

cell death 8 (Table 15A). TOSO, a cell surface protein and inhibitor of apoptosis, was also found upregulated in E-LDL treated cells. CARD8, an antagonist of caspase 9, CFLAR a caspase 8 like apoptosis regulator, caspase 1 and 6 and the anti-death protein IER3 were found downregulated (Table 15B). The proapoptotic gene BNIP3L was also reduced.

5.2. E-LDL Promotes the Survival of Freshly Isolated Monocytes and Predifferentiated Macrophages

These GeneChip data indicate that antiapoptotic genes are induced by E-LDL that may protect the cells from apoptosis. To test this hypothesis purified monocytes were cultivated in serum-free macrophage medium supplemented with M-CSF. E-LDL (40 µg/ml) was added for 24 h immediately after purification. The supernatants were used to detect histone-associated DNA-fragments with the Cell Death Detection ELISA. The amount of nucleosomes released from monocytes cultivated with M-CSF only or M-CSF and enzyme cocktail (EC, used to prepare E-LDL) as control was nearly 3-fold higher (absorbance: 1.12 ± 0.56) than from monocytes incubated with E-LDL (absorbance: 0.38 ± 0.32). These experiments were performed with monocytes from 8 different donors and the difference is statistically significant with $p < 0.003$. We received similar results with the supernatant from 4 d predifferentiated macrophages in serum-free macrophage medium supplemented with M-CSF and then treated with E-LDL (40 µg/ml) for 24 h. 4 d differentiated macrophages were furthermore incubated with Ox-LDL (100 µg/ml) but apoptotic cell death was comparable to control cells (not shown).

In addition, the cells were stained with Trypan blue. 8 to 10% of monocytes/macrophages cultivated in the presence of M-CSF or Ox-LDL were dead, whereas in E-LDL treated dishes only 1 to 3% of the cells stained blue.

5.3. TOSO mRNA is Strongly Induced in E-LDL but not Ox-LDL Generated Foam Cells

TOSO mRNA is hardly detectable by Northern blot analysis in freshly isolated monocytes and in vitro differentiated macrophages (Fig. 44 A and B). However, in monocytes incubated with E-LDL TOSO mRNA was found strongly induced after 24 h (Fig. 44 A). Enzyme cocktail and native LDL were used as controls and did not induce TOSO mRNA. The Northern blot was stripped and subsequently hybridized with a CD36 probe recently identified to be induced by native LDL and E-LDL. GAPDH was used as a loading control.

In a second experiment 4 d predifferentiated macrophages were loaded with E-LDL (40 µg/ml) or Ox-LDL (100 µg/ml) for 24 h. TOSO mRNA was only found upregulated in E-LDL

treated cells. The Northern blot was subsequently hybridized with an adipophilin probe, a sensitive marker of lipid loading in monocytes and macrophages, and the expression of adipophilin was strongly upregulated in Ox-LDL and E-LDL treated macrophages (Fig. 44 B). To obtain more quantitative experimental data on TOSO gene expression a TaqMan assay was established. Relative TOSO mRNA expression is 0.9 ± 0.4 in M-CSF differentiated cells and Ox-LDL and EC did not alter TOSO mRNA with a relative value of 1.5 ± 0.2 and 1.6 ± 0.3, respectively. In E-LDL treated cells TOSO mRNA expression is 7.1 ± 3.9 ($p = 0.007$). HDL_3-treatment subsequent to E-LDL loading reduced TOSO mRNA to 3.4 ± 3.2, however this was not a significant effect (Fig. 44 C).

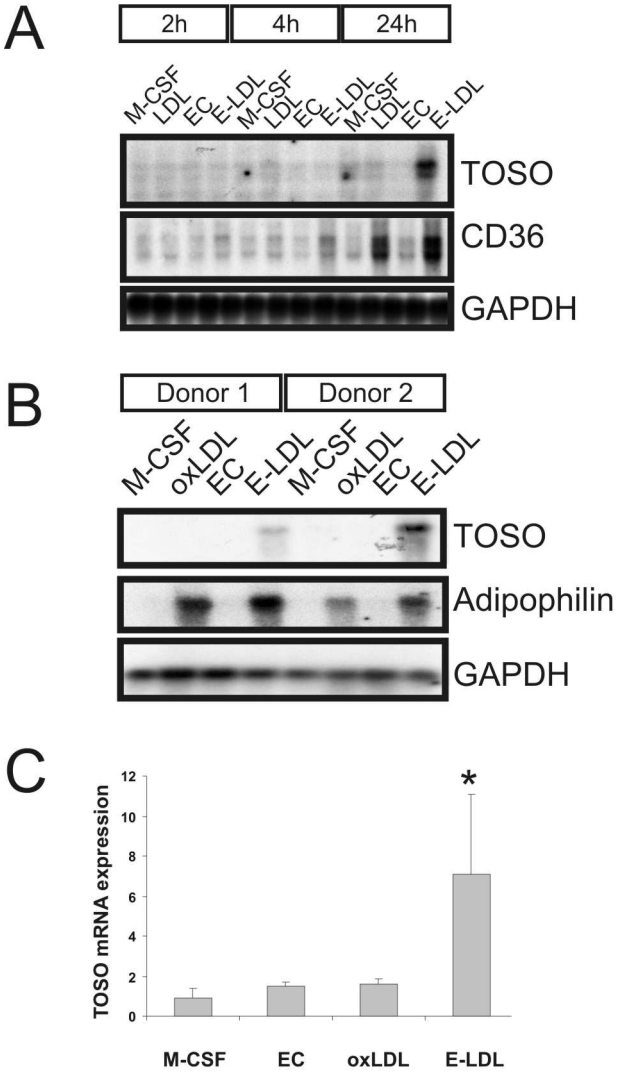

Figure 44. TOSO mRNA expression in macrophage foam cells. (A) TOSO mRNA expression in primary macrophages cultivated in M-CSF alone for 5 d (M-CSF) or M-CSF for 4d and additional 2 h, 4 h or 24 h with either 100 µg/ml LDL, EC or E-LDL was analyzed by Northern blot. Expression of CD36 mRNA and GAPDH was also determined. **(B)** TOSO mRNA expression in primary human macrophages cultivated in M-CSF alone for 5 d or M-CSF for 4 d and additional 24 h with either 100 µg/ml Ox-LDL, EC or E-LDL was analyzed by Northern blot. Adipophilin and GAPDH were determined in the identical mRNA samples. **(C)**. TOSO mRNA was determined by real-time RT-PCR in primary human macrophages cultivated in M-CSF alone for 5 d or M-CSF for 4 d and additional 24 h with either EC, 100 µg/ml Ox-LDL or 40 µg/ml E-LDL. 100 µg/ml HDL were added after E-LDL loading for 24 h and TOSO mRNA was analyzed. TOSO mRNA expression was normalized to GAPDH and the mean values ± std dev from three independent experiments are shown.

5.4. Surface Expression of CD95 and CD95L During Differentiation and Upon E-LDL Loading

TOSO was initially described to inhibit CD95 induced apoptosis. However, the abundance of CD95 and CD95L on E-LDL generated foam cells has not been investigated so far. The surface levels of CD95 and CD95L were determined during differentiation and foam cell formation. Monocytes isolated from 7 different donors were cultivated for 3 days and the expression of CD95 and CD95L was found significantly upregulated during differentiation (Fig. 45).

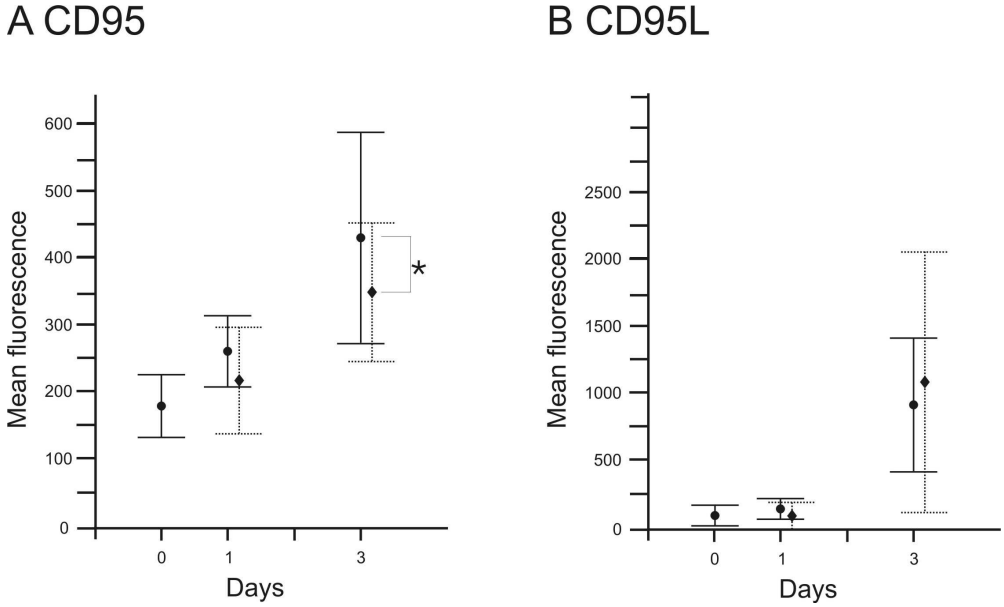

Figure 45. CD95 and CD95L surface expression in E-LDL incubated primary macrophages. Primary human macrophages were incubated with E-LDL (dashed line) or EC (solid line) as control for 1 d, 2 d or 3 d. CD95 and CD95L were measured by flow cytometry.

The mean fluorescence signal for CD95 rose from 180 ± 32 in freshly isolated cells to 416 ± 162 in 3 d macrophages, CD95L was 23 ± 12 in freshly isolated monocytes and 892 ± 587 in 3 d differentiated cells. The surface expression of CD95 and CD95L was also measured in cells treated with E-LDL for 24 h and 72 h. The 24 h incubation did not influence the expression of CD95 and CD95L. CD95 was found slightly reduced with a mean fluorescence of 337 ± 112 in macrophages incubated with E-LDL for 3 d whereas CD95L expression was not altered. The soluble form of CD95 (sCD95) has been shown to be an inhibitor of apoptosis and therefore was determined in the supernatants by ELISA. sCD95 in controls was 113 ± 29 pg/ml, in EC treated cells 110 ± 35 pg/ml and 105 ± 36 pg/ml in E-LDL generated foam cells. Therefore, we can exclude that the enhanced survival of foam cells observed after 24 h incubation is caused by a downregulation of CD95 or CD95L or induction of sCD95.

5.5. Expression of $FLIP_L$ and FADD

It was suggested that TOSO blocks apoptosis by enhancing FLICE-like inhibitory protein long form ($FLIP_{L)}$ abundance. $FLIP_L$ was determined in E-LDL and Ox-LDL loaded macrophages by immunoblot. Neither $FLIP_L$ nor FADD or CD163 expression, used as a loading control, were influenced by lipid loading (Fig. 46 A). Furthermore, recombinant TOSO was expressed in COS-7 cells with a C-terminal V5-tag. Production of the recombinant protein was confirmed by immunoblot using the anti-V5 antibody. The level of FLIPL or FADD was not influenced by the expression of recombinant TOSO (Fig. 46 B).

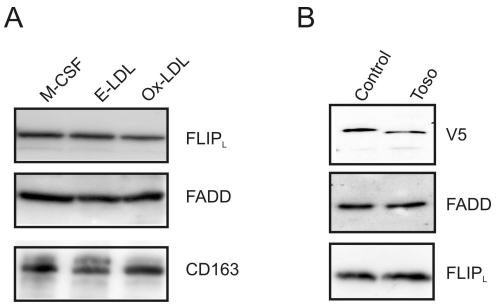

Figure 46. $FLIP_L$ and FADD in foam cells and COS-7 cells expressing recombinant TOSO. (A) $FLIP_L$ and FADD were determined in primary human macrophages cultivated in M-CSF alone for 5 d or M-CSF for 4 d and additional 24 h with either E-LDL or Ox-LDL by immunoblot. **(B)** COS-7 cells stably expressing recombinant TOSO with a V5-tag or rezepin with a V5-tag as control were analyzed for the abundance of V5, FADD and $FLIP_L$ by immunoblot.

5.6. TOSO mRNA is Strongly Induced in Macrophages After Phagocytosis

E-LDL contains large amounts of free fatty acids and is most likely taken up by phagocytosis. The influence of free fatty acids on TOSO mRNA expression was analyzed by TaqMan real-time RT-PCR. Human blood monocytes were incubated with γ-linolenic acid (50 μM and 100 μM) or eicosapentaenoic acid (EPA) (50 μM and 100 μM) complexed to BSA for 24 h in serum free medium supplemented with M-CSF. Control cells were cultivated in the same medium with lipid-free BSA. A slight but significant ($p = 0.02$) increase of TOSO mRNA was observed in macrophages treated with 100 μM EPA with a relative expression of 4.4 ± 0.3 when compared to controls with 2.7 ± 1 (Fig. 47 A).

TOSO mRNA was also determined in macrophages incubated with Bluebeads that are taken up by phagocytosis. The relative expression of TOSO mRNA in controls was 2.2 ± 0.4, in E-LDL incubated macrophages 4.0 ± 0.6 ($p = 0.009$ vs. control) and in macrophages with Bluebeads 6.2 ± 0.5 ($p = 0.003$ vs. control, $p = 0.01$ vs. E-LDL) (Fig. 47 B).

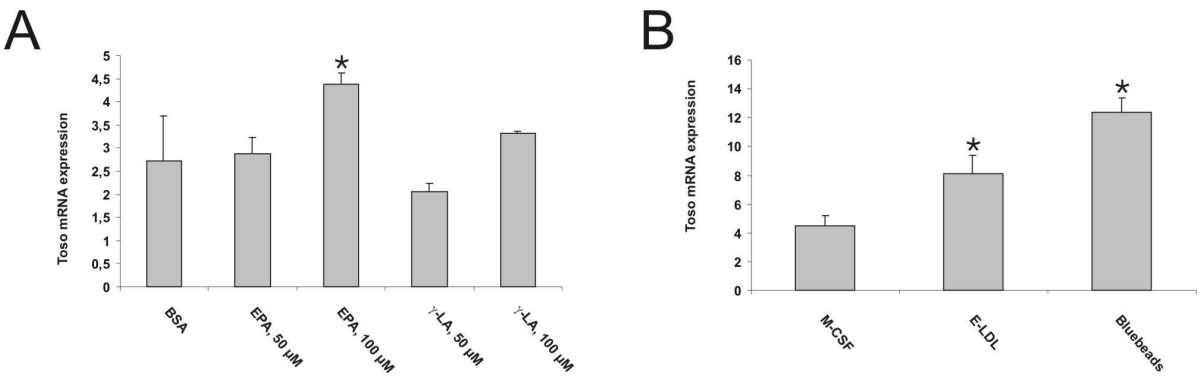

Figure 47. TOSO mRNA expression in macrophages incubated with free fatty acids or Bluebeads and in different cells and tissues. (A) TOSO mRNA expression in primary macrophages cultivated in M-CSF alone for 4 d and additional 24 h with either BSA, eicosapentaenoic acid (EPA) or γ-linolenic acid (γ-LA). TOSO mRNA expression was normalized to GAPDH and the mean values ± std dev from three independent experiments are shown. **(B)** TOSO mRNA was determined by real-time RT-PCR in primary human macrophages cultivated in M-CSF alone for 5 d or M-CSF for 4 d and additional 24 h with either E-LDL or Bluebeads.

5.7. Recombinant Expression of TOSO

The complete cDNA of TOSO was amplified by RT-PCR using RNA isolated from lipid-laden macrophages, cloned in pcDNA3.1D/V5-His-TOPO (Invitrogen) and sequenced.

5.8. Phagocytic Activity of COS-7 Cells Expressing TOSO

Uptake of Fluoresbrite Yellow Green Microspheres was measured in COS-7 cells either expressing recombinant TOSO or recepin as a control protein after 1 h or 2 h incubation. Four independent experiments were performed and indicate that phagocytic activity is not elevated in COS-7 cells with recombinant TOSO (not shown).

5.9. TOSO mRNA Expression in Different Human Tissues

The TOSO cDNA fragment was used to hybridize a human multiple tissue blot. TOSO mRNA was most abundant in lymph nodes followed by the spleen, the appendix, the thymus and peripheral blood leukocytes. TOSO mRNA was also detected in the bowel. Expression was similar in fetal and adult tissues (Fig. 48).

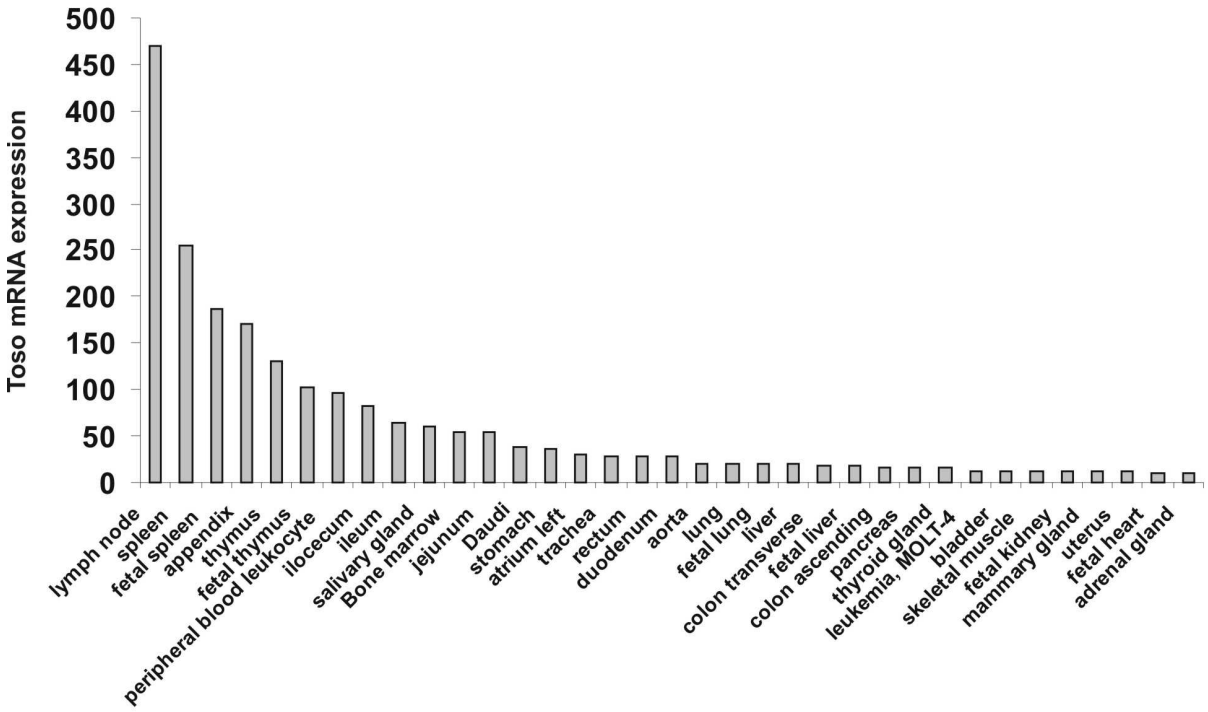

Figure 48. TOSO mRNA expression in different cells and tissues. TOSO mRNA was analyzed in different tissues and cell lines. A normalized dot blot containing mRNAs of different human tissues and cell lines was hybridized with a radioactively labeled TOSO cDNA probe and signals were analyzed using a phosphoimager. The relative tissue expression of TOSO mRNA is shown.

VI. DISCUSSION

1. ABCA1 Interacting PDZ Proteins

Different ABCA1 interacting PDZ proteins are published in the literature. PDZ proteins normally function as molecular scaffolds by mediating protein-protein interactions through multiple interaction modules, thereby clustering membrane proteins, cytoskeletal elements, trafficking machinery, and signal transduction molecules into multimeric complexes at distinct membrane domains [277; 278].

The importance of the PDZ interaction for ABCA1 function is not clear so far. The interactions with SNTA1 and SNTB1 were reported to stabilize ABCA1 and thereby enhance ABCA1-mediated lipid efflux [54; 55], indicating that the SNTB2, also shown to interact with ABCA1 [56], might do the same. On the other hand, Lin7 was also shown to interact with ABCA1, but with no influence on ABCA1 half-life [54]. As the PDZ interaction relies on a free, intact C-terminal PDZ binding motif ([54], this work) the class I motif of ABCA1 (ESYV) would play an important role in the association with PDZ proteins. In contrast, data from experiments with different C-terminal deletion constructs of ABCA1 only show moderate influence of the PDZ motif on lipid efflux. Furthermore chimeric constructs, in which the ABCA1 C-terminus is substituted by either the ABCA4 or ABCA7 C-terminus, show that ABCA1 could stimulate efflux without a PDZ-binding motif, but requires a motif more upstream which is also present in ABCA4 [279]. Most of the data are generated in HEK293 cells, besides the influence of SNTB1 on lipid efflux that was also shown in primary skin fibroblasts and bone marrow-derived macrophages.

In this work, additional PDZ proteins that in vitro are able to bind to the ABCA1 C-terminus were identified (Fig. 49). The interaction of ABCA1 with TAX1BP3, GIPC1, Scribble and MAGI3 observed in the yeast two-hybrid screen was confirmed by different methods and the interaction was shown to depend on a free, intact C-terminus. For Scribble and MAGI3, both containing more than one PDZ domain, the interaction was mapped to PDZ domain 1, nevertheless it is possible that also other domains interact with ABCA1 as not all individual domains were included on the PDZ-array. As PDZ domain 1 of Scribble was not fully included on the clone isolated from the yeast two-hybrid screen this may indicate that either this part of domain 1 was sufficient to interact with ABCA1 in yeast or that PDZ domain 3 is also involved in this association.

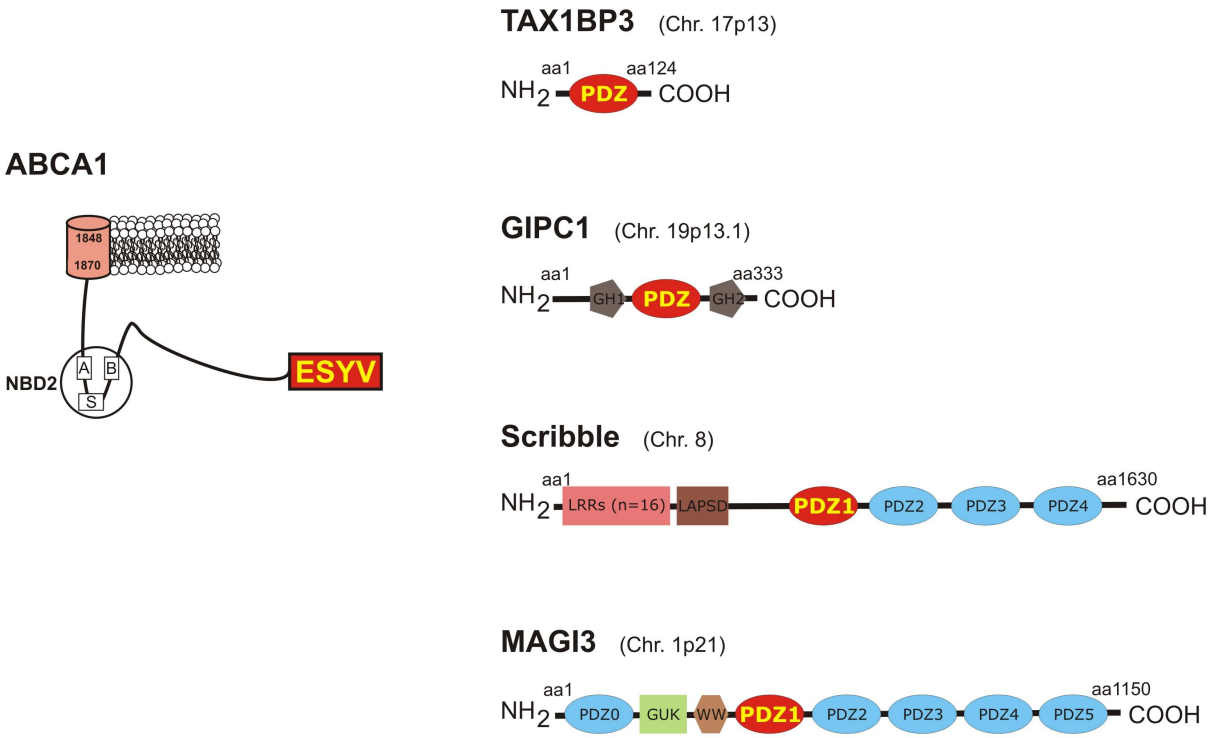

Figure 49. ABCA1 interacting PDZ proteins identified in this work. The C-terminal part of ABCA1 from the last TMD to the C-terminal PDZ binding motif is shown together with the structure of the identified PDZ proteins and their chromosomal location. The PDZ binding motif and the interacting PDZ domains are displayed in red. aa, amino acid; COOH, C-terminus; GH, GIPC1 homology domain; LAPSD, LRR and PDZ-specific domain; LRR, Leucin-rich Repeat domain; NH_2, N-terminus; PDZ, PSD95/Discs-large/ZO-1 domain.

TAX1BP3 is a 124 amino acid protein containing no additional interaction motifs besides the PDZ domain. Recent data suggest that it may act as negative regulator of PDZ-based scaffolding by blocking the PDZ binding sequence and preventing complex formation [280]. Furthermore TAX1BP3 was shown to interact with the human T-lymphotropic virus Tax oncoprotein and the high risk human papilloma virus (HPV) 16 E6 oncoprotein [281; 282] and is suggested to alter RhoA signaling to the c-fos serum response element [283]. In addition, it was described to interact with L-glutaminase [284] and to modulate the Wnt/β-catenin pathway by interacting with β-catenin [285].

GIPC1 is one of the three members of the human GIPC family [286] that is able to interact with various proteins including G protein coupled receptors (GPCRs), tyrosine kinase receptors and membrane proteins, pointing to a function of GIPC1 in GPCR signaling. The regulator of G protein signaling (RGS) 19, which is mainly found in clathrin-coated vesicles, forms a complex with GIPC1. This suggests a function for the GIPC1/RGS19 complex in vesicular trafficking and endocytosis (reviewed in [287]).

Scribble is a leucine-rich (LRR) and PDZ (LAP) protein that is known to regulate apical-basal polarity in epithelia of Drosophila [288]. Human Scribble was reported to be a functional homolog of this tumor suppressor [289]. In humans and Drosophila it was also shown to influence cell-cycle [290; 291]. Data from mice indicate an important role for Scribble in

development and planar cell polarity [292; 293]. In addition, Scribble was demonstrated to be involved in recycling and signaling of the GPCR thyrotropin (TSH) receptor (TSHR) [294]. Scribble is reported to be degraded upon interaction with the HPV 16 and 18 E6 oncoprotein, in contrast to TAX1BP3 that seems to be a gain of function for HPV 16 E6 and is not degraded [282].

MAGI3 comprises five PDZ domains, 2 WW domains and a guanylate kinase domain, enabling various protein interactions. These includes phosphatase and tensin homolog (PTEN), receptor tyrosine phosphatase-β, frizzled, transforming growth factor α precursor, and the GPCRs β1-adrenergic receptor and lysophosphatidic acid (LPA) receptor LPA_2 [295-300]. Furthermore, it is targeted by the HPV 16 and 18 E6 proteins for degradation and also interacts with HTVL-1 Tax [301; 302].

Notably GIPC1, Scribble and MAGI3 are related to GPCR signaling. This may indicate that these PDZ proteins cluster ABCA1 together with GPCRs or bind to either ABCA1 or GPCRs. It was already demonstrated that PDZ proteins retain GPCRs at the plasma membrane [294; 303-305]. Therefore, it is possible that these PDZ interactions retains the putative ABCA1/GPCR-complex or, according to the cell type or stimulus, ABCA1 or GPCRs at the cell surface. TAX1BP3, Scribble, and MAGI3 are altered by viral oncoproteins and therefore another interesting question would be to determine if viral oncoproteins are able to influence ABCA1 activity by modifying its PDZ interactions.

Taking into account the tissue distribution of the PDZ proteins analyzed in this work ABCA1/PDZ protein interaction may be highly cell type or compartment specific and the situation in other cell types than HEK293 may be different. For example, scavenger receptor class B type I (SR-BI) was shown to be regulated by PDZK1, a multi-PDZ domain containing adaptor protein, in a tissue-specific and post-transcriptional manner. PDZK1 knock-out mice reveal 95% and 50% reduced SR-BI expression in liver and proximal intestine, respectively. In contrast, expression in steroidogenic tissues (adrenal, ovary, and testis) was unchanged. The situation for ABCA1 might be similar and additional experiments are needed to clarify the role of the ABCA1/PDZ interaction.

2. AOX1 Interacts with ABCA1 and Influences ABCA1-related Functions

In this work, AOX1 was demonstrated to associate with and influence ABCA1-mediated functions. Knock-down of AOX1 expression leads to decreased lipid efflux and enhanced phagocytic activity in HepG2 cells, supporting the involvement of ABCA1 in the modulation of phagocytic uptake in type I- and type II phagocytosis [64]. These cellular phenotypes are comparable to the phenotype of ABCA1-deficient monocytes and/or fibroblasts, that also

show enhanced phagocytic activity and defective apoA-I-dependent cholesterol efflux [306; 307].

The physiological function of AOX1 is not yet fully characterized. Although AOX1 is well-described as a xenobiotic metabolizing enzyme its physiological substrates and functions are poorly understood. AOX1 derived ROS are directly implicated in free radical damage in liver and brain during ethanol metabolism [201; 308-311]. Alcohol dehydrogenase produces acetaldehyde and NADH from ethanol. Both are substrates for AOX1 and could lead to the formation of ROS in certain tissues [216; 312; 313]. Alcohol-mediated ROS injury of the liver was shown to operate directly through the combined activities of AOX1 and its close homolog xanthine oxidoreductase (XOR) [201; 309; 310; 312] by an iron-dependent process, suggesting involvement of hydroxyl radicals in tissue damage [309; 311; 312]. In alcoholics without cirrhosis a SNP in the first intron of AOX1 is in direction changed compared to controls and alcoholics with cirrhosis. This SNP may alter AOX1 transcription by influencing AOX1 promoter activity or may be linked to a yet unknown SNP that affects AOX1 transcription or activity. Further experiments are required to determine its relevance and function. Recently AOX1 was shown to be regulated in a NAD(P)H oxidase-mediated manner in VSMC and this regulation was induced by thrombin [314]. NAD(P)H oxidase generated ROS is implied in several signal transduction pathways in VSMC [315], in host defense in professional phagocytes [316], and contributes to M-CSF induced monocyte/macrophage survival via regulation of Akt and p38 MAPK [317]. Akt is a kinase downstream from PI3K, and PI3K/Akt pathways are involved in various biological processes, including the PDGF-dependent suppression of ABCA1 expression in VSMC [42]. Akt activity is reduced by ABCA1 [43] and HDL-mediated activation of the PI3K/Akt pathways results in eNOS-mediated nitric oxide production [44]. These data support a complex regulatory network of AOX1, ABCA1, HDL, NAD(P)H oxidase, PI3K/Akt, and ROS formation that might influence various biological processes including insulin signaling, atherosclerosis and phagocytosis.

Moderate alcohol consumption is associated with a decreased risk of cardiovascular diseases [318] and more than 50% of this effect is due to an increase in HDL-cholesterol [319; 320]. Moreover, moderate alcohol consumption increases the capacity of serum to induce cholesterol efflux from J774 mouse macrophages, which might be mediated by ABCA1 [321]. Taken together, these data and our recent results suggest that (i) AOX1 itself by direct interaction, and/or (ii) AOX1-derived ROS could influence ABCA1 activity. Nevertheless, the role of AOX1 in alcohol metabolism is controversially discussed. Recent data from Castro et al. suggest that XOR and not AOX1 itself contributes to the bioactivation of ethanol to acetaldehyde [322]. In this scenario, the function of AOX1 and its homologs has to be explored in more detail.

On the other hand alcohol and retinol were supposed to be metabolized in part by the same enzymes [203], and AOX1 was suggested to be identical to retinal oxidase [198], thus being involved in the biogenesis of RA. 9-cis RA and all-*trans* RA (ATRA) are both transcriptional modulators for RAR/RXR target genes, and thereby induce ABCA1 and HDL maturation [204], which is under strong transcriptional control through LXR/RXR. In rabbit liver two pathways for RA biosynthesis exist. One of them involves the cryptozoic NAD^+-dependent retinal dehydrogenase and the other the oxygen-dependent retinal oxidase (=AOX1). Both catalyze the same reaction with an activity ratio of 59% and 41% under experimental conditions [199]. While the metabolic significance is unclear, it is possible that NAD^+/NADH tissue levels affect the rate of retinal oxidation. Retinal dehydrogenase may be more effective under conditions with high NAD^+ levels while retinal oxidase may maintain basic RA level in liver and circulation [199]. The involvement of AOX1 in retinoid metabolism is further supported by chicken AOX1, which also posses retinaldehyde oxidase activity [323]. Recent data from our laboratory [204] demonstrate the effect of retinoids on lipid efflux in macrophages. A strong up-regulation of genes involved in cellular cholesterol homeostasis, including ABCA1, was observed. Considering that AOX1 might be involved in retinoid metabolism and ABCA1 is a retinoid responsive gene, we expected that AOX1 might influence ABCA1 on the transcriptional level. Surprisingly our findings indicate that the effect of AOX1 knock-down on ABCA1 activity is not due to changes in mRNA or protein expression of ABCA1.

AOX1 was also reported to catalyzes the predominant reductive pathway of ziprasidone (Geodon, Zeldox), an atypical antipsychotic agent for the treatment of schizophrenia [324]. Interestingly ziprasidone was reported to have favorable effects on total cholesterol, LDL, and HDL levels in patients [325], which may be due to altered ABCA1 activity. On the other hand, AOX1 was shown to be a dioxin inducible gene [205]. This effect may be due to AHR-mediated downregulation of PPARα [326], as AOX1 mRNA and protein expression were recently shown do be suppressed by PPARα agonists [228]. TCDD is a persistent environmental pollutant accumulating in fat. Intoxication in humans often leads to elevated plasma total cholesterol and TG levels [327; 328] and long-term effects in addition to hyperlipidaemia include chloracne, psychic disorders, and/or nervous system lesions [328]. As only total cholesterol was measured in these studies this could also mean that TCDD increases HDL, but as TG are elevated, too, and atherosclerotic plaques, increased intima-thickness and ischaemic heart disease are common in these patients this can be ruled out. The observed hyperlipidaemia in TCDD patients and the inverse regulation of ABCA1 and AOX1 by PPARα [34; 228] are not consistent with our model that AOX1 positively influences ABCA1 activity that is supported by our data and the influence of ziprasidone on plasma lipids. Further experiments are necessary to clarify this point.

Immunohistochemical data show a cell-specific expression of AOX1 in different human tissues (liver, kidney, adrenal gland, testis, ovary), which differ at least in part from previous results [222]. Interestingly, the cell types that express high amounts of AOX1 also express high levels of ABCA1. This further underlines the physiological association of ABCA1 and AOX1 at the cellular level.

The impact of hepatic ABCA1 on plasma HDL levels is well described (reviewed in [329]) and as the liver is important for detoxification the presence of AOX1 as xenobiotic-metabolising enzyme [197] makes sense. Taken together these data suggest a role for the ABCA1/AOX1 complex in detoxification, even it has to be clarified in detail. In contrast, the roles of ABCA1 and AOX1 in kidney, adrenal gland and Leydig cells are less clear. While in kidney it may be similar to the liver, the co-expression of AOX1 and ABCA1 in steroidogenic tissue suggests another function. Data from $ABCA1^{-/-}$ mice showed impaired fertility due to reduced sperm count, reduced intratesticular testosterone levels and reduction of Leydig cells lipid droplets in these animals [53]. In males, testosterone is primary secreted by Leydig cells and to a lesser extent by the adrenal cortex, both expressing high levels of AOX1 that is coexpressed with ABCA1. Taken together these data may imply involvement of the AOX1/ABCA1-complex in steroid hormone metabolism. It will be interesting to find out if the dual roles of the AOX1/ABCA1-complex in detoxification and steroid hormone metabolism underlie a common mechanism.

Analysis of the expression of AOX1 and ABCA1 in normal liver compared to HCC indicates a reduced expression of AOX1 in cancer cells, while ABCA1 expression is increased. In RCC the expression of both proteins compared to normal kidney is reduced. In addition our results in HCC show a direct correlation of AOX1 and ABCA1 expression, which is not found in RCC. These findings suggest that in cancer the interaction of AOX1 and ABCA1 may be disturbed, which in context with the possible involvement of AOX1 in retinoid-metabolism could influence cell differentiation/proliferation. Intriguingly both AOX1 and ABCA1 are significantly correlated with positive nodal status in renal cell and hepatocellular carcinomas (RCC: AOX1: p=0,001; ABCA1: p=0,029 and HCC: AOX1: p=0,005; ABCA1: p=0,021). In HCC also a significant correlation with metastatic status (AOX1: p=0,037; ABCA1: p=0,014) is detectable. Interestingly, in contrast to HCC and RCC, AOX1 expression was maintained in LCT and specific for the Leydig cell population. These findings indicate that AOX1, depending on the type of cancer and eventually in combination with ABCA1, might be useful as a histopathologic tumor-marker. Our findings are consistent with recent observations [330], who reported strong expression of AOX1 in pancreatic acinar cells, reduced expression in chronic pancreatitis, and loss of AOX1 in malignant pancreatic adenocarcinoma cells.

In conclusion, we have demonstrated that AOX1 associates with and modulates ABCA1 function. The molecular mechanism and a putative complex regulatory network of AOX1, ABCA1, HDL, NAD(P)H oxidase, PI3K/Akt, ROS formation and retinoids has still to be clarified and is subject of our ongoing work.

3. ABCA7 Regulation and Function

Yeast two-hybrid screens were performed to identify ABCA7 C-terminal interacting proteins and the expression and regulation of the two isoforms of ABCA7, namely type I and type II, was analyzed in different human tissues and during differentiation in different cell types. Although eight candidates were identified in the yeast two-hybrid screen, none of them could be confirmed in neither yeast or in pull-down assays. This indicates that they were false positive interaction partners.

Recent data concerning the two ABCA7 isoforms indicate that in HEK293 type I was localized to the plasma membrane, while type II was mainly found in the ER [68]. Although both isoforms display quite similar tissue expression they seem to be regulated in differentiation in different manners. This could be the result of isoform-specific promoters, sharing common factors for basal transcription and specific factors activated during differentiation. Therefore, analysis of the promoter of ABCA7 type I was performed, but in the meantime a competitive paper appeared, supporting our data and in addition demonstrating regulation of ABCA7 by SREBP-2 [73]. Therefore, we focused on the putative alternative promoter of ABCA7. In silico analysis of both promoters resulted in various potential transcription factors that might regulate ABCA7 transcription. Experiments to verify the transcriptional activity of the second promoter and to evaluate the biological relevance of these transcription factors are currently performed and the comparison of both promoters may give further clues about the regulation of both isoforms.

Interestingly our data indicate that DMSO upregulates both ABCA7 isoforms, but mainly type II in HL-60 cells. This is of particular interest as the tumor suppressor PTEN is also upregulated in DMSO treated HL-60 cells [331]. PTEN is a PI3K antagonist, influencing PI3K/Akt signaling, which in HL-60 cells controls progression of cell cycle [332; 333]. Moreover PI3K and PTEN were shown to be involved in autophagy [47; 334]. Further data possibly linking ABCA7 to autophagy are based on keratinocytes. ABCA7 was reported to be upregulated during terminal keratinocyte differentiation [72] and autophagy was also reported to be implied in this process [335]. More detailed analysis of the ABCA7 expression under this conditions revealed upregulation of ABCA7 isoform II, while isoform I is downregulated.

The recent findings that ABCA7 is involved in phagocytosis [73; 75] are in agreement with our data demonstrating upregulation of ABCA7 isoform I during monocytes to macrophages differentiation, as macrophages are professional phagocytes.
Considering these data, we would suggest different functions for the two isoforms of ABCA7. Isoform I localizes to the plasma membrane and is upregulated during monocyte to macrophage differentiation, indicating an involvement in phagocytic processes. In contrast, isoform II localizes to intracellular membranes and is upregulated together with PTEN in HL-60 cells and during terminal keratinocyte differentiation, pointing to a function in the autophagic pathway. This further supports our current model of the dual mechanism of ABCA1/ABCA7 in lipid-efflux/apoptosis/autophagy. Further experiments are necessary to confirm this hypothesis.

4. Identification of TOSO as Lipid-sensitive Gene

Numerous studies demonstrate that macrophages in atherosclerotic lesions undergo apoptosis and thereby contribute to plaque rupture [250]. Macrophages incubated with Ox-LDL in vitro transform to foam cells and undergo apoptotic stress supporting the established in vivo observations [254]. However, cholesterol loading and apoptosis alone do not explain the accumulation of monocytes/macrophages in early atherosclerotic lesions, which may be caused by enhanced recruitment of monocytes into the arterial wall. Atherogenic lipoproteins were shown to induce the release of monocyte chemotactic protein 1 (MCP-1) from macrophages that may attract monocytes to cross the endothelium [260]. Alternatively, the increased number of monocytes/macrophages may be also the result of a prolonged life span of monocytes/macrophages. This idea is supported by in vitro experiments using lower amounts [255], less oxidized [336] or aggregated [256] Ox-LDL preparations. These authors describe a prolonged survival of cultivated macrophages and even a proliferative response of these cells. In the current study, we demonstrate that E-LDL promotes the survival of monocytes and macrophages cultivated in serum-free medium supplemented with M-CSF. E-LDL is used at low concentrations and E-LDL is much more effective in foam cell formation when compared to Ox-LDL or acetylated LDL [259]. The in vivo relevance of E-LDL was demonstrated by immunohistochemistry and is further supported by the ability of E-LDL to activate complement [337]. Spontaneous cell death of monocytes/macrophages is mediated in vivo and in vitro by apoptosis and CD95/CD95L is at least partly involved [338]. In the current work, we demonstrate an enhanced survival of E-LDL loaded macrophages indicated by a reduced release of histone associated DNA and a higher number of viable cells. Reduction of CD95, CD95L or upregulation of sCD95, that may explain survival, were ruled out.

GeneChip experiments revealed the upregulation of antiapoptotic genes and the suppression of proapoptotic genes in E-LDL treated cells. The upregulation of TOSO by E-LDL was confirmed by Northern blot analysis and Real-time RT-PCR. TOSO was recently identified as a cell surface inhibitor of Fas-, tumor necrosis factor- and FADD- induced apoptosis in T cells [339]. Mechanistically, TOSO was suggested to inhibit apoptosis by reducing caspase 8 processing through the induction of $FLIP_L$ expression [339]. Whereas reduced caspase 8 activity was also found in E-LDL generated foam cells (not shown) expression of $FLIP_L$ was not altered. A second study shows that TOSO directly binds FADD and this may disrupt the formation of the death-inducing signaling complex [340]. Cholesterol- and cholinephospholipid-efflux catalyzed by the ABCA1, that is induced in foam cells upon Ox-LDL and E-LDL loading, may also depend on FADD binding to the C-terminus of ABCA1 [57]. ABCA1 was also suggested to be a phosphatidylserine translocase that facilitates phosphatidylserine exofacial flipping, an early event in apoptotic cells [341]. Therefore, association of FADD with different surface receptors or with ABCA1 may be a central mechanism that connects lipid metabolism, proliferation and apoptosis.

This is the first study that demonstrates an induction of TOSO in foam cells indicative for a function of TOSO in the development of atherosclerotic lesions and plaque rupture. TOSO was found induced in E-LDL generated foam cells and the use of Ox-LDL in concentrations that were recently shown to be toxic to monocytes/macrophages [251] do not induce TOSO mRNA. However, Ox-LDL, especially aggregated Ox-LDL, has also been published to prolong the survival of monocytes/macrophages [255]. Therefore it may be speculated that this effect is due to lipoprotein aggregation and a switch of the uptake pathway from scavenger receptors (e.g. CD36; LOX-1) [342] to phagocytic pathways (e.g. Fcγ-receptors), as aggregated lipoproteins are taken up by monocytes via phagocytosis [343]. This hypothesis is supported by the finding that the uptake of phagobeads also induces TOSO mRNA. E-LDL particles are preferentially internalized via non-specific and specific opsonin-receptor-mediated type I and type II phagocytosis that implies complement and Fcγ-receptors and may in part depend on ABCA1 [64; 259; 344]. Therefore, it is concluded together with the data shown here, that the type of atherogenic lipoprotein and the mode of its uptake may decide about prolonged survival or apoptosis of macrophages in the atherosclerotic lesion.

VII. SUMMARY

The ATP-binding cassette transporters A1 (ABCA1) and A7 (ABCA7) are inversely regulated under loading and deloading conditions and we were interested in protein/protein interactions of these transporters. The main topic was to identify, verify and characterize these interactions.

In case of ABCA7, the yeast two-hybrid approach led to false positive results, and therefore we focused on the expression and regulation of the two published isoforms. Albeit having similar tissue distribution, the two isoforms show different regulation by stimulation, indicating the use of alternative promoters. This caused us to analyze the promoter of the long isoform in more detail and we were able to map the core promoter region. Analyzes of the putative alternative promoter might enable us to understand the regulatory differences between both isoforms. Due to our initial experiments and data from the literature, we would suggest different functions for the two isoforms of ABCA7. Isoform I localizes to the plasma membrane and is upregulated during monocyte to macrophage differentiation, indicating involvment in phagocytic processes. In contrast, isoform II localizes to intracellular membranes and is upregulated together with phosphatase and tensin homolog in HL-60 cells and during terminal keratinocyte differentiation, pointing to a function in the autophagic pathway. Further experiments are necessary to confirm this hypothesis.

ABCA1 regulates plasma high-density lipoprotein levels and its cellular function is mediated through various protein interactions. One aim was to identify and confirm new ABCA1 C-terminus interacting PDZ proteins. By different methods seven new PDZ candidates were identified, and four of them, namely GAIP C-terminus-interacting protein1 (GIPC1), Tax1 (human T-cell leukemia virus type I) binding protein 3 (TAX1BP3), Scribble, and Membrane associated guanylate kinase, WW and PDZ domain containing 3 (MAGI3) were confirmed to bind to ABCA1 by different methods. Together with the known ABCA1 interacting PDZ proteins and their different tissue expression this may indicate that PDZ proteins are able to regulate ABCA1 trafficking and/or function in a tissue or even cell compartment specific manner.

The cytosolic molybdo-flavoenzyme aldehyde oxidase 1 (AOX1), known as xenobiotic metabolizing enzyme, was previously suggested as an ABCA1 interacting protein. In this work it was shown that knock-down of AOX1 by siRNA significantly reduced ABCA1-dependent lipid-efflux and enhanced phagocytic uptake in HepG2 cells. ABCA1 and AOX1 were found coexpressed in certain human cell types, namely hepatocytes, kidney proximal tubular epithelial cells, Leydig cells and cells of the adrenal cortex. Deregulation of ABCA1 and AOX1 in hepatocellular- and renal cell-carcinomas was observed, suggesting that AOX1, perhaps in context with ABCA1, might be used as tumor marker. The involvement of AOX1 in

metabolism of ethanol and xenobiotics is of particular interest, as it might link ABCA1 to detoxification, a process in which many ABC-transporters are involved.

Finally, as ABCA1 through its interaction with Fas-associated via death domain (FADD) might influence apoptosis, we searched for apoptotic genes regulated by modified lipoproteins in a similar manner as ABCA1. Uptake of modified lipoproteins by macrophages causes foam cell formation and promotes the development of atherosclerotic lesions. Atherogenic lipoproteins exert cytotoxic effects and induce necrosis or apoptosis under certain conditions but may also enhance macrophage survival. GeneChip experiments were performed to identify genes that are regulated in macrophages treated with enzymatically modified low-density lipoprotein (E-LDL). Expression of TOSO, protecting cells against CD95- or tumor necrosis factor-mediated apoptosis, was found induced by E-LDL. Concomitantly, reduced apoptosis was detected in E-LDL loaded macrophages compared to oxidized LDL incubated cells or controls. Abundance of the caspase inhibitor FLICE-like inhibitory protein long form ($FLIP_L$) was suggested to mediate the antiapoptotic properties of TOSO; however, $FLIP_L$ expression is induced neither in E-LDL laden macrophages nor in COS-7 cells overexpressing TOSO. E-LDL represents coreless liposome like particles and may be taken up by Fc- and complement-receptor dependent phagocytosis. Internalization of phagobeads by monocytes and macrophages upregulates TOSO but phagocytosis was not altered by TOSO in COS-7 cells. These data indicate that E-LDL-generated foam cells are protected from cell death most likely through the expression of TOSO by a mechanism independent of $FLIP_L$.

ABCA1 and ABCA7 may be related but exert distinct functions in the lipid-efflux/apoptosis/autophagy complex. While the function of ABCA1 is highly modulated by protein interactions, ABCA7 might be more affected by transcriptional regulation.

VIII. REFERENCES

[1] C.A.Doige, G.F.Ames, ATP-dependent transport systems in bacteria and humans: relevance to cystic fibrosis and multidrug resistance Annu.Rev.Microbiol. 47, (1993) 291-319.

[2] J.E.Walker, M.Saraste, M.J.Runswick, N.J.Gay, Distantly related sequences in the alpha- and beta-subunits of ATP synthase, myosin, kinases and other ATP-requiring enzymes and a common nucleotide binding fold EMBO J. 1, (1982) 945-951.

[3] C.F.Higgins, M.P.Gallagher, M.L.Mimmack, S.R.Pearce, A family of closely related ATP-binding subunits from prokaryotic and eukaryotic cells Bioessays 8, (1988) 111-116.

[4] D.C.Gadsby, P.Vergani, L.Csanady, The ABC protein turned chloride channel whose failure causes cystic fibrosis Nature 440, (2006) 477-483.

[5] J.R.Riordan, J.M.Rommens, B.Kerem, N.Alon, R.Rozmahel, Z.Grzelczak, J.Zielenski, S.Lok, N.Plavsic, J.L.Chou, ., Identification of the cystic fibrosis gene: cloning and characterization of complementary DNA Science 245, (1989) 1066-1073.

[6] W.E.Kaminski, A.Piehler, J.J.Wenzel, ABC A-subfamily transporters: structure, function and disease Biochim.Biophys.Acta 1762, (2006) 510-524.

[7] A.Decottignies, A.Goffeau, Complete inventory of the yeast ABC proteins Nat.Genet. 15, (1997) 137-145.

[8] W.E.Kaminski, E.Orso, W.Diederich, J.Klucken, W.Drobnik, G.Schmitz, Identification of a novel human sterol-sensitive ATP-binding cassette transporter (ABCA7) Biochem.Biophys.Res.Commun. 273, (2000) 532-538.

[9] W.E.Kaminski, A.Piehler, K.Pullmann, M.Porsch-Ozcurumez, C.Duong, G.M.Bared, C.Buchler, G.Schmitz, Complete coding sequence, promoter region, and genomic structure of the human ABCA2 gene and evidence for sterol-dependent regulation in macrophages Biochem.Biophys.Res.Commun. 281, (2001) 249-258.

[10] J.Klucken, C.Buchler, E.Orso, W.E.Kaminski, M.Porsch-Ozcurumez, G.Liebisch, M.Kapinsky, W.Diederich, W.Drobnik, M.Dean, R.Allikmets, G.Schmitz, ABCG1 (ABC8), the human homolog of the Drosophila white gene, is a regulator of macrophage cholesterol and phospholipid transport Proc.Natl.Acad.Sci.U.S.A 97, (2000) 817-822.

[11] T.Langmann, J.Klucken, M.Reil, G.Liebisch, M.F.Luciani, G.Chimini, W.E.Kaminski, G.Schmitz, Molecular cloning of the human ATP-binding cassette transporter 1 (hABC1): evidence for sterol-dependent regulation in macrophages Biochem.Biophys.Res.Commun. 257, (1999) 29-33.

[12] T.Langmann, R.Mauerer, A.Zahn, C.Moehle, M.Probst, W.Stremmel, G.Schmitz, Real-time reverse transcription-PCR expression profiling of the complete human ATP-binding cassette transporter superfamily in various tissues Clin.Chem. 49, (2003) 230-238.

[13] C.R.Pullinger, H.Hakamata, P.N.Duchateau, C.Eng, B.E.Aouizerat, M.H.Cho, C.J.Fielding, J.P.Kane, Analysis of hABC1 gene 5' end: additional peptide sequence, promoter region, and four polymorphisms Biochem.Biophys.Res.Commun. 271, (2000) 451-455.

[14] M.Bodzioch, E.Orso, J.Klucken, T.Langmann, A.Bottcher, W.Diederich, W.Drobnik, S.Barlage, C.Buchler, M.Porsch-Ozcurumez, W.E.Kaminski, H.W.Hahmann, K.Oette, G.Rothe, C.Aslanidis, K.J.Lackner, G.Schmitz, The gene encoding ATP-binding cassette transporter 1 is mutated in Tangier disease Nat.Genet. 22, (1999) 347-351.

[15] A.Brooks-Wilson, M.Marcil, S.M.Clee, L.H.Zhang, K.Roomp, M.van Dam, L.Yu, C.Brewer, J.A.Collins, H.O.Molhuizen, O.Loubser, B.F.Ouelette, K.Fichter, K.J.Ashbourne-Excoffon, C.W.Sensen, S.Scherer, S.Mott, M.Denis, D.Martindale, J.Frohlich, K.Morgan, B.Koop, S.Pimstone, J.J.Kastelein, J.Genest, Jr., M.R.Hayden, Mutations in ABC1 in Tangier disease and familial high-density lipoprotein deficiency Nat.Genet. 22, (1999) 336-345.

[16] S.Rust, M.Rosier, H.Funke, J.Real, Z.Amoura, J.C.Piette, J.F.Deleuze, H.B.Brewer, N.Duverger, P.Denefle, G.Assmann, Tangier disease is caused by mutations in the gene encoding ATP-binding cassette transporter 1 Nat.Genet. 22, (1999) 352-355.

[17] E.Orso, C.Broccardo, W.E.Kaminski, A.Bottcher, G.Liebisch, W.Drobnik, A.Gotz, O.Chambenoit, W.Diederich, T.Langmann, T.Spruss, M.F.Luciani, G.Rothe, K.J.Lackner, G.Chimini, G.Schmitz, Transport of lipids from golgi to plasma membrane is defective in tangier disease patients and Abc1-deficient mice Nat.Genet. 24, (2000) 192-196.

[18] R.M.Lawn, D.P.Wade, M.R.Garvin, X.Wang, K.Schwartz, J.G.Porter, J.J.Seilhamer, A.M.Vaughan, J.F.Oram, The Tangier disease gene product ABC1 controls the cellular apolipoprotein-mediated lipid removal pathway J.Clin.Invest 104, (1999) R25-R31.

[19] A.M.Vaughan, J.F.Oram, ABCA1 redistributes membrane cholesterol independent of apolipoprotein interactions J.Lipid Res. 44, (2003) 1373-1380.

[20] G.Szakacs, T.Langmann, C.Ozvegy, E.Orso, G.Schmitz, A.Varadi, B.Sarkadi, Characterization of the ATPase cycle of human ABCA1: implications for its function as a regulator rather than an active transporter Biochem.Biophys.Res.Commun. 288, (2001) 1258-1264.

[21] A.R.Tanaka, S.Abe-Dohmae, T.Ohnishi, R.Aoki, G.Morinaga, K.Okuhira, Y.Ikeda, F.Kano, M.Matsuo, N.Kioka, T.Amachi, M.Murata, S.Yokoyama, K.Ueda, Effects of mutations of ABCA1 in the first extracellular domain on subcellular trafficking and ATP binding/hydrolysis J.Biol.Chem. 278, (2003) 8815-8819.

[22] R.Ross, Atherosclerosis is an inflammatory disease Am.Heart J. 138, (1999) S419-S420.

[23] A.J.Mendez, G.Lin, D.P.Wade, R.M.Lawn, J.F.Oram, Membrane lipid domains distinct from cholesterol/sphingomyelin-rich rafts are involved in the ABCA1-mediated lipid secretory pathway J.Biol.Chem. 276, (2001) 3158-3166.

[24] E.B.Neufeld, A.T.Remaley, S.J.Demosky, J.A.Stonik, A.M.Cooney, M.Comly, N.K.Dwyer, M.Zhang, J.Blanchette-Mackie, S.Santamarina-Fojo, H.B.Brewer,

Jr., Cellular Localization and Trafficking of the Human ABCA1 Transporter J.Biol.Chem. 276, (2001) 27584.

[25] M.van Eck, I.S.Bos, W.E.Kaminski, E.Orso, G.Rothe, J.Twisk, A.Bottcher, E.S.Van Amersfoort, T.A.Christiansen-Weber, W.P.Fung-Leung, T.J.Van Berkel, G.Schmitz, Leukocyte ABCA1 controls susceptibility to atherosclerosis and macrophage recruitment into tissues Proc.Natl.Acad.Sci.U.S.A 99, (2002) 6298-6303.

[26] R.J.Aiello, D.Brees, P.A.Bourassa, L.Royer, S.Lindsey, T.Coskran, M.Haghpassand, O.L.Francone, Increased atherosclerosis in hyperlipidemic mice with inactivation of ABCA1 in macrophages Arterioscler.Thromb.Vasc.Biol. 22, (2002) 630-637.

[27] R.R.Singaraja, C.Fievet, G.Castro, E.R.James, N.Hennuyer, S.M.Clee, N.Bissada, J.C.Choy, J.C.Fruchart, B.M.McManus, B.Staels, M.R.Hayden, Increased ABCA1 activity protects against atherosclerosis J.Clin.Invest 110, (2002) 35-42.

[28] M.Porsch-Ozcurumez, T.Langmann, S.Heimerl, H.Borsukova, W.E.Kaminski, W.Drobnik, C.Honer, C.Schumacher, G.Schmitz, The zinc finger protein 202 (ZNF202) is a transcriptional repressor of ATP binding cassette transporter A1 (ABCA1) and ABCG1 gene expression and a modulator of cellular lipid efflux J.Biol.Chem. 276, (2001) 12427-12433.

[29] T.Langmann, M.Porsch-Ozcurumez, S.Heimerl, M.Probst, C.Moehle, M.Taher, H.Borsukova, D.Kielar, W.E.Kaminski, E.Dittrich-Wengenroth, G.Schmitz, Identification of sterol-independent regulatory elements in the human ATP-binding cassette transporter A1 promoter - Role of Sp1/3, E-box binding factors, and an oncostatin M-responsive element J.Biol.Chem. 277, (2002) 14443-14450.

[30] X.Gan, R.Kaplan, J.G.Menke, K.Macnaul, Y.Chen, C.P.Sparrow, G.Zhou, S.D.Wright, T.Q.Cai, Dual mechanisms of ABCA1 regulation by geranylgeranyl pyrophosphate J.Biol.Chem. 276, (2001) 48702-48708.

[31] G.Schmitz, T.Langmann, Transcriptional regulatory networks in lipid metabolism control ABCA1 expression Biochim.Biophys.Acta 1735, (2005) 1-19.

[32] P.Costet, Y.Luo, N.Wang, A.R.Tall, Sterol-dependent transactivation of the ABC1 promoter by the liver X receptor/retinoid X receptor J.Biol.Chem. 275, (2000) 28240-28245.

[33] K.Schwartz, R.M.Lawn, D.P.Wade, ABC1 gene expression and ApoA-I-mediated cholesterol efflux are regulated by LXR Biochem.Biophys.Res.Commun. 274, (2000) 794-802.

[34] G.Chinetti, S.Lestavel, V.Bocher, A.T.Remaley, B.Neve, I.P.Torra, E.Teissier, A.Minnich, M.Jaye, N.Duverger, H.B.Brewer, J.C.Fruchart, V.Clavey, B.Staels, PPAR-alpha and PPAR-gamma activators induce cholesterol removal from human macrophage foam cells through stimulation of the ABCA1 pathway Nat.Med. 7, (2001) 53-58.

[35] A.Chawla, W.A.Boisvert, C.H.Lee, B.A.Laffitte, Y.Barak, S.B.Joseph, D.Liao, L.Nagy, P.A.Edwards, L.K.Curtiss, R.M.Evans, P.Tontonoz, A PPAR gamma-LXR-ABCA1 pathway in macrophages is involved in cholesterol efflux and atherogenesis Mol.Cell 7, (2001) 161-171.

[36] A.C.Li, C.J.Binder, A.Gutierrez, K.K.Brown, C.R.Plotkin, J.W.Pattison, A.F.Valledor, R.A.Davis, T.M.Willson, J.L.Witztum, W.Palinski, C.K.Glass, Differential inhibition of macrophage foam-cell formation and atherosclerosis in mice by PPARalpha, beta/delta, and gamma J.Clin.Invest 114, (2004) 1564-1576.

[37] Y.Wang, J.F.Oram, Unsaturated fatty acids inhibit cholesterol efflux from macrophages by increasing degradation of ATP-binding cassette transporter A1 J.Biol.Chem. 277, (2002) 5692-5697.

[38] Y.Wang, J.F.Oram, Unsaturated fatty acids phosphorylate and destabilize ABCA1 through a phospholipase D2 pathway J.Biol.Chem. 280, (2005) 35896-35903.

[39] Y.Uehara, T.Engel, Z.Li, C.Goepfert, S.Rust, X.Zhou, C.Langer, C.Schachtrup, J.Wiekowski, S.Lorkowski, G.Assmann, A.von Eckardstein, Polyunsaturated fatty acids and acetoacetate downregulate the expression of the ATP-binding cassette transporter A1 Diabetes 51, (2002) 2922-2928.

[40] Y.Sun, M.Hao, Y.Luo, C.P.Liang, D.L.Silver, C.Cheng, F.R.Maxfield, A.R.Tall, Stearoyl-CoA desaturase inhibits ATP-binding cassette transporter A1-mediated cholesterol efflux and modulates membrane domain structure J.Biol.Chem. 278, (2003) 5813-5820.

[41] P.R.Shepherd, Mechanisms regulating phosphoinositide 3-kinase signalling in insulin-sensitive tissues Acta Physiol Scand. 183, (2005) 3-12.

[42] S.Nagao, K.Murao, H.Imachi, W.M.Cao, X.Yu, J.Li, K.Matsumoto, T.Nishiuchi, R.A.Ahmed, N.C.Wong, K.Ueda, T.Ishida, Platelet derived growth factor regulates ABCA1 expression in vascular smooth muscle cells FEBS Lett. 580, (2006) 4371-4376.

[43] Y.D.Landry, M.Denis, S.Nandi, S.Bell, A.M.Vaughan, X.Zha, ATP-binding cassette transporter A1 expression disrupts raft membrane microdomains through its ATPase-related functions J.Biol.Chem. 281, (2006) 36091-36101.

[44] J.R.Nofer, G.M.van der, M.Tolle, I.Wolinska, L.K.von Wnuck, H.A.Baba, U.J.Tietge, A.Godecke, I.Ishii, B.Kleuser, M.Schafers, M.Fobker, W.Zidek, G.Assmann, J.Chun, B.Levkau, HDL induces NO-dependent vasorelaxation via the lysophospholipid receptor S1P3 J.Clin.Invest 113, (2004) 569-581.

[45] D.Kim, G.Z.Cheng, C.W.Lindsley, H.Yang, J.Q.Cheng, Targeting the phosphatidylinositol-3 kinase/Akt pathway for the treatment of cancer Curr.Opin.Investig.Drugs 6, (2005) 1250-1258.

[46] D.L.Williams, C.Li, T.Ha, T.Ozment-Skelton, J.H.Kalbfleisch, J.Preiszner, L.Brooks, K.Breuel, J.B.Schweitzer, Modulation of the phosphoinositide 3-kinase pathway alters innate resistance to polymicrobial sepsis J.Immunol. 172, (2004) 449-456.

[47] A.Petiot, E.Ogier-Denis, E.F.Blommaart, A.J.Meijer, P.Codogno, Distinct classes of phosphatidylinositol 3'-kinases are involved in signaling pathways that control macroautophagy in HT-29 cells J.Biol.Chem. 275, (2000) 992-998.

[48] C.L.Wellington, E.K.Walker, A.Suarez, A.Kwok, N.Bissada, R.Singaraja, Y.Z.Yang, L.H.Zhang, E.James, J.E.Wilson, O.Francone, B.M.McManus, M.R.Hayden, ABCA1 mRNA and protein distribution patterns predict multiple different roles and levels of regulation Lab Invest 82, (2002) 273-283.

[49] Q.Wu, S.Sucheta, S.Azhar, K.M.Menon, Lipoprotein enhancement of ovarian theca-interstitial cell steroidogenesis: relative contribution of scavenger receptor class B (type I) and adenosine 5'-triphosphate- binding cassette (type A1) transporter in high-density lipoprotein-cholesterol transport and androgen synthesis Endocrinology 144, (2003) 2437-2445.

[50] G.Schmitz, W.E.Kaminski, M.Porsch-Ozcurumez, J.Klucken, E.Orso, M.Bodzioch, C.Buechler, W.Drobnik, ATP-Binding Cassette Transporter A1 (ABCA1) in Macrophages: A Dual Function in Inflammation and Lipid Metabolism? Pathobiology 67, (1999) 236-240.

[51] G.Schmitz, W.E.Kaminski, E.Orso, ABC transporters in cellular lipid trafficking Curr.Opin.Lipidol. 11, (2000) 493-501.

[52] T.A.Christiansen-Weber, J.R.Voland, Y.Wu, K.Ngo, B.L.Roland, S.Nguyen, P.A.Peterson, W.P.Fung-Leung, Functional loss of ABCA1 in mice causes severe placental malformation, aberrant lipid distribution, and kidney glomerulonephritis as well as high-density lipoprotein cholesterol deficiency Am.J.Pathol. 157, (2000) 1017-1029.

[53] D.M.Selva, V.Hirsch-Reinshagen, B.Burgess, S.Zhou, J.Chan, S.McIsaac, M.R.Hayden, G.L.Hammond, A.W.Vogl, C.L.Wellington, The ATP-binding cassette transporter 1 mediates lipid efflux from Sertoli cells and influences male fertility J.Lipid Res. 45, (2004) 1040-1050.

[54] Y.Munehira, T.Ohnishi, S.Kawamoto, A.Furuya, K.Shitara, M.Imamura, T.Yokota, S.Takeda, T.Amachi, M.Matsuo, N.Kioka, K.Ueda, Alpha1-syntrophin modulates turnover of ABCA1 J.Biol.Chem. 279, (2004) 15091-15095.

[55] K.Okuhira, M.L.Fitzgerald, D.A.Sarracino, J.J.Manning, S.A.Bell, J.L.Goss, M.W.Freeman, Purification of ATP-binding cassette transporter A1 and associated binding proteins reveals the importance of beta1-syntrophin in cholesterol efflux J.Biol.Chem. 280, (2005) 39653-39664.

[56] C.Buechler, A.Boettcher, S.M.Bared, M.C.Probst, G.Schmitz, The carboxyterminus of the ATP-binding cassette transporter A1 interacts with a beta2-syntrophin/utrophin complex Biochem.Biophys.Res.Commun. 293, (2002) 759-765.

[57] C.Buechler, S.M.Bared, C.Aslanidis, M.Ritter, W.Drobnik, G.Schmitz, Molecular and functional interaction of the ATP-binding cassette transporter A1 with Fas-associated death domain protein J.Biol.Chem. 277, (2002) 41307-41310.

[58] W.C.Yeh, J.L.Pompa, M.E.McCurrach, H.B.Shu, A.J.Elia, A.Shahinian, M.Ng, A.Wakeham, W.Khoo, K.Mitchell, W.S.El Deiry, S.W.Lowe, D.V.Goeddel, T.W.Mak, FADD: essential for embryo development and signaling from some, but not all, inducers of apoptosis Science 279, (1998) 1954-1958.

[59] S.Balachandran, E.Thomas, G.N.Barber, A FADD-dependent innate immune mechanism in mammalian cells Nature 432, (2004) 401-405.

[60] J.R.Nofer, A.T.Remaley, R.Feuerborn, I.Wolinnska, T.Engel, E.A.von, G.Assmann, Apolipoprotein A-I activates Cdc42 signaling through the ABCA1 transporter J.Lipid Res. 47, (2006) 794-803.

[61] K.Hirano, F.Matsuura, K.Tsukamoto, Z.Zhang, A.Matsuyama, K.Takaishi, R.Komuro, T.Suehiro, S.Yamashita, Y.Takai, Y.Matsuzawa, Decreased expression of a

member of the Rho GTPase family, Cdc42Hs, in cells from Tangier disease - the small G protein may play a role in cholesterol efflux FEBS Lett. 484, (2000) 275-279.

[62] J.R.Nofer, R.Feuerborn, B.Levkau, A.Sokoll, U.Seedorf, G.Assmann, Involvement of Cdc42 signaling in apoA-I-induced cholesterol efflux J.Biol.Chem. 278, (2003) 53055-53062.

[63] T.Engel, A.Lueken, G.Bode, U.Hobohm, S.Lorkowski, B.Schlueter, S.Rust, P.Cullen, M.Pech, G.Assmann, U.Seedorf, ADP-ribosylation factor (ARF)-like 7 (ARL7) is induced by cholesterol loading and participates in apolipoprotein AI-dependent cholesterol export FEBS Lett. 566, (2004) 241-246.

[64] S.M.Bared, C.Buechler, A.Boettcher, R.Dayoub, A.Sigruener, M.Grandl, C.Rudolph, A.Dada, G.Schmitz, Association of ABCA1 with syntaxin 13 and flotillin-1 and enhanced phagocytosis in tangier cells Mol.Biol.Cell 15, (2004) 5399-5407.

[65] W.E.Kaminski, A.Piehler, G.Schmitz, Genomic organization of the human cholesterol-responsive ABC transporter ABCA7: tandem linkage with the minor histocompatibility antigen HA-1 gene Biochem.Biophys.Res.Commun. 278, (2000) 782-789.

[66] S.Abe-Dohmae, Y.Ikeda, M.Matsuo, M.Hayashi, K.Okuhira, K.Ueda, S.Yokoyama, Human ABCA7 supports apolipoprotein-mediated release of cellular cholesterol and phospholipid to generate high density lipoprotein J.Biol.Chem. 279, (2004) 604-611.

[67] M.Hayashi, S.Abe-Dohmae, M.Okazaki, K.Ueda, S.Yokoyama, Heterogeneity of high density lipoprotein generated by ABCA1 and ABCA7 J.Lipid Res. 46, (2005) 1703-1711.

[68] Y.Ikeda, S.Abe-Dohmae, Y.Munehira, R.Aoki, S.Kawamoto, A.Furuya, K.Shitara, T.Amachi, N.Kioka, M.Matsuo, S.Yokoyama, K.Ueda, Posttranscriptional regulation of human ABCA7 and its function for the apoA-I-dependent lipid release Biochem.Biophys.Res.Commun. 311, (2003) 313-318.

[69] W.S.Kim, M.L.Fitzgerald, K.Kang, K.Okuhira, S.A.Bell, J.J.Manning, S.L.Koehn, N.Lu, K.J.Moore, M.W.Freeman, Abca7 null mice retain normal macrophage phosphatidylcholine and cholesterol efflux activity despite alterations in adipose mass and serum cholesterol levels J.Biol.Chem. 280, (2005) 3989-3995.

[70] P.Linsel-Nitschke, A.W.Jehle, J.Shan, G.Cao, D.Bacic, D.Lan, N.Wang, A.R.Tall, Potential role of ABCA7 in cellular lipid efflux to apoA-I J.Lipid Res. 46, (2005) 86-92.

[71] N.Wang, D.Lan, M.Gerbod-Giannone, P.Linsel-Nitschke, A.W.Jehle, W.Chen, L.O.Martinez, A.R.Tall, ATP-binding cassette transporter A7 (ABCA7) binds apolipoprotein A-I and mediates cellular phospholipid but not cholesterol efflux J.Biol.Chem. 278, (2003) 42906-42912.

[72] D.Kielar, W.E.Kaminski, G.Liebisch, A.Piehler, J.J.Wenzel, C.Mohle, S.Heimerl, T.Langmann, S.O.Friedrich, A.Bottcher, S.Barlage, W.Drobnik, G.Schmitz, Adenosine triphosphate binding cassette (ABC) transporters are expressed and regulated during terminal keratinocyte differentiation: a potential role for ABCA7 in epidermal lipid reorganization J.Invest Dermatol. 121, (2003) 465-474.

[73] N.Iwamoto, S.Abe-Dohmae, R.Sato, S.Yokoyama, ABCA7 expression is regulated by cellular cholesterol through the SREBP2 pathway and associated with phagocytosis J.Lipid Res. 47, (2006) 1915-1927.

[74] G.E.Grau, G.Chimini, Immunopathological consequences of the loss of engulfment genes: the case of ABCA1 J.Soc.Biol. 199, (2005) 199-206.

[75] A.W.Jehle, S.J.Gardai, S.Li, P.Linsel-Nitschke, K.Morimoto, W.J.Janssen, R.W.Vandivier, N.Wang, S.Greenberg, B.M.Dale, C.Qin, P.M.Henson, A.R.Tall, ATP-binding cassette transporter A7 enhances phagocytosis of apoptotic cells and associated ERK signaling in macrophages J.Cell Biol. 174, (2006) 547-556.

[76] A.M.Vaughan, J.F.Oram, ABCG1 redistributes cell cholesterol to domains removable by high density lipoprotein but not by lipid-depleted apolipoproteins J.Biol.Chem. 280, (2005) 30150-30157.

[77] K.Nakamura, M.A.Kennedy, A.Baldan, D.D.Bojanic, K.Lyons, P.A.Edwards, Expression and regulation of multiple murine ATP-binding cassette transporter G1 mRNAs/isoforms that stimulate cellular cholesterol efflux to high density lipoprotein J.Biol.Chem. 279, (2004) 45980-45989.

[78] N.Wang, D.Lan, W.Chen, F.Matsuura, A.R.Tall, ATP-binding cassette transporters G1 and G4 mediate cellular cholesterol efflux to high-density lipoproteins Proc.Natl.Acad.Sci.U.S.A 101, (2004) 9774-9779.

[79] N.Wang, D.L.Silver, P.Costet, A.R.Tall, Specific binding of ApoA-I, enhanced cholesterol efflux, and altered plasma membrane morphology in cells expressing ABC1 J.Biol.Chem. 275, (2000) 33053-33058.

[80] N.Wang, D.L.Silver, C.Thiele, A.R.Tall, ATP-binding cassette transporter A1 (ABCA1) functions as a cholesterol efflux regulatory protein J.Biol.Chem. 276, (2001) 23742-23747.

[81] J.F.Oram, R.M.Lawn, M.R.Garvin, D.P.Wade, ABCA1 is the cAMP-inducible apolipoprotein receptor that mediates cholesterol secretion from macrophages J.Biol.Chem. 275, (2000) 34508-34511.

[82] S.Lorkowski, S.Rust, T.Engel, E.Jung, K.Tegelkamp, E.A.Galinski, G.Assmann, P.Cullen, Genomic sequence and structure of the human ABCG1 (ABC8) gene Biochem.Biophys.Res.Commun. 280, (2001) 121-131.

[83] M.A.Kennedy, A.Venkateswaran, P.T.Tarr, I.Xenarios, J.Kudoh, N.Shimizu, P.A.Edwards, Characterization of the human ABCG1 gene: liver X receptor activates an internal promoter that produces a novel transcript encoding an alternative form of the protein J.Biol.Chem. 276, (2001) 39438-39447.

[84] A.Baldan, P.Tarr, R.Lee, P.A.Edwards, ATP-binding cassette transporter G1 and lipid homeostasis Curr.Opin.Lipidol. 17, (2006) 227-232.

[85] C.Cavelier, I.Lorenzi, L.Rohrer, A.von Eckardstein, Lipid efflux by the ATP-binding cassette transporters ABCA1 and ABCG1 Biochim.Biophys.Acta 1761, (2006) 655-666.

[86] I.C.Gelissen, M.Harris, K.A.Rye, C.Quinn, A.J.Brown, M.Kockx, S.Cartland, M.Packianathan, L.Kritharides, W.Jessup, ABCA1 and ABCG1 synergize to

mediate cholesterol export to apoA-I Arterioscler.Thromb.Vasc.Biol. 26, (2006) 534-540.

[87] A.Baldan, P.Tarr, C.S.Vales, J.Frank, T.K.Shimotake, S.Hawgood, P.A.Edwards, Deletion of the transmembrane transporter ABCG1 results in progressive pulmonary lipidosis J.Biol.Chem. 281, (2006) 29401-29410.

[88] E.C.Dell'Angelica, C.Mullins, S.Caplan, J.S.Bonifacino, Lysosome-related organelles FASEB J. 14, (2000) 1265-1278.

[89] J.P.Luzio, V.Poupon, M.R.Lindsay, B.M.Mullock, R.C.Piper, P.R.Pryor, Membrane dynamics and the biogenesis of lysosomes Mol.Membr.Biol. 20, (2003) 141-154.

[90] W.Li, M.E.Rusiniak, S.Chintala, R.Gautam, E.K.Novak, R.T.Swank, Murine Hermansky-Pudlak syndrome genes: regulators of lysosome-related organelles Bioessays 26, (2004) 616-628.

[91] R.Clark, G.M.Griffiths, Lytic granules, secretory lysosomes and disease Curr.Opin.Immunol. 15, (2003) 516-521.

[92] M.Huizing, W.A.Gahl, Disorders of vesicles of lysosomal lineage: the Hermansky-Pudlak syndromes Curr.Mol.Med. 2, (2002) 451-467.

[93] R.A.Spritz, P.W.Chiang, N.Oiso, A.Alkhateeb, Human and mouse disorders of pigmentation Curr.Opin.Genet.Dev. 13, (2003) 284-289.

[94] S.L.Shiflett, J.Kaplan, D.M.Ward, Chediak-Higashi Syndrome: a rare disorder of lysosomes and lysosome related organelles Pigment Cell Res. 15, (2002) 251-257.

[95] D.M.Ward, S.L.Shiflett, J.Kaplan, Chediak-Higashi syndrome: a clinical and molecular view of a rare lysosomal storage disorder Curr.Mol.Med. 2, (2002) 469-477.

[96] Y.Tomita, T.Suzuki, Genetics of pigmentary disorders Am.J.Med.Genet.C.Semin.Med.Genet. 131C, (2004) 75-81.

[97] J.Stinchcombe, G.Bossi, G.M.Griffiths, Linking albinism and immunity: the secrets of secretory lysosomes Science 305, (2004) 55-59.

[98] N.V.Morgan, S.Pasha, C.A.Johnson, J.R.Ainsworth, R.A.Eady, B.Dawood, C.McKeown, R.C.Trembath, J.Wilde, S.P.Watson, E.R.Maher, A germline mutation in BLOC1S3/reduced pigmentation causes a novel variant of Hermansky-Pudlak syndrome (HPS8) Am.J.Hum.Genet. 78, (2006) 160-166.

[99] M.Starcevic, E.C.Dell'Angelica, Identification of snapin and three novel proteins (BLOS1, BLOS2, and BLOS3/reduced pigmentation) as subunits of biogenesis of lysosome-related organelles complex-1 (BLOC-1) J.Biol.Chem. 279, (2004) 28393-28401.

[100] E.C.Dell'Angelica, The building BLOC(k)s of lysosomes and related organelles Curr.Opin.Cell Biol. 16, (2004) 458-464.

[101] R.Gautam, E.K.Novak, J.Tan, K.Wakamatsu, S.Ito, R.T.Swank, Interaction of Hermansky-Pudlak Syndrome genes in the regulation of lysosome-related organelles Traffic. 7, (2006) 779-792.

[102] F.Y.Teng, Y.Wang, B.L.Tang, The syntaxins Genome Biol. 2, (2001) REVIEWS3012.

[103] L.Huang, Y.M.Kuo, J.Gitschier, The pallid gene encodes a novel, syntaxin 13-interacting protein involved in platelet storage pool deficiency Nat.Genet. 23, (1999) 329-332.

[104] J.E.Rothman, F.T.Wieland, Protein sorting by transport vesicles Science 272, (1996) 227-234.

[105] L.Lu, H.Horstmann, C.Ng, W.Hong, Regulation of Golgi structure and function by ARF-like protein 1 (Arl1) J.Cell Sci. 114, (2001) 4543-4555.

[106] V.K.Lloyd, D.A.Sinclair, M.Alperyn, T.A.Grigliatti, Enhancer of garnet/deltaAP-3 is a cryptic allele of the white gene and identifies the intracellular transport system for the white protein Genome 45, (2002) 296-312.

[107] T.Plosch, A.Kosters, A.K.Groen, F.Kuipers, The ABC of hepatic and intestinal cholesterol transport Handb.Exp.Pharmacol.(2005) 465-482.

[108] L.Liscum, J.J.Klansek, Niemann-Pick disease type C Curr.Opin.Lipidol. 9, (1998) 131-135.

[109] P.G.Pentchev, H.S.Kruth, M.E.Comly, J.D.Butler, M.T.Vanier, D.A.Wenger, S.Patel, Type C Niemann-Pick disease. A parallel loss of regulatory responses in both the uptake and esterification of low density lipoprotein-derived cholesterol in cultured fibroblasts J.Biol.Chem. 261, (1986) 16775-16780.

[110] E.J.Blanchette-Mackie, N.K.Dwyer, L.M.Amende, H.S.Kruth, J.D.Butler, J.Sokol, M.E.Comly, M.T.Vanier, J.T.August, R.O.Brady, ., Type-C Niemann-Pick disease: low density lipoprotein uptake is associated with premature cholesterol accumulation in the Golgi complex and excessive cholesterol storage in lysosomes Proc.Natl.Acad.Sci.U.S.A 85, (1988) 8022-8026.

[111] P.G.Pentchev, E.J.Blanchette-Mackie, L.Liscum, Biological implications of the Niemann-Pick C mutation Subcell.Biochem. 28, (1997) 437-451.

[112] L.Liscum, J.R.Faust, Low density lipoprotein (LDL)-mediated suppression of cholesterol synthesis and LDL uptake is defective in Niemann-Pick type C fibroblasts J.Biol.Chem. 262, (1987) 17002-17008.

[113] P.E.Kuwabara, M.Labouesse, The sterol-sensing domain: multiple families, a unique role? Trends Genet. 18, (2002) 193-201.

[114] M.S.Brown, J.L.Goldstein, A proteolytic pathway that controls the cholesterol content of membranes, cells, and blood Proc.Natl.Acad.Sci.U.S.A 96, (1999) 11041-11048.

[115] J.L.Goldstein, M.S.Brown, Regulation of the mevalonate pathway Nature 343, (1990) 425-430.

[116] J.L.Goldstein, R.B.Rawson, M.S.Brown, Mutant mammalian cells as tools to delineate the sterol regulatory element-binding protein pathway for feedback regulation of lipid synthesis Arch.Biochem.Biophys. 397, (2002) 139-148.

[117] J.D.Horton, J.L.Goldstein, M.S.Brown, SREBPs: activators of the complete program of cholesterol and fatty acid synthesis in the liver J.Clin.Invest 109, (2002) 1125-1131.

[118] R.E.Soccio, J.L.Breslow, StAR-related lipid transfer (START) proteins: mediators of intracellular lipid metabolism J.Biol.Chem. 278, (2003) 22183-22186.

[119] F.Alpy, C.Tomasetto, Give lipids a START: the StAR-related lipid transfer (START) domain in mammals J.Cell Sci. 118, (2005) 2791-2801.

[120] Y.Tsujishita, J.H.Hurley, Structure and lipid transport mechanism of a StAR-related domain Nat.Struct.Biol. 7, (2000) 408-414.

[121] O.Hatano, A.Takakusu, M.Nomura, K.Morohashi, Identical origin of adrenal cortex and gonad revealed by expression profiles of Ad4BP/SF-1 Genes Cells 1, (1996) 663-671.

[122] B.C.Chung, K.J.Matteson, R.Voutilainen, T.K.Mohandas, W.L.Miller, Human cholesterol side-chain cleavage enzyme, P450scc: cDNA cloning, assignment of the gene to chromosome 15, and expression in the placenta Proc.Natl.Acad.Sci.U.S.A 83, (1986) 8962-8966.

[123] K.Morohashi, K.Sogawa, T.Omura, Y.Fujii-Kuriyama, Gene structure of human cytochrome P-450(SCC), cholesterol desmolase J.Biochem.(Tokyo) 101, (1987) 879-887.

[124] R.S.Sparkes, I.Klisak, W.L.Miller, Regional mapping of genes encoding human steroidogenic enzymes: P450scc to 15q23-q24, adrenodoxin to 11q22; adrenodoxin reductase to 17q24-q25; and P450c17 to 10q24-q25 DNA Cell Biol. 10, (1991) 359-365.

[125] W.L.Miller, Molecular biology of steroid hormone synthesis Endocr.Rev. 9, (1988) 295-318.

[126] S.M.Black, J.A.Harikrishna, G.D.Szklarz, W.L.Miller, The mitochondrial environment is required for activity of the cholesterol side-chain cleavage enzyme, cytochrome P450scc Proc.Natl.Acad.Sci.U.S.A 91, (1994) 7247-7251.

[127] D.STONE, O.HECHTER, Studies on ACTH action in perfused bovine adrenals: aspects of progesterone as an intermediary in corticosteroidogenesis Arch.Biochem. 54, (1955) 121-128.

[128] J.J.FERGUSON, Jr., PROTEIN SYNTHESIS AND ADRENOCORTICOTROPIN RESPONSIVENESS J.Biol.Chem. 238, (1963) 2754-2759.

[129] L.D.Garren, R.L.Ney, W.W.Davis, Studies on the role of protein synthesis in the regulation of corticosterone production by adrenocorticotropic hormone in vivo Proc.Natl.Acad.Sci.U.S.A 53, (1965) 1443-1450.

[130] L.D.Garren, W.W.Davis, R.M.Crocco, R.L.Ney, Puromycin analogs: action of adrenocorticotropic hormone and the role of glycogen Science 152, (1966) 1386-1388.

[131] B.J.Clark, J.Wells, S.R.King, D.M.Stocco, The purification, cloning, and expression of a novel luteinizing hormone-induced mitochondrial protein in MA-10 mouse Leydig tumor cells. Characterization of the steroidogenic acute regulatory protein (StAR) J.Biol.Chem. 269, (1994) 28314-28322.

[132] D.Lin, T.Sugawara, J.F.Strauss, III, B.J.Clark, D.M.Stocco, P.Saenger, A.Rogol, W.L.Miller, Role of steroidogenic acute regulatory protein in adrenal and gonadal steroidogenesis Science 267, (1995) 1828-1831.

[133] T.Sugawara, J.A.Holt, D.Driscoll, J.F.Strauss, III, D.Lin, W.L.Miller, D.Patterson, K.P.Clancy, I.M.Hart, B.J.Clark, ., Human steroidogenic acute regulatory protein: functional activity in COS-1 cells, tissue-specific expression, and mapping of the structural gene to 8p11.2 and a pseudogene to chromosome 13 Proc.Natl.Acad.Sci.U.S.A 92, (1995) 4778-4782.

[134] S.Mesiano, R.B.Jaffe, Developmental and functional biology of the primate fetal adrenal cortex Endocr.Rev. 18, (1997) 378-403.

[135] G.D.Hammer, K.L.Parker, B.P.Schimmer, Minireview: transcriptional regulation of adrenocortical development Endocrinology 146, (2005) 1018-1024.

[136] Migeon C.J., Donohoue P.A., Adrenal disorders, in: Kappy MS, Blizzard RM, Migeon CJ (Eds.), Wilkins´ The Diagnosis and Management of Endocrine Disorders in Childhood and Adolescence,Charles C Thomas, Springfield, IL, 1994, pp. 717-856.

[137] R.N.Yu, M.Ito, J.L.Jameson, The murine Dax-1 promoter is stimulated by SF-1 (steroidogenic factor-1) and inhibited by COUP-TF (chicken ovalbumin upstream promoter-transcription factor) via a composite nuclear receptor-regulatory element Mol.Endocrinol. 12, (1998) 1010-1022.

[138] K.Kawabe, T.Shikayama, H.Tsuboi, S.Oka, K.Oba, T.Yanase, H.Nawata, K.Morohashi, Dax-1 as one of the target genes of Ad4BP/SF-1 Mol.Endocrinol. 13, (1999) 1267-1284.

[139] C.Hoyle, V.Narvaez, G.Alldus, R.Lovell-Badge, A.Swain, Dax1 expression is dependent on steroidogenic factor 1 in the developing gonad Mol.Endocrinol. 16, (2002) 747-756.

[140] M.Ito, R.Yu, J.L.Jameson, DAX-1 inhibits SF-1-mediated transactivation via a carboxy-terminal domain that is deleted in adrenal hypoplasia congenita Mol.Cell Biol. 17, (1997) 1476-1483.

[141] P.A.Crawford, C.Dorn, Y.Sadovsky, J.Milbrandt, Nuclear receptor DAX-1 recruits nuclear receptor corepressor N-CoR to steroidogenic factor 1 Mol.Cell Biol. 18, (1998) 2949-2956.

[142] A.K.Iyer, E.R.McCabe, Molecular mechanisms of DAX1 action Mol.Genet.Metab 83, (2004) 60-73.

[143] K.Jeays-Ward, C.Hoyle, J.Brennan, M.Dandonneau, G.Alldus, B.Capel, A.Swain, Endothelial and steroidogenic cell migration are regulated by WNT4 in the developing mammalian gonad Development 130, (2003) 3663-3670.

[144] H.Mizusaki, K.Kawabe, T.Mukai, E.Ariyoshi, M.Kasahara, H.Yoshioka, A.Swain, K.Morohashi, Dax-1 (dosage-sensitive sex reversal-adrenal hypoplasia congenita critical region on the X chromosome, gene 1) gene transcription is regulated by wnt4 in the female developing gonad Mol.Endocrinol. 17, (2003) 507-519.

[145] K.D.Wagner, N.Wagner, A.Schedl, The complex life of WT1 J.Cell Sci. 116, (2003) 1653-1658.

[146] M.W.Nachtigal, Y.Hirokawa, D.L.Enyeart-VanHouten, J.N.Flanagan, G.D.Hammer, H.A.Ingraham, Wilms' tumor 1 and Dax-1 modulate the orphan nuclear receptor SF-1 in sex-specific gene expression Cell 93, (1998) 445-454.

[147] J.Kim, D.Prawitt, N.Bardeesy, E.Torban, C.Vicaner, P.Goodyer, B.Zabel, J.Pelletier, The Wilms' tumor suppressor gene (wt1) product regulates Dax-1 gene expression during gonadal differentiation Mol.Cell Biol. 19, (1999) 2289-2299.

[148] S.Y.Park, J.L.Jameson, Minireview: transcriptional regulation of gonadal development and differentiation Endocrinology 146, (2005) 1035-1042.

[149] N.di Clemente, N.Josso, L.Gouedard, C.Belville, Components of the anti-Mullerian hormone signaling pathway in gonads Mol.Cell Endocrinol. 211, (2003) 9-14.

[150] S.Nef, L.F.Parada, Cryptorchidism in mice mutant for Insl3 Nat.Genet. 22, (1999) 295-299.

[151] J.Schmahl, E.M.Eicher, L.L.Washburn, B.Capel, Sry induces cell proliferation in the mouse gonad Development 127, (2000) 65-73.

[152] J.Brennan, J.Karl, B.Capel, Divergent vascular mechanisms downstream of Sry establish the arterial system in the XY gonad Dev.Biol. 244, (2002) 418-428.

[153] A.J.Ross, B.Capel, Signaling at the crossroads of gonad development Trends Endocrinol.Metab 16, (2005) 19-25.

[154] D.B.Menke, J.Koubova, D.C.Page, Sexual differentiation of germ cells in XX mouse gonads occurs in an anterior-to-posterior wave Dev.Biol. 262, (2003) 303-312.

[155] I.R.Adams, A.McLaren, Sexually dimorphic development of mouse primordial germ cells: switching from oogenesis to spermatogenesis Development 129, (2002) 1155-1164.

[156] H.H.Yao, L.DiNapoli, B.Capel, Meiotic germ cells antagonize mesonephric cell migration and testis cord formation in mouse gonads Development 130, (2003) 5895-5902.

[157] M.Buehr, S.Gu, A.McLaren, Mesonephric contribution to testis differentiation in the fetal mouse Development 117, (1993) 273-281.

[158] H.Merchant-Larios, N.Moreno-Mendoza, M.Buehr, The role of the mesonephros in cell differentiation and morphogenesis of the mouse fetal testis Int.J.Dev.Biol. 37, (1993) 407-415.

[159] J.Martineau, K.Nordqvist, C.Tilmann, R.Lovell-Badge, B.Capel, Male-specific cell migration into the developing gonad Curr.Biol. 7, (1997) 958-968.

[160] C.Tilmann, B.Capel, Mesonephric cell migration induces testis cord formation and Sertoli cell differentiation in the mammalian gonad Development 126, (1999) 2883-2890.

[161] H.H.Yao, W.Whoriskey, B.Capel, Desert Hedgehog/Patched 1 signaling specifies fetal Leydig cell fate in testis organogenesis Genes Dev. 16, (2002) 1433-1440.

[162] J.Brennan, C.Tilmann, B.Capel, Pdgfr-alpha mediates testis cord organization and fetal Leydig cell development in the XY gonad Genes Dev. 17, (2003) 800-810.

[163] K.Kitamura, M.Yanazawa, N.Sugiyama, H.Miura, A.Iizuka-Kogo, M.Kusaka, K.Omichi, R.Suzuki, Y.Kato-Fukui, K.Kamiirisa, M.Matsuo, S.Kamijo,

M.Kasahara, H.Yoshioka, T.Ogata, T.Fukuda, I.Kondo, M.Kato, W.B.Dobyns, M.Yokoyama, K.Morohashi, Mutation of ARX causes abnormal development of forebrain and testes in mice and X-linked lissencephaly with abnormal genitalia in humans Nat.Genet. 32, (2002) 359-369.

[164] J.B.Kerr, C.M.Knell, The fate of fetal Leydig cells during the development of the fetal and postnatal rat testis Development 103, (1988) 535-544.

[165] H.B.Ariyaratne, S.Chamindrani Mendis-Handagama, Changes in the testis interstitium of Sprague Dawley rats from birth to sexual maturity Biol.Reprod. 62, (2000) 680-690.

[166] R.Habert, H.Lejeune, J.M.Saez, Origin, differentiation and regulation of fetal and adult Leydig cells Mol.Cell Endocrinol. 179, (2001) 47-74.

[167] F.Pierucci-Alves, A.M.Clark, L.D.Russell, A developmental study of the Desert hedgehog-null mouse testis Biol.Reprod. 65, (2001) 1392-1402.

[168] A.M.Clark, K.K.Garland, L.D.Russell, Desert hedgehog (Dhh) gene is required in the mouse testis for formation of adult-type Leydig cells and normal development of peritubular cells and seminiferous tubules Biol.Reprod. 63, (2000) 1825-1838.

[169] F.Umehara, G.Tate, K.Itoh, N.Yamaguchi, T.Douchi, T.Mitsuya, M.Osame, A novel mutation of desert hedgehog in a patient with 46,XY partial gonadal dysgenesis accompanied by minifascicular neuropathy Am.J.Hum.Genet. 67, (2000) 1302-1305.

[170] P.Canto, D.Soderlund, E.Reyes, J.P.Mendez, Mutations in the desert hedgehog (DHH) gene in patients with 46,XY complete pure gonadal dysgenesis J.Clin.Endocrinol.Metab 89, (2004) 4480-4483.

[171] L.Gnessi, S.Basciani, S.Mariani, M.Arizzi, G.Spera, C.Wang, C.Bondjers, L.Karlsson, C.Betsholtz, Leydig cell loss and spermatogenic arrest in platelet-derived growth factor (PDGF)-A-deficient mice J.Cell Biol. 149, (2000) 1019-1026.

[172] K.J.Teerds, D.G.De Rooij, F.F.Rommerts, d.T.van, I, C.J.Wensing, Turnover time of Leydig cells and other interstitial cells in testes of adult rats Arch.Androl 23, (1989) 105-111.

[173] J.B.Kerr, K.Donachie, F.F.Rommerts, Selective destruction and regeneration of rat Leydig cells in vivo. A new method for the study of seminiferous tubular-interstitial tissue interaction Cell Tissue Res. 242, (1985) 145-156.

[174] R.Molenaar, D.G.De Rooij, F.F.Rommerts, H.J.van der Molen, Repopulation of Leydig cells in mature rats after selective destruction of the existent Leydig cells with ethylene dimethane sulfonate is dependent on luteinizing hormone and not follicle-stimulating hormone Endocrinology 118, (1986) 2546-2554.

[175] K.J.Teerds, D.G.De Rooij, F.F.Rommerts, C.J.Wensing, Development of a new Leydig cell population after the destruction of existing Leydig cells by ethane dimethane sulphonate in rats: an autoradiographic study J.Endocrinol. 126, (1990) 229-236.

[176] A.K.Christensen, K.C.Peacock, Increase in Leydig cell number in testes of adult rats treated chronically with an excess of human chorionic gonadotropin Biol.Reprod. 22, (1980) 383-391.

[177] K.J.Teerds, D.G.De Rooij, F.F.Rommerts, C.J.Wensing, The regulation of the proliferation and differentiation of rat Leydig cell precursor cells after EDS administration or daily HCG treatment J.Androl 9, (1988) 343-351.

[178] K.J.Teerds, F.F.Rommerts, H.J.van de Kant, D.G.De Rooij, Leydig cell number and function in the adult cynomolgus monkey (Macaca fascicularis) is increased by daily hCG treatment but not by daily FSH treatment J.Reprod.Fertil. 87, (1989) 141-146.

[179] S.M.Mendis-Handagama, P.A.Watkins, S.J.Gelber, T.J.Scallen, The effect of chronic luteinizing hormone treatment on adult rat Leydig cells Tissue Cell 30, (1998) 64-73.

[180] S.M.Mendis-Handagama, H.B.Ariyaratne, Differentiation of the adult Leydig cell population in the postnatal testis Biol.Reprod. 65, (2001) 660-671.

[181] K.C.Lo, Z.Lei, C.Rao, J.Beck, D.J.Lamb, De novo testosterone production in luteinizing hormone receptor knockout mice after transplantation of leydig stem cells Endocrinology 145, (2004) 4011-4015.

[182] W.M.Geissler, D.L.Davis, L.Wu, K.D.Bradshaw, S.Patel, B.B.Mendonca, K.O.Elliston, J.D.Wilson, D.W.Russell, S.Andersson, Male pseudohermaphroditism caused by mutations of testicular 17 beta-hydroxysteroid dehydrogenase 3 Nat.Genet. 7, (1994) 34-39.

[183] P.J.O'Shaughnessy, P.J.Baker, M.Heikkila, S.Vainio, A.P.McMahon, Localization of 17beta-hydroxysteroid dehydrogenase/17-ketosteroid reductase isoform expression in the developing mouse testis--androstenedione is the major androgen secreted by fetal/neonatal leydig cells Endocrinology 141, (2000) 2631-2637.

[184] L.Lin, J.C.Achermann, The adrenal Horm.Res. 62 Suppl 3, (2004) 22-29.

[185] P.E.Jira, H.R.Waterham, R.J.Wanders, J.A.Smeitink, R.C.Sengers, R.A.Wevers, Smith-Lemli-Opitz syndrome and the DHCR7 gene Ann.Hum.Genet. 67, (2003) 269-280.

[186] H.S.Bose, T.Sugawara, J.F.Strauss, III, W.L.Miller, The pathophysiology and genetics of congenital lipoid adrenal hyperplasia. International Congenital Lipoid Adrenal Hyperplasia Consortium N.Engl.J.Med. 335, (1996) 1870-1878.

[187] J.C.Achermann, J.J.Meeks, B.Jeffs, U.Das, P.E.Clayton, C.G.Brook, J.L.Jameson, Molecular and structural analysis of two novel StAR mutations in patients with lipoid congenital adrenal hyperplasia Mol.Genet.Metab 73, (2001) 354-357.

[188] T.Tajima, K.Fujieda, N.Kouda, J.Nakae, W.L.Miller, Heterozygous mutation in the cholesterol side chain cleavage enzyme (p450scc) gene in a patient with 46,XY sex reversal and adrenal insufficiency J.Clin.Endocrinol.Metab 86, (2001) 3820-3825.

[189] N.Katsumata, M.Ohtake, T.Hojo, E.Ogawa, T.Hara, N.Sato, T.Tanaka, Compound heterozygous mutations in the cholesterol side-chain cleavage enzyme gene (CYP11A) cause congenital adrenal insufficiency in humans J.Clin.Endocrinol.Metab 87, (2002) 3808-3813.

[190] M.Kagimoto, J.S.Winter, K.Kagimoto, E.R.Simpson, M.R.Waterman, Structural characterization of normal and mutant human steroid 17 alpha-hydroxylase

genes: molecular basis of one example of combined 17 alpha-hydroxylase/17,20 lyase deficiency Mol.Endocrinol. 2, (1988) 564-570.

[191] W.L.Miller, Steroid 17alpha-hydroxylase deficiency--not rare everywhere J.Clin.Endocrinol.Metab 89, (2004) 40-42.

[192] W.G.Beamer, H.O.Sweet, R.T.Bronson, J.G.Shire, D.N.Orth, M.T.Davisson, Adrenocortical dysplasia: a mouse model system for adrenocortical insufficiency J.Endocrinol. 141, (1994) 33-43.

[193] D.M.Hurley, D.Accili, C.A.Stratakis, M.Karl, N.Vamvakopoulos, E.Rorer, K.Constantine, S.I.Taylor, G.P.Chrousos, Point mutation causing a single amino acid substitution in the hormone binding domain of the glucocorticoid receptor in familial glucocorticoid resistance J.Clin.Invest 87, (1991) 680-686.

[194] T.Kino, R.H.Stauber, J.H.Resau, G.N.Pavlakis, G.P.Chrousos, Pathologic human GR mutant has a transdominant negative effect on the wild-type GR by inhibiting its translocation into the nucleus: importance of the ligand-binding domain for intracellular GR trafficking J.Clin.Endocrinol.Metab 86, (2001) 5600-5608.

[195] D.S.Geller, J.Rodriguez-Soriano, B.A.Vallo, S.Schifter, M.Bayer, S.S.Chang, R.P.Lifton, Mutations in the mineralocorticoid receptor gene cause autosomal dominant pseudohypoaldosteronism type I Nat.Genet. 19, (1998) 279-281.

[196] L.Lin, J.C.Achermann, Inherited adrenal hypoplasia: not just for kids! Clin.Endocrinol.(Oxf) 60, (2004) 529-537.

[197] R.S.Obach, P.Huynh, M.C.Allen, C.Beedham, Human liver aldehyde oxidase: inhibition by 239 drugs J.Clin.Pharmacol. 44, (2004) 7-19.

[198] S.Tomita, M.Tsujita, Y.Ichikawa, Retinal oxidase is identical to aldehyde oxidase FEBS Lett. 336, (1993) 272-274.

[199] D.Y.Huang, Y.Ichikawa, Two different enzymes are primarily responsible for retinoic acid synthesis in rabbit liver cytosol Biochem.Biophys.Res.Commun. 205, (1994) 1278-1283.

[200] Y.Moriwaki, T.Yamamoto, K.Higashino, Distribution and pathophysiologic role of molybdenum-containing enzymes Histol.Histopathol. 12, (1997) 513-524.

[201] S.Shaw, E.Jayatilleke, The role of aldehyde oxidase in ethanol-induced hepatic lipid peroxidation in the rat Biochem.J. 268, (1990) 579-583.

[202] R.M.Wright, J.L.McManaman, J.E.Repine, Alcohol-induced breast cancer: a proposed mechanism Free Radic.Biol.Med. 26, (1999) 348-354.

[203] X.D.Wang, Alcohol, vitamin A, and cancer Alcohol 35, (2005) 251-258.

[204] T.Langmann, G.Liebisch, C.Moehle, R.Schifferer, R.Dayoub, S.Heiduczek, M.Grandl, A.Dada, G.Schmitz, Gene expression profiling identifies retinoids as potent inducers of macrophage lipid efflux Biochim.Biophys.Acta 1740, (2005) 155-161.

[205] Y.M.Yang, D.Y.Huang, G.F.Liu, J.C.Zhong, K.Du, Y.F.Li, X.H.Song, Effects of 2,3,7,8-tetrachlorodibenzo-p-dioxin on vitamin A metabolism in mice J.Biochem.Mol.Toxicol. 19, (2005) 327-335.

[206] M.L.Calzi, C.Raviolo, E.Ghibaudi, L.de Gioia, M.Salmona, G.Cazzaniga, M.Kurosaki, M.Terao, E.Garattini, Purification, cDNA cloning, and tissue distribution of bovine liver aldehyde oxidase J.Biol.Chem. 270, (1995) 31037-31045.

[207] G.Carpani, M.Racchi, P.Ghezzi, M.Terao, E.Garattini, Purification and characterization of mouse liver xanthine oxidase Arch.Biochem.Biophys. 279, (1990) 237-241.

[208] M.Terao, M.Kurosaki, G.Saltini, S.Demontis, M.Marini, M.Salmona, E.Garattini, Cloning of the cDNAs coding for two novel molybdo-flavoproteins showing high similarity with aldehyde oxidase and xanthine oxidoreductase J.Biol.Chem. 275, (2000) 30690-30700.

[209] M.Terao, M.Kurosaki, M.Marini, M.A.Vanoni, G.Saltini, V.Bonetto, A.Bastone, C.Federico, S.Saccone, R.Fanelli, M.Salmona, E.Garattini, Purification of the aldehyde oxidase homolog 1 (AOH1) protein and cloning of the AOH1 and aldehyde oxidase homolog 2 (AOH2) genes. Identification of a novel molybdo-flavoprotein gene cluster on mouse chromosome 1 J.Biol.Chem. 276, (2001) 46347-46363.

[210] E.Garattini, R.Mendel, M.J.Romao, R.Wright, M.Terao, Mammalian molybdo-flavoenzymes, an expanding family of proteins: structure, genetics, regulation, function and pathophysiology Biochem.J. 372, (2003) 15-32.

[211] R.Berger, E.Mezey, K.P.Clancy, G.Harta, R.M.Wright, J.E.Repine, R.H.Brown, M.Brownstein, D.Patterson, Analysis of aldehyde oxidase and xanthine dehydrogenase/oxidase as possible candidate genes for autosomal recessive familial amyotrophic lateral sclerosis Somat.Cell Mol.Genet. 21, (1995) 121-131.

[212] M.Terao, M.Kurosaki, S.Demontis, S.Zanotta, E.Garattini, Isolation and characterization of the human aldehyde oxidase gene: conservation of intron/exon boundaries with the xanthine oxidoreductase gene indicates a common origin Biochem.J. 332 (Pt 2), (1998) 383-393.

[213] R.M.Wright, L.K.Weigel, M.Varella-Garcia, G.Vaitaitis, J.E.Repine, Molecular cloning, refined chromosomal mapping, and structural analysis of the human gene encoding aldehyde oxidase (AOX1), a candidate for the ALS2 gene. Redox Rep. 3, (1997) 135-144.

[214] R.M.Wright, G.M.Vaitaitis, L.K.Weigel, T.B.Repine, J.L.McManaman, J.E.Repine, Identification of the candidate ALS2 gene at chromosome 2q33 as a human aldehyde oxidase gene Redox Rep. 1, (1995) 313-321.

[215] R.Javahery, A.Khachi, K.Lo, B.Zenzie-Gregory, S.T.Smale, DNA sequence requirements for transcriptional initiator activity in mammalian cells Mol.Cell Biol. 14, (1994) 116-127.

[216] R.M.Wright, M.G.Riley, L.K.Weigel, L.A.Ginger, D.A.Costantino, J.L.McManaman, Activation of the human aldehyde oxidase (hAOX1) promoter by tandem cooperative Sp1/Sp3 binding sites: identification of complex architecture in the hAOX upstream DNA that includes a proximal promoter, distal activation sites, and a silencer element DNA Cell Biol. 19, (2000) 459-474.

[217] D.Y.Huang, A.Furukawa, Y.Ichikawa, Molecular cloning of retinal oxidase/aldehyde oxidase cDNAs from rabbit and mouse livers and functional expression of

recombinant mouse retinal oxidase cDNA in Escherichia coli Arch.Biochem.Biophys. 364, (1999) 264-272.

[218] R.M.Wright, D.A.Clayton, M.G.Riley, J.L.McManaman, J.E.Repine, cDNA cloning, sequencing, and characterization of male and female rat liver aldehyde oxidase (rAOX1). Differences in redox status may distinguish male and female forms of hepatic APX J.Biol.Chem. 274, (1999) 3878-3886.

[219] M.Kurosaki, S.Demontis, M.M.Barzago, E.Garattini, M.Terao, Molecular cloning of the cDNA coding for mouse aldehyde oxidase: tissue distribution and regulation in vivo by testosterone Biochem.J. 341 (Pt 1), (1999) 71-80.

[220] S.Yoshihara, K.Tatsumi, Purification and characterization of hepatic aldehyde oxidase in male and female mice Arch.Biochem.Biophys. 338, (1997) 29-34.

[221] S.Yoshihara, K.Tatsumi, Involvement of growth hormone as a regulating factor in sex differences of mouse hepatic aldehyde oxidase Biochem.Pharmacol. 53, (1997) 1099-1105.

[222] Y.Moriwaki, T.Yamamoto, S.Takahashi, Z.Tsutsumi, T.Hada, Widespread cellular distribution of aldehyde oxidase in human tissues found by immunohistochemistry staining Histol.Histopathol. 16, (2001) 745-753.

[223] S.P.Rivera, H.H.Choi, B.Chapman, M.J.Whitekus, M.Terao, E.Garattini, O.Hankinson, Identification of aldehyde oxidase 1 and aldehyde oxidase homologue 1 as dioxin-inducible genes Toxicology 207, (2005) 401-409.

[224] M.R.Probst, S.Reisz-Porszasz, R.V.Agbunag, M.S.Ong, O.Hankinson, Role of the aryl hydrocarbon receptor nuclear translocator protein in aryl hydrocarbon (dioxin) receptor action Mol.Pharmacol. 44, (1993) 511-518.

[225] A.Fujisawa-Sehara, K.Sogawa, M.Yamane, Y.Fujii-Kuriyama, Characterization of xenobiotic responsive elements upstream from the drug-metabolizing cytochrome P-450c gene: a similarity to glucocorticoid regulatory elements Nucleic Acids Res. 15, (1987) 4179-4191.

[226] H.Reyes, S.Reisz-Porszasz, O.Hankinson, Identification of the Ah receptor nuclear translocator protein (Arnt) as a component of the DNA binding form of the Ah receptor Science 256, (1992) 1193-1195.

[227] J.J.Reiners, Jr., A.R.Cantu, T.A.Rupp, Coordinate modulation of murine hepatic xanthine oxidase activity and the cytochrome P-450 system by interferons J.Interferon Res. 10, (1990) 109-118.

[228] M.Neumeier, J.Weigert, A.Schaffler, T.S.Weiss, C.Schmidl, R.Buttner, C.Bollheimer, C.Aslanidis, J.Scholmerich, C.Buechler, Aldehyde oxidase 1 is highly abundant in hepatic steatosis and is downregulated by adiponectin and fenofibric acid in hepatocytes in vitro Biochem.Biophys.Res.Commun. 350, (2006) 731-735.

[229] C.Beedham, D.J.Critchley, D.J.Rance, Substrate specificity of human liver aldehyde oxidase toward substituted quinazolines and phthalazines: a comparison with hepatic enzyme from guinea pig, rabbit, and baboon Arch.Biochem.Biophys. 319, (1995) 481-490.

[230] C.Bendotti, E.Prosperini, M.Kurosaki, E.Garattini, M.Terao, Selective localization of mouse aldehyde oxidase mRNA in the choroid plexus and motor neurons Neuroreport 8, (1997) 2343-2349.

[231] C.K.Tang, G.H.Yi, J.H.Yang, L.S.Liu, Z.Wang, C.G.Ruan, Y.Z.Yang, Oxidized LDL upregulated ATP binding cassette transporter-1 in THP-1 macrophages Acta Pharmacol.Sin. 25, (2004) 581-586.

[232] P.Codogno, A.J.Meijer, Autophagy and signaling: their role in cell survival and cell death Cell Death.Differ. 12 Suppl 2, (2005) 1509-1518.

[233] D.J.Klionsky, J.M.Cregg, W.A.Dunn, Jr., S.D.Emr, Y.Sakai, I.V.Sandoval, A.Sibirny, S.Subramani, M.Thumm, M.Veenhuis, Y.Ohsumi, A unified nomenclature for yeast autophagy-related genes Dev.Cell 5, (2003) 539-545.

[234] B.Levine, D.J.Klionsky, Development by self-digestion: molecular mechanisms and biological functions of autophagy Dev.Cell 6, (2004) 463-477.

[235] E.Bergamini, G.Cavallini, A.Donati, Z.Gori, The role of macroautophagy in the ageing process, anti-ageing intervention and age-associated diseases Int.J.Biochem.Cell Biol. 36, (2004) 2392-2404.

[236] S.Rodriguez-Enriquez, L.He, J.J.Lemasters, Role of mitochondrial permeability transition pores in mitochondrial autophagy Int.J.Biochem.Cell Biol. 36, (2004) 2463-2472.

[237] T.Shintani, D.J.Klionsky, Autophagy in health and disease: a double-edged sword Science 306, (2004) 990-995.

[238] A.Kuma, M.Hatano, M.Matsui, A.Yamamoto, H.Nakaya, T.Yoshimori, Y.Ohsumi, T.Tokuhisa, N.Mizushima, The role of autophagy during the early neonatal starvation period Nature 432, (2004) 1032-1036.

[239] N.Mizushima, A.Yamamoto, M.Matsui, T.Yoshimori, Y.Ohsumi, In vivo analysis of autophagy in response to nutrient starvation using transgenic mice expressing a fluorescent autophagosome marker Mol.Biol.Cell 15, (2004) 1101-1111.

[240] E.Ogier-Denis, P.Codogno, Autophagy: a barrier or an adaptive response to cancer Biochim.Biophys.Acta 1603, (2003) 113-128.

[241] P.Boya, R.A.Gonzalez-Polo, N.Casares, J.L.Perfettini, P.Dessen, N.Larochette, D.Metivier, D.Meley, S.Souquere, T.Yoshimori, G.Pierron, P.Codogno, G.Kroemer, Inhibition of macroautophagy triggers apoptosis Mol.Cell Biol. 25, (2005) 1025-1040.

[242] J.J.Lum, D.E.Bauer, M.Kong, M.H.Harris, C.Li, T.Lindsten, C.B.Thompson, Growth factor regulation of autophagy and cell survival in the absence of apoptosis Cell 120, (2005) 237-248.

[243] P.G.Clarke, Developmental cell death: morphological diversity and multiple mechanisms Anat.Embryol.(Berl) 181, (1990) 195-213.

[244] G.E.Mortimore, G.Miotto, R.Venerando, M.Kadowaki, Autophagy Subcell.Biochem. 27, (1996) 93-135.

[245] E.F.Blommaart, J.J.Luiken, P.J.Blommaart, G.M.van Woerkom, A.J.Meijer, Phosphorylation of ribosomal protein S6 is inhibitory for autophagy in isolated rat hepatocytes J.Biol.Chem. 270, (1995) 2320-2326.

[246] T.Kanazawa, I.Taneike, R.Akaishi, F.Yoshizawa, N.Furuya, S.Fujimura, M.Kadowaki, Amino acids and insulin control autophagic proteolysis through different signaling pathways in relation to mTOR in isolated rat hepatocytes J.Biol.Chem. 279, (2004) 8452-8459.

[247] S.Mordier, C.Deval, D.Bechet, A.Tassa, M.Ferrara, Leucine limitation induces autophagy and activation of lysosome-dependent proteolysis in C2C12 myotubes through a mammalian target of rapamycin-independent signaling pathway J.Biol.Chem. 275, (2000) 29900-29906.

[248] E.F.Blommaart, U.Krause, J.P.Schellens, H.Vreeling-Sindelarova, A.J.Meijer, The phosphatidylinositol 3-kinase inhibitors wortmannin and LY294002 inhibit autophagy in isolated rat hepatocytes Eur.J.Biochem. 243, (1997) 240-246.

[249] J.L.Goldstein, Y.K.Ho, S.K.Basu, M.S.Brown, Binding site on macrophages that mediates uptake and degradation of acetylated low density lipoprotein, producing massive cholesterol deposition Proc.Natl.Acad.Sci.U.S.A 76, (1979) 333-337.

[250] P.Libby, Y.J.Geng, M.Aikawa, U.Schoenbeck, F.Mach, S.K.Clinton, G.K.Sukhova, R.T.Lee, Macrophages and atherosclerotic plaque stability Curr.Opin.Lipidol. 7, (1996) 330-335.

[251] H.S.Liao, T.Kodama, Y.J.Geng, Expression of class A scavenger receptor inhibits apoptosis of macrophages triggered by oxidized low density lipoprotein and oxysterol Arterioscler.Thromb.Vasc.Biol. 20, (2000) 1968-1975.

[252] R.Kinscherf, H.P.Deigner, C.Usinger, J.Pill, M.Wagner, H.Kamencic, D.Hou, M.Chen, W.Schmiedt, M.Schrader, G.Kovacs, K.Kato, J.Metz, Induction of mitochondrial manganese superoxide dismutase in macrophages by oxidized LDL: its relevance in atherosclerosis of humans and heritable hyperlipidemic rabbits FASEB J. 11, (1997) 1317-1328.

[253] E.Lagasse, I.L.Weissman, Enforced expression of Bcl-2 in monocytes rescues macrophages and partially reverses osteopetrosis in op/op mice Cell 89, (1997) 1021-1031.

[254] H.P.Deigner, R.Claus, G.A.Bonaterra, C.Gehrke, N.Bibak, M.Blaess, M.Cantz, J.Metz, R.Kinscherf, Ceramide induces aSMase expression: implications for oxLDL-induced apoptosis FASEB J. 15, (2001) 807-814.

[255] J.A.Hamilton, D.Myers, W.Jessup, F.Cochrane, R.Byrne, G.Whitty, S.Moss, Oxidized LDL can induce macrophage survival, DNA synthesis, and enhanced proliferative response to CSF-1 and GM-CSF Arterioscler.Thromb.Vasc.Biol. 19, (1999) 98-105.

[256] J.A.Hamilton, W.Jessup, A.J.Brown, G.Whitty, Enhancement of macrophage survival and DNA synthesis by oxidized-low-density-lipoprotein (LDL)-derived lipids and by aggregates of lightly oxidized LDL Biochem.J. 355, (2001) 207-214.

[257] S.Bhakdi, B.Dorweiler, R.Kirchmann, J.Torzewski, E.Weise, J.Tranum-Jensen, I.Walev, E.Wieland, On the pathogenesis of atherosclerosis: enzymatic

transformation of human low density lipoprotein to an atherogenic moiety J.Exp.Med. 182, (1995) 1959-1971.

[258] S.Bhakdi, Complement and atherogenesis: the unknown connection Ann.Med. 30, (1998) 503-507.

[259] M.Kapinsky, M.Torzewski, C.Buchler, C.Q.Duong, G.Rothe, G.Schmitz, Enzymatically degraded LDL preferentially binds to CD14(high) CD16(+) monocytes and induces foam cell formation mediated only in part by the class B scavenger-receptor CD36 Arterioscler.Thromb.Vasc.Biol. 21, (2001) 1004-1010.

[260] M.Klouche, S.Gottschling, V.Gerl, W.Hell, M.Husmann, B.Dorweiler, M.Messner, S.Bhakdi, Atherogenic properties of enzymatically degraded LDL: selective induction of MCP-1 and cytotoxic effects on human macrophages Arterioscler.Thromb.Vasc.Biol. 18, (1998) 1376-1385.

[261] E.Stoyanova, A.Tesch, V.W.Armstrong, E.Wieland, Enzymatically degraded low density lipoproteins are more potent inducers of egr-1 mRNA than oxidized or native low density lipoproteins Clin.Biochem. 34, (2001) 483-490.

[262] C.Buechler, M.Ritter, C.Q.Duong, E.Orso, M.Kapinsky, G.Schmitz, Adipophilin is a sensitive marker for lipid loading in human blood monocytes Biochim.Biophys.Acta 1532, (2001) 97-104.

[263] S.R.Han, A.Momeni, K.Strach, P.Suriyaphol, D.Fenske, K.Paprotka, S.I.Hashimoto, M.Torzewski, S.Bhakdi, M.Husmann, Enzymatically modified LDL induces cathepsin H in human monocytes: potential relevance in early atherogenesis Arterioscler.Thromb.Vasc.Biol. 23, (2003) 661-667.

[264] Y.Gluzman, SV40-transformed simian cells support the replication of early SV40 mutants Cell 23, (1981) 175-182.

[265] D.P.Aden, A.Fogel, S.Plotkin, I.Damjanov, B.B.Knowles, Controlled synthesis of HBsAg in a differentiated human liver carcinoma-derived cell line Nature 282, (1979) 615-616.

[266] S.J.Collins, R.C.Gallo, R.E.Gallagher, Continuous growth and differentiation of human myeloid leukaemic cells in suspension culture Nature 270, (1977) 347-349.

[267] U.Schneider, H.U.Schwenk, G.Bornkamm, Characterization of EBV-genome negative "null" and "T" cell lines derived from children with acute lymphoblastic leukemia and leukemic transformed non-Hodgkin lymphoma Int.J.Cancer 19, (1977) 621-626.

[268] J.Stohr, G.Schindler, G.Rothe, G.Schmitz, Enhanced upregulation of the Fc gamma receptor IIIa (CD16a) during in vitro differentiation of ApoE4/4 monocytes Arterioscler.Thromb.Vasc.Biol. 18, (1998) 1424-1432.

[269] W.Drobnik, H.Borsukova, A.Bottcher, A.Pfeiffer, G.Liebisch, G.J.Schutz, H.Schindler, G.Schmitz, Apo AI/ABCA1-dependent and HDL3-mediated lipid efflux from compositionally distinct cholesterol-based microdomains Traffic. 3, (2002) 268-278.

[270] E.G.BLIGH, W.J.DYER, A rapid method of total lipid extraction and purification Can.J.Biochem.Physiol 37, (1959) 911-917.

[271] O.H.Lowry, N.J.ROSEBROUGH, A.L.FARR, R.J.RANDALL, Protein measurement with the Folin phenol reagent J.Biol.Chem. 193, (1951) 265-275.

[272] E.Wieland, S.Parthasarathy, D.Steinberg, Peroxidase-dependent metal-independent oxidation of low density lipoprotein in vitro: a model for in vivo oxidation? Proc.Natl.Acad.Sci.U.S.A 90, (1993) 5929-5933.

[273] G.W.Duff, E.Atkins, The detection of endotoxin by in vitro production of endogenous pyrogen: comparison with limulus amebocyte lysate gelation J.Immunol.Methods 52, (1982) 323-331.

[274] C.T.Chien, P.L.Bartel, R.Sternglanz, S.Fields, The two-hybrid system: a method to identify and clone genes for proteins that interact with a protein of interest Proc.Natl.Acad.Sci.U.S.A 88, (1991) 9578-9582.

[275] S.Fields, O.Song, A novel genetic system to detect protein-protein interactions Nature 340, (1989) 245-246.

[276] L.Dini, A.Lentini, G.D.Diez, M.Rocha, L.Falasca, L.Serafino, F.Vidal-Vanaclocha, Phagocytosis of apoptotic bodies by liver endothelial cells J.Cell Sci. 108 (Pt 3), (1995) 967-973.

[277] B.Brone, J.Eggermont, PDZ proteins retain and regulate membrane transporters in polarized epithelial cell membranes Am.J.Physiol Cell Physiol 288, (2005) C20-C29.

[278] C.Campo, A.Mason, D.Maouyo, O.Olsen, D.Yoo, P.A.Welling, Molecular mechanisms of membrane polarity in renal epithelial cells Rev.Physiol Biochem.Pharmacol. 153, (2005) 47-99.

[279] M.L.Fitzgerald, K.Okuhira, G.F.Short, III, J.J.Manning, S.A.Bell, M.W.Freeman, ATP-binding cassette transporter A1 contains a novel C-terminal VFVNFA motif that is required for its cholesterol efflux and ApoA-I binding activities J.Biol.Chem. 279, (2004) 48477-48485.

[280] C.Alewine, O.Olsen, J.B.Wade, P.A.Welling, TIP-1 has PDZ scaffold antagonist activity Mol Biol.Cell 17, (2006) 4200-4211.

[281] R.Rousset, S.Fabre, C.Desbois, F.Bantignies, P.Jalinot, The C-terminus of the HTLV-1 Tax oncoprotein mediates interaction with the PDZ domain of cellular proteins Oncogene 16, (1998) 643-654.

[282] L.Hampson, C.Li, A.W.Oliver, H.C.Kitchener, I.N.Hampson, The PDZ protein Tip-1 is a gain of function target of the HPV16 E6 oncoprotein Int.J.Oncol. 25, (2004) 1249-1256.

[283] C.Reynaud, S.Fabre, P.Jalinot, The PDZ protein TIP-1 interacts with the Rho effector rhotekin and is involved in Rho signaling to the serum response element J.Biol.Chem. 275, (2000) 33962-33968.

[284] L.Olalla, J.C.Aledo, G.Bannenberg, J.Marquez, The C-terminus of human glutaminase L mediates association with PDZ domain-containing proteins FEBS Lett. 488, (2001) 116-122.

[285] M.Kanamori, P.Sandy, S.Marzinotto, R.Benetti, C.Kai, Y.Hayashizaki, C.Schneider, H.Suzuki, The PDZ protein tax-interacting protein-1 inhibits beta-catenin

transcriptional activity and growth of colorectal cancer cells J.Biol.Chem. 278, (2003) 38758-38764.

[286] M.Katoh, GIPC gene family (Review) Int.J.Mol.Med. 9, (2002) 585-589.

[287] M.Abramow-Newerly, A.A.Roy, C.Nunn, P.Chidiac, RGS proteins have a signalling complex: interactions between RGS proteins and GPCRs, effectors, and auxiliary proteins Cell Signal. 18, (2006) 579-591.

[288] D.Bilder, N.Perrimon, Localization of apical epithelial determinants by the basolateral PDZ protein Scribble Nature 403, (2000) 676-680.

[289] L.E.Dow, A.M.Brumby, R.Muratore, M.L.Coombe, K.A.Sedelies, J.A.Trapani, S.M.Russell, H.E.Richardson, P.O.Humbert, hScrib is a functional homologue of the Drosophila tumour suppressor Scribble Oncogene 22, (2003) 9225-9230.

[290] K.Nagasaka, S.Nakagawa, T.Yano, S.Takizawa, Y.Matsumoto, T.Tsuruga, K.Nakagawa, T.Minaguchi, K.Oda, O.Hiraike-Wada, H.Ooishi, T.Yasugi, Y.Taketani, Human homolog of Drosophila tumor suppressor Scribble negatively regulates cell-cycle progression from G1 to S phase by localizing at the basolateral membrane in epithelial cells Cancer Sci. 97, (2006) 1217-1225.

[291] A.Brumby, J.Secombe, J.Horsfield, M.Coombe, N.Amin, D.Coates, R.Saint, H.Richardson, A genetic screen for dominant modifiers of a cyclin E hypomorphic mutation identifies novel regulators of S-phase entry in Drosophila Genetics 168, (2004) 227-251.

[292] J.N.Murdoch, D.J.Henderson, K.Doudney, C.Gaston-Massuet, H.M.Phillips, C.Paternotte, R.Arkell, P.Stanier, A.J.Copp, Disruption of scribble (Scrb1) causes severe neural tube defects in the circletail mouse Hum.Mol.Genet. 12, (2003) 87-98.

[293] K.Zarbalis, S.R.May, Y.Shen, M.Ekker, J.L.Rubenstein, A.S.Peterson, A focused and efficient genetic screening strategy in the mouse: identification of mutations that disrupt cortical development PLoS.Biol. 2, (2004) E219.

[294] O.Lahuna, M.Quellari, C.Achard, S.Nola, G.Meduri, C.Navarro, N.Vitale, J.P.Borg, M.Misrahi, Thyrotropin receptor trafficking relies on the hScrib-betaPIX-GIT1-ARF6 pathway EMBO J. 24, (2005) 1364-1374.

[295] Y.Wu, D.Dowbenko, S.Spencer, R.Laura, J.Lee, Q.Gu, L.A.Lasky, Interaction of the tumor suppressor PTEN/MMAC with a PDZ domain of MAGI3, a novel membrane-associated guanylate kinase J.Biol.Chem. 275, (2000) 21477-21485.

[296] K.Adamsky, K.Arnold, H.Sabanay, E.Peles, Junctional protein MAGI-3 interacts with receptor tyrosine phosphatase beta (RPTPbeta) and tyrosine-phosphorylated proteins J.Cell Sci. 116, (2003) 1279-1289.

[297] R.Yao, Y.Natsume, T.Noda, MAGI-3 is involved in the regulation of the JNK signaling pathway as a scaffold protein for frizzled and Ltap Oncogene 23, (2004) 6023-6030.

[298] J.L.Franklin, K.Yoshiura, P.J.Dempsey, G.Bogatcheva, L.Jeyakumar, K.S.Meise, R.S.Pearsall, D.Threadgill, R.J.Coffey, Identification of MAGI-3 as a

transforming growth factor-alpha tail binding protein Exp.Cell Res. 303, (2005) 457-470.

[299] J.He, M.Bellini, H.Inuzuka, J.Xu, Y.Xiong, X.Yang, A.M.Castleberry, R.A.Hall, Proteomic analysis of beta1-adrenergic receptor interactions with PDZ scaffold proteins J.Biol.Chem. 281, (2006) 2820-2827.

[300] H.Zhang, D.Wang, H.Sun, R.A.Hall, C.C.Yun, MAGI-3 regulates LPA-induced activation of Erk and RhoA Cell Signal. 19, (2007) 261-268.

[301] M.Thomas, R.Laura, K.Hepner, E.Guccione, C.Sawyers, L.Lasky, L.Banks, Oncogenic human papillomavirus E6 proteins target the MAGI-2 and MAGI-3 proteins for degradation Oncogene 21, (2002) 5088-5096.

[302] M.Ohashi, M.Sakurai, M.Higuchi, N.Mori, M.Fukushi, M.Oie, R.J.Coffey, K.Yoshiura, Y.Tanaka, M.Uchiyama, M.Hatanaka, M.Fujii, Human T-cell leukemia virus type 1 Tax oncoprotein induces and interacts with a multi-PDZ domain protein, MAGI-3 Virology 320, (2004) 52-62.

[303] Z.Xia, J.A.Gray, B.A.Compton-Toth, B.L.Roth, A direct interaction of PSD-95 with 5-HT2A serotonin receptors regulates receptor trafficking and signal transduction J.Biol.Chem. 278, (2003) 21901-21908.

[304] K.W.Roche, S.Standley, J.McCallum, L.C.Dune, M.D.Ehlers, R.J.Wenthold, Molecular determinants of NMDA receptor internalization Nat.Neurosci. 4, (2001) 794-802.

[305] Y.Xiang, B.Kobilka, The PDZ-binding motif of the beta2-adrenoceptor is essential for physiologic signaling and trafficking in cardiac myocytes Proc.Natl.Acad.Sci.U.S.A 100, (2003) 10776-10781.

[306] X.Zha, J.Genest, Jr., R.McPherson, Endocytosis is enhanced in Tangier fibroblasts: possible role of ATP-binding cassette protein A1 in endosomal vesicular transport J.Biol.Chem. 276, (2001) 39476-39483.

[307] X.Zha, A.Gauthier, J.Genest, R.McPherson, Secretory vesicular transport from the Golgi is altered during ATP-binding cassette protein A1 (ABCA1)-mediated cholesterol efflux J.Biol.Chem. 278, (2003) 10002-10005.

[308] S.C.Bondy, J.Orozco, Effects of ethanol treatment upon sources of reactive oxygen species in brain and liver Alcohol Alcohol 29, (1994) 375-383.

[309] S.Shaw, E.Jayatilleke, The role of cellular oxidases and catalytic iron in the pathogenesis of ethanol-induced liver injury Life Sci. 50, (1992) 2045-2052.

[310] S.Shaw, E.Jayatilleke, Cimetidine as a scavenger of ethanol-induced free radicals Alcohol 9, (1992) 363-367.

[311] S.Shaw, J.Eng, E.Jayatilleke, Ethanol-induced free radical injury to the hepatocyte glucagon receptor Alcohol 12, (1995) 273-277.

[312] L.Mira, L.Maia, L.Barreira, C.F.Manso, Evidence for free radical generation due to NADH oxidation by aldehyde oxidase during ethanol metabolism Arch.Biochem.Biophys. 318, (1995) 53-58.

[313] R.M.Wright, L.K.Weigel, J.E.Repine, Aldehyde oxidase generates deoxyribonucleic acid single strand nicks in vitro Redox Rep. 1, (1995) 313-321.

[314] A.E.Vendrov, N.R.Madamanchi, Z.S.Hakim, M.Rojas, M.S.Runge, Thrombin and NAD(P)H oxidase-mediated regulation of CD44 and BMP4-Id pathway in VSMC, restenosis, and atherosclerosis Circ.Res. 98, (2006) 1254-1263.

[315] K.K.Griendling, D.Sorescu, M.Ushio-Fukai, NAD(P)H oxidase: role in cardiovascular biology and disease Circ.Res. 86, (2000) 494-501.

[316] B.M.Babior, NADPH oxidase Curr.Opin.Immunol. 16, (2004) 42-47.

[317] Y.Wang, M.M.Zeigler, G.K.Lam, M.G.Hunter, T.D.Eubank, V.V.Khramtsov, S.V.Tridandapani, C.K.Sen, C.B.Marsh, The Role of the NADPH Oxidase Complex, p38 MAPK and Akt in Regulating Human Monocyte/Macrophage Survival Am.J.Respir.Cell Mol.Biol.(2006).

[318] E.B.Rimm, P.Williams, K.Fosher, M.Criqui, M.J.Stampfer, Moderate alcohol intake and lower risk of coronary heart disease: meta-analysis of effects on lipids and haemostatic factors BMJ 319, (1999) 1523-1528.

[319] W.P.Castelli, J.T.Doyle, T.Gordon, C.G.Hames, M.C.Hjortland, S.B.Hulley, A.Kagan, W.J.Zukel, Alcohol and blood lipids. The cooperative lipoprotein phenotyping study Lancet 2, (1977) 153-155.

[320] M.H.Criqui, L.D.Cowan, H.A.Tyroler, S.Bangdiwala, G.Heiss, R.B.Wallace, R.Cohn, Lipoproteins as mediators for the effects of alcohol consumption and cigarette smoking on cardiovascular mortality: results form the Lipid Research Clinics Follow-up Study Am.J.Epidemiol. 126, (1987) 629-637.

[321] J.W.Beulens, A.Sierksma, A.van Tol, N.Fournier, T.van Gent, J.L.Paul, H.F.Hendriks, Moderate alcohol consumption increases cholesterol efflux mediated by ABCA1 J.Lipid Res. 45, (2004) 1716-1723.

[322] G.D.Castro, A.M.Delgado de Layno, M.H.Costantini, J.A.Castro, Cytosolic xanthine oxidoreductase mediated bioactivation of ethanol to acetaldehyde and free radicals in rat breast tissue. Its potential role in alcohol-promoted mammary cancer Toxicology 160, (2001) 11-18.

[323] M.Terao, M.Kurosaki, M.M.Barzago, E.Varasano, A.Boldetti, A.Bastone, M.Fratelli, E.Garattini, Avian and Canine Aldehyde Oxidases: NOVEL INSIGHTS INTO THE BIOLOGY AND EVOLUTION OF MOLYBDO-FLAVOENZYMES J.Biol.Chem. 281, (2006) 19748-19761.

[324] C.Beedham, J.J.Miceli, R.S.Obach, Ziprasidone metabolism, aldehyde oxidase, and clinical implications J.Clin.Psychopharmacol. 23, (2003) 229-232.

[325] R.R.Brown, M.W.Estoup, Comparison of the metabolic effects observed in patients treated with ziprasidone versus olanzapine Int.Clin.Psychopharmacol. 20, (2005) 105-112.

[326] Z.Shaban, S.El-Shazly, S.Abdelhady, I.Fattouh, K.Muzandu, M.Ishizuka, K.Kimura, A.Kazusaka, S.Fujita, Down regulation of hepatic PPARalpha function by AhR ligand J.Vet.Med.Sci. 66, (2004) 1377-1386.

[327] A.Geusau, K.Abraham, K.Geissler, M.O.Sator, G.Stingl, E.Tschachler, Severe 2,3,7,8-tetrachlorodibenzo-p-dioxin (TCDD) intoxication: clinical and laboratory effects Environ.Health Perspect. 109, (2001) 865-869.

[328] D.Pelclova, Z.Fenclova, J.Preiss, B.Prochazka, J.Spacil, Z.Dubska, B.Okrouhlik, E.Lukas, P.Urban, Lipid metabolism and neuropsychological follow-up study of workers exposed to 2,3,7,8- tetrachlordibenzo- p-dioxin Int.Arch.Occup.Environ.Health 75 Suppl, (2002) S60-S66.

[329] J.F.Oram, J.W.Heinecke, ATP-binding cassette transporter A1: a cell cholesterol exporter that protects against cardiovascular disease Physiol Rev. 85, (2005) 1343-1372.

[330] T.Crnogorac-Jurcevic, R.Gangeswaran, V.Bhakta, G.Capurso, S.Lattimore, M.Akada, M.Sunamura, W.Prime, F.Campbell, T.A.Brentnall, E.Costello, J.Neoptolemos, N.R.Lemoine, Proteomic analysis of chronic pancreatitis and pancreatic adenocarcinoma Gastroenterology 129, (2005) 1454-1463.

[331] Y.R.Lee, H.J.Shim, H.N.Yu, E.K.Song, J.Park, K.B.Kwon, J.W.Park, H.W.Rho, B.H.Park, M.K.Han, J.S.Kim, Dimethylsulfoxide induces upregulation of tumor suppressor protein PTEN through nuclear factor-kappaB activation in HL-60 cells Leuk.Res. 29, (2005) 401-405.

[332] A.Cappellini, G.Tabellini, M.Zweyer, R.Bortul, P.L.Tazzari, A.M.Billi, F.Fala, L.Cocco, A.M.Martelli, The phosphoinositide 3-kinase/Akt pathway regulates cell cycle progression of HL60 human leukemia cells through cytoplasmic relocalization of the cyclin-dependent kinase inhibitor p27(Kip1) and control of cyclin D1 expression Leukemia 17, (2003) 2157-2167.

[333] M.C.Seminario, P.Precht, R.P.Wersto, M.Gorospe, R.L.Wange, PTEN expression in PTEN-null leukaemic T cell lines leads to reduced proliferation via slowed cell cycle progression Oncogene 22, (2003) 8195-8204.

[334] S.Arico, A.Petiot, C.Bauvy, P.F.Dubbelhuis, A.J.Meijer, P.Codogno, E.Ogier-Denis, The tumor suppressor PTEN positively regulates macroautophagy by inhibiting the phosphatidylinositol 3-kinase/protein kinase B pathway J.Biol.Chem. 276, (2001) 35243-35246.

[335] D.C.De, R.Wattiaux, Functions of lysosomes Annu.Rev.Physiol 28, (1966) 435-492.

[336] B.Bjorkerud, S.Bjorkerud, Contrary effects of lightly and strongly oxidized LDL with potent promotion of growth versus apoptosis on arterial smooth muscle cells, macrophages, and fibroblasts Arterioscler.Thromb.Vasc.Biol. 16, (1996) 416-424.

[337] M.Torzewski, M.Klouche, J.Hock, M.Messner, B.Dorweiler, J.Torzewski, H.E.Gabbert, S.Bhakdi, Immunohistochemical demonstration of enzymatically modified human LDL and its colocalization with the terminal complement complex in the early atherosclerotic lesion Arterioscler.Thromb.Vasc.Biol. 18, (1998) 369-378.

[338] P.A.Kiener, P.M.Davis, G.C.Starling, C.Mehlin, S.J.Klebanoff, J.A.Ledbetter, W.C.Liles, Differential induction of apoptosis by Fas-Fas ligand interactions in human monocytes and macrophages J.Exp.Med. 185, (1997) 1511-1516.

[339] Y.Hitoshi, J.Lorens, S.I.Kitada, J.Fisher, M.LaBarge, H.Z.Ring, U.Francke, J.C.Reed, S.Kinoshita, G.P.Nolan, Toso, a cell surface, specific regulator of Fas-induced apoptosis in T cells Immunity. 8, (1998) 461-471.

[340] Y.Song, C.O.Jacob, The mouse cell surface protein TOSO regulates Fas/Fas ligand-induced apoptosis through its binding to Fas-associated death domain J.Biol.Chem. 280, (2005) 9618-9626.

[341] Y.Hamon, C.Broccardo, O.Chambenoit, M.F.Luciani, F.Toti, S.Chaslin, J.M.Freyssinet, P.F.Devaux, J.McNeish, D.Marguet, G.Chimini, ABC1 promotes engulfment of apoptotic cells and transbilayer redistribution of phosphatidylserine Nat.Cell Biol. 2, (2000) 399-406.

[342] S.Horiuchi, Y.Sakamoto, M.Sakai, Scavenger receptors for oxidized and glycated proteins Amino.Acids 25, (2003) 283-292.

[343] H.F.Hoff, T.B.Cole, Macrophage uptake of low-density lipoprotein modified by 4-hydroxynonenal. An ultrastructural study Lab Invest 64, (1991) 254-264.

[344] S.Bhakdi, M.Torzewski, K.Paprotka, S.Schmitt, H.Barsoom, P.Suriyaphol, S.R.Han, K.J.Lackner, M.Husmann, Possible protective role for C-reactive protein in atherogenesis: complement activation by modified lipoproteins halts before detrimental terminal sequence Circulation 109, (2004) 1870-1876.

[*] Figures 1, 6, 8 (lower part), 10, 11, 25 and Table 1 were generated at our institute and provided by Prof. Dr. Gerd Schmitz.

Eidesstattliche Erklärung

Ich erkläre hiermit an Eides Statt, dass ich die vorliegende Arbeit ohne unzulässige Hilfe Dritter und ohne Benutzung anderer als der angegebenen Hilfsmittel angefertigt habe; die aus anderen Quellen direkt oder indirekt übernommenen Daten und Konzepte sind unter Angabe des Literaturzitats gekennzeichnet.

Die in der Danksagung aufgeführten Personen haben mir in der jeweils beschrieben Weise unentgeltlich geholfen.

Weitere Personen waren an der inhaltlich-materiellen Herstellung der vorliegenden Arbeit nicht beteiligt. Insbesondere habe ich hierfür nicht die entgeltliche Hilfe eines Promotionsberaters oder anderer Personen in Anspruch genommen. Niemand hat von mir weder unmittelbar noch mittelbar geldwerte Leistungen für Arbeiten erhalten, die im Zusammenhang mit dem Inhalt der vorgelegten Dissertation stehen.

Die Arbeit wurde bisher weder im In- noch im Ausland in gleicher oder ähnlicher Form einer anderen Prüfungsbehörde vorgelegt.

Ich versichere an Eides Statt, dass ich nach bestem Wissen die reine Wahrheit gesagt und nichts verschwiegen habe.

Vor Aufnahme der obigen Versicherung an Eides Statt wurde ich über die Bedeutung der eidesstattlichen Versicherung und die strafrechtlichen Folgen einer unrichtigen oder unvollständigen eidesstattlichen Versicherung belehrt.

.....

Alexander Sigrüner